Doctoral Dissertation

Collapse Analysis of Ship Hull Girder Using Hydro-elastoplastic Beam Model

HAN HTOO HTOO KO

June 2020

Graduate School of Engineering
Osaka University

Collapse Analysis of Ship Hull Girder Using Hydro-elastoplastic Beam Model

By

HAN HTOO HTOO KO

A Dissertation for Doctor of Engineering Degree submitted to

Graduate School of Engineering

Department of Naval Architecture and Ocean Engineering

Osaka University

in

July 2020

Supervised by

Prof. Dr. Masahiko Fujikubo

Committee members

Prof. Dr. Kazuhiro Iijima

Prof. Dr. Naoki Osawa

Prof. Dr. Ninshu Ma

Abstract

Ultimate longitudinal hull girder strength is the most fundamental strength to ensure the structural safety of ships. Not only a peak strength but also a post-ultimate strength behavior and collapse extent need to be evaluated to assess the risk of failure. After reaching the ultimate strength, the capacity of hull girder decreases because of buckling, and inertia force is taking a supporting role to satisfy the equilibrium condition. Another important aspect of hull girder collapse in waves is a fluid-structure interaction (FSI). The hull girder collapse is, therefore, essentially a dynamic behavior and needs to consider nonlinear structural behavior and FSI. Such behavior can be called hydro-elastoplastic response.

In the present study, a simplified method named FE-smith method is developed to analyze the hydro-elastoplastic response of a ship hull girder. The Smith method which is employed for the progressive collapse analysis of hull girder cross sections is coupled with the beam finite element with consideration of FSI. The validation is made through a comparison with the analysis employing 3D-shell FE model. Parametric studies are performed to investigate the effect of some dynamic and hydrodynamic parameters on the collapse behavior.

The theory and methodology underlying the proposed FE-smith method are presented first. The average stress-average strain relationship of structural elements used in Smith method is transformed to the average stress-average plastic strain relationship and introduced in beam element as a pseudo strain hardening/softening effect. The nonlinear stiffness equation for a whole ship can be derived in the standard FE approach. Two types of average stress-average strain relationship are adopted, using those obtained by rule formula and by nonlinear FEM. It has been confirmed from the comparison of results that the FE-smith method can capture the essential collapse behavior of hull girder cross section in shorter time with reasonable accuracy.

The FE-smith method is then extended to the dynamic collapse analysis considering the hydro-static/dynamic forces which are the function of hull girder motions and deformation. By applying impulsive bending loads, dynamic collapse behavior of a uniform beam model is analyzed. Reasonable collapse behavior can be obtained by FE-smith method with much shorter computation time. It has been found that the shorter the

load duration, the smaller the collapse extent even when the maximum applied load is the same.

The validation of the proposed hydro-elastoplastic beam model is performed by the comparison with nonlinear FE analysis taking a 5,250 TEU container ship as a subject ship. In the FE analysis, 3D-shell model is used for the collapsing midship part and beam model for the rest part. Assumed load distribution is applied in an impulsive manner instead of real wave loads. It has been found that FE-smith method that employs the average stress-average strain curves obtained by nonlinear FEM can provide more reasonable prediction of the collapse behavior than those by rule formula, together with its limitation in the application arising from the assumption of a plane cross section for beam element.

The parametric dependency of hull girder collapse is investigated. The effect of applied load duration, added mass and fluid damping on the collapse behavior and extent is investigated. Damping effect generally reduces the collapse extent. The added mass has more complicated effects on the collapse extent, as it is related both to the reactions against accelerated hull girder deformation and to the natural vibrations that affects the bending moment history exerted at cross sections.

Finally, the conclusions of main findings are drawn and suggestion for future work are described.

Acknowledgement

First of all, I would like to express my deep and sincere gratitude to my research supervisor Prof. Dr. Masahiko Fujikubo for accepting me as a graduate student, giving me the opportunity to do this study. I have learnt a lot of things from basics to advance including conducting research and writing academic papers under his guidance. Without his kind support and encouragement, this dissertation would not have been materialized.

Secondly, my deepest appreciation goes to Assistant Prof. Dr. Akira Tatsumi. This dissertation would not have been completed without his enormous and generous contribution. I also would like to express my gratitude to him as I have learnt a lot from his advice and constructive comments.

Thirdly, I am grateful to Prof. Dr. Kazuhiro Iijima. Discussion with him has been insightful. And I would like to thank my dissertation committee members : Prof. Dr. Naoki Osawa, Prof. Dr. Ninshu Ma and again Prof. Dr. Kazuhiro Iijima for their time, constructive comments and review on this work. I would like to appreciate Dr. Sherif Rashed for providing me kind support and valuable advice. My special thanks go to Mr. Kenji Nakano and Mr. Shuta Tatsukawa for the assistant in this study.

This study was financially supported by Japanese Government (MEXT Scholarship). I would like to acknowledge with gratitude for their financial support during 5 years study in Japan. Also I owe my gratitude to my supervisor again for financial support partly in my study extension period.

Finally, I would like to deeply thank to the support and encouragement of my family and Mr. Set Naing.

Thanks to my lab members for giving me their kind hearts and warm atmosphere for my stay in lab. I also would like to appreciate the warm encouragement from my friends from Japan and Myanmar. Special thanks go to my senior, Dr. Thaw Tar for his support and encouragement.

Table of contents

Nomenclature

u_x = axial displacement

u_z = displacement in z direction

θ_y = rotational displacement around y axis

ü = acceleration

ε_x = axial strain

ε^p = plastic strain

E = elastic modulus

$[K_a]$ = axial stiffness matrix of a beam element

$[K_b]$ = bending stiffness matrix of a beam element

ω_0 = natural frequency

δu = virtual displacement

w_{local} = local panel deflection

w_{global} = global panel deflection

A_0 = maximum magnitude of global panel deflection confined between the transverse frames and longitudinal girder

B_0 = maximum magnitude of local deflection of panel

m = number of buckling half wave in longitudinal direction of panel

n = number of buckling half wave in transverse direction of panel

β = slenderness ratio of panel

t = thickness of the plate

σ_Y = yield stress

ω = wave frequency

Φ = total velocity potential

ϕ = velocity potential

φ_0 = incident wave potential

φ_4 = scattering potential

k_0 = wave number

A_{ij} = added mass coefficient

B_{ij} = wave damping coefficient

A'_{ij} = non-dimensional added mass coefficient

B'_{ij} = non-dimensional wave damping coefficient

S_H = submerged body surface

g = acceleration due to gravity

η = wave amplitude

n_j = normal vector in j direction

ρ_{sea} = seawater density

ρ = density of material

A_s = area of ship's cross section per unit length of ship

B_w = breadth of ship's cross section at waterplane

List of tables

List of figures

Chapter 1

Introduction

1.1 Background

Ships contribute to human lives in many ways. Economics and transportation are main contribution sectors of the ship's role. Nowadays, maritime transport demand is getting higher according to the increase of markets and global trade. Variety of goods such as oil, material, gas and food are handled by maritime transport.

Collapse of ship can lead not only to loss of human lives but also severe environmental impact depending on the good she carries. One of the worst oil pollutions is due to the collapse of MV Prestige in 2012, Fig 1. 1. About 500,000 tonnes of oil are spilled into the ocean and got polluted thousands of miles as can be seen in Fig 1. 2. This accident caused huge damage to wild life and fishing industry. Also, tragedy of 8000TEU container ship MOL-Comfort happened in June 2013. The ship collapsed amidship and broke into two pieces as shown in Fig 1. 3 and Fig 1. 4. Such kind of accident alerts researchers to investigate more about the ship collapse behavior. IACS (International Association of Classification Society) also strengthened the rules for safety of ship hull girder.

Fig 1. 1 MV Prestige accident

Image source : https://safety4sea.com/cm-learn-from-the-past-prestige-sinking-one-of-the-worst-oil-spills-in-europe/

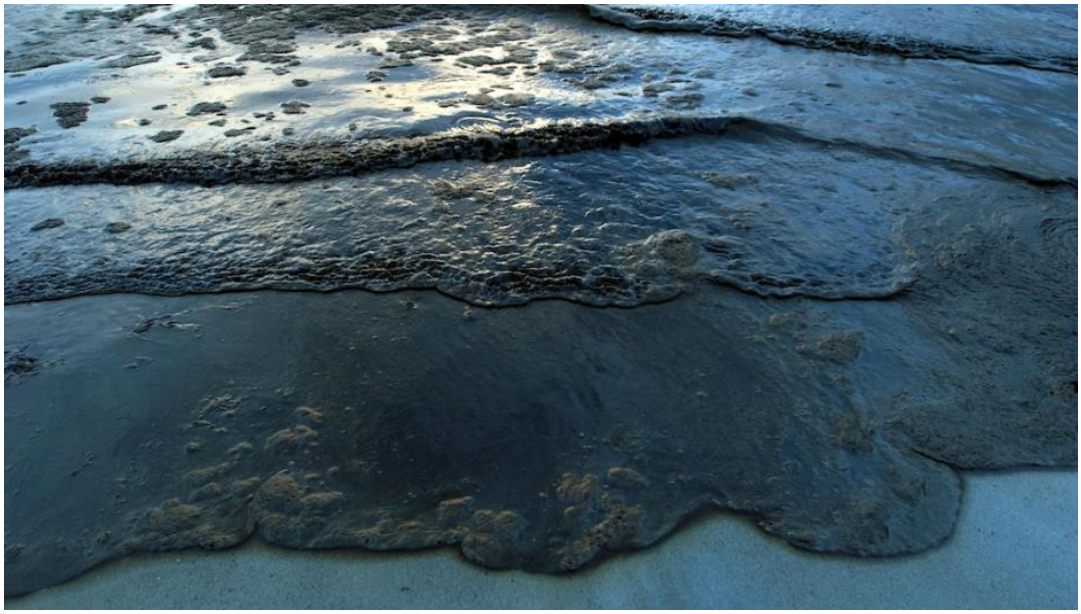

Fig 1. 2 Consequence of oil spill

Image source : https://www.pri.org/stories/2012-10-16/prestige-oil-spill-trial-opens-spain

Fig 1. 3 MOL-Comfort accident

Image source : https://maritimecyprus.com/2014/10/03/classnk-investigative-panel-publishes-report-on-mol-comfort-incident/

Fig 1. 4 MOL-Comfort accident

Image source : https://www.vesselfinder.com/news/3036-IACS-releases-comment-regarding-MOL-Comfort-report

1.2 Hull girder collapse behavior

Ship on her voyage is subjected to various kinds of loads such as hydrodynamic load, cargo load and sometimes unexpected extreme wave load. Hull girder collapse occurs when those external applied loads are getting larger than its capacity. To know the safety level of ship, longitudinal ultimate hull girder strength is the important study. Fig 1. 5 shows the moment curvature curve of a ship hull girder cross section. As the external load is increased, internal bending moment of ship hull girder is getting increased. Progressive collapse of plate and stiffened panel members occur due to buckling and plastic collapse under hull girder bending. At last, hull girder attains its ultimate strength. Ultimate strength of the ship hull girder is obtained from the peak point of the moment-curvature curve as shown in Fig 1. 5.

Beyond the ultimate strength, capacity of hull girder is gradually decreased. Decreasing its capacity does not mean external force will be decreasing. Since the capacity is not enough to carry the external force, inertia force is taking a supporting role to satisfy the equilibrium condition for a whole ship. Since the unbalance between the

external force and capacity is compensated by inertia force, this behavior becomes a dynamic behavior.

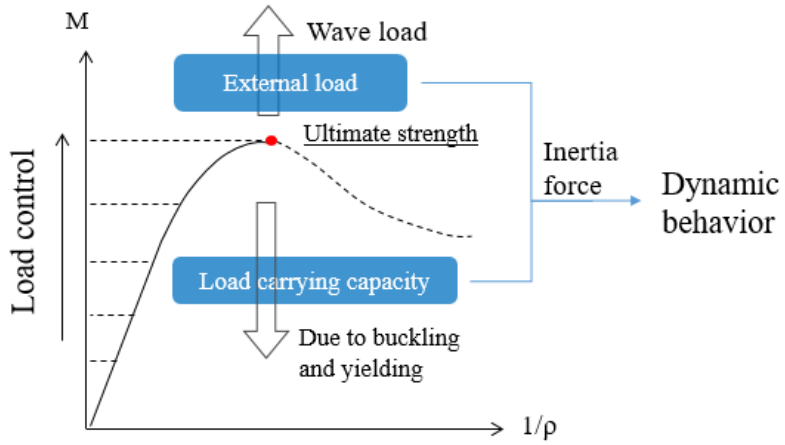

Fig 1. 5 Moment-curvature curve of hull girder

Another important aspect of ship hull girder collapse in waves is a fluid-structure interaction. As shown in Fig 1. 6, during the collapse process, structural deformation rapidly increases and the deformation of a whole ship leads to the change of the distribution of fluid pressure, and this in turn affects the ship motions. Such variations of pressure and motion again affect the collapse behavior. This interaction between hydrostatic/hydrodynamic forces and elastoplastic deformation need to be considered to predict the hull girder collapse in wave.

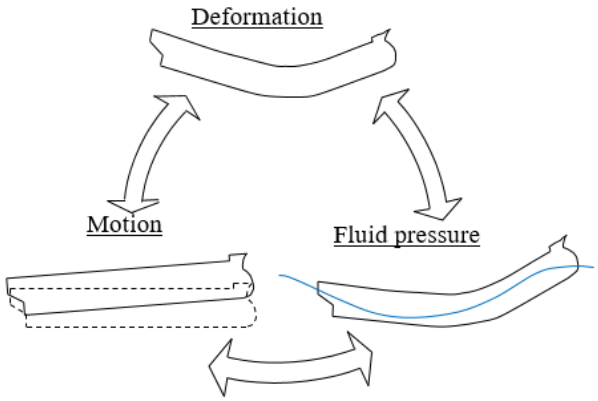

Fig 1. 6 Fluid structure interaction

Therefore, collapse of the ship is a dynamic behavior which needs the consideration of nonlinear structural behavior and fluid structure interaction. This is called *Hydro-Elastoplastic Response* [1]

1.3 Research works on the ultimate strength and post-ultimate strength behavior of hull girder

Brief introduction to the history of the study on ultimate longitudinal hull girder strength of ships is described. Research into ultimate hull girder strength started from the 19th century. Breakthrough research work on this topic were done by Thomas Young [2] and John [3]. Thomas Young is the first researcher who calculated the bending moment distribution and shear force along the ship hull girder, and John is the one who used the beam theory to calculate the bending moment of the ship hull girder by making fundamental assumption of ship length is equal to the wavelength.

After their works, researchers are trying to attempt in different ways to estimate the ultimate ship hull girder strength. Proposed methods are

1. Caldwell's method
2. Smith method
3. Non-Linear Finite Element Method (NFEM) and
4. Idealized Structural Unit Method (ISUM)

Caldwell[4] firstly proposed the method to calculate ship hull girder strength in 1965. He idealized the bottom stiffened panels of the ship cross section as the panels of equivalent plate thickness and considered a buckling factor. This assumed all the bottom stiffened panel collapse at the same time.

Then, Smith[5] proposed a method which could consider the progressive collapse of stiffened panels of cross section under longitudinal bending. In Smith method, cross-section is divided into plate or stiffened panel elements and the ultimate hull girder strength is calculated based on average stress-average strain of each element, which was calculated in advance considering the effect of buckling and yielding. In that way, it could capture the progressive collapse behavior of hull girder subjected to longitudinal bending.

In 1991 and 1992, Yao and Nikolov proposed a simple analytical method to calculate the progressive collapse behavior of ship's hull based on Smith method [6,7]. This method is developed as in-house code, HULLST. Because of its efficiency, Smith method is also adopted in the Common Structural Rules for Bulk Carriers and Oil Tankers[8] developed by IACS. CSR applied the Gordo-Soares formulae to calculate the required average stress-average strain curves [9].

On the other hand, with a rapid development of computational capabilities, NFEM comes into the practical use for ultimate strength analyses. Highly accurate and efficient shell elements for NFEM were proposed e.g. by Thomas J.R. Hughes et al. [10,11] and by T.Belytschko et al. [12] including one point-quadrature element [13], and their applicability to transient problems with material and geometric nonlinearities has been demonstrated[14]. Chen et al. [15] performed first hull girder collapse analysis by NFEM in 1983 by using 1+1/2 model and Valsgaard et al.[16] by using 1/2+1/2 model in 1991. Ikeda et.al [17] performed the collapse analysis of oil tankers to know the effect of thickness corrosion on ultimate strength by using explicit LS-dyna in 2001. Three tankers of 1/2+1/2 models were adopted. Although NFEM implicit analysis takes longer time than explicit analysis, Amlashi and Moan [18,19] performed the implicit analysis of bulk carrier by using 1/2+1+1/2 model. Most recently, Tatsumi and Fujikubo [20] published an article about the effect of bottom local loads on ultimate hull girder strength on 8000 TEU and 14000 TEU container ships. The effect is investigated by analyzing 1/2+1+1/2 model by implicit MSC.Marc.

ISUM was originally developed by Ueda and Rashed [21]. ISUM is similar to the traditional FEM but element size is significantly larger as member-size scale and thus the calculation time is more effective than FEM. Most recent ISUM elements were developed by Fujikubo et.al[22,23] and Paik et.al. [24]. In 2013, Pei Z et.al [25] performed the progressive collapse behavior of the whole ship bulk carrier model in extreme sea by using three different approaches, ISUM/FEM, implicit NFEM and HULLST. Singularity distribution method is used to find the water pressure. In this system, load is calculated by considering the rigid body motion while progressive collapse behavior considered the local and global deflection of hull girder. The fluid-structure interactions are not taken into account.

Hull girder ultimate strength is the fundamental subject to ensure the safety of ship. In addition to the ultimate strength, the post-ultimate strength behavior is important also from the viewpoint of risk assessment including consequence analysis. In 2006, Lehmann explained that bending moment and curvature curve obtained from force control or displacement control is far from reality when the working bending moment is larger than hull girder capacity. He considered the bending moment-curvature relationship that gives the equilibrium state after collapse as shown in Fig. 1.7 [26] considering the snap-though type relationship as shown. It is however not reasonable to explain the post-ultimate state using the capacity curve alone. It can be explained by considering the fluid-structure interaction effect as described above.

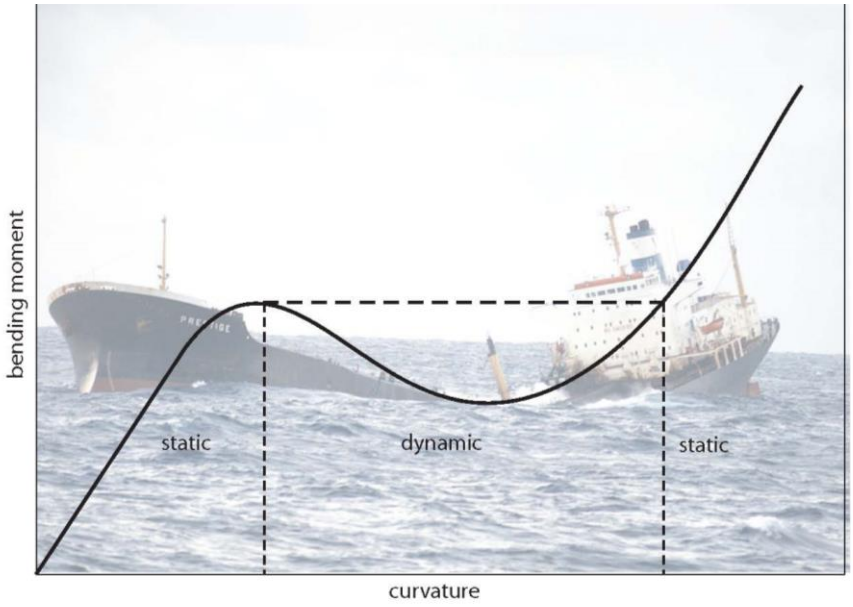

Fig 1. 7 Relationship between bending moment and curvature of a ship in seaway [26]

Post ultimate strength behavior of hull girder in waves was investigated numerically and experimentally by Iijima et al. and Xu et al. [1,27,28]. In those studies, hull girder was considered as two rigid bodies connected by a nonlinear rotational spring which represents the non-linear bending moment and rotation relationship. The model includes the consideration of hydro-elastoplastic response and the reduction of capacity beyond the ultimate strength. This model expresses the hull girder deflection in terms of

rotation angle which is regarded as an integrated value of plastic curvature over a certain longitudinal length. However, in order to predict the progressive collapse behavior in more detail including the spread of failures of plate and stiffened panel members, it is necessary to develop the method that can cope with the curvature or strains of individual sections or elements. NFEM is the most accurate and powerful approach for this purpose but it requires extremely large computation effort and time for the time-domain analysis of a whole ship considering hydro-elastoplastic effects.

A simplified static analysis method was proposed by Tanaka et.al [29], in which a hull girder was idealized as a non-uniform beam using conventional beam finite elements and the progressive collapse of each elements or sections are evaluated applying Smith method. In addition to longitudinal curvatures, warping effects due to torsional moments were considered for the collapse analysis of container ships under combined bending and torsional moments. The application of this extended Smith method to the dynamic collapse analysis of a hull girder is considered to be one possible approach to develop a practical method of hydro-elastoplastic response analysis of ship hull girder in waves.

1.4 Objective

Based on the above-mentioned background, the objective of this study is to develop a simplified method of collapse analysis of ship hull girder using hydro-elastoplastic beam model and to validate its effectiveness through a comparison with the results obtained by NFEM analysis. Parametric studies are performed using the developed method to investigate the dependency of hull girder collapse behavior on some loading and hydrodynamic parameters.

First, the Smith method is coupled with the conventional beam finite element by considering the change in the axial stiffness of longitudinal members due to buckling and yielding as a pseudo strain hardening/softening effect. The method is named as FE-Smith method and its applicability to the static collapse analysis of hull girder cross section is examined. The FE-Smith method is then extended for the dynamic collapse analysis of a whole ship hull girder considering fluid-structure interaction. A series of dynamic

collapse analysis of a ship hull girder under impulsive excitation with different load durations is performed using the proposed hydro-elastoplastic beam model. The results are compared with those obtained by the explicit NFEM analysis using the 3D shell model for the collapsing midship part. Finally, a series of dynamic collapse analyses of hull girder is performed with a focus on the effect of applied load durations and added-mass and fluid-damping forces on the collapse extent.

1.5 Organization of thesis

In Chapter 2, the theory and methodology underlying the proposed FE-Smith method that incorporate the Smith method into the elastoplastic beam FE analysis is presented. The average stress-average strain relationship of structural elements used in the original Smith method is transformed to the average stress-average plastic strain relationship and introduced to the beam element as a pseudo strain hardening/softening effect. Ultimate longitudinal bending strength of a hull girder cross section is analyzed by the FE-Smith method and NFEM, and the fundamental accuracy of the FE-smith method is discussed.

In Chapter 3, the hydro-elastoplastic beam model is developed. The FE-smith method is extended to the dynamic collapse analysis with consideration of the hydro-static and dynamic forces which are the function of hull girder motions and deformation. The solution procedures for the dynamic and elastoplastic analyses are described. Dynamic collapse behavior of a uniform beam model mounted on the hydrostatic spring is analyzed considering added mass and damping force effects. The characteristic of the hydro-elastoplastic behavior of a hull girder under impulsive bending loads is discussed.

In Chapter 4, the validation of the proposed hydro-elastoplastic beam model is performed through a comparison with NLFEA analysis. 5250 TEU container ship is taken as a subject ship and modelled as a non-uniform beam. In NFEM, 3D shell model is used for the collapsing midship part and beam model for the rest part. Considering the whipping response of container ships, an assumed external load distribution is applied in an impulsive manner instead of real wave loads. The accuracy of the proposed model is

examined in terms of the collapse mode, the time history of collapse response, the bending moment-curvature relationship of cross section and the final collapse extent.

In Chapter 5, the parametric dependency of hull girder collapse is investigated by the proposed model. The effect of applied load duration, added mass and wave damping forces in the collapse behavior and extent are discussed.

In Chapter 6, the conclusions with a summary of main findings are drawn. The suggestion for future work are also described.

Chapter 2

Ultimate Strength Analysis of a Hull Girder Cross Section

2.1 Introduction

Prediction of ultimate hull girder strength is essential to know the safety level of the ships. The Smith method is the effective and widely used method to calculate the progressive collapse behavior of hull girder, which is also adopted by IACS/CSR. Non-Linear Finite Element Method is also a powerful and precise method to investigate the ultimate strength. But due to its requirement of large computation time and computation power, simplified method which is called FE-smith method is proposed in this chapter. The ultimate hull girder strength of uniform cross section is investigated by FE-smith method. NFEA are also performed by commercial software, LS-dyna (Explicit) and MSC.Marc (Implicit) to measure the accuracy and capability of FE-smith method. Midship section of 5250 TEU container ship is adopted and 3 frame space midship part is used as an analysis model.

Details of collapse mode of hull girder are discussed by NFEM and compared with FE-smith method. Although certain differences can be found in comparison between them, it can be concluded that FE-smith method can capture the basic collapse behavior. Differences between the two methods are mainly due to the assumption of Smith method. There is also uncertainty of modeling accuracy and boundary condition in NFEM which are discussed in this chapter.

2.2 Smith method

Smith method is the robust and also widely used method to calculate the ultimate longitudinal bending hull girder strength. Procedure of Smith method are

(1) The first step is to divide the cross section into elements. Way of element division is shown in Fig 2. 1. The geometric center of each element shown in Fig 2. 2 is used as the integration point for the calculation of cross-sectional stiffness.

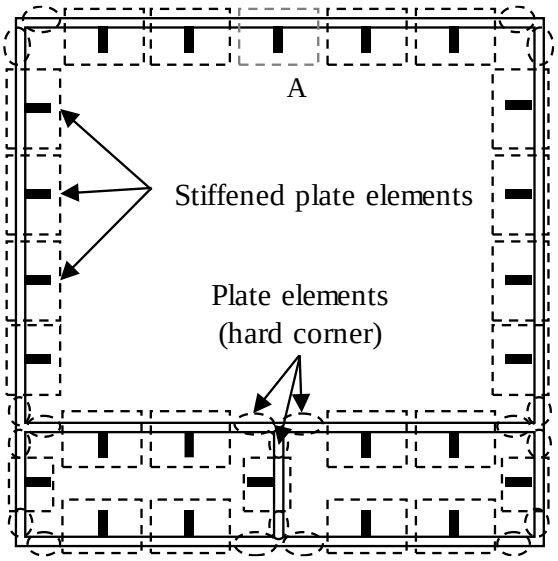

Fig 2. 1 Elements of Smith method

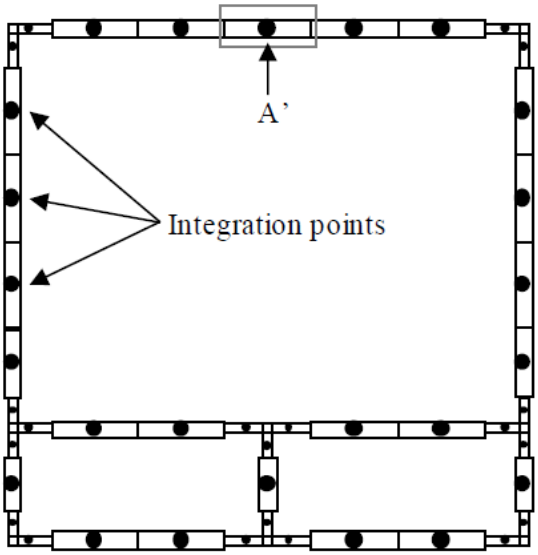

Fig 2. 2 Location of integration points

(2) Then average stress-average strain of each element under axial tensile and compressive loads considering the effect of buckling/yielding are prepared in advance before ultimate hull girder strength calculation. One assumption of Smith method is that there is no interaction between adjacent elements of the cross section.

(3) Ultimate bending strength of hull girder is attained by giving the curvature increment to the cross section under the assumption that the plane cross section remains plane. Using prepared average stress-average strain curves of elements, tangential stiffness of each element at current increment is calculated. From the distribution of tangential axial stiffness of each element, position of instantaneous neutral axis of the cross-section is updated.

(4) The tangential bending stiffness of the cross section about the instantaneous neutral axis is evaluated and bending moment increment is obtained by multiplying the stiffness with applied curvature increment.

(5) Strain increment of each element under the applied curvature value is calculated under the assumption of the plane cross section and stress increment is determined from the average stress-average strain curve.

(6) Obtained increment of bending moment, curvature, stress and strain are added to the values at last incremental step and continue next step.

(7) Ultimate longitudinal bending strength of a hull girder cross section is obtained from the peak bending moment of the bending moment-curvature relationship.

2.3 FE-smith method

In FE-smith method, hull girder is considered as an aggregation of finite beam elements discretized longitudinally. Consider Euler-Bernoulli beam element of length *L* with two end nodes, *i* and *j*, as shown in Fig 2. 3. In this case, nodal displacment vector $\{u\}$ and nodal force vector $\{F\}$ consists of axial and bending components.

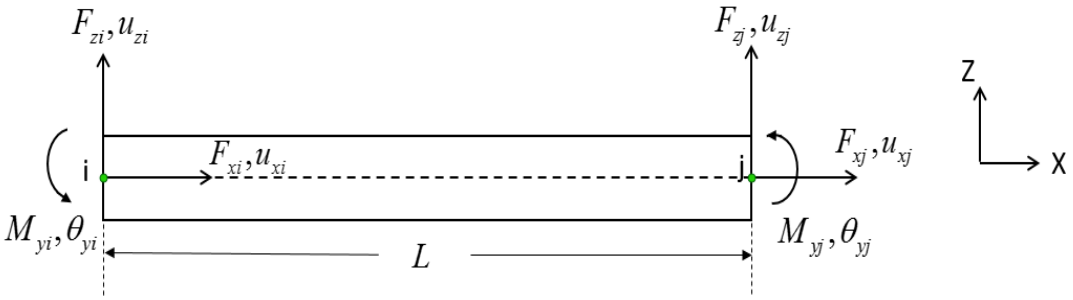

Fig 2. 3 Finite beam element

Let the subscript a represents axial components and b represents bending components. Then $\{u\}$ and $\{F\}$ can be written in the form of

$$\{u\} = \begin{Bmatrix} u_a \\ u_b \end{Bmatrix} \qquad \{F\} = \begin{Bmatrix} F_a \\ F_b \end{Bmatrix} \qquad \text{Eq (2.1)}$$

Each axial and bending components can be decomposed into

$$\{u_a\} = \begin{Bmatrix} u_{xi} \\ u_{xj} \end{Bmatrix} \qquad \{F_a\} = \begin{Bmatrix} F_{xi} \\ F_{xj} \end{Bmatrix} \qquad \text{Eq (2.2)}$$

$$\{u_b\} = \begin{Bmatrix} u_{zi} \\ \theta_{yi} \\ u_{zj} \\ \theta_{yj} \end{Bmatrix} \qquad \{F_b\} = \begin{Bmatrix} F_{zi} \\ F_{yi} \\ F_{zj} \\ F_{yj} \end{Bmatrix} \qquad \text{Eq (2.3)}$$

Shape function of the axial displacment u_a and bending deformation u_b are defined by linear and cubic interpolation functions.

$$u_a = \alpha_1 + \alpha_2 x \qquad \text{Eq (2.4)}$$

$$u_b = \beta_1 + \beta_2 x + \beta_3 x^2 + \beta_4 x^3 \qquad \text{Eq (2.5)}$$

By using the condition at x=0 and x=L , the coefficients α and β can be obtained in the form of

$$u_a = \begin{bmatrix} 1 - \frac{x}{L} & \frac{x}{L} \end{bmatrix} \begin{Bmatrix} u_{xi} \\ u_{xj} \end{Bmatrix} = [A_a]\{u_a\} \qquad \text{Eq (2.6)}$$

$$u_b = \begin{bmatrix} 1 & x & x^3 & x^3 \end{bmatrix} \begin{bmatrix} 1 & 0 & 0 & 0 \\ 0 & 1 & 0 & 0 \\ -\frac{3}{L^2} & \frac{2}{L} & \frac{3}{L^2} & -\frac{1}{L} \\ \frac{2}{L^2} & \frac{1}{L^2} & -\frac{2}{L^2} & \frac{1}{L} \end{bmatrix} \begin{Bmatrix} u_{zi} \\ \theta_{yi} \\ u_{zj} \\ \theta_{yj} \end{Bmatrix} = [A_b]\{u_b\} \qquad \text{Eq (2.7)}$$

Since Euler-Bernoulli beam is considered, cross section is remained plane as assumed in Smith method and the axial strain of the element is given by

$$\varepsilon_x = \frac{du_a}{dx} - z\frac{d^2u_b}{dx^2} = [B_a]\{u_a\} - z[B_b]\{u_b\} = [B]\{u\} \qquad \text{Eq (2.8)}$$

where z = distance from neutral axis

By using the principle of virtual work, element stiffness matrix can be written as

$$\{F\} = \int_V [B]^T \sigma_x dV \qquad \text{Eq (2.9)}$$

Here, σ_x = axial stress. If the material is in the elastic state where Young's Modulus is E

$$\{F\} = [K_e]\{u\} \qquad \text{Eq (2.10)}$$

$[K_e]$ is elastic stiffness composed of axial and bending components as

$$[K_e] = \begin{bmatrix} K_a & K_{ab} \\ K_{ba} & K_b \end{bmatrix} \qquad \text{Eq (2.11)}$$

$$[K_a] = \int_V [B_a]^T E [B_a] dV \qquad \text{Eq (2.12)}$$

$$[K_b] = \int_V z^2 [B_b]^T E [B_b] dV \qquad \text{Eq (2.13)}$$

$$[K_{ab}] = [K_{ba}]^T = -\int_V z [B_a]^T E [B_b] dV \qquad \text{Eq (2.14)}$$

In FE-smith method, the ship hull girder cross-section is divided into elements according to the Smith method. Location of integration point of each element is as shown in Fig 2. 2. Then, the average stress-average strain relationship of each element under axial load is prepared so that these relationships can be used as nonlinear material stress-strain relationship which can be expressed as

$$\sigma_x = f(\varepsilon_x) \qquad \text{Eq (2.15)}$$

Since the axial displacement u_a is considered as an independent degree of freedom of the beam element *ij*, the axial deformation caused by the shift of the neutral axis can be automatically considered.

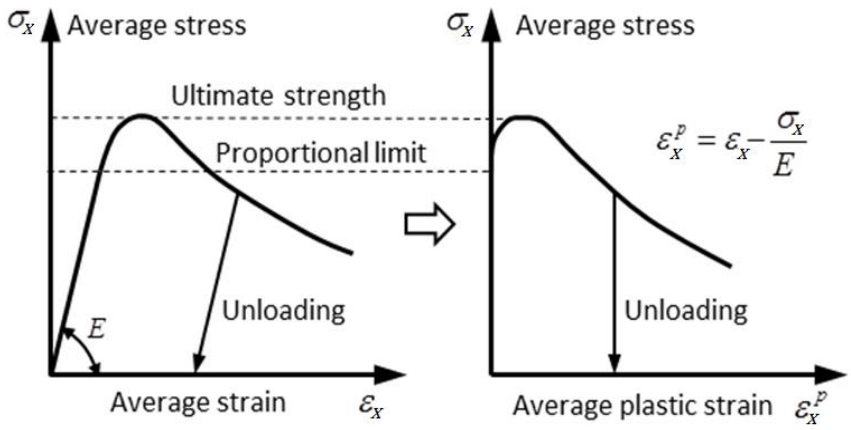

Fig 2. 4 Treatment of average stress-average strain relationship

In addition, the average stress-average strain relationship of structural elements, $\sigma_x=H(\varepsilon_x)$, which is usually highly nonlinear and has a reduction of the capacity after ultimate strength is transformed into the average stress-average plastic strain relationship, $\sigma_x=H'(\varepsilon_x^p)$, as shown in Fig 2. 4 and regarded as a pseudo strain-hardening/softening behaviors. This transformation gives an easy and general approach to implement the Smith method in the conventional FE analysis, since the consideration of strain hardening/softening effect is readily available in many FE analysis codes. It also gives a robust way to obtain convergence of solutions and also to detect the elastic unloading under repeated loads, which is indispensable in the dynamic elastoplastic analyses. The average plastic strain ε_x^p is calculated as

$$\varepsilon_x^p = \varepsilon_x - \frac{\sigma_x}{E} \qquad \text{Eq (2.16)}$$

Unloading stiffness is assumed to be given by the elastic stiffness even after yielding/buckling of the element. This is not correct since the unloading stiffness will be smaller because of the buckling damage of the structural element.

2.4 FE-smith analysis

Ultimate strength of uniform cross section hull girder is calculated by taking the one beam element for the region of 3 frame space length with simply-supported condition as shown in Fig 2. 5. Ultimate bending moment is obtained by applying the same magnitude of rotational angle θ_y in the hogging direction. Midship section of 5250 TEU container ship is adopted as shown in Fig 2. 6.

Average stress-average strain curve must be calculated prior to the beam element analysis. Two approaches are used to calculate the average stress-average strain relationship in this study as

1. Gordo-Soares formulae (CSR equation)
2. Nonlinear Finite Element Analysis by Msc.Marc (Applying Periodic-Boundary Condition)

Preparation of average stress-average strain curve are explained in Appendix A. FE-smith analysis using the first approach of average stress-average strain curve is named as FE-smith (CSR) and the second is as FE-smith (PBC) and are compared in Appendix B.

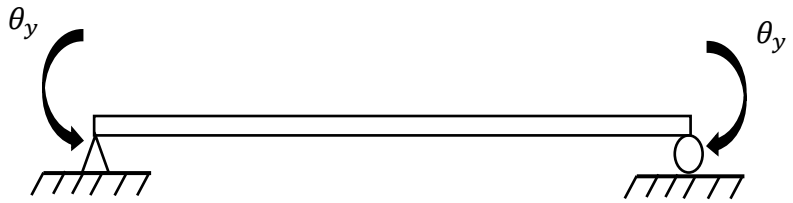

Fig 2. 5 Simply supported beam model for static analysis

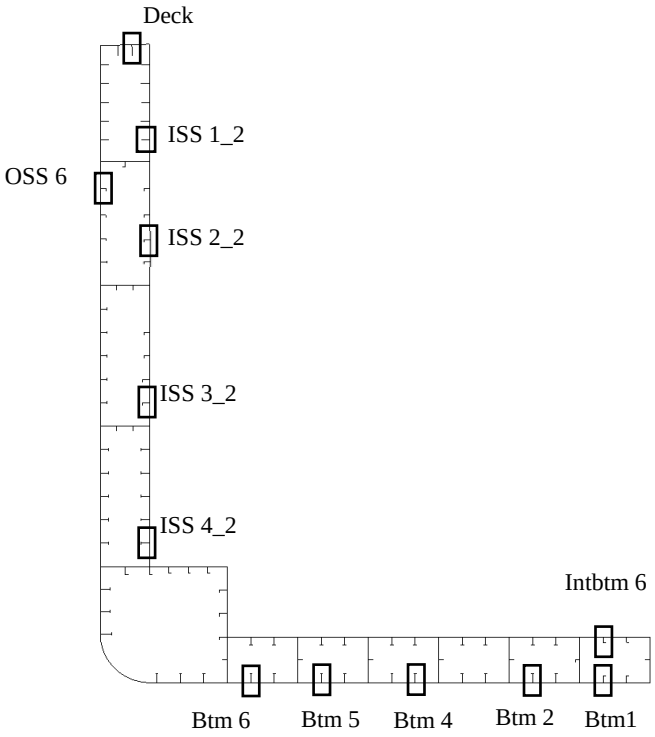

Fig 2. 6 Midship cross section of 5250 TEU container ship

2.5 Nonlinear finite element analysis

Since FE-smith model adopts the 3 frame space length as one beam element, 3 frame space shell elements model is modelled as midship part as shown in Fig 2. 7. Edges nodes of shell element model is constrained as rigid body (nodal rigid body option for LS-dyna and RBE2 for Msc.Marc) by setting the Node A and Node B as master nodes. Node A is fixed in X, Y, Z, θ_x and θ_z and node B is fixed in Y, Z, θ_x and θ_z direction. To satisfy the symmetric condition, all the nodes along the center girder are constrained not only in θ_x and θ_z direction but also in Y-direction.

Flange of stiffeners is divided into 4 elements and web into 6 elements. Plate between the two stiffeners is divided into 8 elements and mesh size is approximately 100mm x 100mm. Element types and material properties of LS-dyna and MSc.Marc are summarized in Table 2. 1. Two types of element model are analyzed in LS-dyna to check the accuracy. For shell element, number of integration point through the thickness direction is set as 5 for both models.

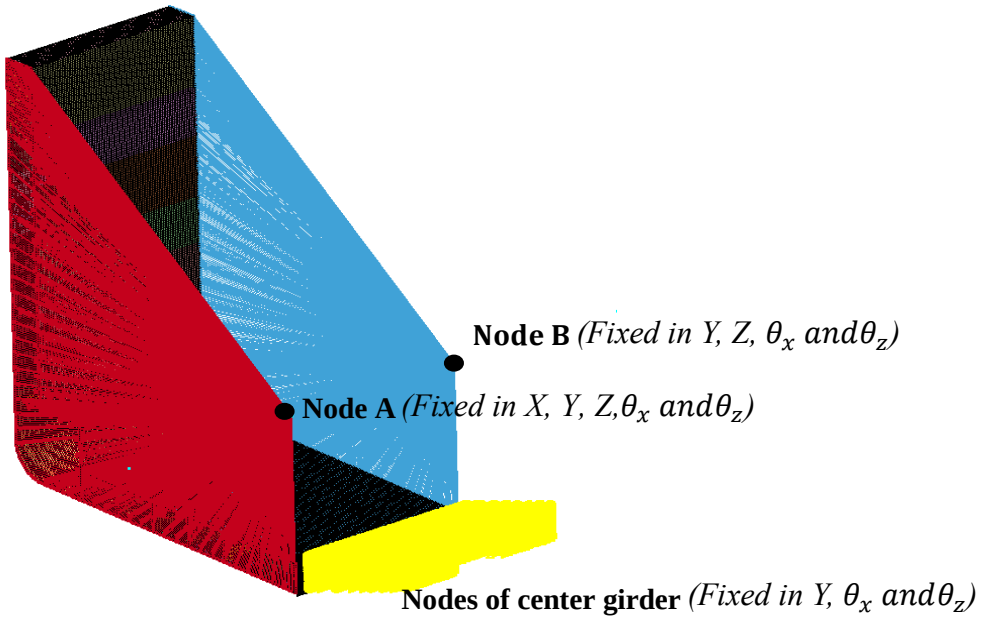

Fig 2. 7 Boundary condition of midship shell element

Table 2. 1 Material properties and Element types of NFEA model

NFEA	Material	Element
MSC.Marc	Elastic-plastic isotropic	Element type -75
LS-Dyna	003 : Plastic Kinematic	Hughes-Liu
	003 : Plastic Kinematic	Belytschko-Tsay

Initial imperfection is also applied to the implicit model only. Global and local deflection is applied to the bottom and inner bottom shell element. Three longitudinal half waves and one transverse half wave are assumed as the initial deflection mode of a local rectangular plate according the aspect ratio of the panel. One global half wave is applied to the region between the transverse frames and longitudinal girders in both longitudinal and transverse directions. Stiffener tripping is not considered. Magnitude of initial deflection is same as described in Eq (A.1) and Eq (A.4).

2.6 Results and discussion

First, the results obtained by FE-smith method are discussed. The bending moment-curvature relationships obtained by FE-smith method are shown in Fig 2. 8. It can be seen that FE-smith (CSR) shows the larger ultimate strength and also smoother load reduction beyond ultimate strength compared to FE-smith (PBC). In larger collapse extent region, load carrying capacity of FE-smith (CSR) is smaller than FE-smith (PBC). These results are directly related to the behavior of average stress-average strain curves shown in Appendix B.

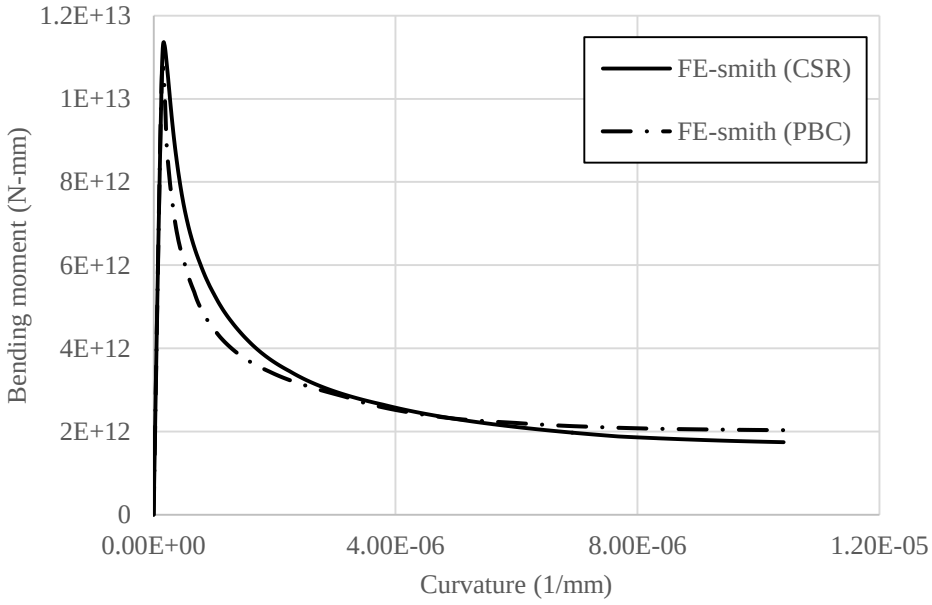

Fig 2. 8 Ultimate hogging strength analysis by FE-smith method

Results obtained from NFEM are shown in Fig 2. 9. For Msc.Marc implicit analysis, with and without initial deflection models are analyzed. To perform the static analysis in LS-dyna dynamic program, quasi-static load is adopted to have the small inertia force so that dynamic effect can be ignored. Static analysis result obtained by Msc.Marc and quasi-static analysis result by LS-dyna are drawn in Fig 2. 9. It can be seen that Marc without initial deflection model gives largest ultimate hogging bending moment. Since there exists a small deflection due to vibration in explicit dynamic analysis, ultimate hogging moment of LS-dyna model gives better agreement with Marc-model analysis

with initial deflection. In Marc analysis, model with initial deflection gives larger load reduction compared to the model without initial deflection. This is because of the difference in collapse region. Model with initial deflection collapsed only one edge frame while both edge frames collapsed in the model without initial deflection as can be seen in Fig 2. 10 and Fig 2. 11. Therefore, unloading process in 2 frame collapse is fairly distributed than 1 frame collapse case.

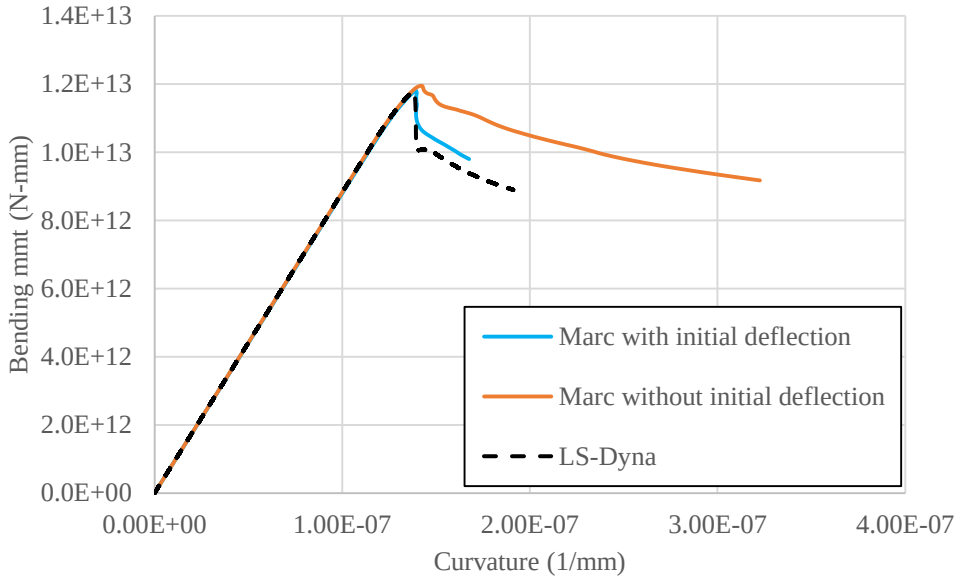

Fig 2. 9 Static analysis results by NFEM

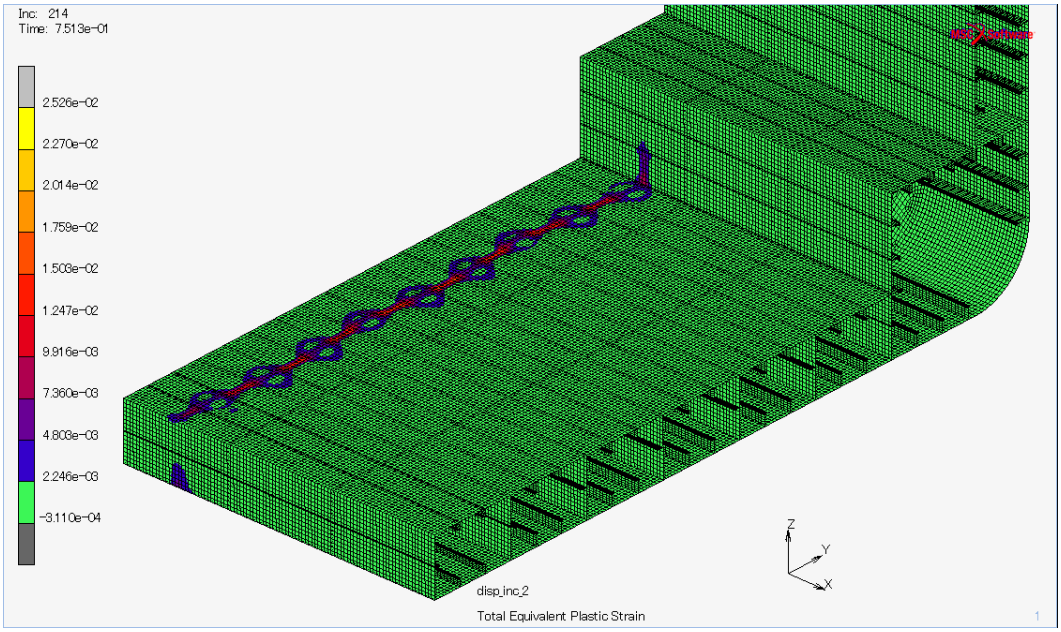

Fig 2. 10 Collapse region of midship part (with initial deflection model)

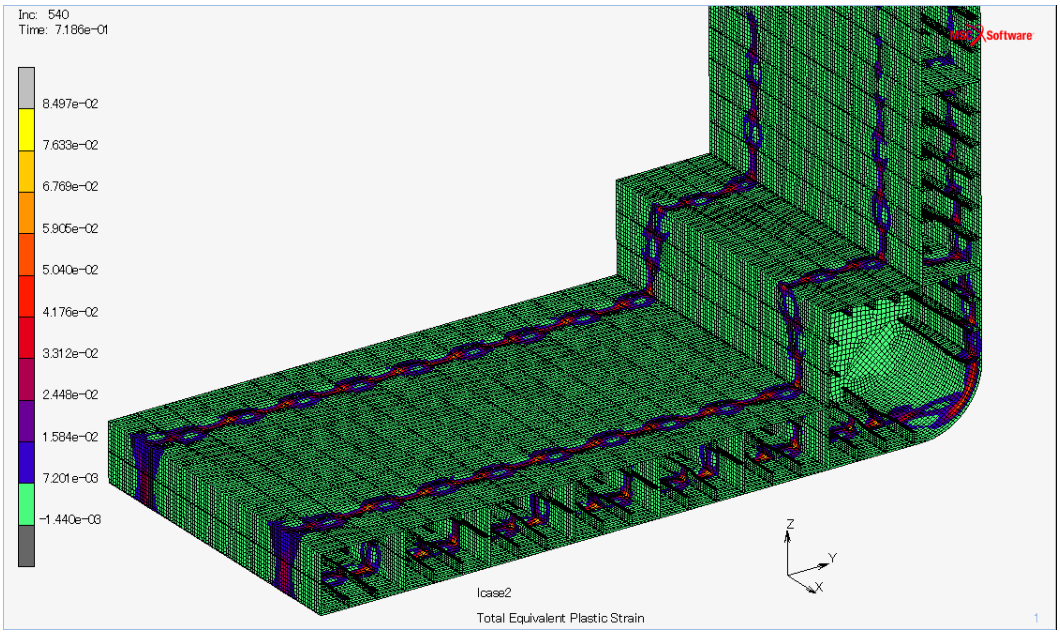

Fig 2. 11 Collapse region of midship part (without initial deflection model)

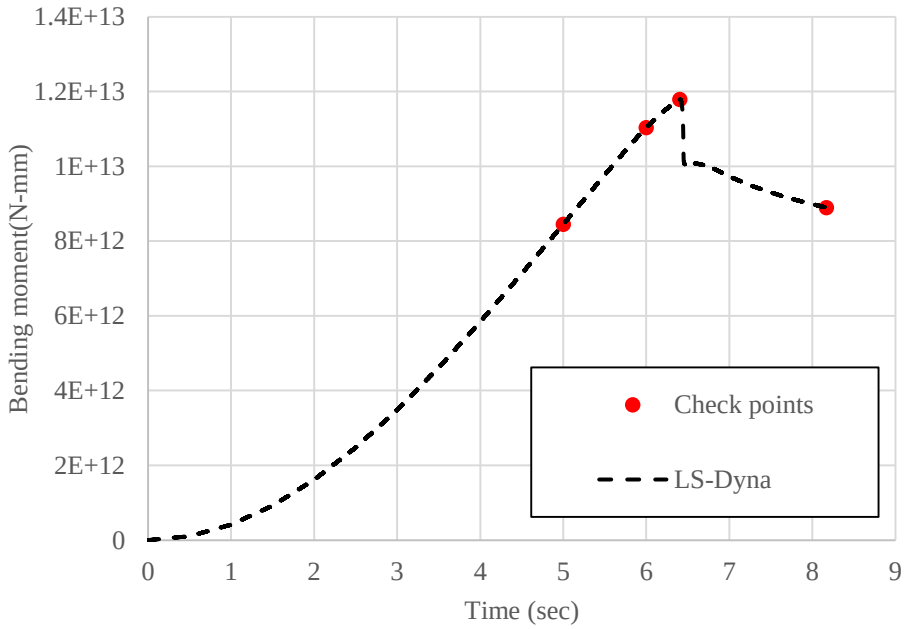

Fig 2. 12 Time history of moment of LS-dyna quasi-static analysis

Detail collapse mode and accumulation of the plastic strain of the model are also checked. Here, only the LS-dyna collapse mode will be explained as the same behavior

occurred between the Msc.Marc and LS-dyna. Fig 2. 12 shows the time history of hogging moment in LS-dyna. Two time step (5sec and 6sec) before ultimate strength, 6.4 sec (at ultimate strength) and end of analysis (8.7 sec) are clarified.

At 5sec, plastic strain in the model found at the edge of the deck area. Accumulation of plastic strain at deck is shown in Fig 2. 14. During 5 sec and 6 sec, there is no plastic strain in the bottom region. At 6.4 sec, hull girder attained its ultimate hogging moment. Between 6 sec and 6.4 sec, plastic strain in bottom region is started from the bottom plate element adjacent to the bilge part of the edge frames as shown in Fig 2. 15(a). This is because bottom plate thickness at those regions has the smallest thickness value. In that way, plate buckling is induced and plate collapsed first in bottom stiffened panel. After that plastic strain propagates towards the center girder alongside of the bottom plate and weaker frame is collapsed at 6.4 sec. Stress distribution of shell mode can be seen in Fig 2. 16. Since the rigid body constraint is applied, it induces the collapse of edge frame. Stress distribution and plastic strain distribution at the end of the analysis and collapse mode of bottom stiffened panels are described in Fig 2. 17, Fig 2. 18 and Fig 2. 19.

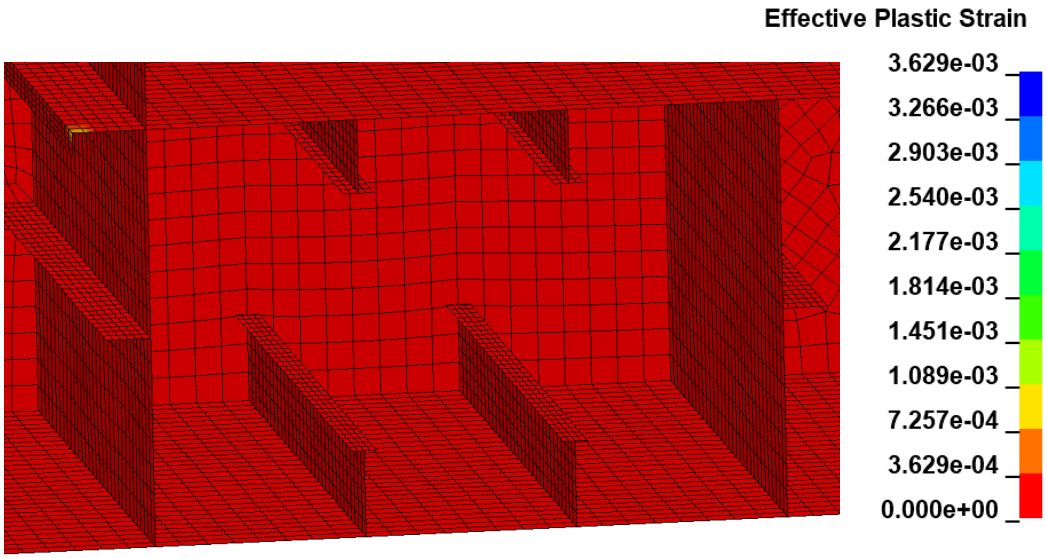

Fig 2. 13 Showing no plastic strain at bottom region at 6 sec

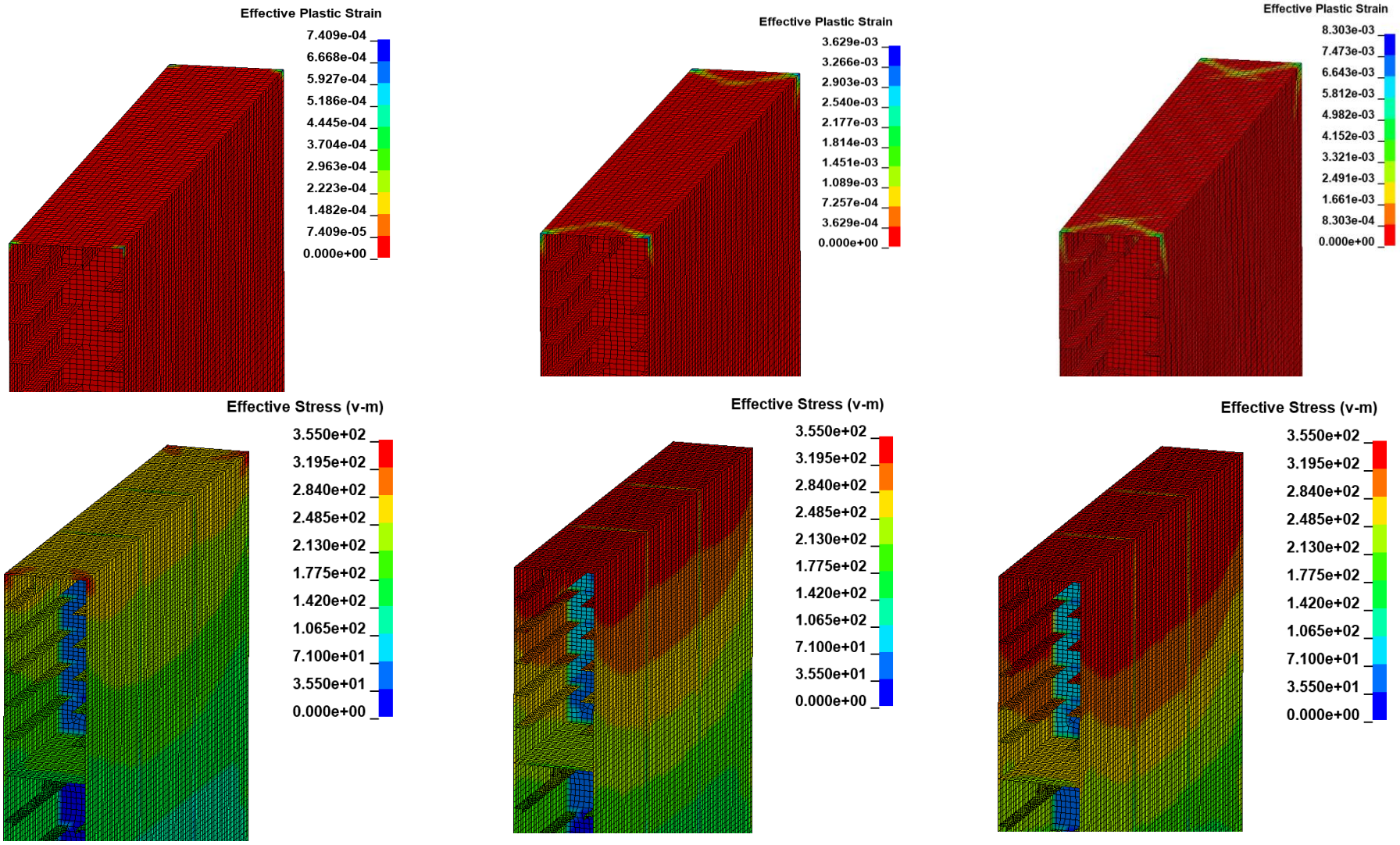

(a) 5sec (b) 6 sec (c) 6.4 sec

Fig 2. 14 Accumulation of plastic strain and stress distribution at deck region

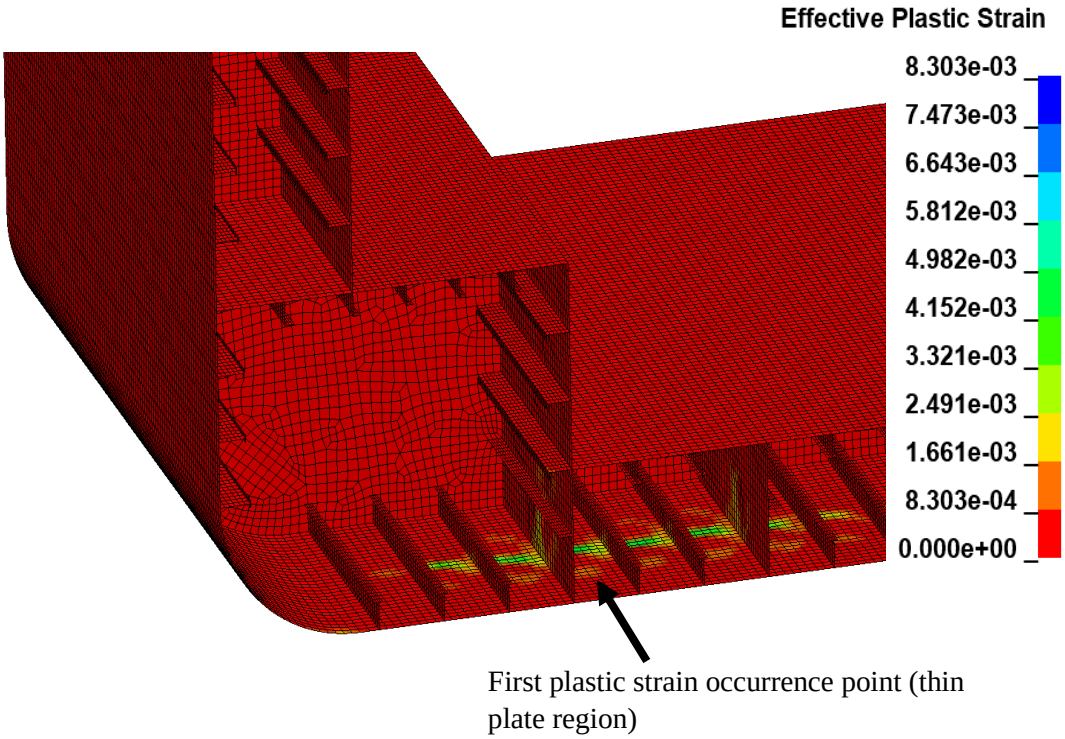

(a) First plastic strain occurrence region in bottom area

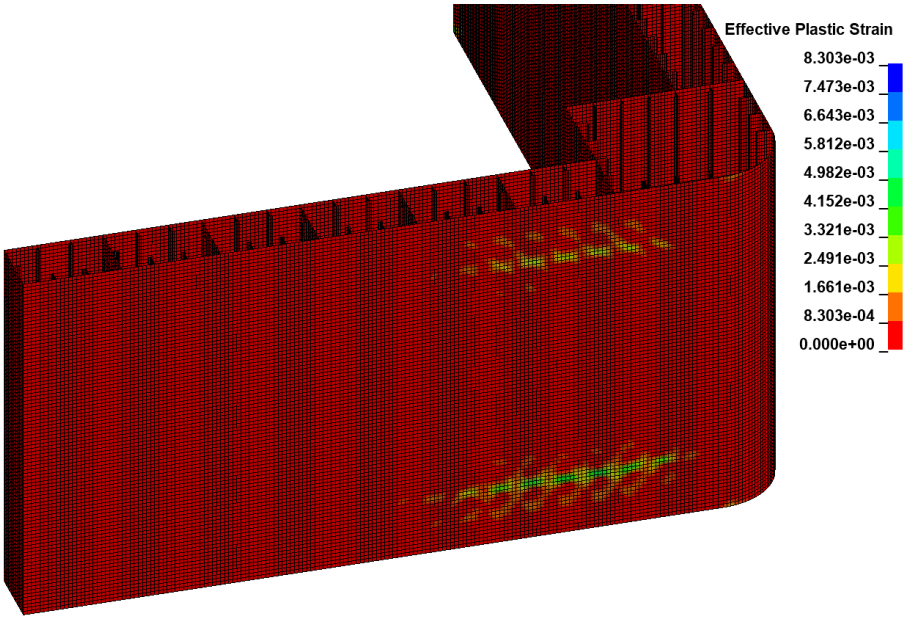

(b) Showing the accumulation of plastic strain at edge frames

Fig 2. 15 Plastic strain distribution at the bottom area at t = 6.4 sec

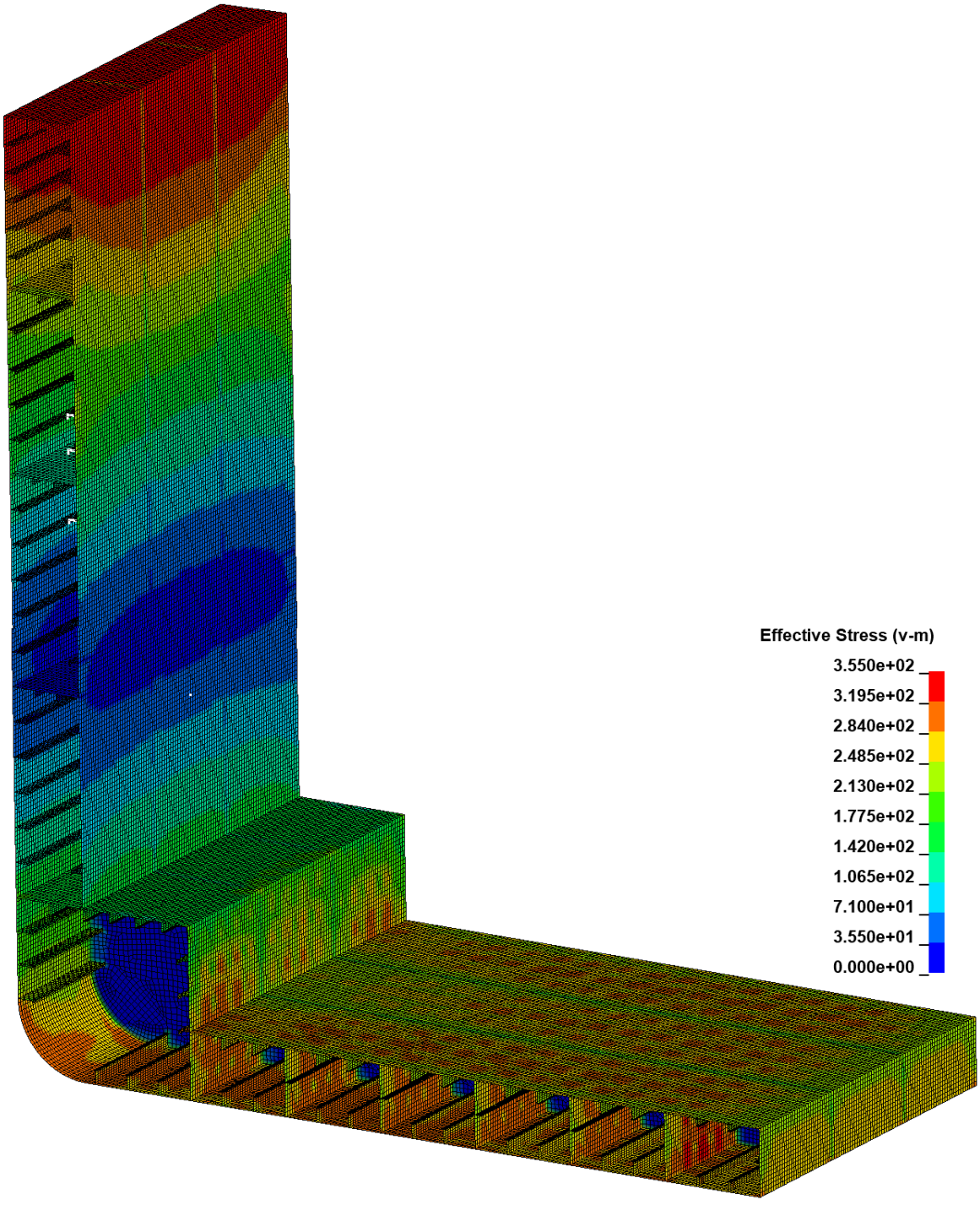

Fig 2. 16 Von Mises stress distribution of shell model at t = 6.4 sec

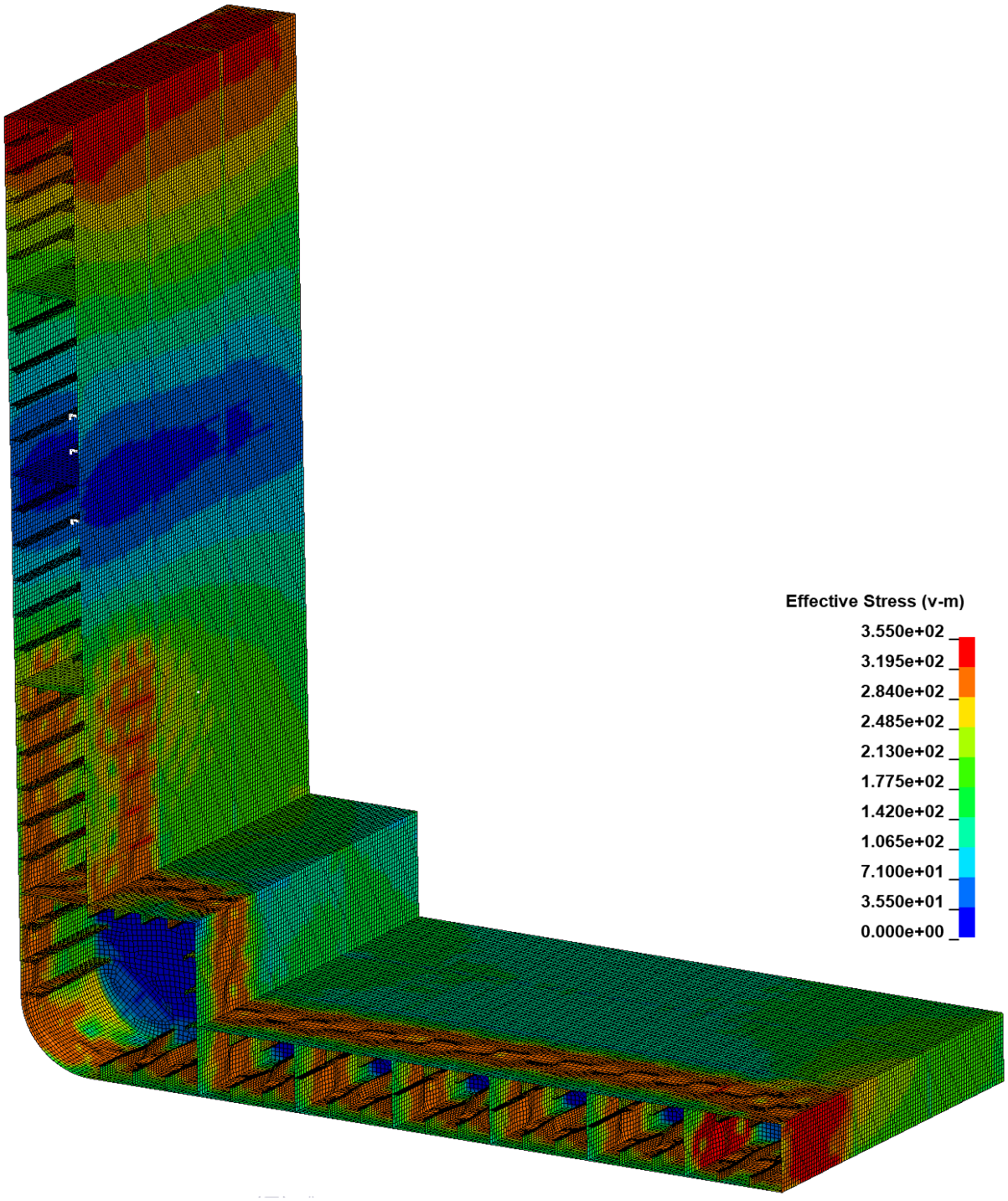

Fig 2. 17 Von Mises stress distribution of shell model at the end of analysis, t = 8.17 sec

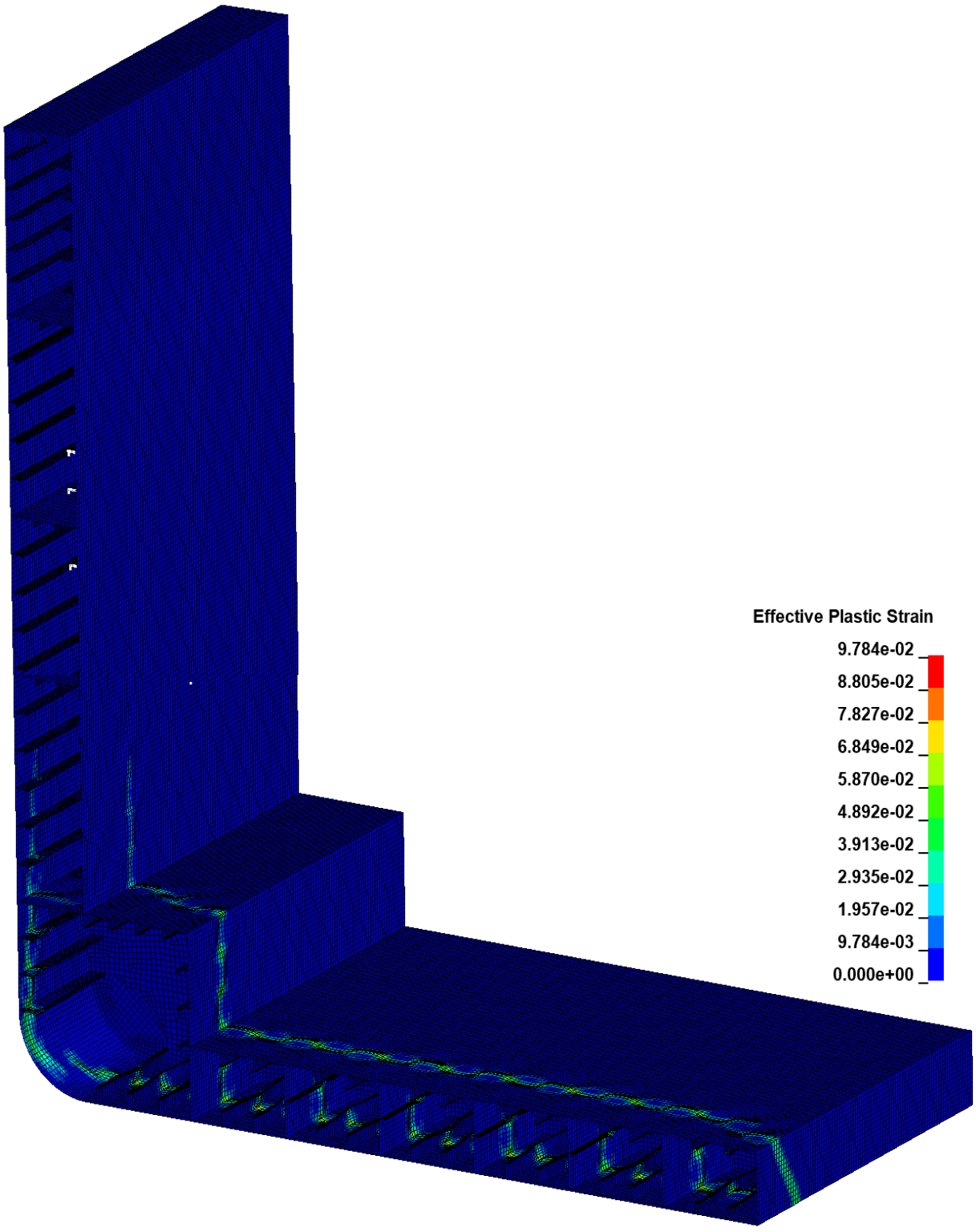

Fig 2. 18 Plastic strain distribution at the end of analysis, t = 8.17 sec

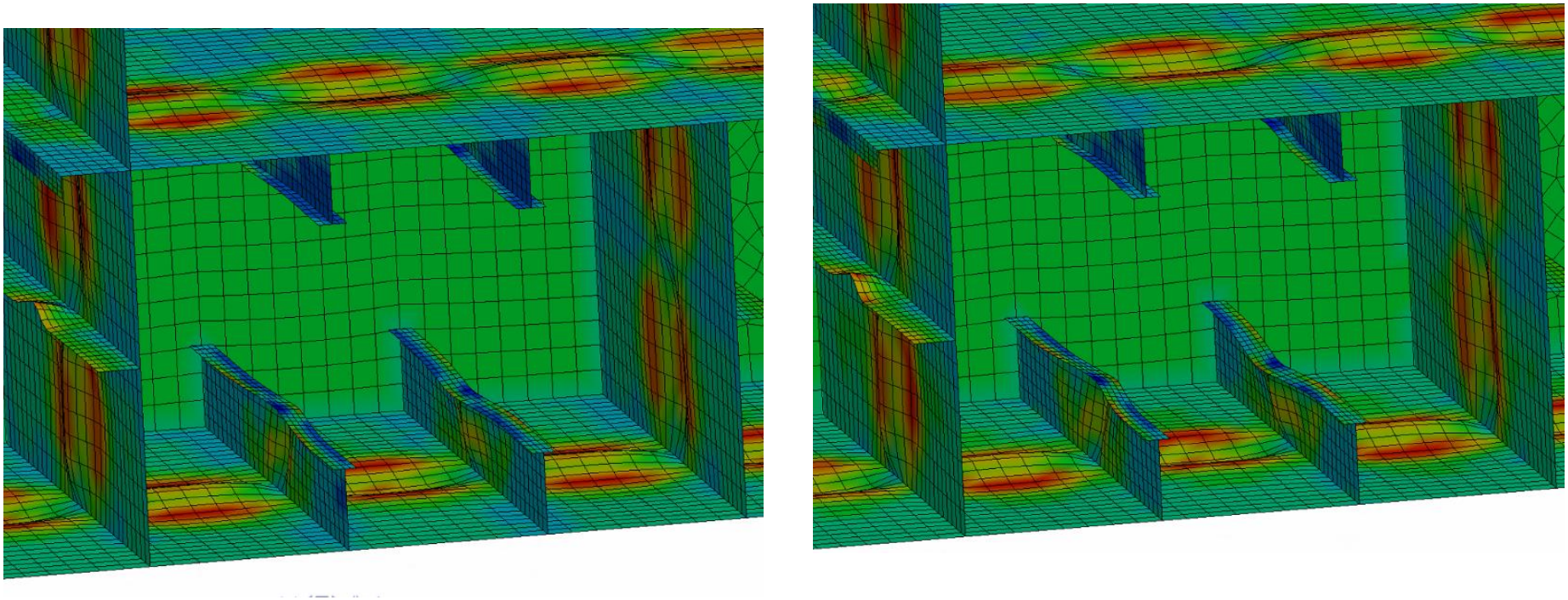

(a) 7 sec

(b) 7.5 sec

Fig 2. 19 Collapse mode of bottom stiffened panels

In Fig 2. 20, results obtained by both FE-smith method and NFEM are compared. Ultimate hogging strength obtained by each analysis are summarized in Table 2.2. From Fig 2. 20, differences can be found in

1. Elastic stiffness
2. Maximum hogging moment
3. Load carrying capacity after the ultimate strength.

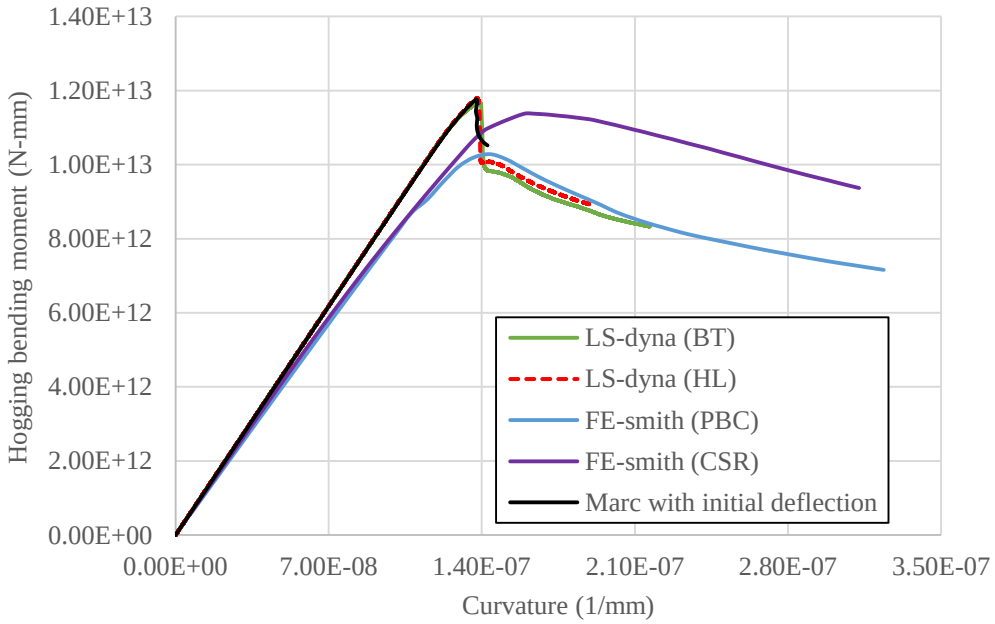

Fig 2. 20 Comparison of static analysis results

Table 2. 2 Ultimate hogging bending moment of cross section obtained by FE-smith method and NFEM

Case	Ultimate Hogging BM (N-mm)
FE-smith (PBC)	1.0760E+13
FE-smith (CSR)	1.1364E+13
LS-dyna (Belytscho-tsay)	1.1668E+13
LS-dyna (Hughes-Liu)	1.1789E+13
Msc.Marc (Implicit)	1.1764E+13

Firstly, difference in load carrying capacity is explained. In case of FE analysis, one edge frame is collapsed among three frames. The resulting localization of plastic deformation and the elastic unloading in the rest parts cause the rapid load reduction capacity just after the ultimate strength. But FE-smith method considered those 3 frames as one beam element and localization does not be happen. That is why load carrying capacity of FE-smith method is smoother and there is no rapid load reduction like NFEM.

It is clear that the difference of the maximum hogging moment and elastic stiffness is because of the difference of average stress- average strain relationship of structural members. Here, the effect of average stress-average strain relationship of structural members is explained by plate buckling mode of CSR equation which is described by Eq (2.17).

$$\sigma_{CR} = min\begin{Bmatrix} \emptyset R_{eHP} \\ \emptyset R_{eHP}\left[\left(\frac{2.25}{\beta_E} - \frac{1.25}{\beta_E^2}\right)\right] \end{Bmatrix} \quad \text{Eq (2.17)}$$

where $\beta_E = 10^3 \frac{s}{t}\sqrt{\frac{\varepsilon R_{eHP}}{E}}$

It can be seen that slenderness ratio β_E is assumed as a function of average strain ε in CSR equation. Such assumption of empirical formula could not estimate the accurate stiffness. Also the assumption of Smith method, 'Interaction with adjacent elements are not considered', influences on the effect of Poisson's ratio which leads to the underestimate of the stiffness.

From the view point of NFEA, the stiffness can be overestimated because of the assigned boundary condition in NFEA model. Since the rigid body constraint is applied at the edges of the shell model, the model is over-constraint which influences on the Poisson's effect, leading to the increase of stiffness. And collapse of edge frame occurred due to over-constraint as described in the previous section. Therefore, not only the FE-smith underestimates the stiffness but also NFEA overestimates the stiffness. One thing to be noted is that effect of Poisson's ratio is dominant here because of the model extent of the NFEA. Since the three frames shell model is adopted with rigid body constraint,

effect of Poisson`s ratio is larger compared to the full length shell model with transverse bulkhead.

Then difference in elastic slope is investigated by modifying the boundary condition. Rather than tying all dofs, FE analysis is done by tying certain dofs as shown in Fig 2. 21.

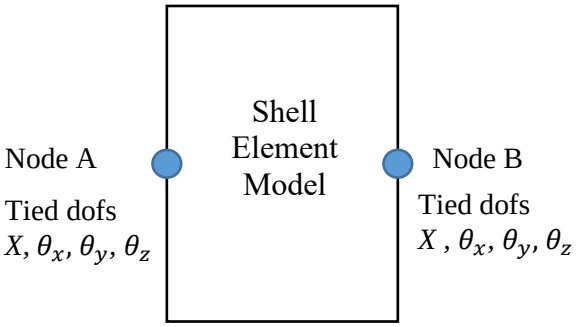

Fig 2. 21 Modified boundary condition for midship shell model

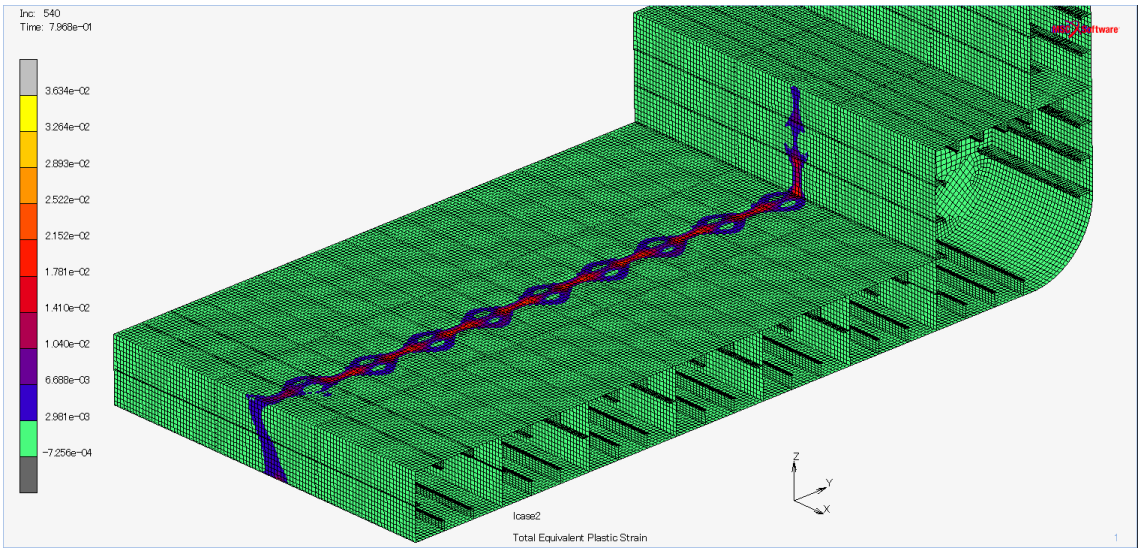

Fig 2. 22 Collapse of mid-frame by modified boundary condition

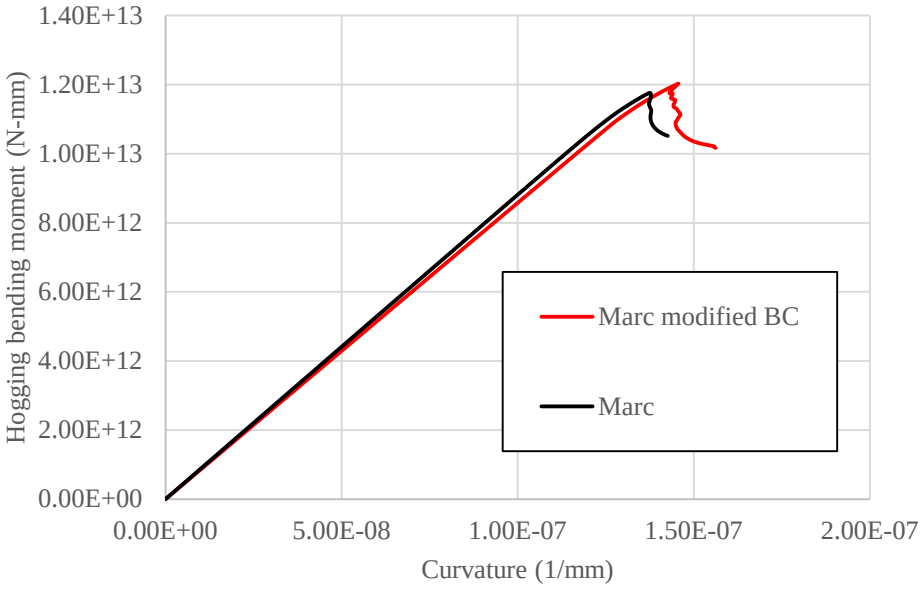

Fig 2. 23 Bending moment and curvature for midship part

If we analyzed again by using the modified boundary condition, mid-frame collapse can be found as shown in Fig 2. 22. Fig 2. 23 compared the modified boundary condition and previous obtained result. Elastic stiffness is slightly reduced and ultimate bending moment is increased to the value of 1.203E+13 N-mm. Detailed collapse mode is same as the result with tying all dofs. Further improvement is necessary with regard to the accuracy of FE-smith method compared to NFEM. However, it is found that essential collapse behavior can be well captured by FE-smith.

The CPU time required for the FE-Smith method was 2.74 min, while that for Msc.Marc, LS-dyna (BT) and LS-dyna (HL) are 19.4 hours, 30 hours and 38.22 hours respectively.

2.7 Conclusions

A simplified method of the progressive collapse analysis of hull girder cross section has been proposed by incorporating the Smith method with the conventional beam finite element, and named FE-smith method. The theory and methodology of the FE-

smith method has been described and its effectiveness has been discussed through a comparison with implicit and explicit NFEM analyses. Conclusions can be drawn as in the following:

1. FE-smith method likely gives a smaller elastic stiffness than the NFEM because of the assumed average-stress average strain relationship of Gordo-Soares formula and of the assumption of the Smith method that the interaction between the elements is not considered.
2. The rigid body boundary condition applied in the NFEM analyses overestimates the elastic stiffness. This is also the reason for FE-smith gives smaller elastic stiffness.
3. FE-smith (CSR) gives the larger ultimate strength and smoother load reduction compared to the FE-smith (PBC) that can considers the effect of localization of plastic deformation in the post-ultimate regime.
4. Though there are rooms for improvement, it has been confirmed that FE-smith can capture the essential collapse behavior of ship hull girder cross section with reasonable accuracy and quite in shorter time.

Chapter 3

Hydro-elastoplastic Beam Model

3.1 Introduction

Ultimate hull girder strength can be obtained from the peak point of moment-curvature curve. However, beyond the ultimate strength, hull girder capacity becomes decrease and unbalanced force between external force and capacity is compensated by the inertia force which leads to the dynamic behavior. Also fluid-structure interaction is inevitable in hull girder collapse. Such non-linear collapse behavior with the effect of plasticity, inertia force and fluid-structure interaction is called hydro-elastoplastic response.

In this chapter, the FE-smith method is extended to the hydro-elastoplastic analysis method. To consider the hydrodynamic forces, hydrodynamic coefficients are calculated by 2D Boundary Element Method (BEM). Structural mass, added mass and hydrodynamic damping force are assumed to be uniformly distributed over an element length. These coefficients are introduced into the corresponding matrix of equation of motions. Regarding static restoring force effect, spring elements are considered and the hull girder model is mounted on the springs. As a fundamental case, the dynamic collapse analysis of uniform beam (box shaped model) is performed using the FE-smith method.

3.2 Hydro-elastoplastic analysis

Equation of motion at time t+Δt is defined as

$$[M]\{\ddot{u}\}^{t+\Delta t} + [C]\{\dot{u}\}^{t+\Delta t} + [K]\{u\}^{t+\Delta t} + \{Q\}^{t+\Delta t} = \{F\}^{t+\Delta t} \qquad \text{Eq (3.1)}$$

where,

$[M]$ = mass matrix

$[C]$ = damping matrix

$[K]$ = stiffness matrix

$\{Q\}$ = internal force vector

$\{F\}$ = external force vector

Each term of Eq (3.1) and consideration of hydro-elastoplastic behavior are explained in the following sections.

3.2.1 Mass matrix and damping matrix

Mass matrix, $[M]$ is the sum of fluid added mass matrix $[M_a]$ and structural mass matrix $[M_s]$. Damping matrix $[C]$ is also represented by the sum of fluid damping matrix $[C_a]$ and structural damping matrix $[C_s]$.

For structural damping, Rayleigh damping is assumed. Here, coefficient of stiffness matrix a_1 is assumed to be zero and a_0 is determined by taking the damping ratio of 2% with respect to the 2-node natural frequency.

$$[C_s] = a_0[M] + a_1[K] \quad \text{Eq (3.2)}$$

$$a_0 = 2\xi\omega_0 \quad \text{Eq (3.3)}$$

ω_0 is calculated from the Eigen value analysis in which wave added mass and static restoring spring are considered.

Structural mass matrix $[M_s]$ is derived by considering the distributed mass over the element as shown in Fig 3. 1. The inertia force per unit length q_z is obtained by

$$q_z = -\rho A_s \cdot \ddot{u} \quad \text{Eq (3.4)}$$

$$\ddot{u} = [A]\{\ddot{u}\} \quad \text{Eq (3.5)}$$

where ρ = density, A_s = the cross-sectional area, $\ddot{u}$ = the acceleration and $\{\ddot{u}\}$ = the nodal acceleration vector.

The principle of virtual work can be represented as

$$\{\delta u\}^T \{F_n\} + \int_L \delta u_z \cdot q_z dx = \int_V \delta\varepsilon_x \cdot \sigma_x dV \quad \text{Eq (3.6)}$$

in which $\int_V \delta\varepsilon_x \cdot \sigma_x dV = \{\delta u\}^T [K]\{u\}$

Using Eq (3.4) and Eq (3.5), Eq (3.6) can be transformed into the form of

$$\{\delta u\}^T \{F_n\} - \int_L [A]\{\delta u\} \cdot \rho A_s [A]\{\ddot{u}\} dx = \{\delta u\}^T [K]\{u\}$$

$$\{F_n\} - \int_L [A]^T \cdot \rho A_s [A]\{\ddot{u}\} dx = [K]\{u\}$$

$$\int_L [A]^T \cdot \rho A_s [A]\{\ddot{u}\} dx + [K]\{u\} = \{F_n\}$$

$$[M_s]\{\ddot{u}\} + [K]\{u\} = \{F_n\} \qquad \text{Eq (3.7)}$$

Structural mass matrix $[M_s]$ can be represented as the following expression.

$$[M_s] = \int_L [A]^T \rho A_s [A] dx \qquad \text{Eq (3.8)}$$

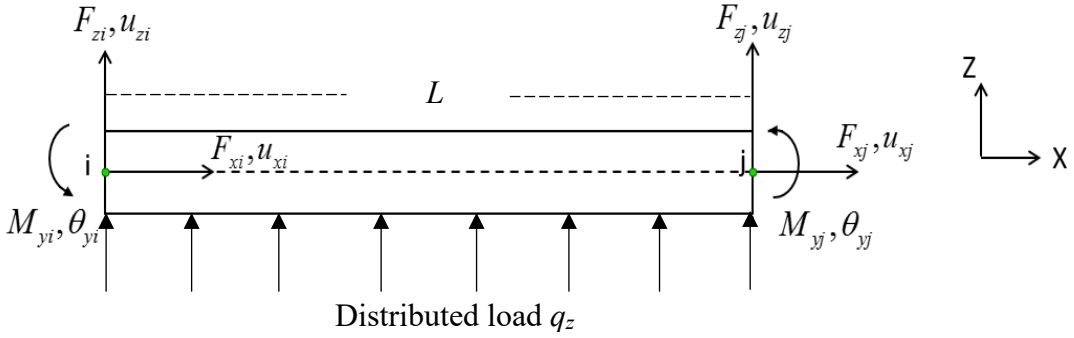

Fig 3. 1 Distributed load on beam element

3.2.2 Stiffness matrix

Stiffness matrix $[K]$ also comprises the fluid part $[K_r]$ and structural stiffness part $[K_{ep}]$. The structural stiffness matrix is given in the form of Eq. (2.12) replacing the Young's modulus *E* with the elastoplastic tangential stiffness given by the Smith method. $[K_{ep}]$ represents the nonlinear structural behavior.

$[K_r]$ is the static buoyancy force along the ship hull girder and can be represented by linear spring element. Here, it is modelled as concentrated spring as shown in Fig 3. 2.

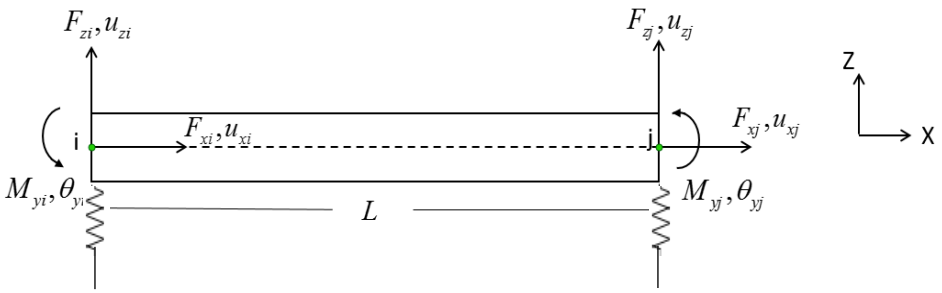

Fig 3. 2 Restoring stiffness spring

In that case, restoring matrix and spring coefficient is defined by the following equations.

$$[K_r] = \frac{kL}{2}\begin{bmatrix} 0 & 0 & 0 & 0 & 0 & 0 \\ 0 & 0 & 0 & 0 & 0 & 0 \\ 0 & 0 & 1 & 0 & 0 & 0 \\ 0 & 0 & 0 & 0 & 0 & 0 \\ 0 & 0 & 0 & 0 & 0 & 0 \\ 0 & 0 & 0 & 0 & 0 & 1 \end{bmatrix} \quad \text{Eq (3.9)}$$

$$k = \rho_{sea} g B_w \quad \text{Eq (3.10)}$$

3.2.3 Hydrodynamic coefficients

Strip method is adopted to consider the hydrodynamic force. In the strip method, submerged part of hull form is cut into two-dimensional strip. Each cross section of ship hull girder is regarded as 2D- strip and the added mass and wave damping forces which contribute to the equation of motion, Eq. (3.1) are calculated from 2D potential theory. Here, the hydrodynamic coefficients for cross section are calculated by 2D Boundary Element (free-surface Green function) Method.

To find the hydrodynamic coefficients of submerged part of cross-sections, flow around the free surface is described by using the linear velocity potential. Nonlinearity due to cross-sectional geometries and nonlinear wave particle motions are not considered. The velocity potential is a scalar function which comes from the assumption that motion

of the fluid is irrotational (ie. vorticity is zero). Velocity potential for the plane progressive wave can be represented by

$$\boldsymbol{\Phi} = Re\left[\phi(x,y)e^{i\omega t}\right] \quad \text{Eq (3.11)}$$

Velocity potential is composed of incident-wave, scattering and radiation potentials and can be described by

$$\phi(x) = \frac{g\eta}{i\omega}\{\varphi_0(x) + \varphi_4(x)\} + \sum_{j=1}^{3} i\omega X_j \varphi_j(x) \quad \text{Eq (3.12)}$$

where $\varphi_j(x)$ represents the flow induced by the jth motion of the body and it can be found by considering that velocity of the fluid is equal to the velocity in the normal direction of the body surface.

$$\varphi \frac{\partial \varphi_j}{\partial n} = n_j \quad \text{Eq (3.13)}$$

Pressure on the hull surface can be calculated from the velocity potentials by the linear theory. Radiation pressure can be written by the following equation.

$$P_R(x) = -\rho i\omega \sum_{j=1}^{3} i\omega X_j \varphi_j(x) \quad \text{Eq (3.14)}$$

Added mass and damping coefficient can be obtained by integrating the radiation pressure at the source points which are located at the integrated mesh panels of the wetted section. Non-dimensional form of added mass and damping coefficient defined for half-breadth can be found

$$A'_{ij} - iB'_{ij} = \frac{A_{ij}}{\rho_{sea} B^2 \gamma_i \gamma_j} - i\frac{B_{ij}}{\rho_{sea} B^2 \gamma_i \gamma_j} = -\int_{S_H} \varphi_j(x,y) n_i dS \quad \text{Eq (3.15)}$$

B = half breadth of cross section

γ_j = 1 for j = 1, 2 (sway, heave) and γ_j = B for j = 3 (roll)

In this study, only added mass and damping in heave direction are adopted.

3.3 Solution Procedures

Implicit time integration scheme using Newmark-β method is used. Newton-Raphson method is adopted for numerical iterations.

3.3.1 Newmark β method

Newmark β method is based on the linear acceleration method. The expression of the velocity and acceleration is

$$\dot{x}(t+\Delta t) = \dot{x}(t) + \Delta t\left[(1-\gamma)\ddot{x}(t) + \gamma\ddot{x}(t+\Delta t)\right] \quad \text{Eq (3.16)}$$

$$x(t+\Delta t) = x(t) + \Delta t\,\dot{x}(t) + \Delta t^2\left[(\tfrac{1}{2}-\beta)\ddot{x}(t) + \beta\ddot{x}(t+\Delta t)\right] \quad \text{Eq (3.17)}$$

Equation of motion at future time $t+\Delta t$ is expressed as

$$M\ddot{x}(t+\Delta t) + C\dot{x}(t+\Delta t) + Kx(t+\Delta t) = F(t+\Delta t) \quad \text{Eq (3.18)}$$

Incremental form of equation of motion can be written as

$$M\ddot{x}(t+\Delta t) + C\dot{x}(t+\Delta t) + Kx(\Delta t) = F(t+\Delta t) - Kx(t) \quad \text{Eq (3.19)}$$

To solve the Eq (2.35) as one unknown variable form, $\ddot{x}(t+\Delta t)$ and $\dot{x}(t+\Delta t)$ are represented by $x(t+\Delta t)$. By using Eq (2.32) and Eq (2.33),

$$\dot{x}(t+\Delta t) = \frac{\gamma}{\beta\Delta t}x(\Delta t) + \left(1-\frac{\gamma}{\beta}\right)\dot{x}(t) + \Delta t\left(1-\frac{\gamma}{2\beta}\right)\ddot{x}(t) \quad \text{Eq (3.20)}$$

$$\ddot{x}(t+\Delta t) = \frac{1}{\beta}\left\{\frac{1}{\Delta t^2}x(\Delta t) - \frac{1}{\Delta t}\dot{x}(t) - \left(\frac{1}{2}-\beta\right)\ddot{x}(t)\right\} \quad \text{Eq (3.21)}$$

From Eq (3.20) and Eq (3.21), incremental form of $x(\Delta t)$ is obtained as

$$x(\Delta t) = \Delta t\,\dot{x}(t) + \Delta t^2\left[\left(\frac{1}{2}-\beta\right)\ddot{x}(t) + \beta\ddot{x}(t+\Delta t)\right] \quad \text{Eq (3.22)}$$

By substituting above equations in eq(3.1), equation of motion can be solved in the form of

$$\left(\frac{1}{\beta\Delta t^2}M + \frac{\gamma}{\beta\Delta t}C + K\right)x(\Delta t) =$$
$$F(t+\Delta t) - Kx(t) + \frac{1}{\beta}M\left\{\frac{x(t)}{\Delta t} + \left(\frac{1}{2}-\beta\right)\ddot{x}(t)\right\} - C\left\{\left(1-\frac{\gamma}{\beta}\right)\dot{x}(t) + \Delta t\left(1-\frac{\gamma}{2\beta}\right)\ddot{x}(t)\right\}$$

Eq (3.23)

γ and β value is taken as 0.5 and 0.25. In this case, Newmark β method is un-conditionally stable.

3.3.2 Return mapping algorithm

In the Smith method, the nonlinear average stress-average strain relationship is considered for stiffened panel elements in the cross section, including the reduction of their post-ultimate strength capacity. In the FE-smith method, such average stress-average strain relationships are transformed to the average stress-average plastic strain relationships as was shown in Fig 2. 4, and the nonlinear material behavior is regarded as a pseudo strain-hardening/softening behavior. In such elastoplastic response analyses, accurate and robust numerical procedures that can deal with the nonlinear stress-strain responses accompanied by elastic unloading behavior is needed.

In this study, elastoplastic problem mentioned above is numerically solved by elastic predictor-plastic corrector algorithm, which is so-called return mapping method. In the case of 1-dimensional problem, the following equation should be solved with respect to incremental plastic multiplier (= absolute value of incremental plastic strain) $\Delta\gamma$;

$$\left|\sigma_{n+1}^{trial}\right| - E\Delta\gamma - \sigma_y\left(\bar{\varepsilon}_n^p + \Delta\gamma\right) = 0 \qquad \text{Eq (3.24)}$$

where σ_{n+1}^{trial} and $\sigma_y\left(\bar{\varepsilon}_n^p + \Delta\gamma\right)$ are trial elastic stress and yield surface at n+1$^{\text{th}}$ step, respectively. $\bar{\varepsilon}_n^p$ denotes the equivalent plastic strain (= absolute value of axial plastic strain). Eq (3.24) means that the elastically-predicted stress σ_{n+1}^{trial} is returned back to the yield surface by the corrector $E\Delta\gamma$ as shown in Fig 3.3. When σ_y is linear function with respect to plastic strain i.e. it follows linear hardening law, $\Delta\gamma$ can be analytically derived. In this study, Newton-Raphson method is adopted to solve Eq (3.24) since the stress-plastic strain curve is nonlinear to represent buckling behavior of structural elements according to Smith's method. More detail of the return mapping algorithm can be found in [30] and [31].

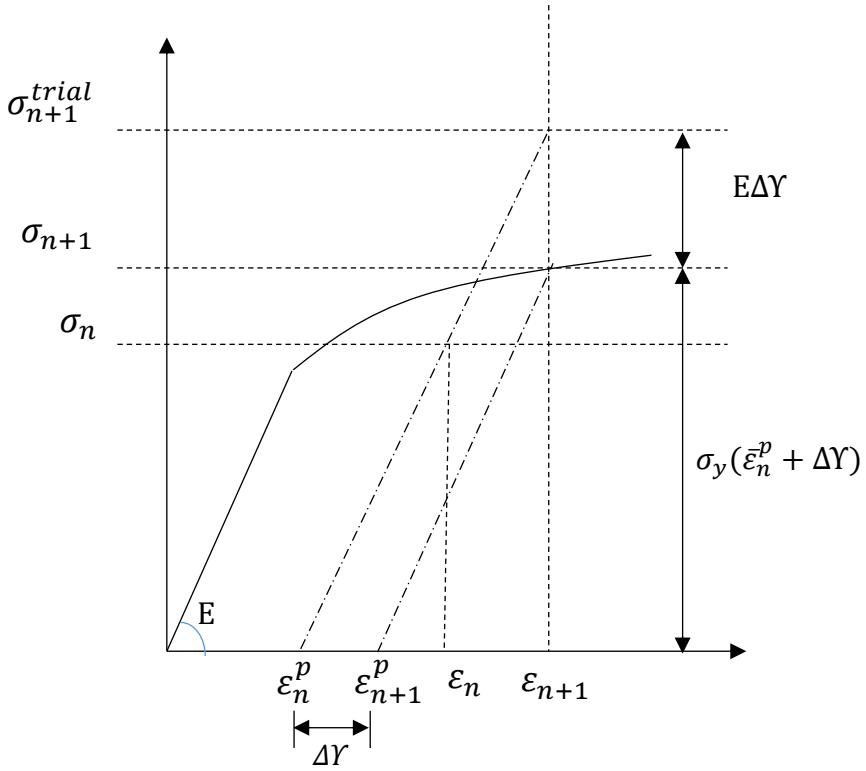

Fig 3. 3 Return mapping algorithm

3.4 Collapse behavior of uniform beam model

In this section, dynamic collapse analysis is performed by FE-smith method. As a fundamental study, a uniform beam having the cross section of Fig 2. 6 is considered. The model is equally divided into 29 beam elements and hydrostatic restoring springs are attached at each node to represent the hydrostatic restoring effect. Principal dimension and material properties of the analysis model can be found in Table 3.1.

Table 3. 1 Principal dimension of hull girder

Length	L	278 m
Breadth	B	39.8 m
Depth	D	23.6 m
Draft	d	13 m

Container ship usually in the hogging condition in stillwater condition because of a fine hull form and container cargos loaded over the full length. So, the hogging collapse is considered in this study, and the distributed loads as shown in Fig.3.5 are applied to the hull girder. Clearly, there is no pitching and heaving motion in this model. Then time history of load applied at each node is shown in Fig 3. 6.

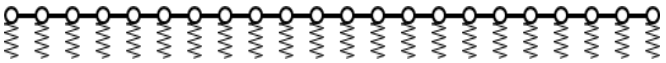

Fig 3. 4 Elasto-plastic beam model

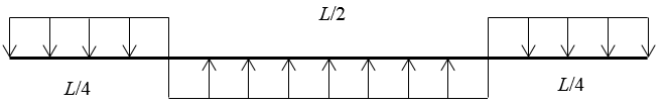

Fig 3. 5 Applied distributed load pattern

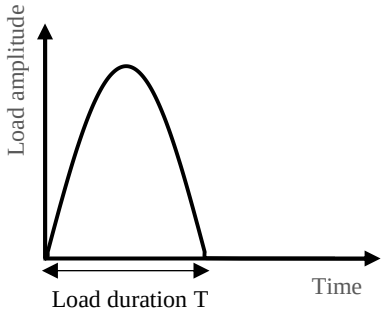

Fig 3. 6 Sinusoidal half wave

Added mass and damping coefficient are calculated assuming a regular wave condition having the period of two times load duration. Relationship between hydrodynamic coefficients and wave frequency for cross section are shown in Fig 3. 7.

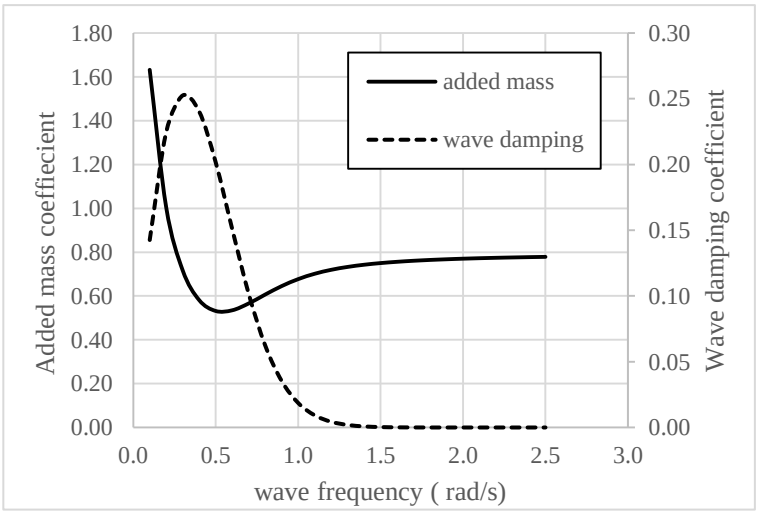

Fig 3. 7 Added mass and wave damping coefficient of cross section in heave direction

3.4.1 Elastic analysis

As the first step of collapse analysis, elastic analysis is performed. Time history of unit magnitude applied load for different load duration cases are shown in Fig 3. 8 and obtained elastic bending moment are shown in Fig 3. 9.

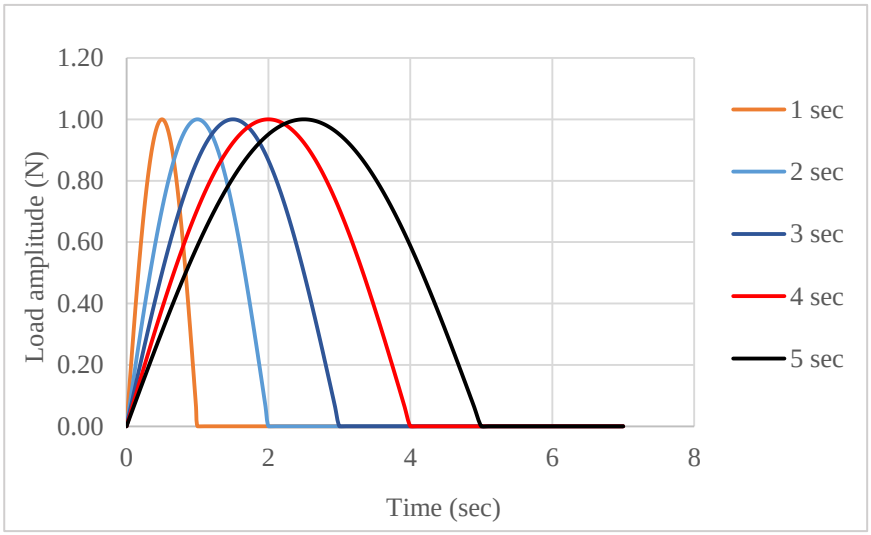

Fig 3. 8 Time history of applied load at node 15 for dynamic elastic analyses

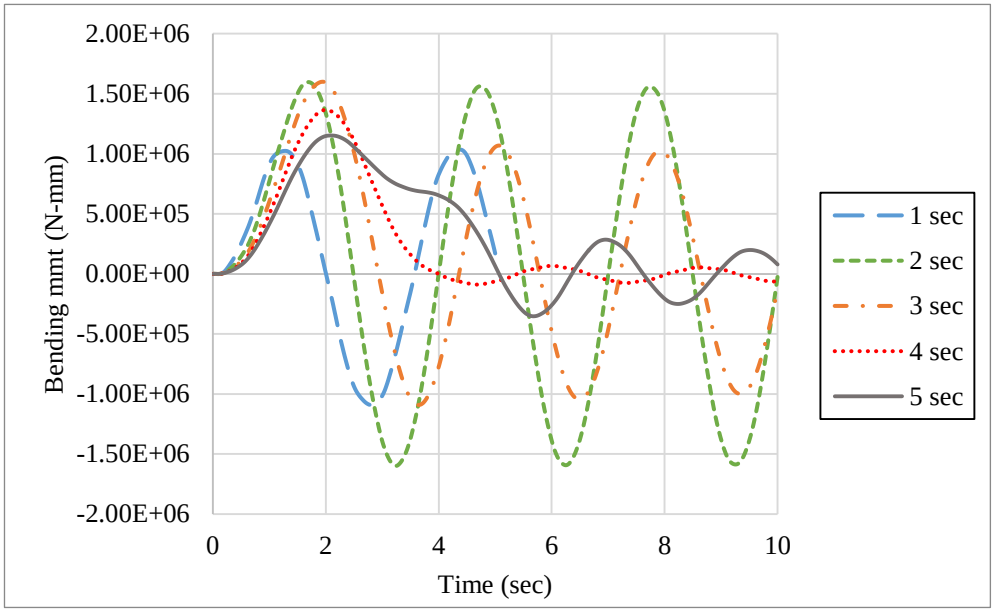

Fig 3. 9 Time history of bending moment at midship obtained by dynamic elastic analyses

3.4.2 Collapse analysis

To analyze the collapsed behavior, the magnitude of externally applied load is determined so that hull girder is subjected to the internal bending moment that is 7% larger than ultimate bending strength of the hull girder. Based on the elastic hogging bending moment obtained from elastic dynamic analysis, the applied load amplitude for collapse analysis of different load duration cases are summarized in Fig 3. 10 and Table 3.2. It can be found that load amplitude of FE-smith (PBC) cases are smaller than FE-smith (CSR) as the ultimate hogging bending moment of FE-smith (PBC) is smaller than FE-smith (CSR).

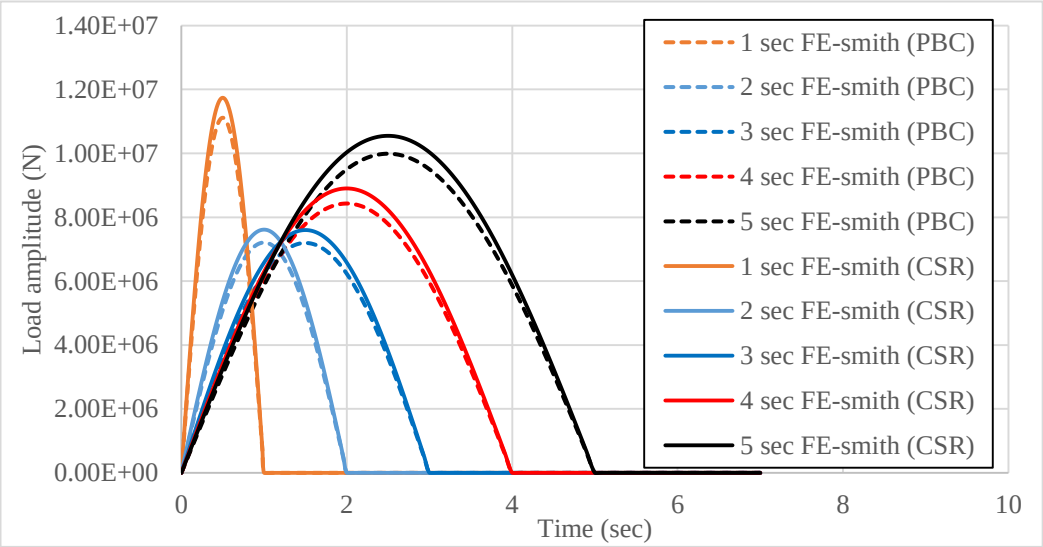

Fig 3. 10 Time history of applied load at node 15 for uniform beam model dynamic collapse analyses

Table 3. 2 Applied load amplitude at node 15 for uniform beam model collapse analysis

Case	Target moment	Load Amplitude x10^6 (N)						
		1 sec	2 sec	2.5 sec	3 sec	3.5 sec	4 sec	5 sec
PBC	1.151E+13	11.11	7.207	7.059	7.195	7.691	8.429	9.988
CSR	1.216E+13	11.74	7.612	7.455	7.599	8.122	8.901	10.55

3.4.3 Results and discussion of FE-smith

Bending moment-curvature relationship of midship obtained by FE-smith (CSR) for different load duration cases are compared in Fig 3. 11 and time history of curvature is shown in Fig 3. 12.

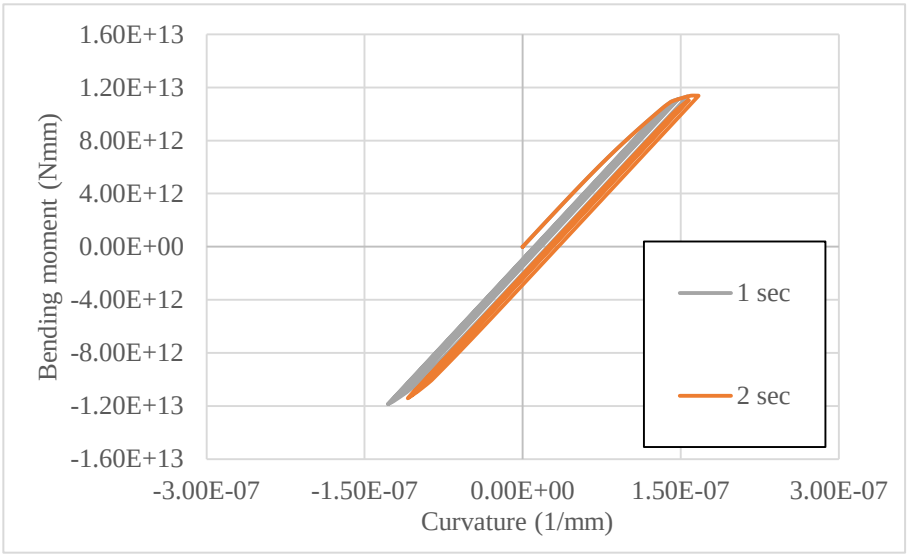

(a) Small structural damage cases

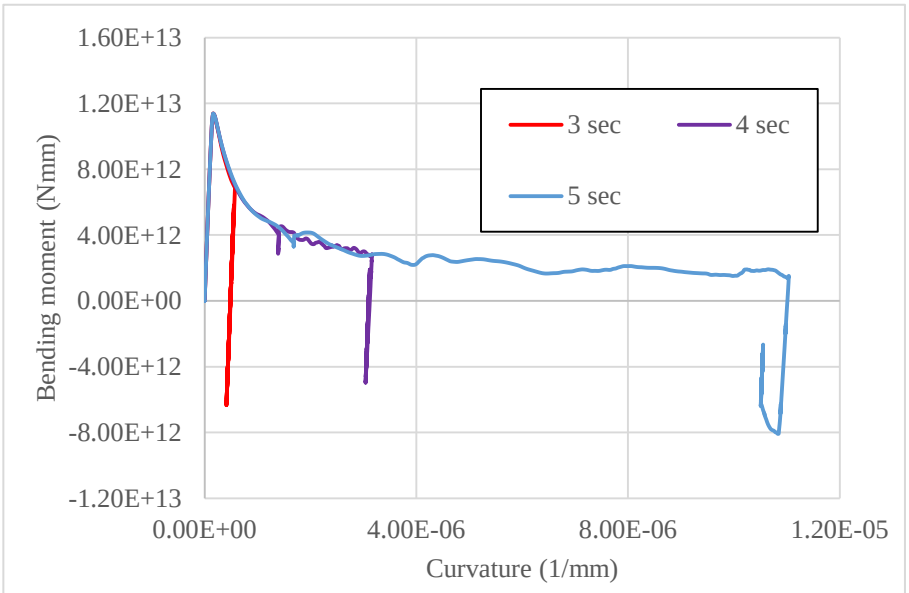

(b) Collapse cases

Fig 3. 11 Bending moment-curvature relationship of midship obtained by FE-smith (CSR)

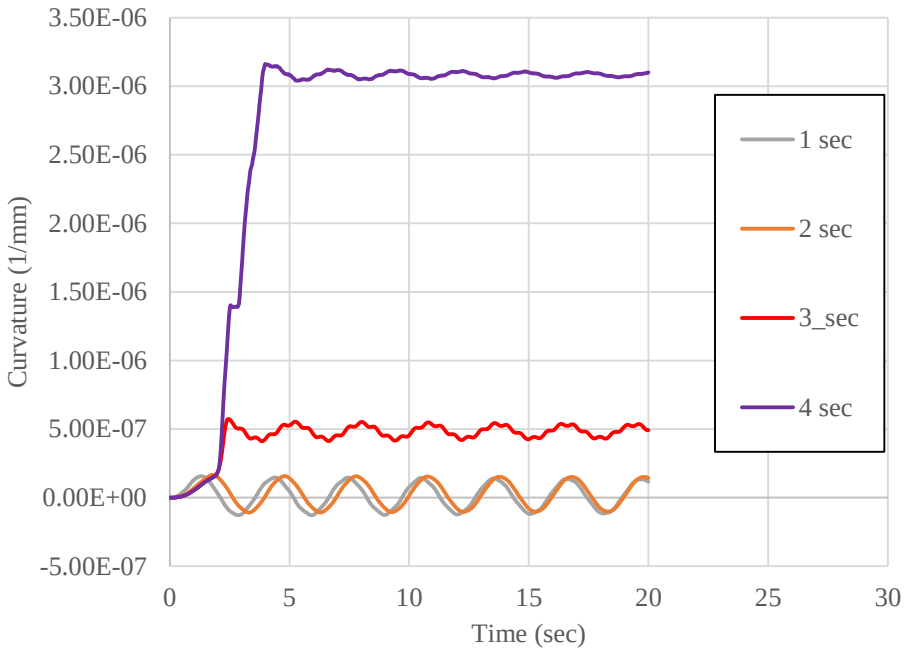

(a) 1 sec to 4 sec load duration

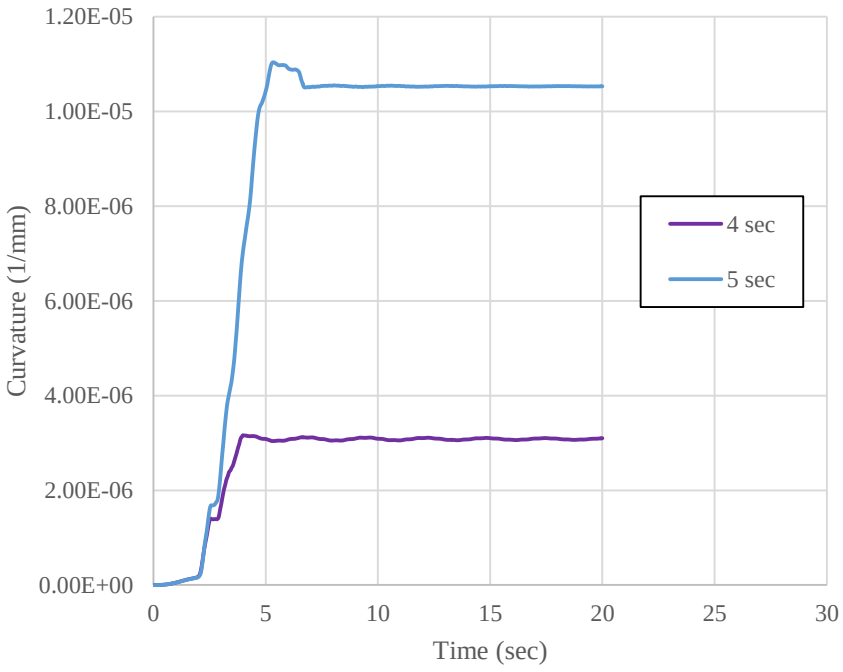

(b) 4 sec and 5 sec load duration

Fig 3. 12 Time history of curvature of midship by FE-smith (CSR)

From the comparison, it can be seen that the longer the load duration, the larger the collapse deformation. During the collapse, we can see that fluctuation as shown in Fig 3. 11 (b) which are result of structural vibration. In case of short load duration, the repeated loading and unloading behavior can be seen as shown in Fig 3. 11(a). Even though, ultimate hull girder strength is not attained in short load duration case, the structure is partially damaged. This kind of repeated load weaken the structure which may can lead to the fatigue failure. Fig 3. 13 and Fig 3. 14 show the results obtained by FE-smith (PBC). Same as FE-smith (CSR), the longer the load duration, the larger the collapse extent. But 2 sec and 5 sec case have different behavior compared to other load duration cases.

There are two loading and unloading behaviors in 2 sec case shown in Fig 3. 13(a). After the first unloading, collapse was extended again rather than having the same collapse extend and vibrate. In 5 sec case, collapse occurred in the sagging condition again. This behavior obtained by FE-smith analyses are discussed in Chapter 4.

Bending moment-curvature relationship for all different load duration cases of FE-smith (CSR) and FE-smith (PBC) are compared in Fig 3. 15. In all the cases, collapse extent obtained by FE-smith (PBC) is larger than those by FE-smith (CSR). The discrepancy between collapse extent is getting smaller for larger load duration. This is because of the rate of load reduction capacity of each element and larger strain region of average stress-average strain relationship in PBC and CSR as shown in Appendix B.

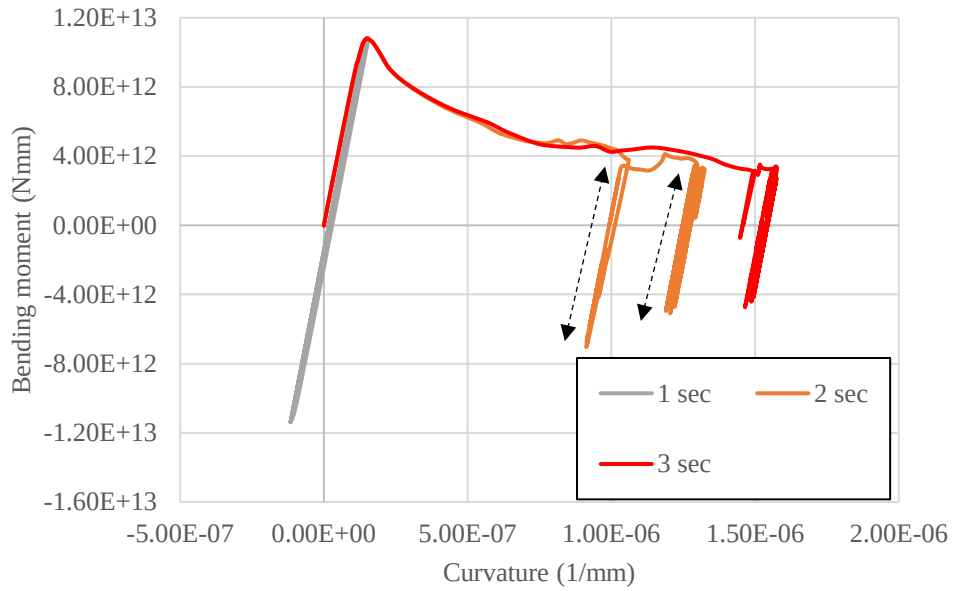

(a) Shorter load duration cases

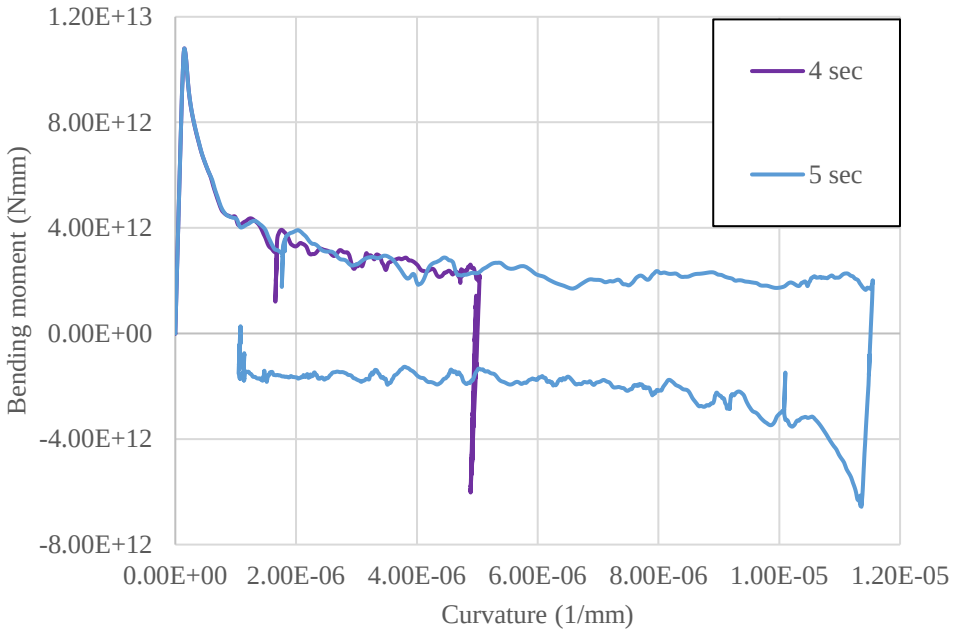

(b) Longer load duration cases

Fig 3. 13 Bending moment-curvature relationship of midship obtained by FE-smith (PBC)

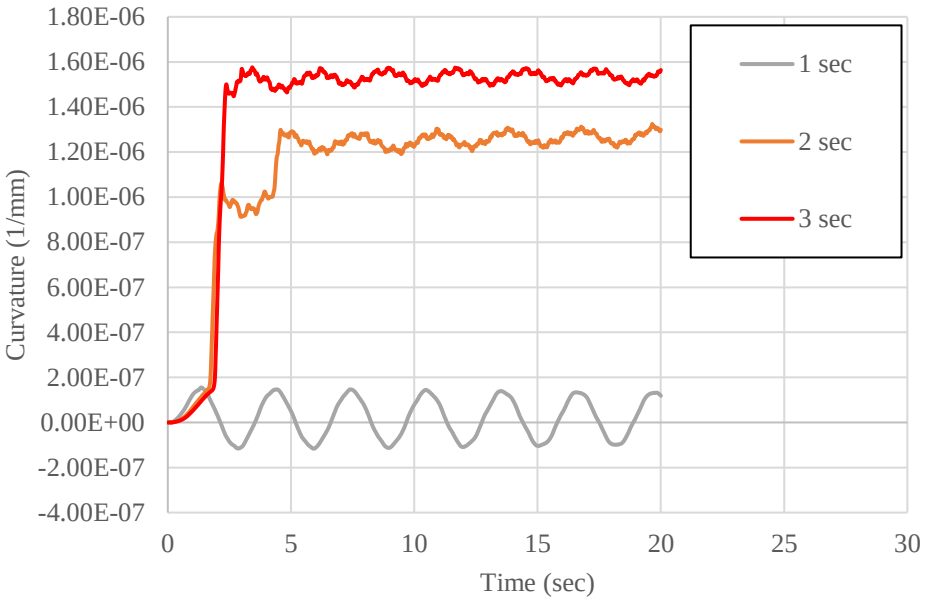

(a) 1 sec to 3 sec load duration

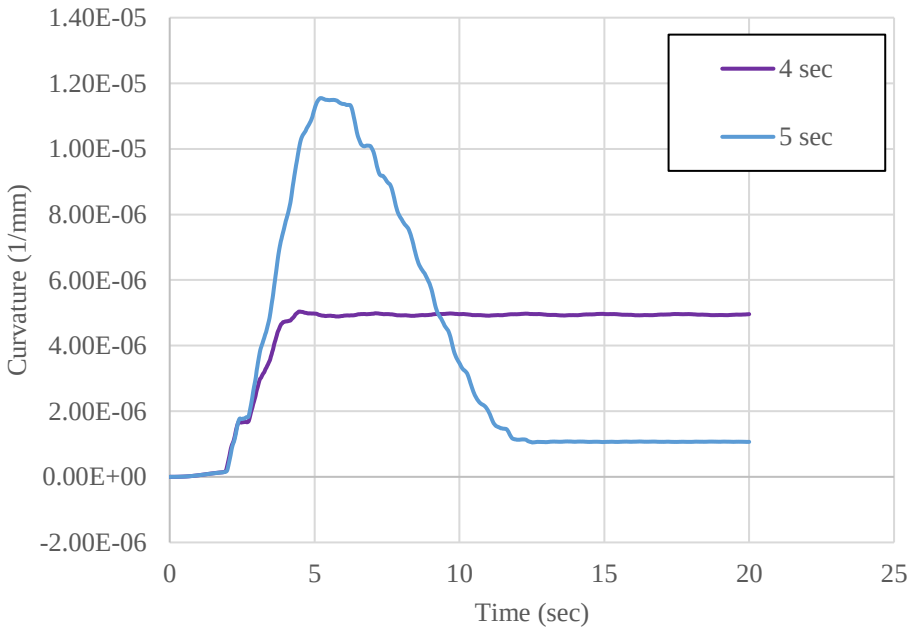

(b) 4 sec and 5 sec load duration

Fig 3. 14 Time history of curvature at midship obtained by FE-smith (PBC) analyses

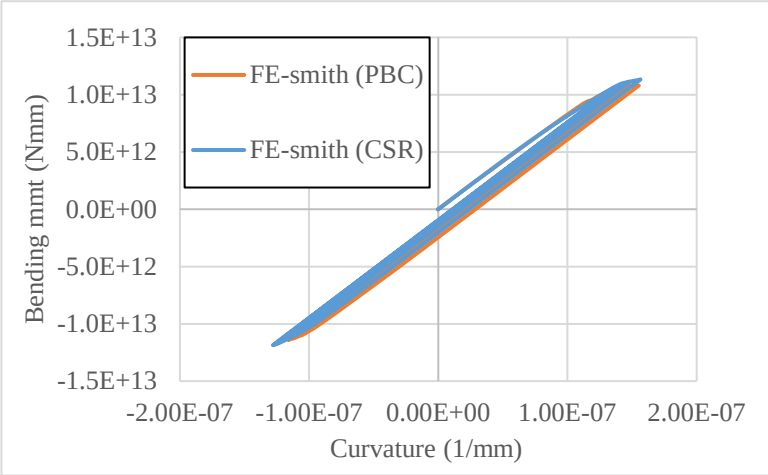

(a) 1 sec load duration

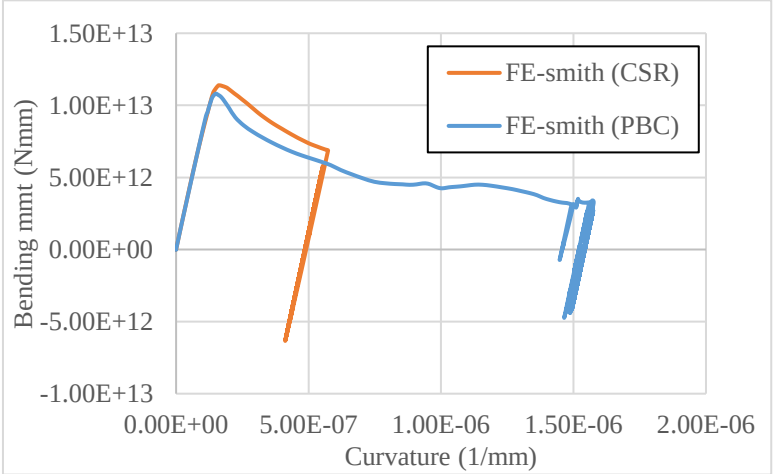

(c) 3 sec load duration

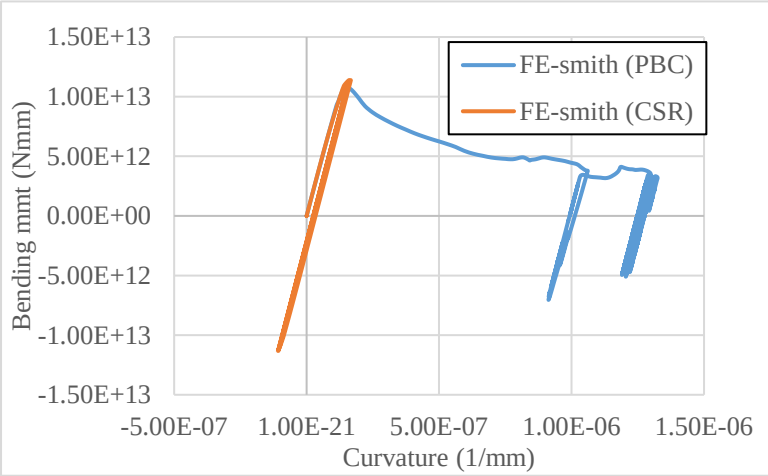

(b) 2 sec load duration

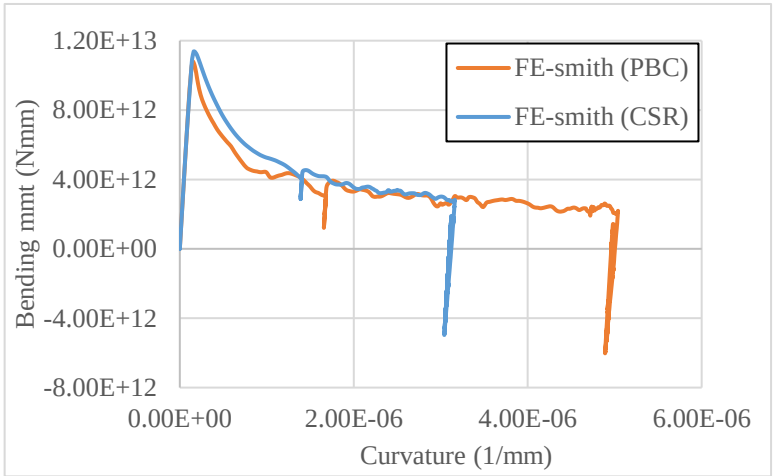

(d) 4 sec load duration

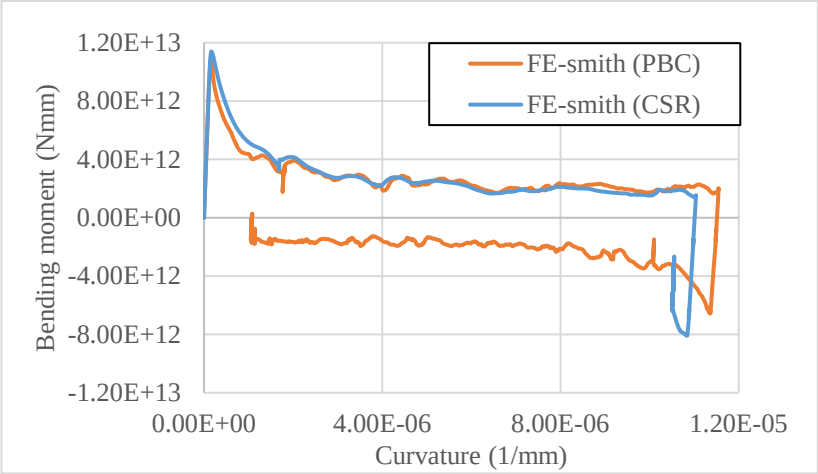

(e) 5 sec load duration

Fig 3. 15 Comparison between bending moment-curvature relationship obtained by FE-smith (PBC) and FE-smith (CSR)

3.7 Conclusions

Time domain collapse analysis of ship hull girder including the consideration of fluid-structure interaction, non-linear structural behavior is developed by coupling the Smith method and conventional finite beam element. Series of analysis are performed by using two types of stress-strain curves and impulsive bending loads with different load duration are applied. Fundamental capability of the FE-smith method is investigated by box-shaped model and it can be concluded that

1. Reasonable collapse behavior of hull girder can be obtained by FE-smith method using simplified beam element.
2. The longer the load duration, the larger the collapse extent of hull girder.
3. Shorter load duration has smaller structural damage. It means short load duration like slamming will have small structural damage.

The validation of the proposed model is made through a comparison with NFEA in Chapter 4.

Chapter 4

Hydro-elastoplastic Analysis of a Ship Hull Girder

4.1 Introduction

In this chapter, a more realistic hull girder shape is adopted to perform the FE-smith analysis. 5250 TEU container ship is used as the analysis model. Also in NFEM, analysis of more precise model is carried out for the comparison purpose. Not only a realistic hull girder shape but also the uniform beam model is analyzed by NFEM including a comparison with the result obtained in Chapter 3. Purpose of the comparison is to understand the degree of accuracy and capability of FE-smith method.

For hull girder model, load distributions are adopted as close as possible to the real ship and initial stillwater load condition is considered. As a fundamental study, assumed external load distribution is applied in an impulsive manner instead of real wave load. Collapse behavior of hull girder obtained by FE-smith (PBC) and FE-smith (CSR) are described. NFEM analysis is performed by using combined 3D shell and beam finite element model, and both global and local collapse behavior are explained in detail. If FE-smith results are compared with NFEA, there must be differences between them as FE-smith a simplified method under the certain assumption. Three different load duration cases are analyzed and compared. Through these analyses, collapse behavior of hull girder and the applicability of FE-smith are discussed.

4.2 Model for analysis

5250 TEU container ship model is regarded as a target analysis model. Offset sections, properties of each section and their corresponding beam elements are shown in Fig 4. 1.

Beam properties	
Beam Elem	Section
1	9
2	9
3	9
4	9
5	8
6	8
7	8
8	7
9	6
10	6
11	5
12	5
13	5
14	5
15	5
16	5
17	4
18	4
19	3
20	2
21	2
22	2
23	2
24	2
25	1
26	1
27	1
28	1
29	1

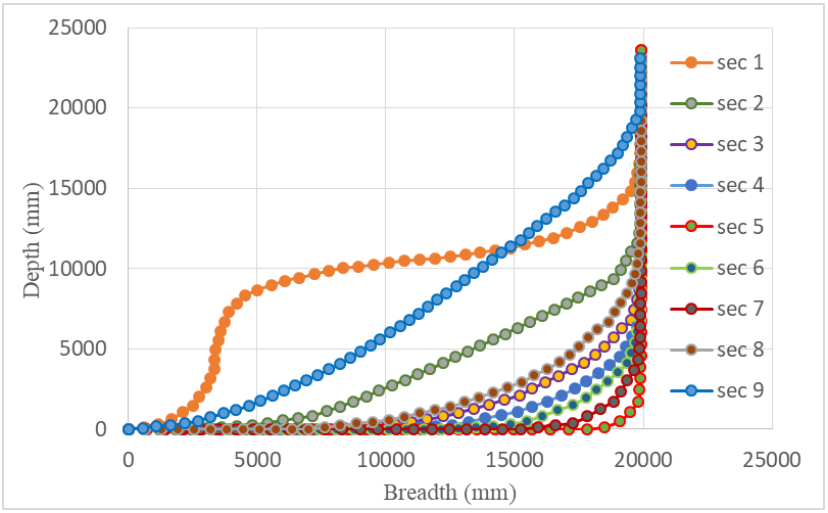

Section properties (unit in millimeter)				
sec id	Ixx	Iyy	Area	CGz
1	1.2047E+14	6.4690E+14	3.1610E+06	13552.09
2	3.2127E+14	1.1511E+15	5.1115E+06	11883.64
3	3.8545E+14	1.2215E+15	4.8578E+06	10924.48
4	3.8587E+14	1.2637E+15	4.8505E+06	10778.93
5	4.1442E+14	1.3230E+15	4.9904E+06	10106.36
6	4.0124E+14	1.3384E+15	5.0291E+06	10565.75
7	3.6914E+14	1.1530E+15	4.7040E+06	10963.70
8	3.2099E+14	1.0897E+15	4.6406E+06	11835.96
9	2.3049E+14	8.2095E+14	4.0244E+06	12712.08

Fig 4. 1 Cross-sections' properties and element division

Container ship is generally in the hogging condition in stillwater. In fact, stillwater loading must be considered to understand the actual collapse behavior. Dead load distribution and buoyancy distribution are employed from the provided drawing data and its bending moment distribution are shown in Fig 4. 2. For collapse case, location of

midship section from provided data is around 119400 mm from FP (Ship's stern). So, beam element 13 is the expected collapse section.

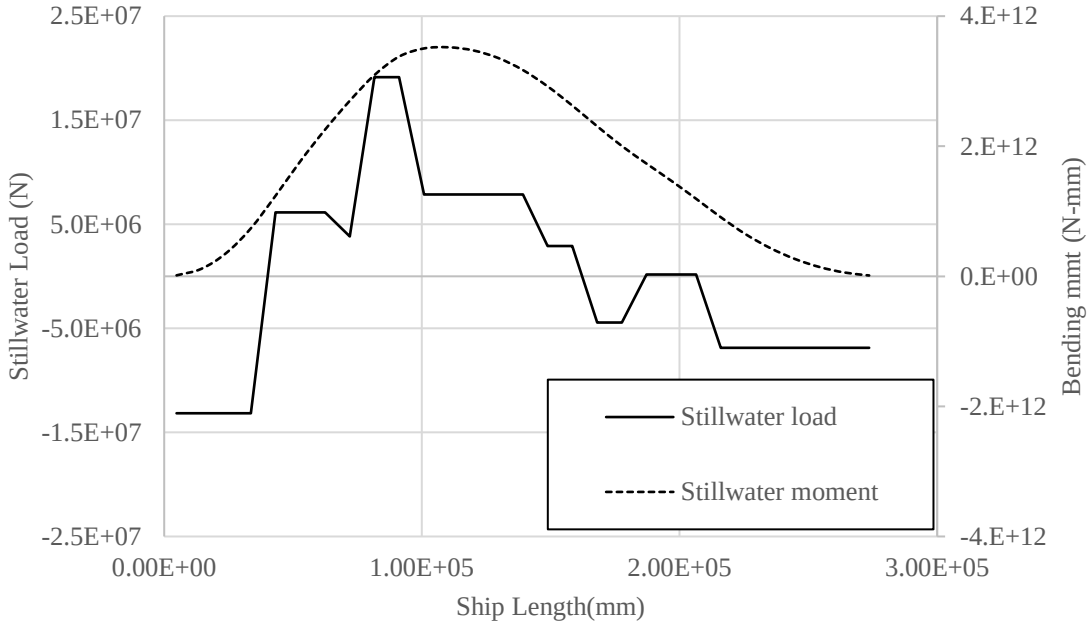

Fig 4. 2 Stillwater load and its moment distribution along the ship hull girder

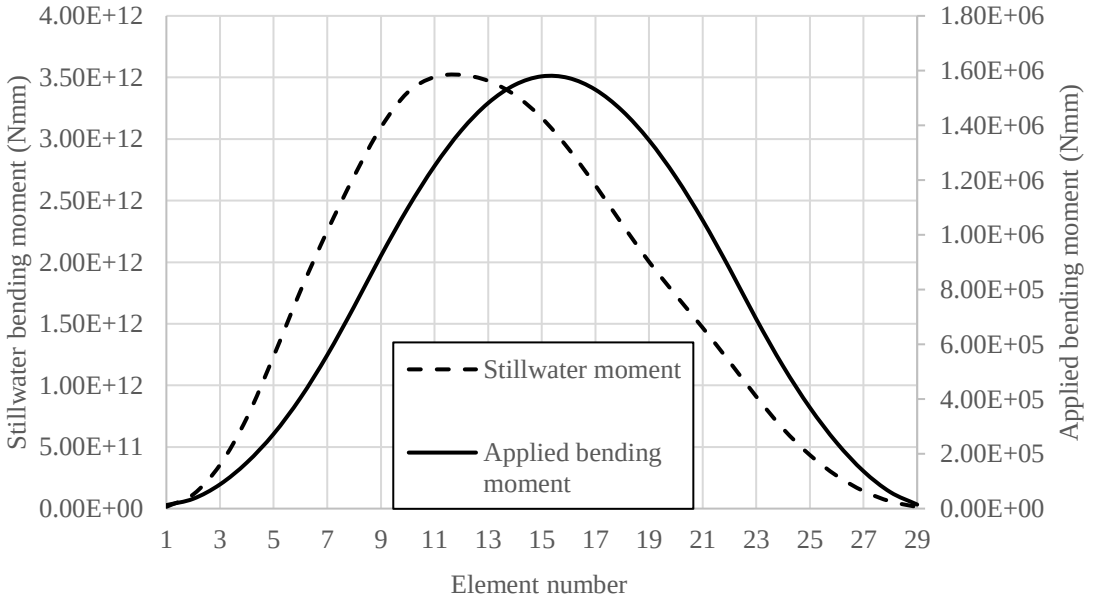

Fig 4. 3 Moment contributions on hull girder by applied load and stillwater load

In case of external hogging moment, load is applied in the same way as uniform beam model. Since container ship model is adopted, applying the same distributed load pattern as uniform beam model might be contradictory. But the reasonable results can be obtained which are discussed in later sections. Beam element 14 is collapsed in the analysis which is the adjacent element of expected collapse beam element. This can be happened as only 9 cross-sectional shapes are considered in FE-smith analysis. Although there exists some discrepancy from the real stillwater moment distribution, it can be considered that the load model and modelling is reasonable as shown in Fig 4. 3.

The analysis for stillwater loads is performed by NFEM also for comparison purpose. In case of NFEM model, combined shell and beam model is used as a dynamic analysis model to reduce the computation time. Since the midship part (element 14) is the target region for collapse analysis, only that region is represented by shell element and the other elements are by elastic beam element. Since FE-smith model adopts the 3 frame space length as one beam element, 3 frame space shell elements model is modelled as midship part. Mass elements are located at each beam node to represent the wave added mass. Spring and damper elements are also attached at each node to consider the buoyancy force and wave damping effect as shown in Fig 4. 4.

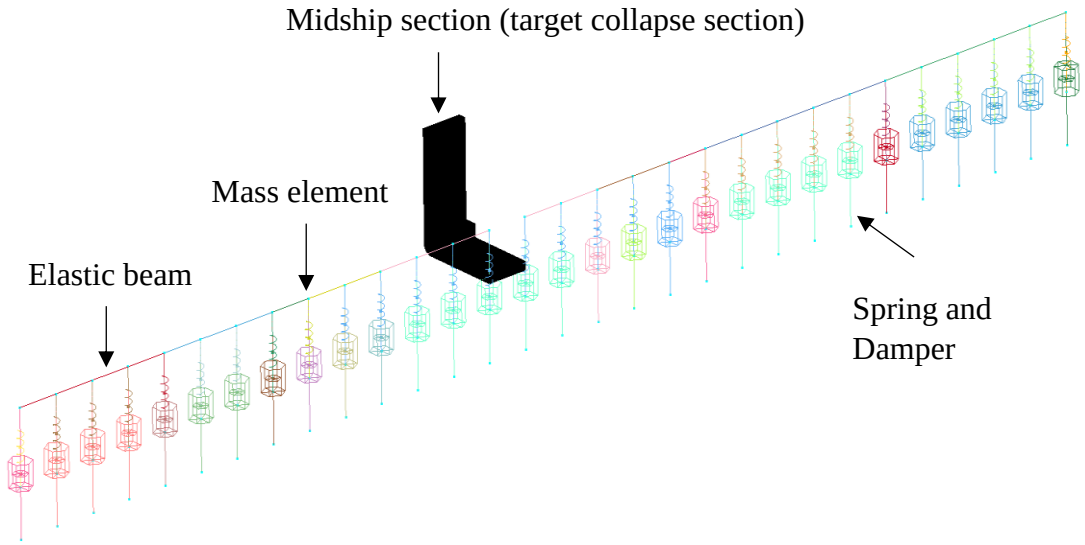

Fig 4. 4 Combined shell and beam FE model

All the ground nodes of spring and damper elements are constrained in all directions. Edges nodes of shell element model is constrained as a rigid cross section (nodal rigid body option for LS-dyna and RBE2 for MSC.Marc) by setting the Node A and Node B as master nodes which are same as static analysis. Node A is fixed in X, θ_x and θ_z and node B is fixed in θ_x and θ_z direction. To satisfy the symmetric condition, all the nodes along the center girder (including the master nodes) are constrained not only in θ_x and θ_z direction but also in Y-direction as described in Fig 4. 5. Elastic beam element nodes are also fixed in Y, θ_x and θ_z direction in the same manner.

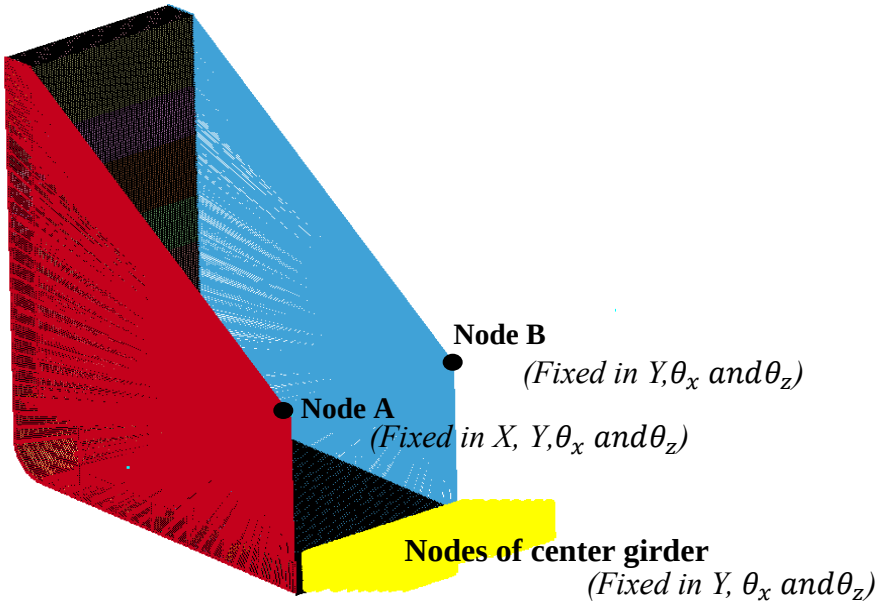

Fig 4. 5 Boundary condition of midship shell element

Table 4. 1 Material properties and element types of LS-dyna model

Model	Material	Element
Shell model	003 : Plastic Kinematic	Hughes-Liu
Beam model	001 : Elastic	Belytschko-Schwer
Spring	S01 : Spring Elastic	Translational spring
Damper	S02 : Damper Viscous	Translational damper
Mass Element	-	-

Mesh size and initial imperfection are as described in section 2.5. Element used for modelling in LS-dyna are described in Table 4.1. Uniform box-shaped model is also analyzed by NFEM to validate the results of Chapter 3. In that case, stillwater loading is not considered.

4.3 Analysis of uniform beam model

In this section, comparison between FE-smith and NFEM analyses for uniform beam model is described. Elastic analysis of NFEA is done by applying the load amplitude of 0.8MN as shown in Fig 4. 6. Here, load duration of 2 sec, 3.5 sec and 5 sec cases are carried out. Applied load distribution pattern is as was shown in Fig 3. 5.

Fig 4. 7 shows the comparison of time history of elastic hogging moment at midship obtained by LS- dyna and FE-smith analyses. Results show the good agreement between them but vibration after loading period shows some difference. This is because of the difference of modelling between them. NFEM adopted the shell element for midship part and beam elements for the rest part. While FE-smith adopted the beam element with ship cross section composed of Smith elements. From the results, we can conclude that modelling and condition of NFEA model is reasonable to perform the dynamic collapse analysis.

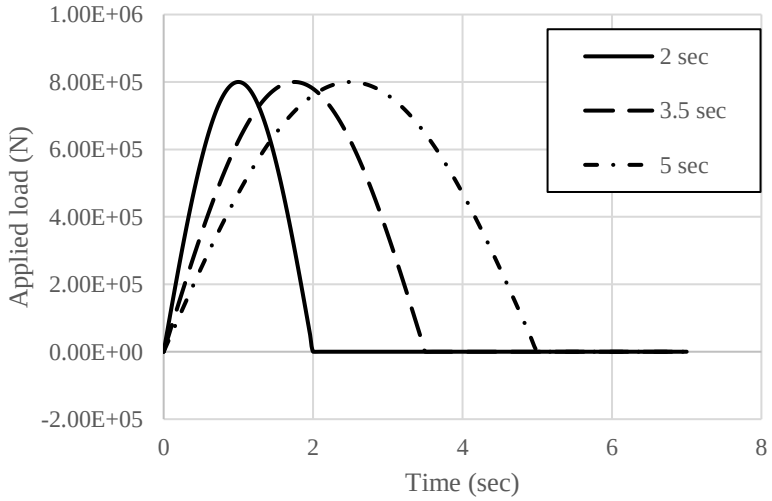

Fig 4. 6 Time history of applied load at node 15 for LS-dyna dynamic elastic analyses of uniform beam model

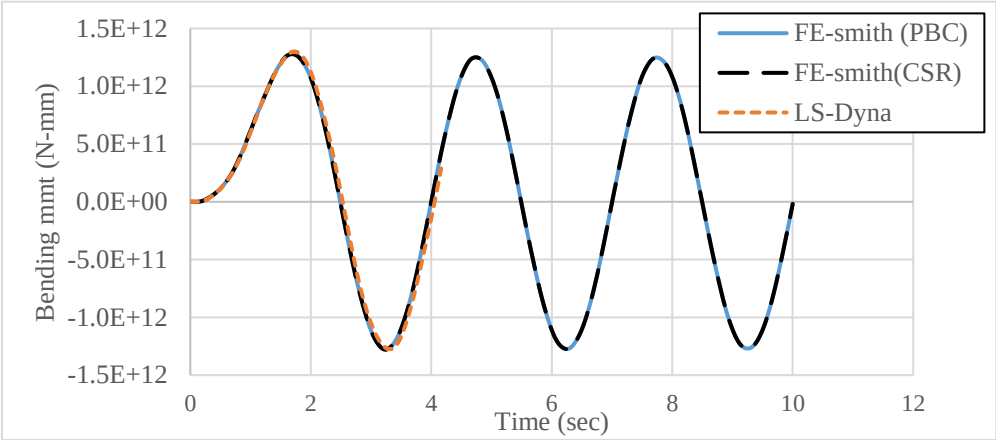

(a) 2 sec load duration

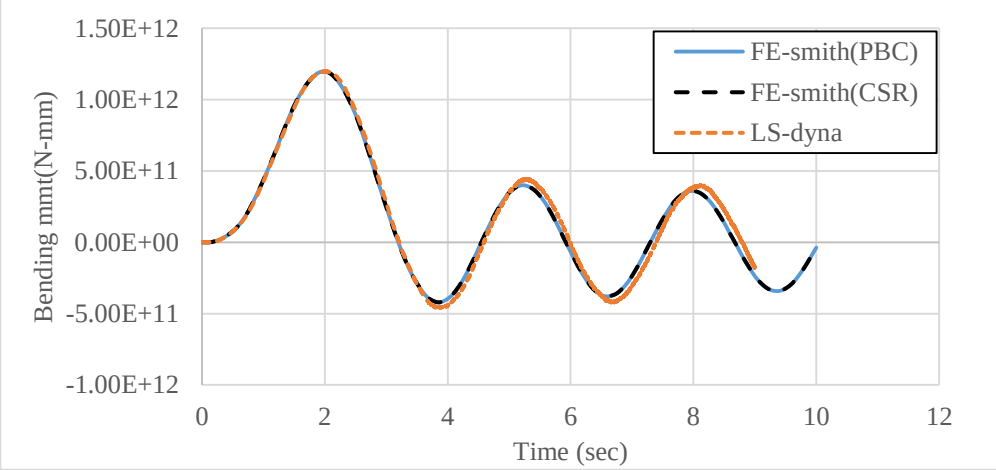

(b) 3.5 sec load duration

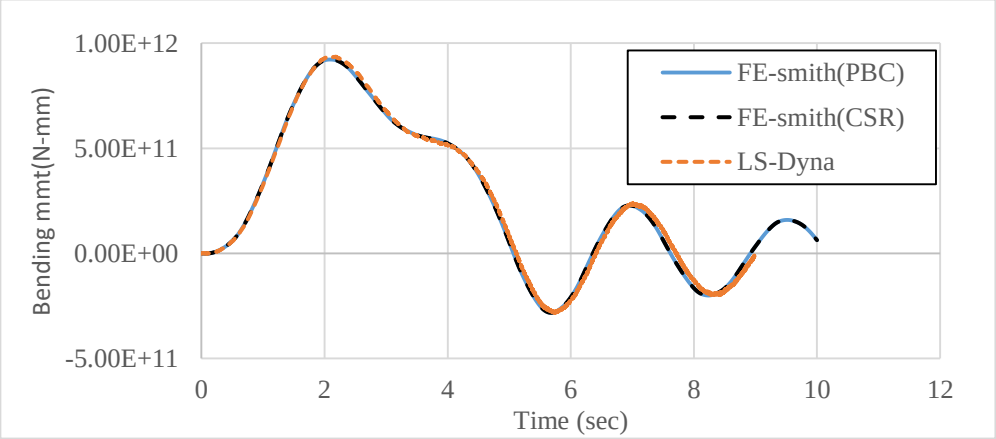

(c) 5 sec load duration

Fig 4. 7 Comparison of time history of elastic hogging moment at midship

Collapse analysis is then performed by applying the load which gives the 7% larger than ultimate hogging bending moment to the hull girder. Time history of applied load for LS-dyna analysis of different load duration cases are drawn in Fig 4. 8.

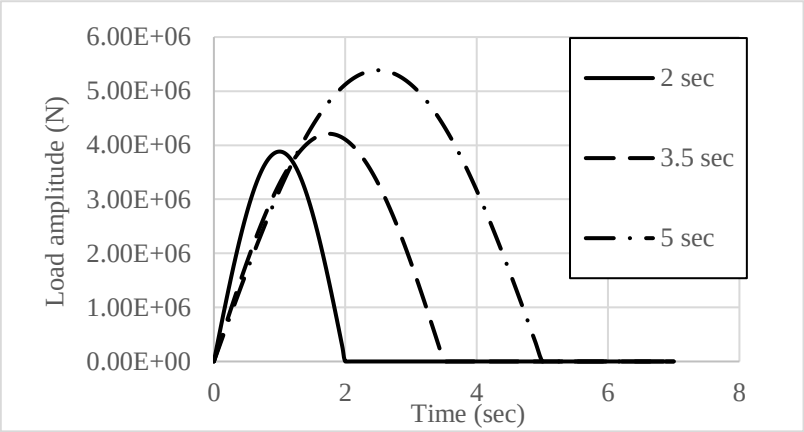

Fig 4. 8 Time history of applied load at node 15 for LS-dyna dynamic collapse analyses

4.3.1 Comparison between FE-smith and NFEA

Discussion is done on the following matters based on the comparison results.

1. Progressive collapse behavior
2. Collapse extent
3. Unloading behavior
4. Behavior in sagging condition after unloading.

Firstly, 3.5 sec load duration case is explained. Both local and global collapse behavior are explained by representative elements of midship cross section as was shown in Fig 2. 6. Collapse mode of selected elements and their collapse sequence are summarized in Table 4. 2. Fig 4. 9 shows the moment-curvature relationship at the collapse element, and the time histories of bending moment and curvature.

Similar to static analysis, plastic strain is initiated at Btm 6. As soon as Btm 6, Btm 5 and Btm 4 of outer bottom shell attained their ultimate strength, hull girder reached to its ultimate strength. Inner bottom cannot give significant additional strength. Plastic strain distribution and stress distribution at ultimate strength is shown in Fig 4. 11 and Fig 4. 11. Then collapse was extended upward and collapse of side shell elements

occurred. Collapse frame is same as the static analysis. All the elements mentioned in Table 4. 2 are collapsed before external hogging moment is zero (i.e. before 3.5 sec).

Table 4. 2 Sequence of collapse and collapse mode of cross section

Collapse sequence	Mode of collapse
Deck	Yielding in tension
Btm 6	Buckling
Btm 5	Buckling
Btm 4	Buckling
Btm 2	Buckling
Intbtm 6	Buckling
Btm 1	Buckling
ISS4_2	Buckling
ISS3_2	Buckling
OSS 6	Buckling
ISS 2_2	Buckling
ISS 1_2	Buckling

Hull girder attained its ultimate hogging moment at 1.74 sec as shown in Fig 4. 9(b). Then load carrying capacity is rapidly decreased with some fluctuation due to the structural vibration. Up to this point, behaviors are similar between FE-smith and LS-dyna. We can see that reduction rate beyond the ultimate strength of each analysis are different. Also if we compare the collapse extent, largest collapse extent is obtained by LS-dyna, second largest one by FE-smith (PBC) and smallest one by FE-smith (CSR). These differences are due to the difference of element average stress-average strain relationship in each analysis as can be seen in Fig 4. 13. The assumption of plane cross section is also another source of uncertainties as found from Fig 4. 12.

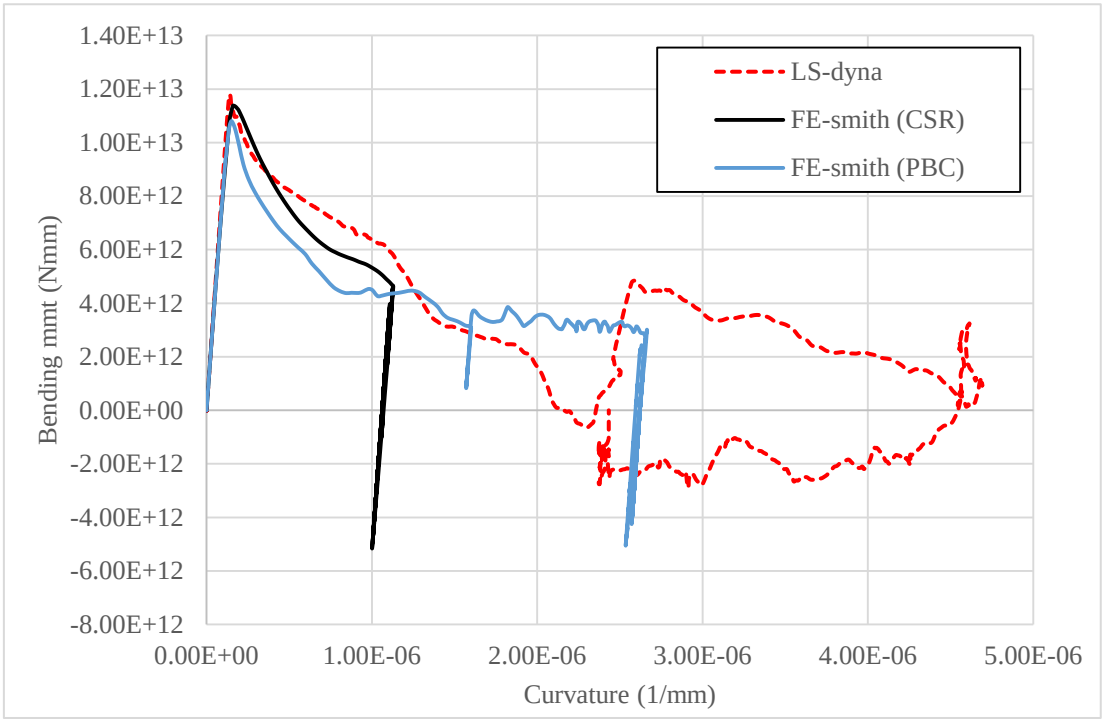

(a) Bending moment and curvature relationship

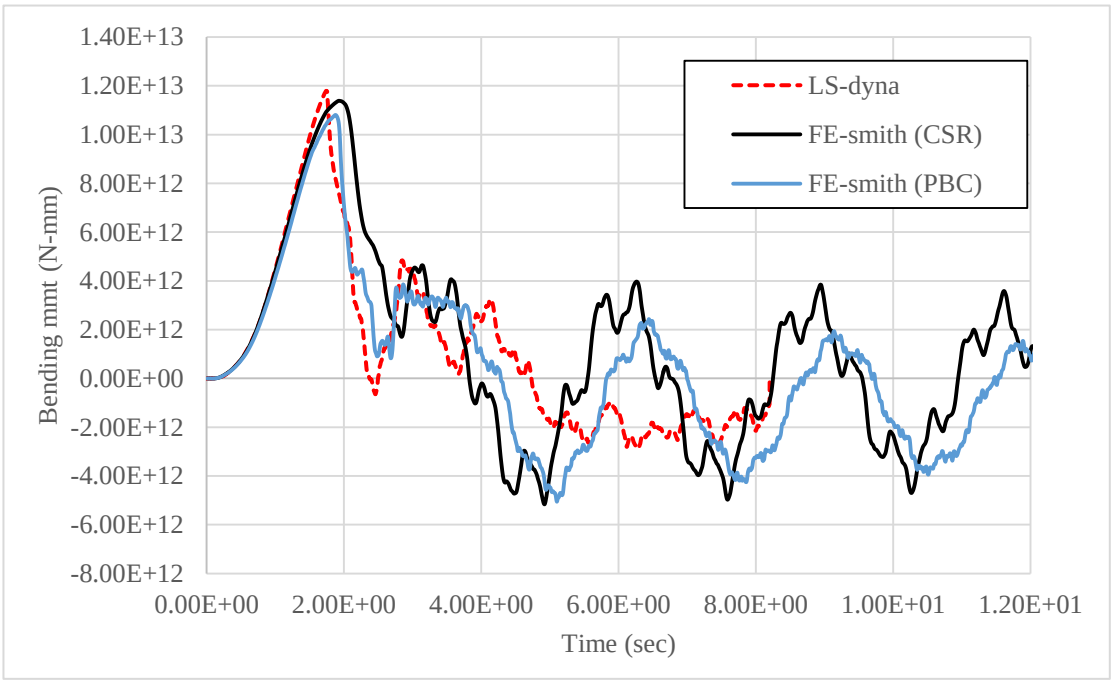

(b) Time history of bending moment

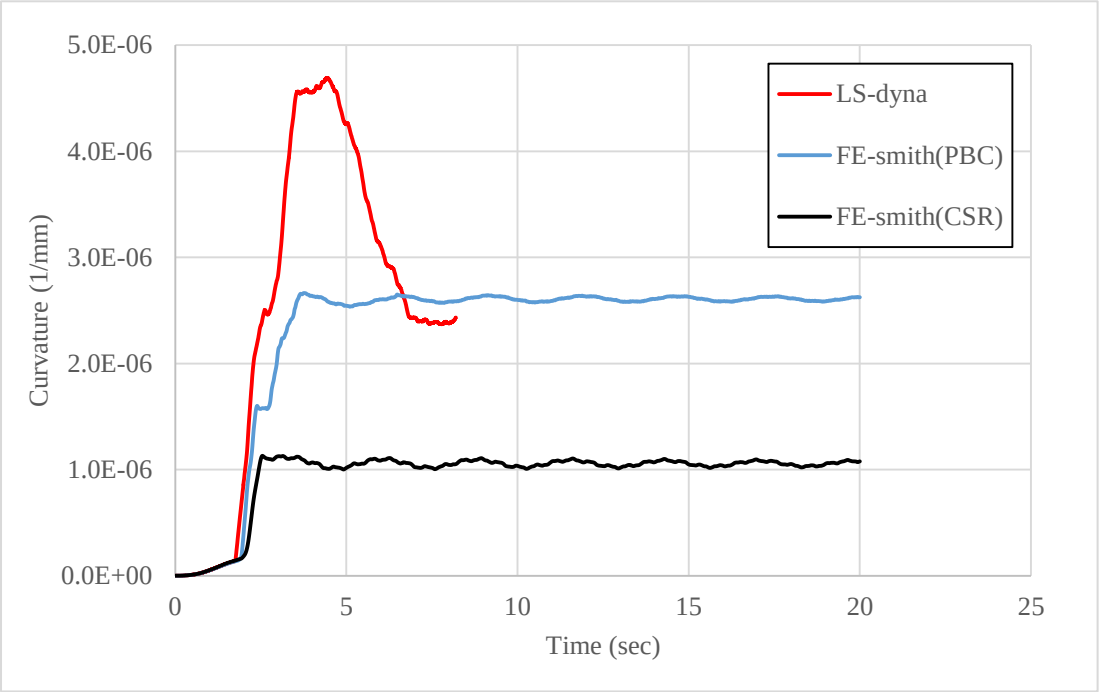

(c) Time history of curvature

Fig 4. 9 Comparison of LS-dyna and FE-smith analyses for 3.5 sec load duration

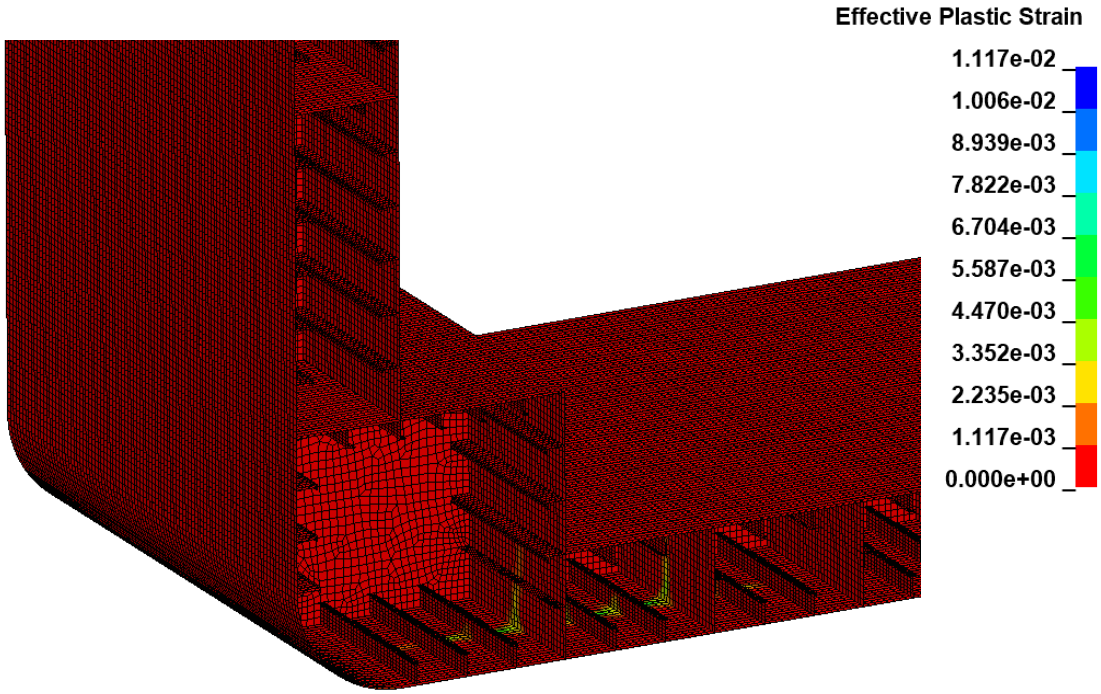

Fig 4. 10 Plastic strain distribution at bottom region at ultimate strength for 3.5 sec load duration

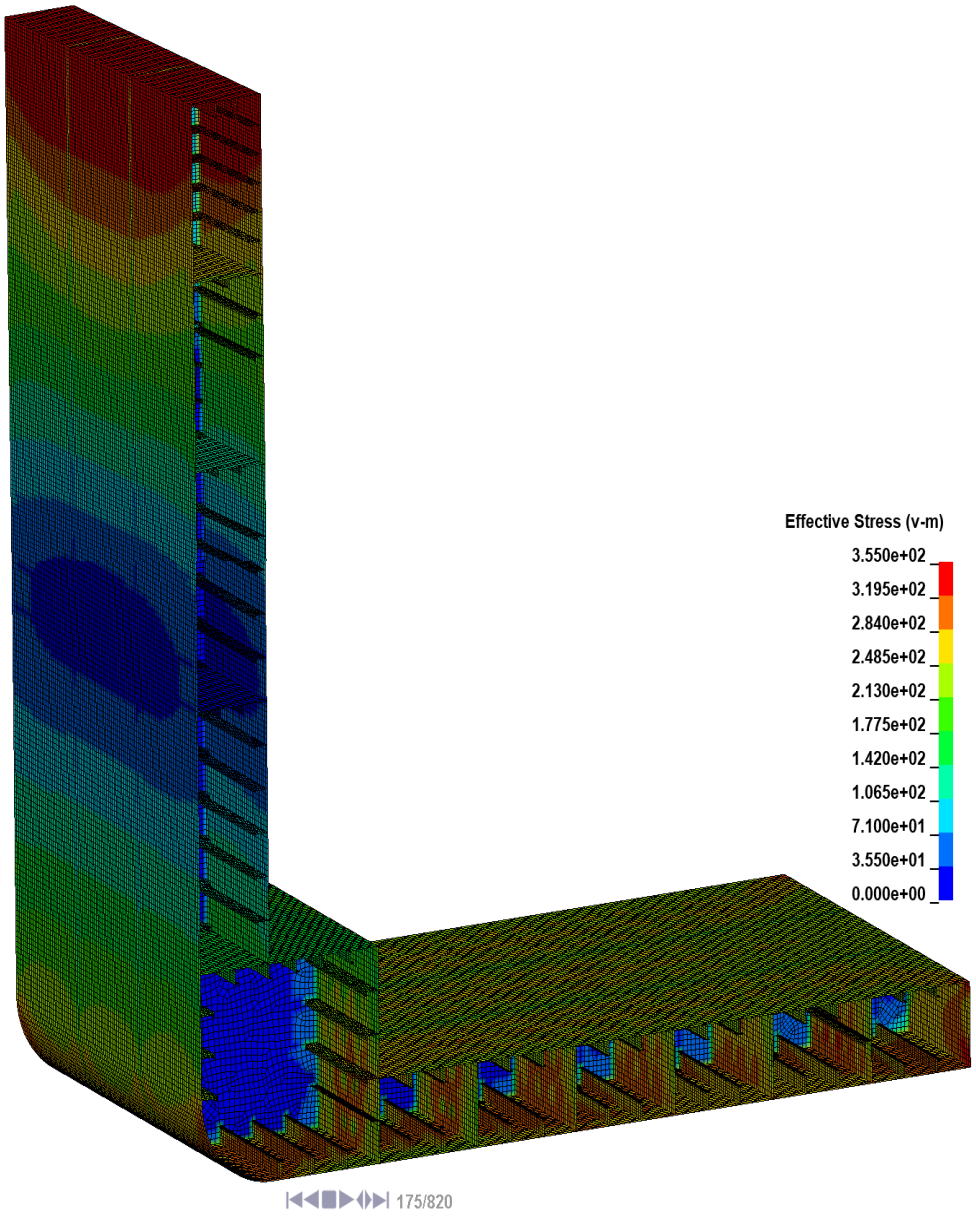

Fig 4. 11 Stress distribution at ultimate strength of 3.5 sec load duration case

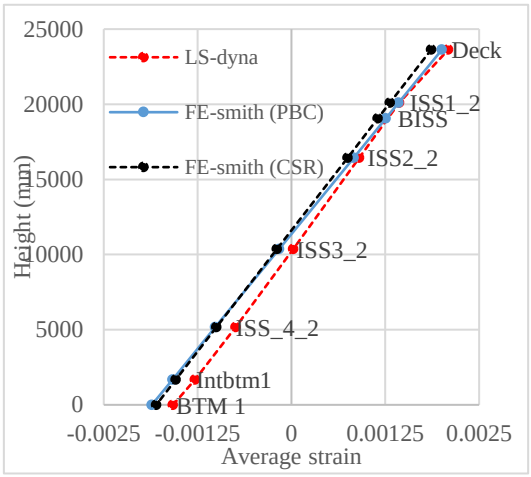

(a) Strain distribution at 1.74 sec

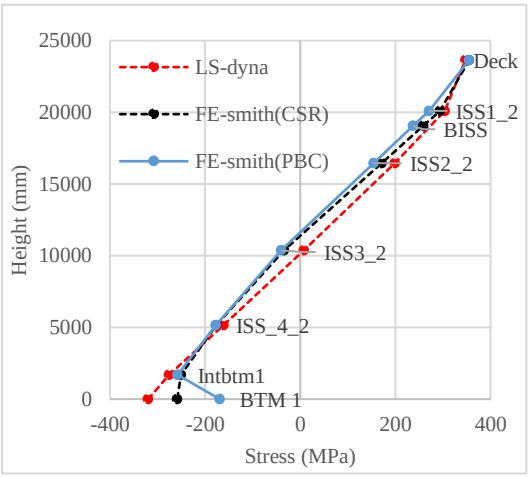

(d) Stress distribution at 1.74 sec

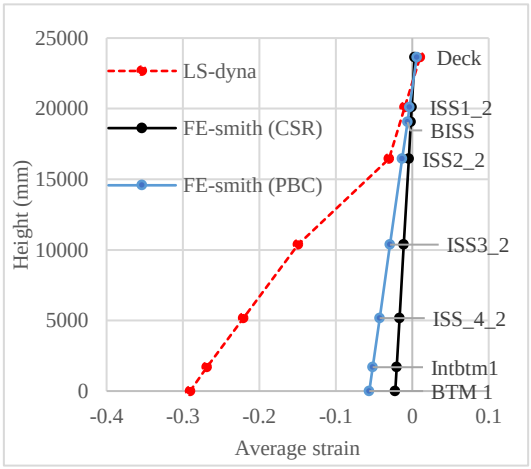

(b) Strain distribution at 4.74 sec

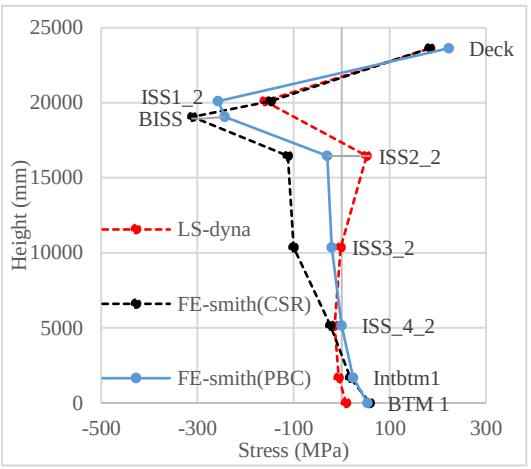

(e) Stress distribution at 4.74 sec

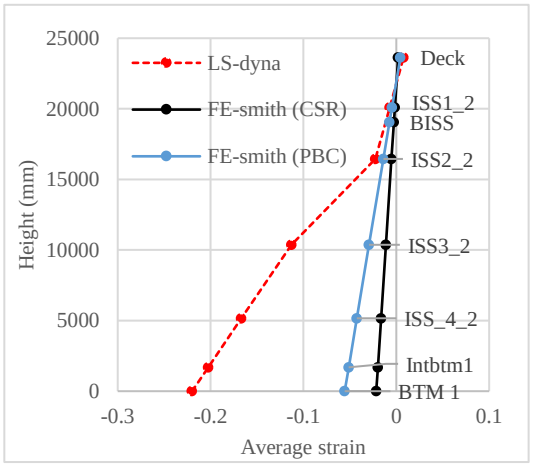

(c) Strain distribution at 6.3 sec

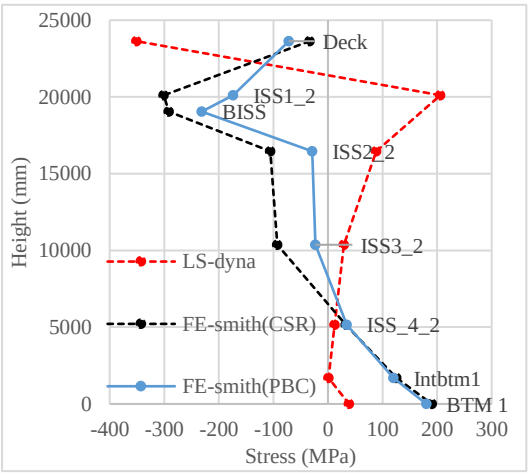

(f) Stress distribution at 6.3 sec

Fig 4. 12 Stress and strain distribution of midship cross section

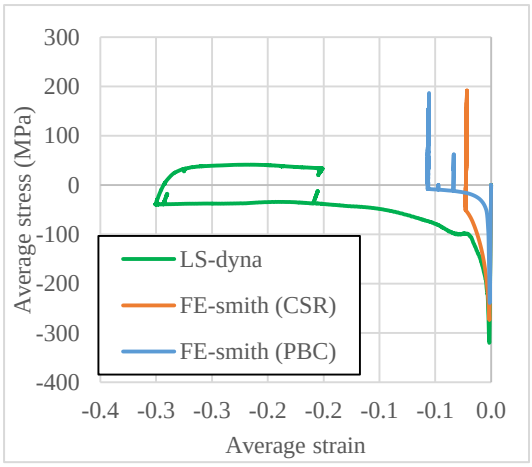

(a) Btm 1 element

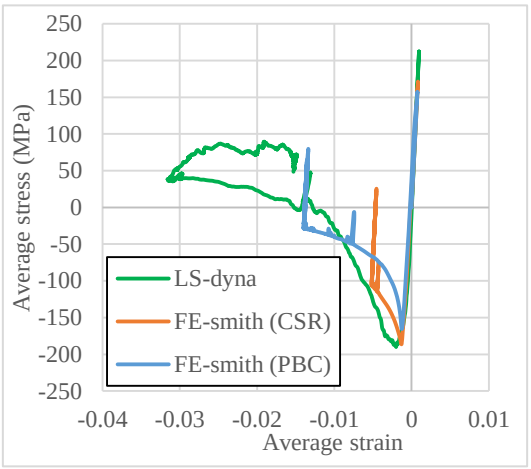

(d) ISS 2_2 element

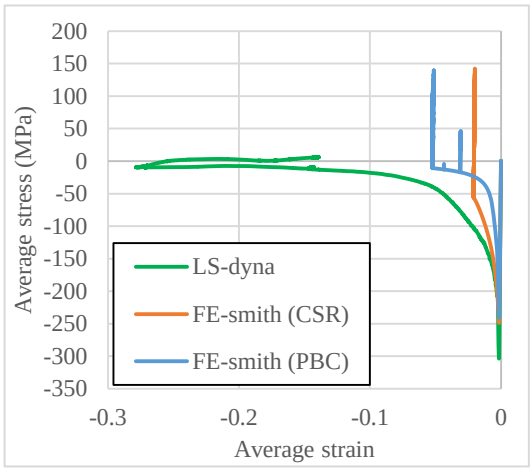

(b) Intbtm 1 element

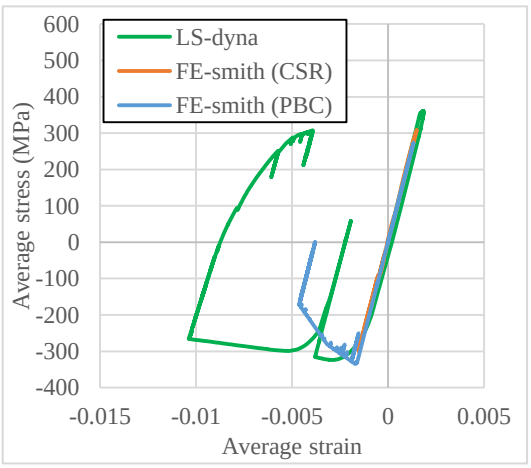

(e) ISS 1_2 element

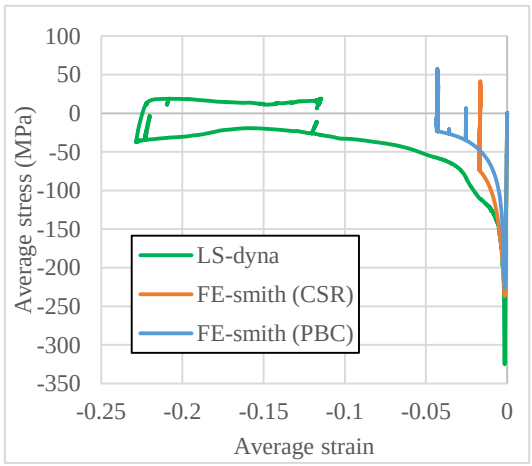

(c) ISS4_2 element

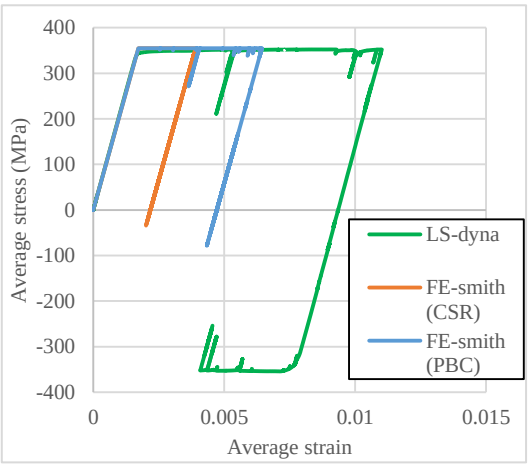

(f) Deck element

Fig 4. 13 Average stress-average strain of selected elements during dynamic collapse

The results obtained for the load duration of 2 sec and 5 sec are shown in Fig 4. 14 and Fig 4. 15, respectively.

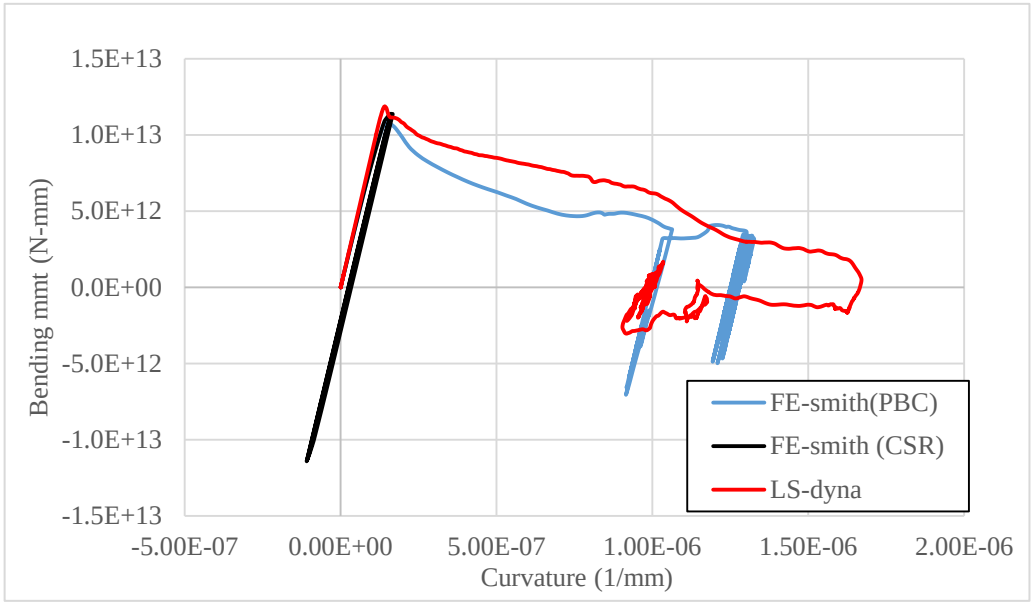

(a) Bending moment and curvature relationship

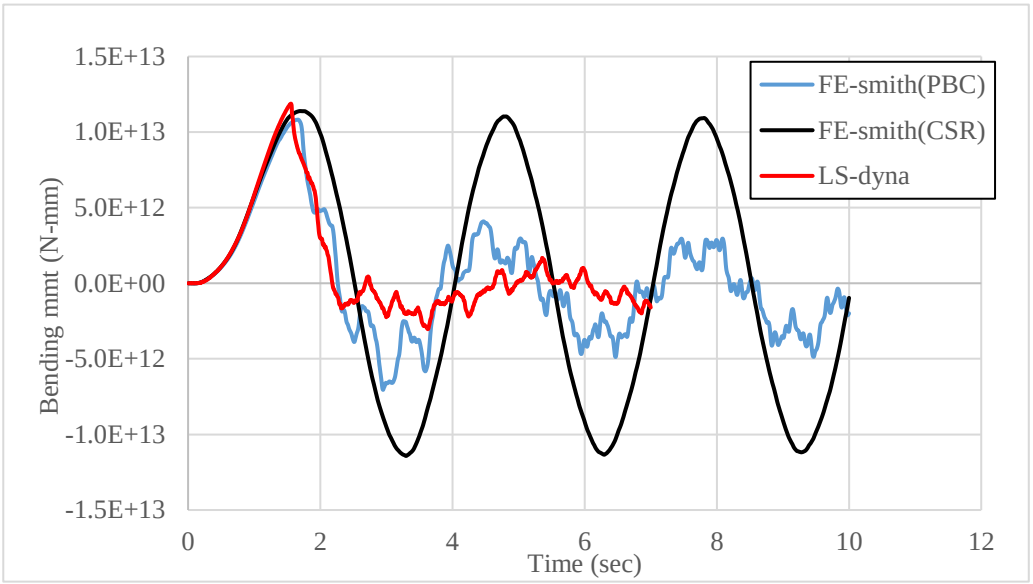

(b) Time history of bending moment

Fig 4. 14 Comparison between LS-dyna and FE-smith analyses for 2 sec load duration

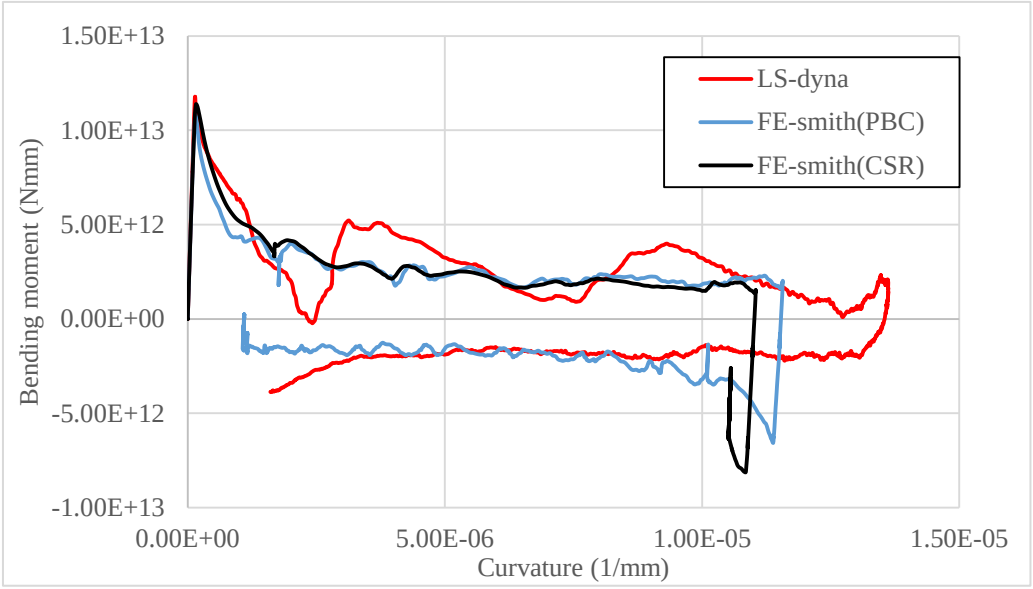

(a) Bending moment and curvature relationship

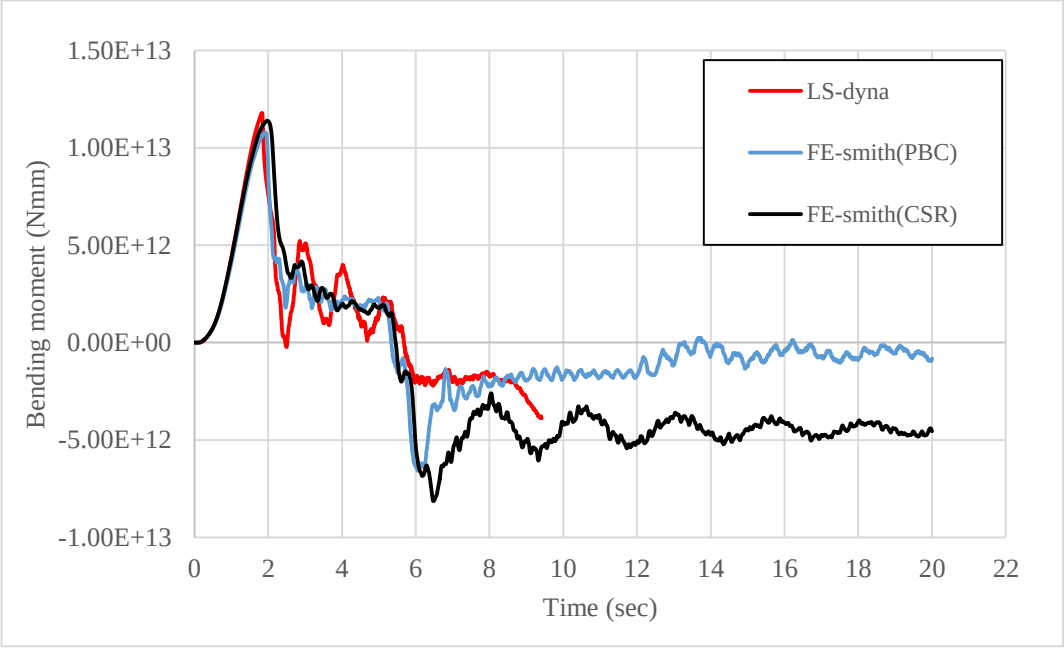

(b) Time history of bending moment

Fig 4. 15 Comparison between LS-dyna and FE-smith analyses for 5 sec load duration

Comparing FE-smith (CSR) and FE-smith (PBC), the latter gives the behavior that is closer to the results by LS-dyna. In particular, FE-smith (CSR) tends to significantly underestimate the collapse extent. This is probably because the reduction of post-ultimate strength capacity of element is smaller than those in FE-smith (PBC) and LS-dyna.

FE-smith analysis clearly has some degrees of uncertainties in the prediction of the collapse behavior of hull girder compared to NFEM, because of its idealization of buckling/plastic collapse behavior of structural elements and assumption of plane cross underlying in Smith method. It has been however confirmed that it can capture the basic characteristic of time-dependent collapse behavior expressed in terms of curvature with reasonable accuracy. In addition, FE-smith (PBC) likely to have better accuracy than FE-smith (CSR) because of its more accurate consideration of the post-ultimate strength behavior of structural elements. It has also capability of improving the average stress-average strain relationships unlike the specified CSR equations.

4.4 Analysis of hull girder model

4.4.1 FE-smith analysis

For hull girder model, stillwater analysis is performed first to set as initial loading condition. Calculation result shows the maximum stillwater hogging moment value 3.52e+12 Nmm at element 12 (between 105,600mm-115,200mm). Provided data is 3.489E+12 Nmm at 106800 mm which is very close to the FE-smith result. Deflection due to stillwater load is shown in Fig 4. 16.

Then elastic analysis is performed by applying unit load amplitude. Load duration of 2sec, 2.5 sec, 3sec, 3.5sec, 4sec and 5 sec are analyzed. Time history of applied load at node 14 for FE-smith analysis are shown in Fig 4. 17. Obtained time history of elastic bending moment of element 14 is shown for each load duration case in Fig 4. 18.

For collapse analyses, load amplitude is determined so that 6% larger than ultimate hogging moment is applied to the ship hull girder. Applied load distribution

pattern on hull girder is same as Fig 3. 5. Time history of total load applied for FE-smith (CSR) and FE-smith (PBC) at node 14 is shown in Fig 4. 19.

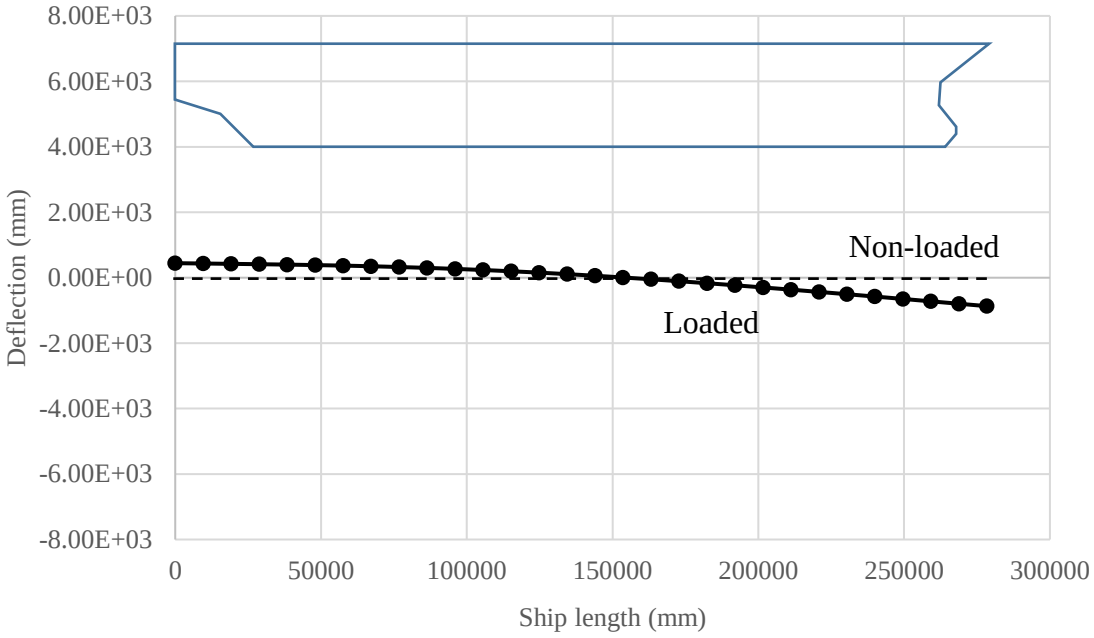

Fig 4. 16 Initial deflection of hull girder due to stillwater load

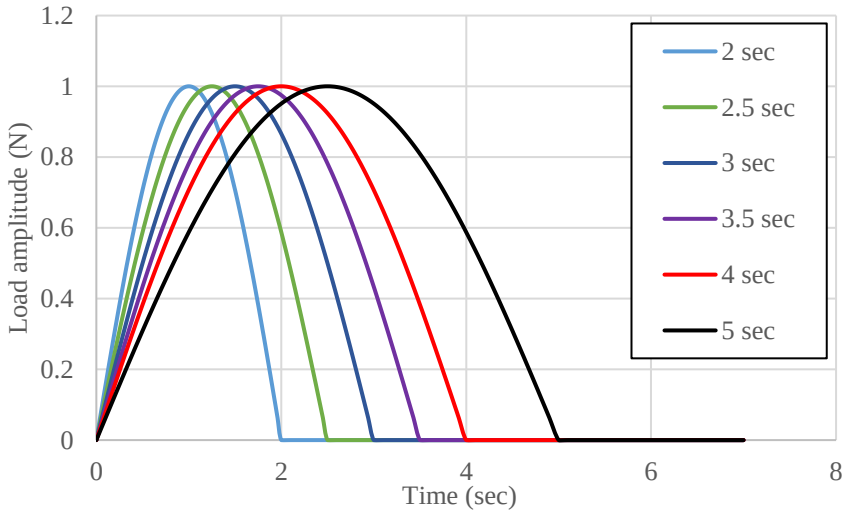

Fig 4. 17 Time history of applied load at node 14 for dynamic elastic analyses

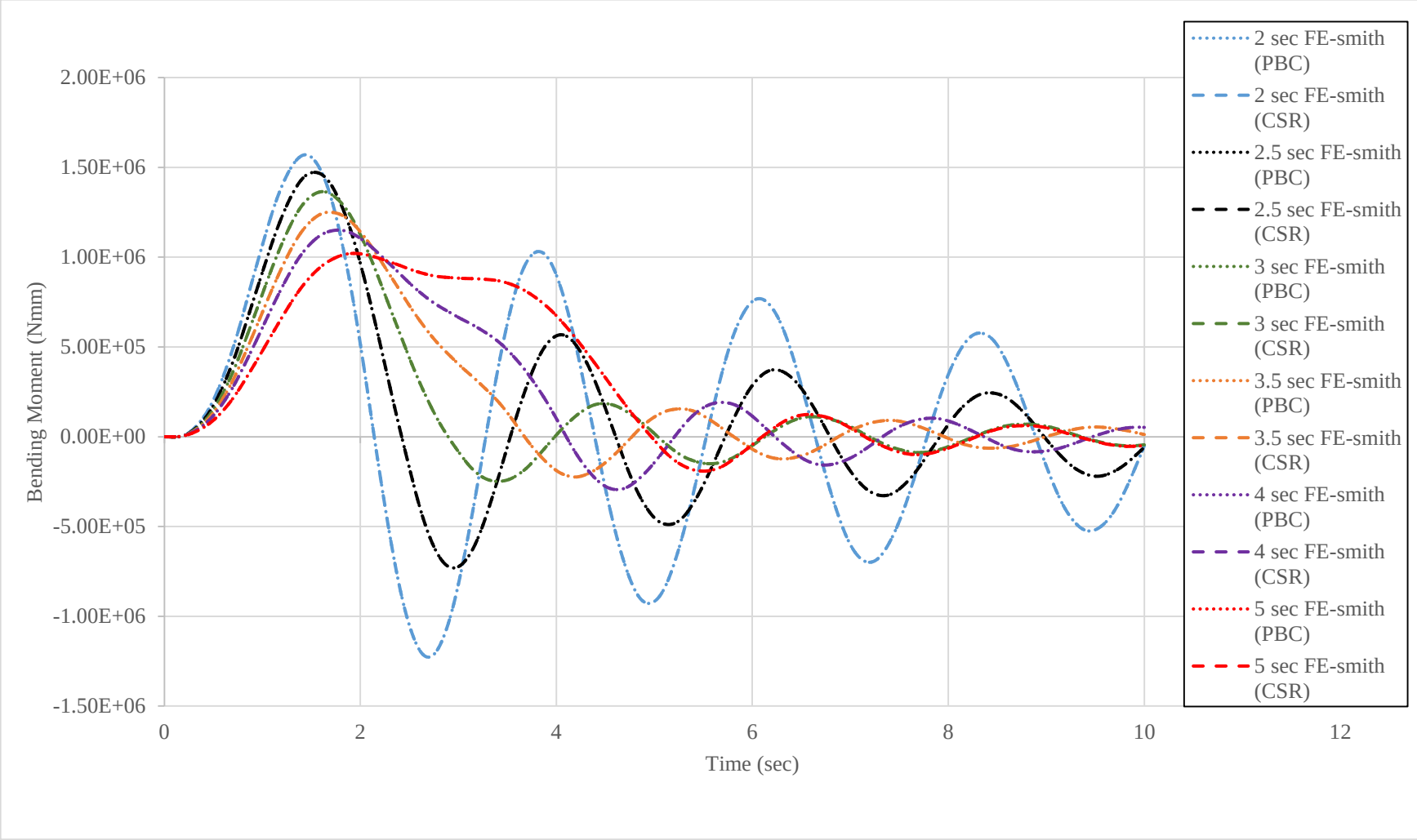

Fig 4. 18 Time history of bending moment at element 14 obtained by FE-smith (CSR) and FE-smith (PBC)

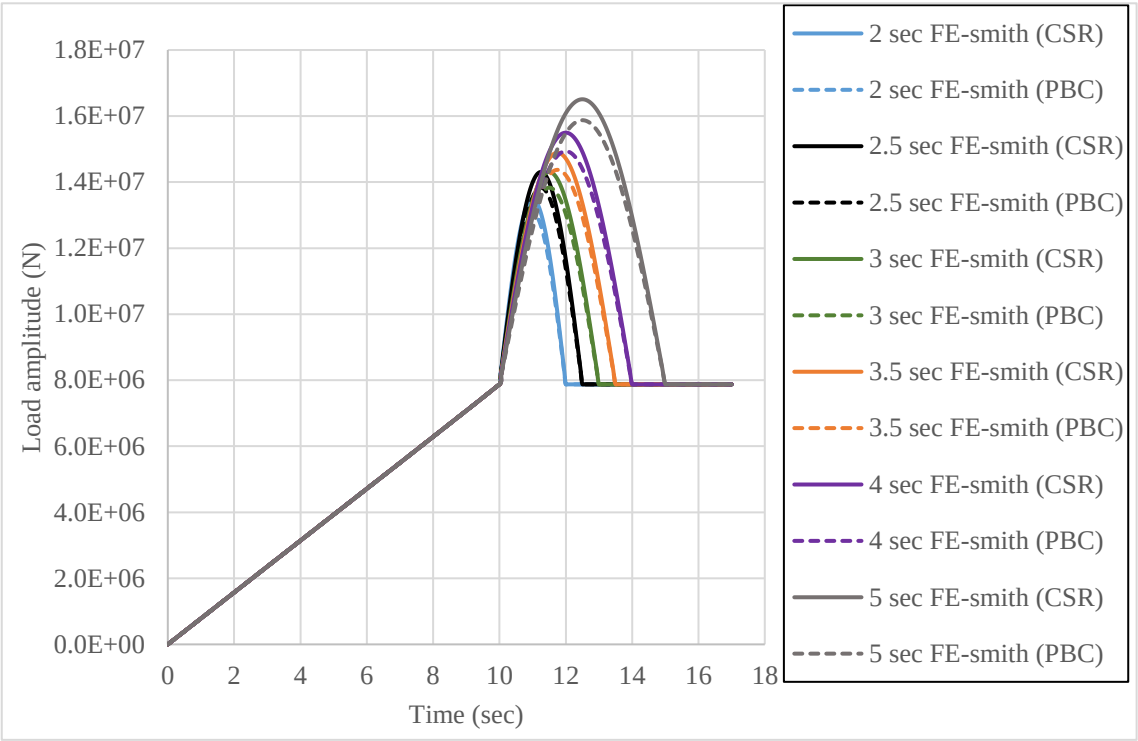

Fig 4. 19 Time history of applied load at node 14 for collapse analyses of FE-smith (CSR)

4.4.2 Analysis using combined 3D-shell and beam FEM

Stillwater load is applied by 10 sec load duration in LS-dyna under quasi-static condition. Load time history curve is as shown in Fig 4. 23. Slowly varying slope is adopted to reduce the noise. For the stillwater load analysis, to reduce the computation time, Belytschko-tsay shell element is used with 5 integration points through the thickness.

Time step determined by LS-dyna is 3.77E-06 sec which is automatically determined by smallest mesh size. Stillwater load is applied by 10 sec load duration which is larger than 2 times of model natural period so that analysis becomes quasi-static. Results in comparison with FE-smith are discussed. Stillwater moment distribution is shown in Fig 4. 20. Moment distribution is not exactly the same with that on real ship because of the different modelling concept but distribution is reasonable and discrepancy is at acceptable level. Since element 14 is shell model, we can see that moment is a little bit deviated from the distribution pattern and discrepancy is large compared to the beam model.

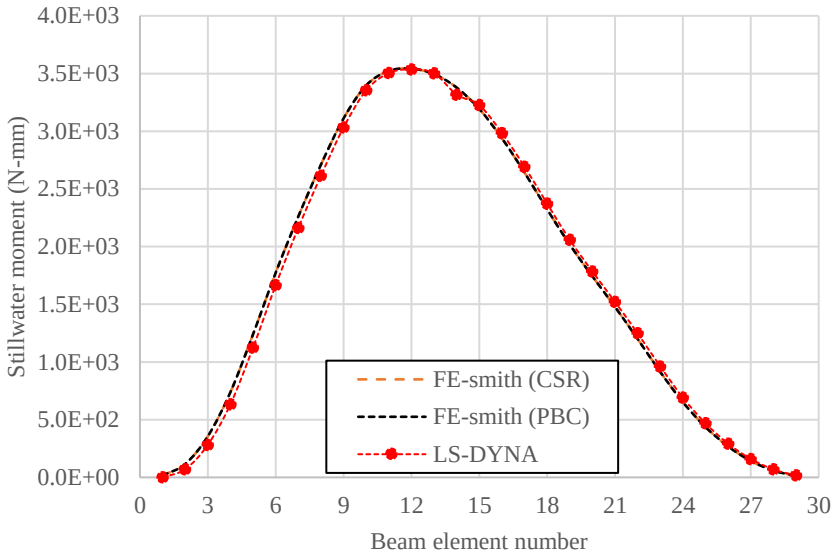

Fig 4. 20 Stillwater hogging moment distribution along the ship length for 3 sec load duration

From Fig 4. 20, it can be concluded that modelling and boundary condition of hull girder model in LS-dyna is reasonable to compare with FE-smith analysis. Stress distribution of shell model under stillwater load for 2.5 sec load duration is shown in Fig 4. 21. It can be seen that model is totally in elastic state. Maximum stress has been found at edge of the deck. Then elastic analysis for the impulsive load duration is carried out. Time history of elastic bending moment are compared and NFEM results show good agreement with FE-smith as described in Fig 4. 22. For the elastic analysis, to reduce the computation time, Belytschko-tsay element is used with 5 integration points through the thickness.

Load amplitude for dynamic collapse analysis is determined based on the elastic analysis and stillwater load analysis. Target bending moment is taken as 6% larger than ultimate hogging moment. Stillwater load is applied during first 10 sec in quasi-static manner followed by hogging moment. Time history of loads applied at each node of beam elements is shown in Fig 4. 23. For collapse analysis, Hughes-Liu shell element is adopted with 5 integration point through thickness. Belytschko-tsay element is not applied for collapse analysis as it could not give the reasonable behavior because of the lack of control in warping mode.

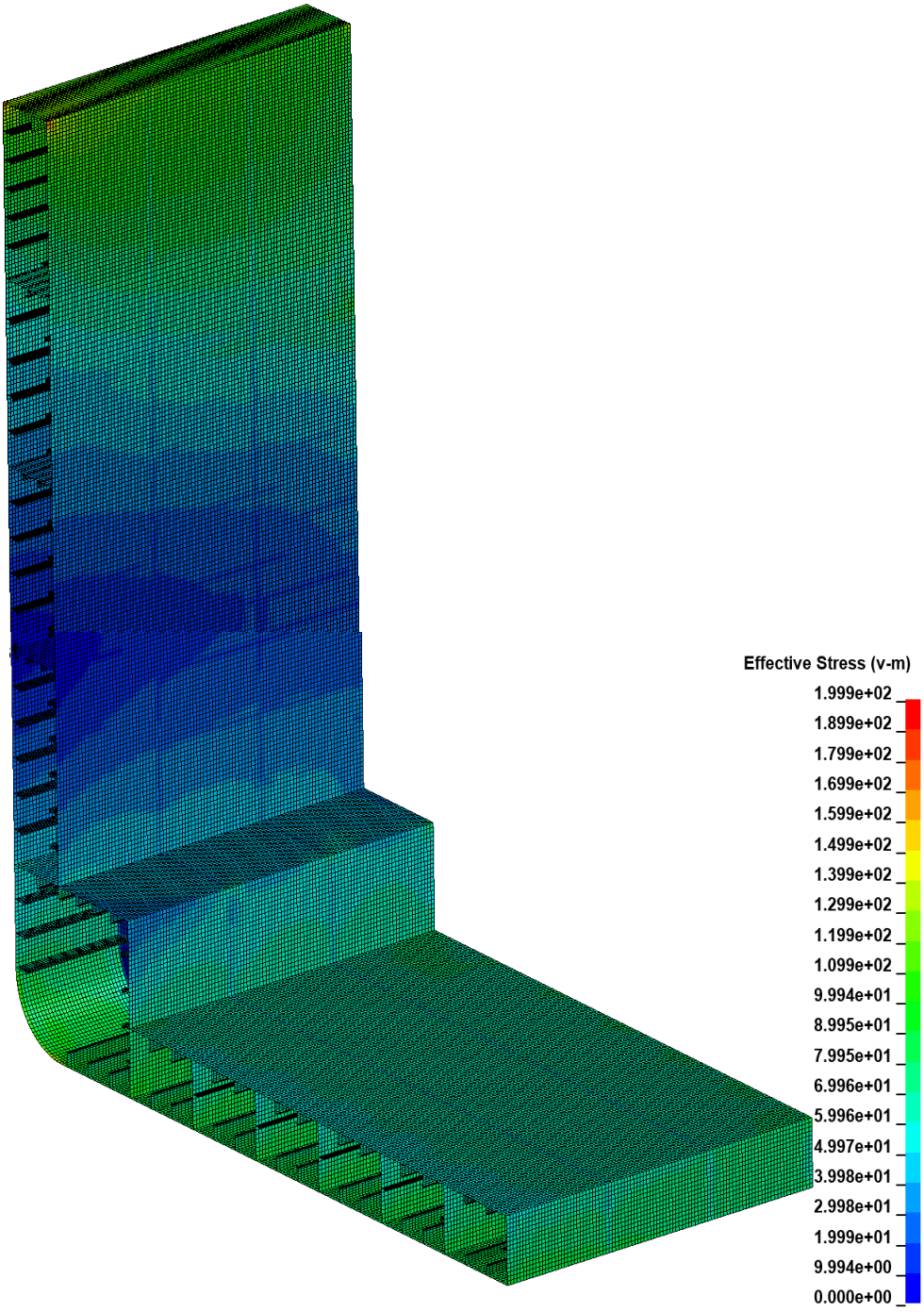

Fig 4. 21 Elastic stress distribution of shell model under stillwater hogging moment

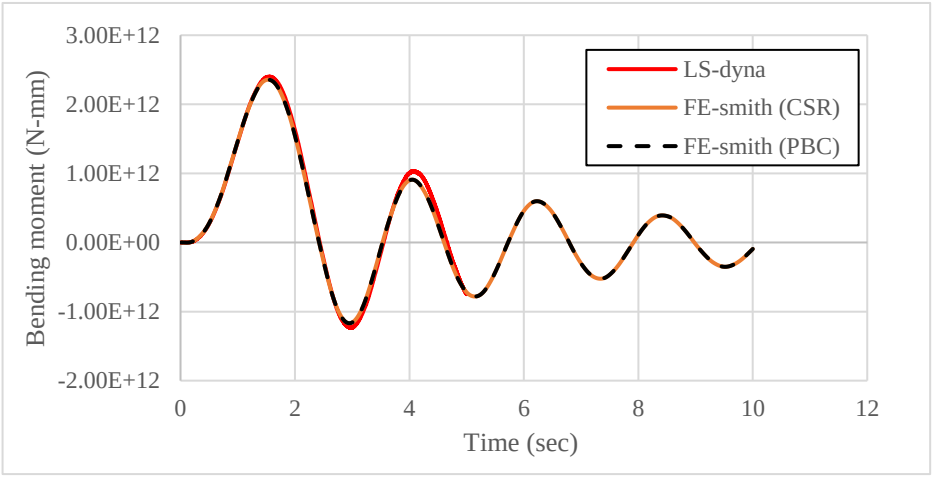

(a) 2.5 sec load duration

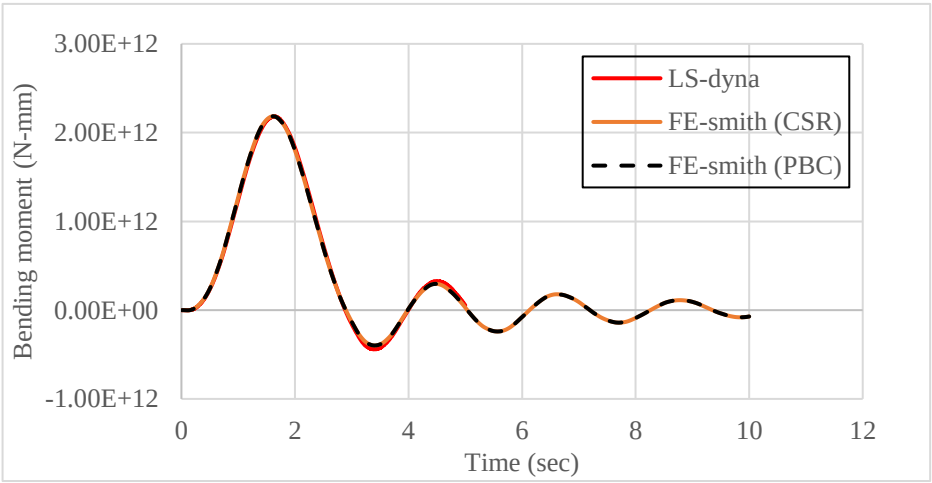

(b) 3sec load duration

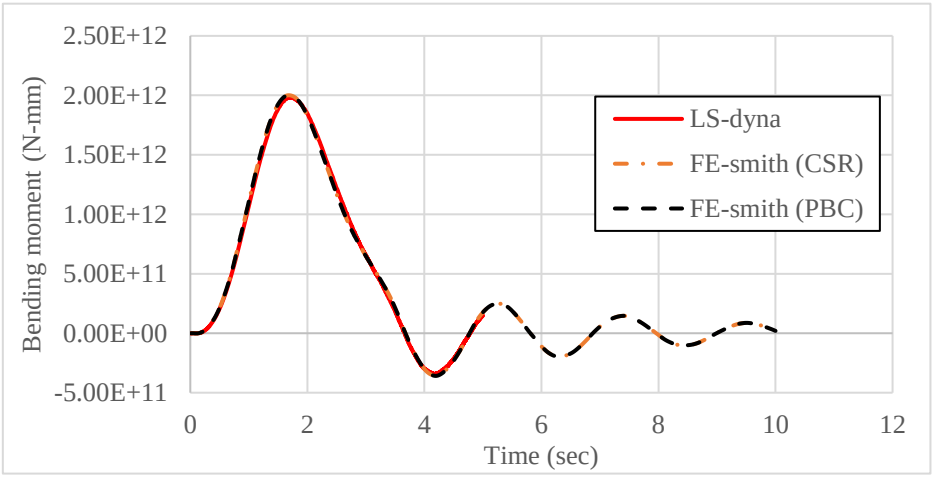

(c) 3.5 sec load duration

Fig 4. 22 Comparison of dynamic elastic moment obtained by LS-dyna and FE-smith

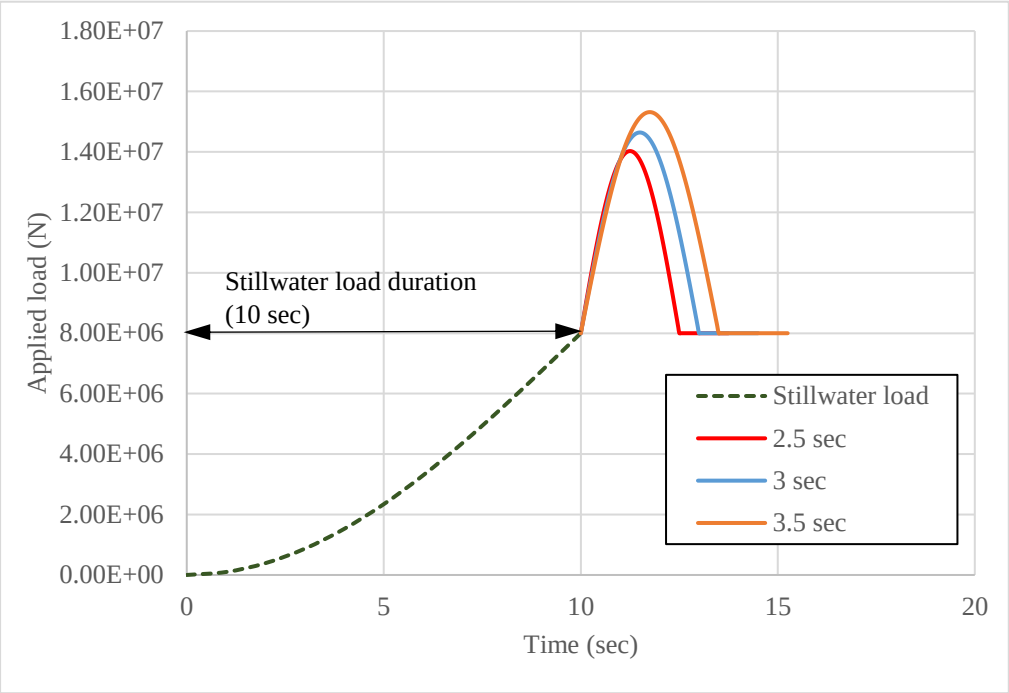

Fig 4. 23 Time history applied load for dynamic collapse analysis in LS-dyna

4.4.3 Results and discussion

Results obtained from FE-smith are firstly discussed. Fig 4. 24 and Fig 4. 25 show the bending-moment curvature relationship and Fig 4. 28 shows the time history of bending moment of element 14 for the different load durations obtained by FE-smith (CSR) and FE-smith (PBC), respectively.

Fig 4. 27 shows the residual deformation of hull girder. Same as uniform beam model, the larger the load duration, the larger the collapse extent. Unlike uniform beam model, residual hogging deflection with hogging residual moment is remained for smaller load duration cases. Also there is no plastic deformation occurred by sagging moment because of the presence of stillwater hogging moment.

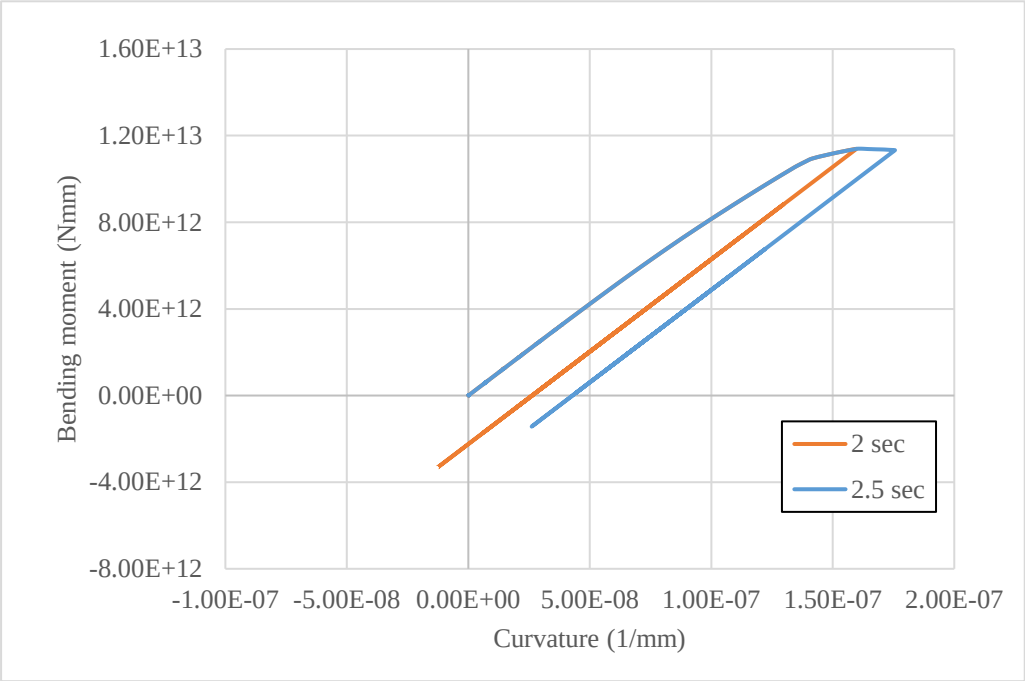

(a) Elasto-plastic case

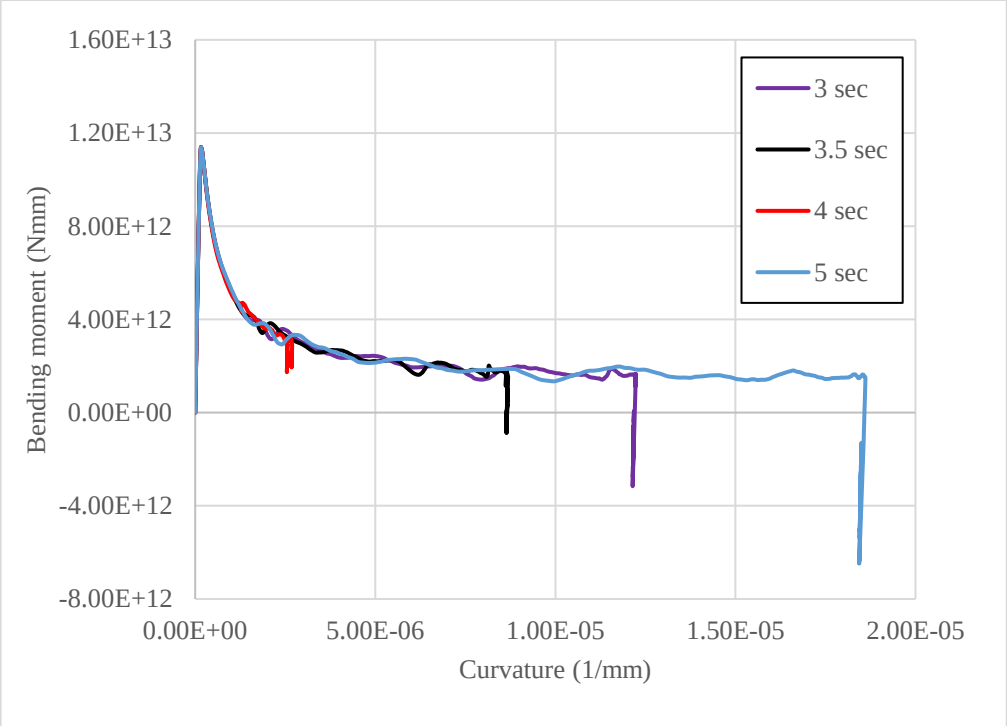

(b) Collapse case

Fig 4. 24 Bending moment-curvture relationship obtained by FE-smith (CSR)

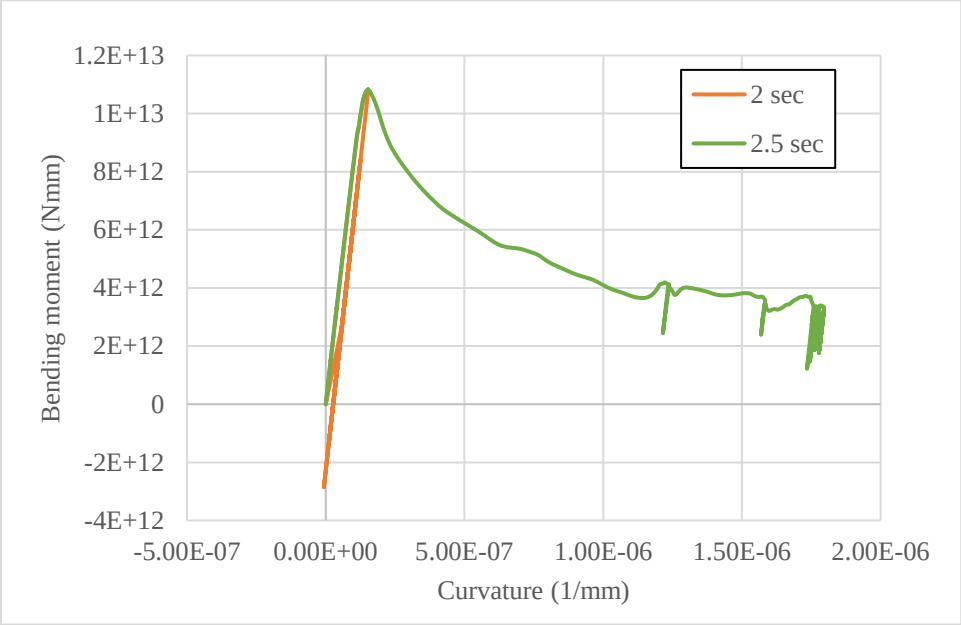

(a) Smaller collapse extent

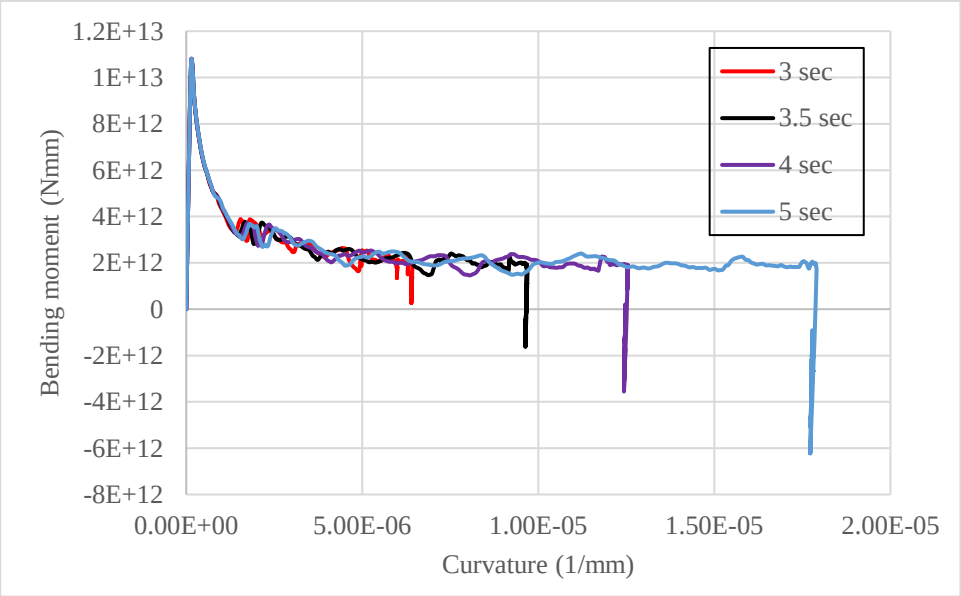

(b) Larger collapse extent

Fig 4. 25 Bending moment and curvature relationship obtained by FE-smith (PBC)

Bending moment and curvature relationships obtained by FE-smith (PBC) and FE-smith (CSR) are compared in Fig 4. 26. We can see that collapse extent of FE-smith (PBC) is larger than FE-smith (CSR) for mall load duration case. But the longer the load duration, the smaller the discrepancy between the collapse extent. This is because of the

element average stress-average strain curve behavior in larger strain region. In smaller strain region, rapid load duration effect of PBC is dominant which results in larger collapse extent. Residual deformations are compared in Fig 4. 27 and bending moment in Fig 4. 28.

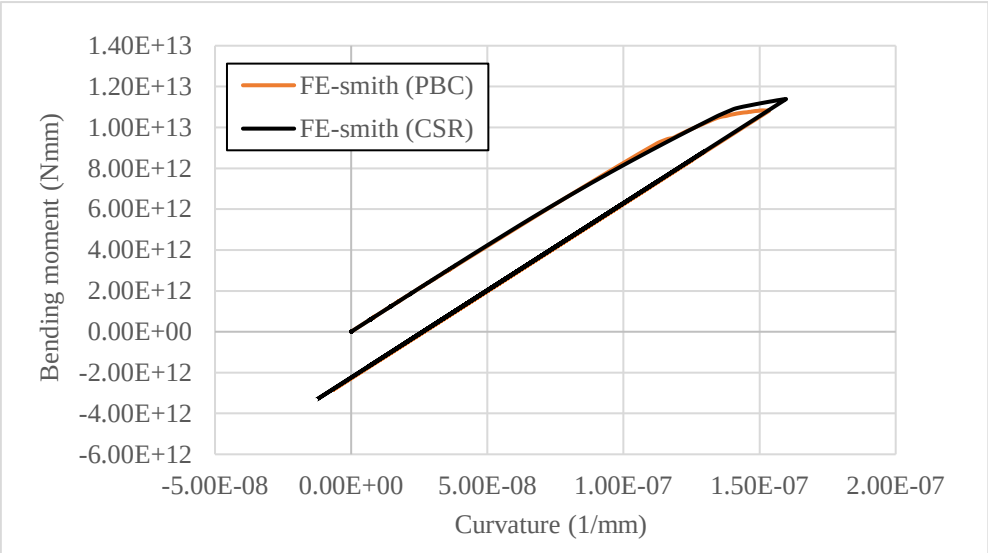

(a) 2 sec load duration case

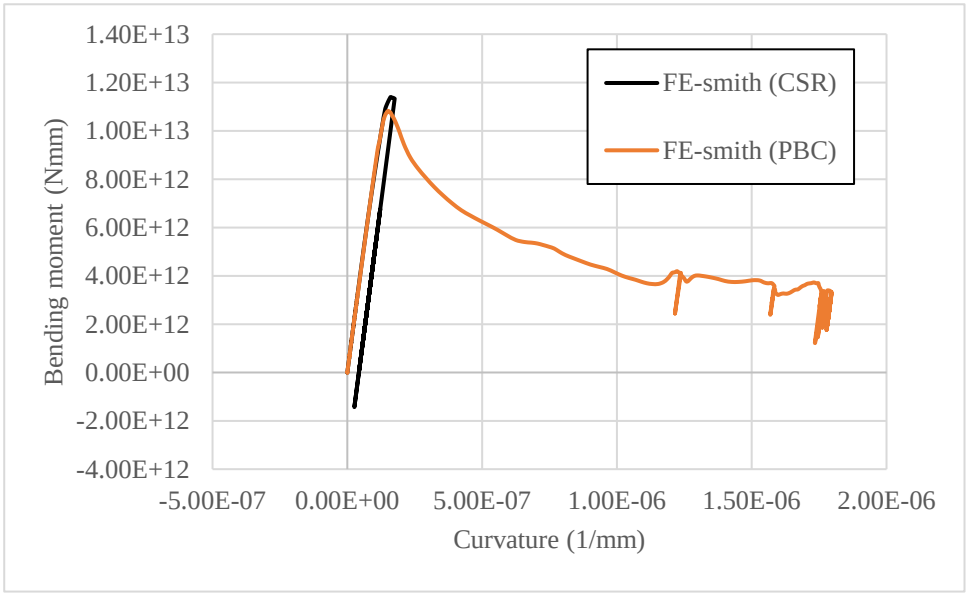

(b) 2.5 sec load duration

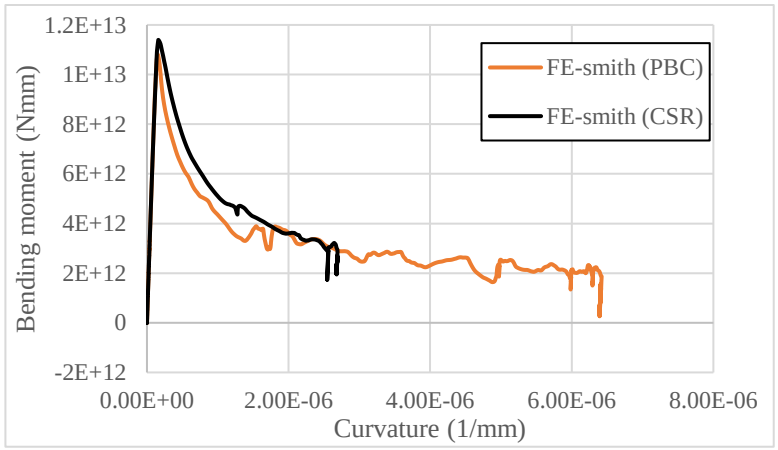

(c) 3 sec load duration

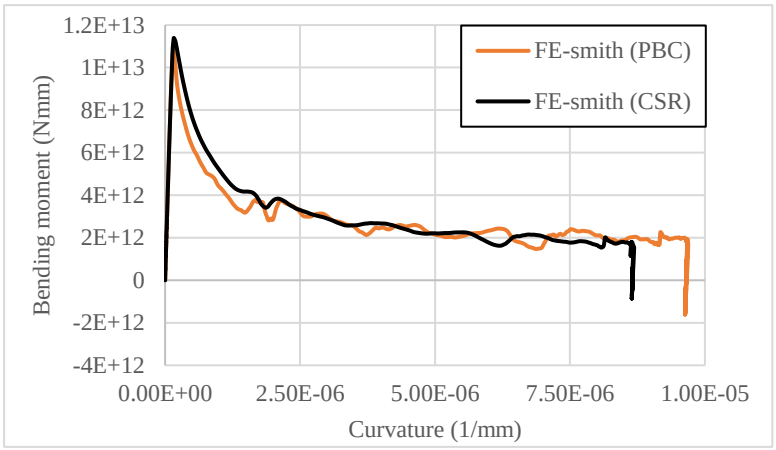

(d) 3.5 sec load duration

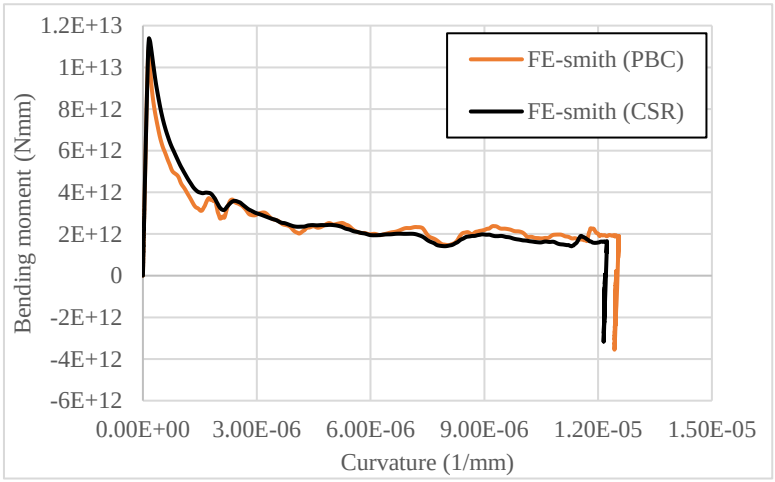

(e) 4 sec load duration

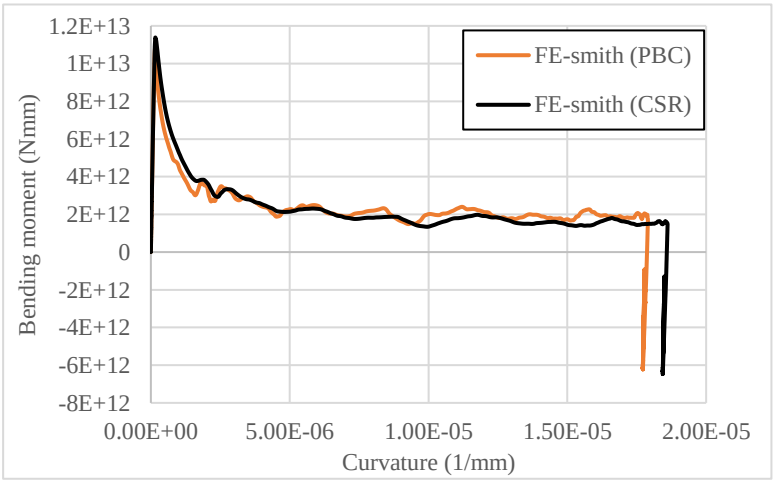

(f) 5 sec load duration

Fig 4. 26 Comparison of bending moment-curvature relationship obtained by FE-smith (CSR) and FE-smtih (PBC)

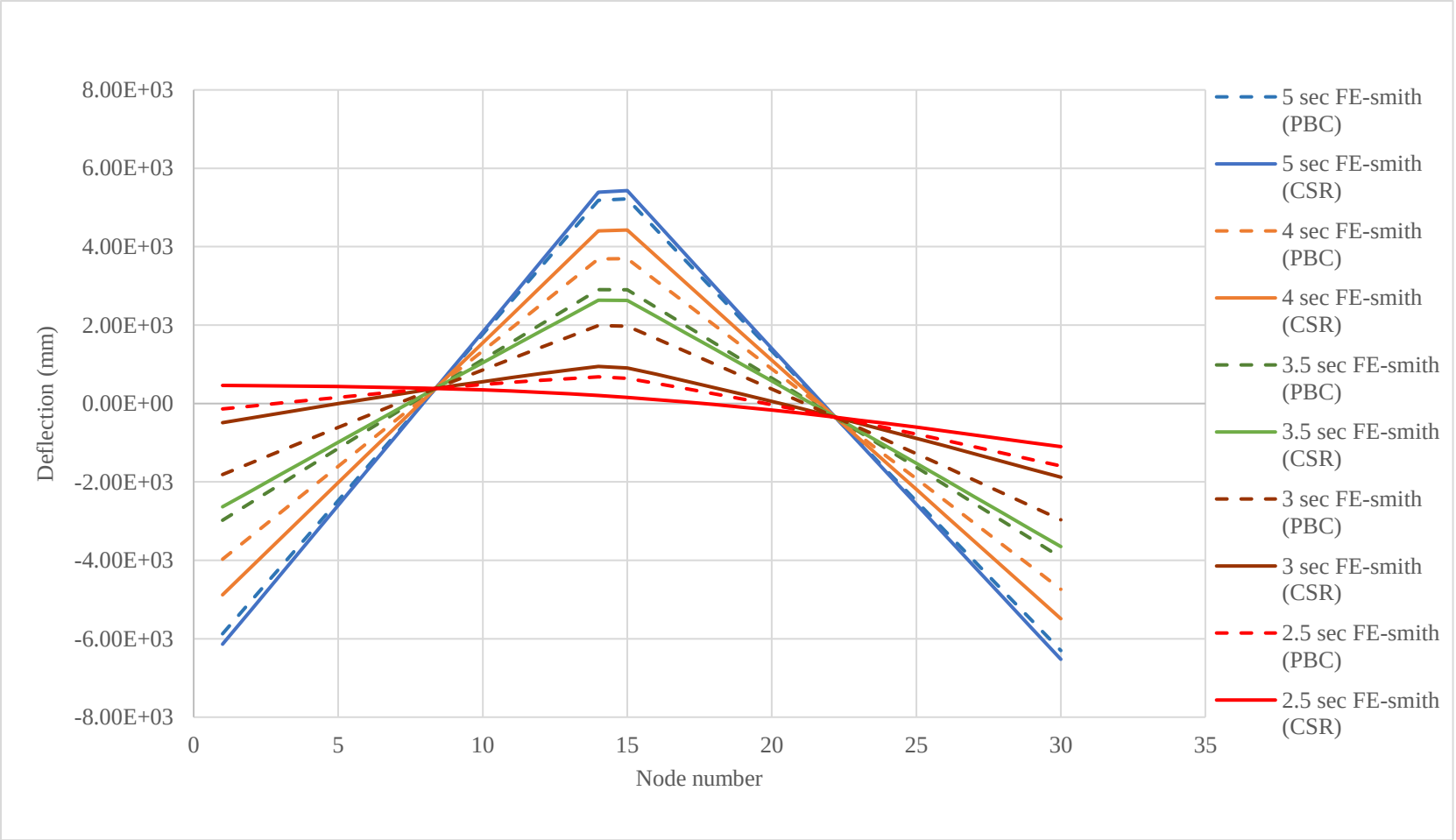

Fig 4. 27 Residual deformation obtained by FE-smith(CSR) and FE-smith(PBC)

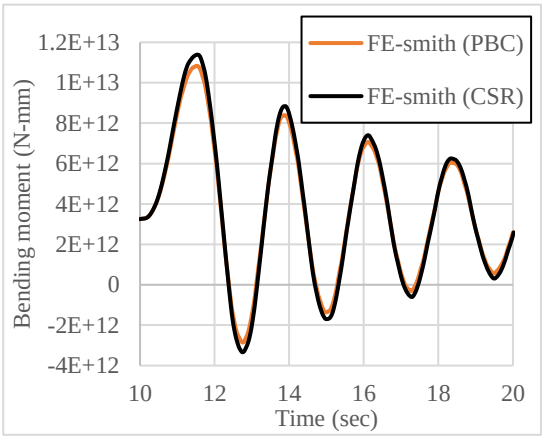

(a) 2 sec load duration

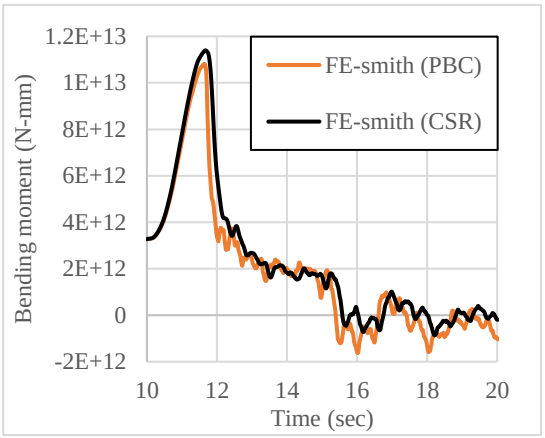

(d) 2.5 sec load duration

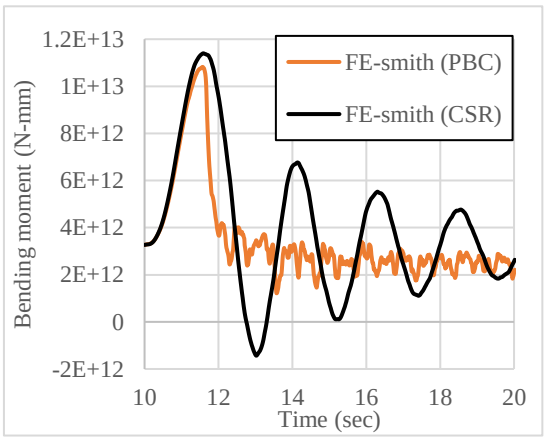

(b) 2.5 sec load duration

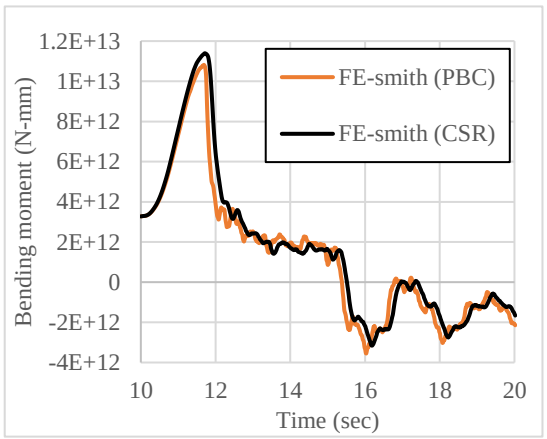

(e) 4 sec load duration

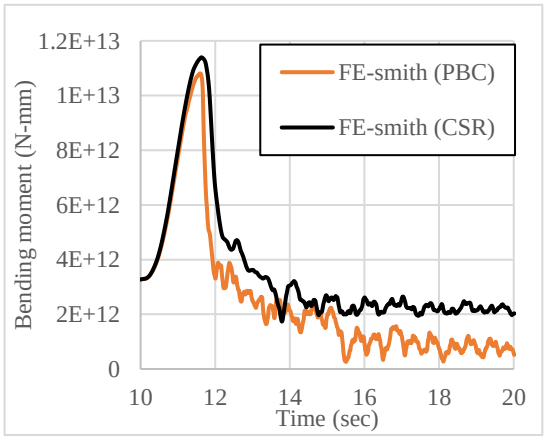

(c) 3 sec load duration

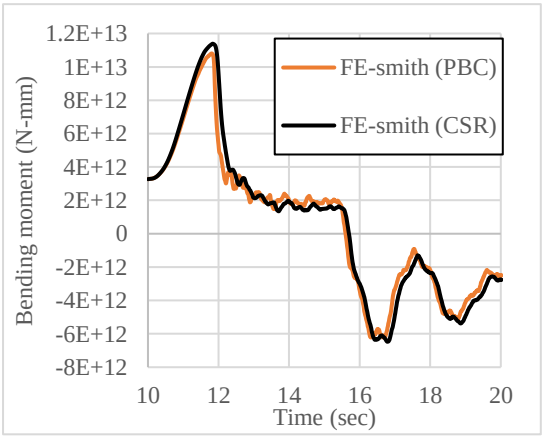

(f) 5 sec load duration

Fig 4. 28 Time history of moment at element 14 obtained by FE-smith

Then NFEA results for 2.5 sec load duration case is explained. Similar to the static analysis, plastic strain of outer bottom plate initiates from the thinnest plate region at 11.28 sec. Ultimate hogging strength is attained at 11.39 sec and plastic strain at the bottom is shown in Fig 4. 29. As we can see in Fig 4. 30(b), the sagging moment does not act on the hull girder due to the presence of stillwater hogging moment. The error in the Smith method in the unloading process does not significantly affect the behavior predicted by FE-smith as can be seen in Fig 4. 32. Element collapse sequence of the cross section and their mode of collapse are same as uniform beam model. Cross-section stress and strain distribution is also drawn in Fig 4. 31 for (1) at ultimate strength, 11.39 sec, (2) at external moment zero, 12.5 sec and end of analysis, 20 sec. Neutral axis at the end of analysis is between Deck and ISS1_2 Element. Strain distribution is linear in FE-smith while LS-dyna is no longer linear after collapse. FE-smith (CSR) does not attain its ultimate strength, while FE-Smith (PBC) gives the result which is better agreement with NFEM similar to the case of uniform beam model.

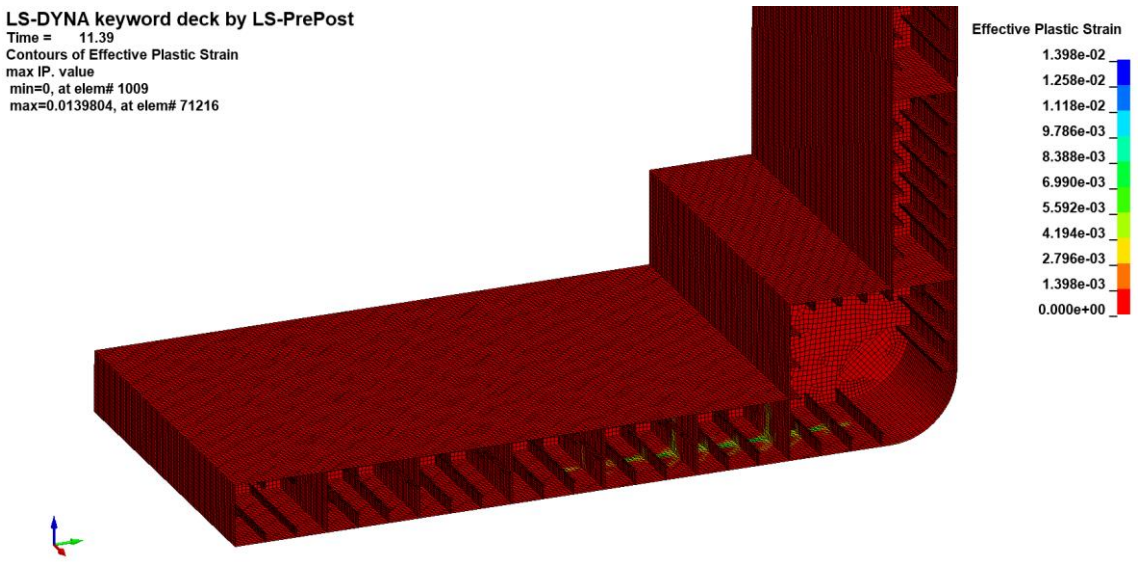

Fig 4. 29 Plastic strain distribution at the bottom at ultimate strength

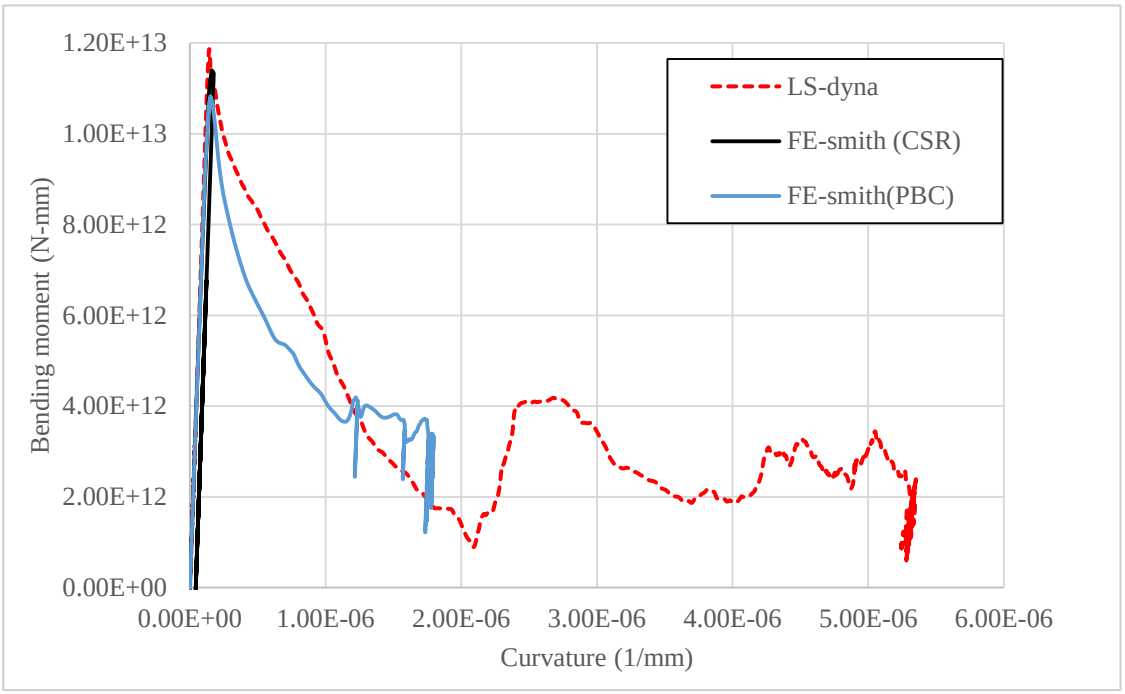

(a) Bending moment-curvature

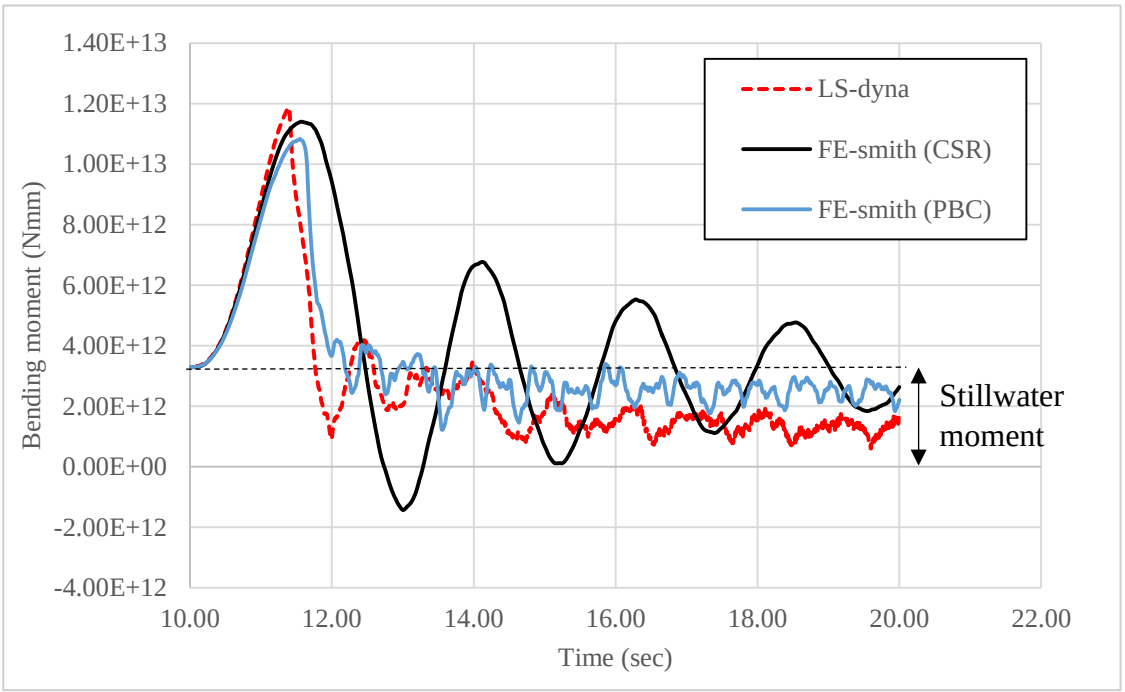

(b) Time history of moment

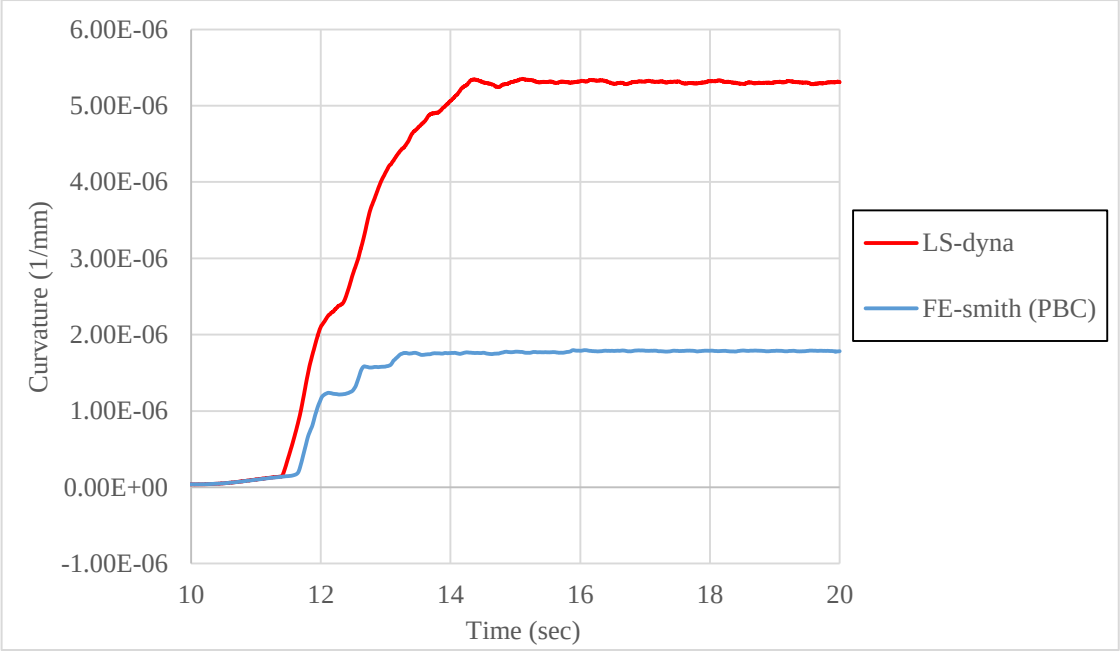

(c) Time history of curvature

Fig 4. 30 Comparison between LS-dyna and FE-smith analyses

Stress distribution of the shell model at ultimate strength and its collapse mode at the end of analysis are shown in Fig 4. 33 and Fig 4. 34 which are similar behavior to the static analysis. But the collapse frame is different from static case and uniform beam model as the hull girder model is analyzed and loading condition are different.

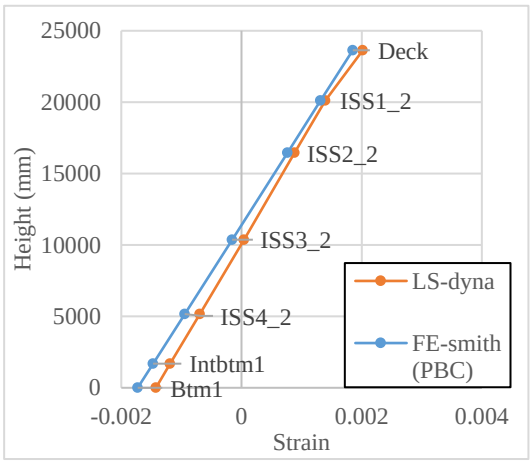

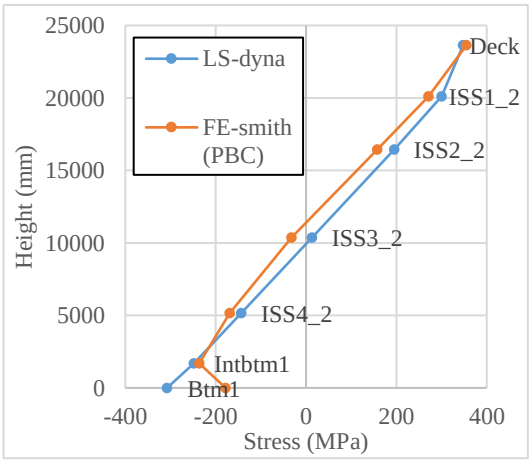

(a) Strain distribution and stress distribution at ultimate strength

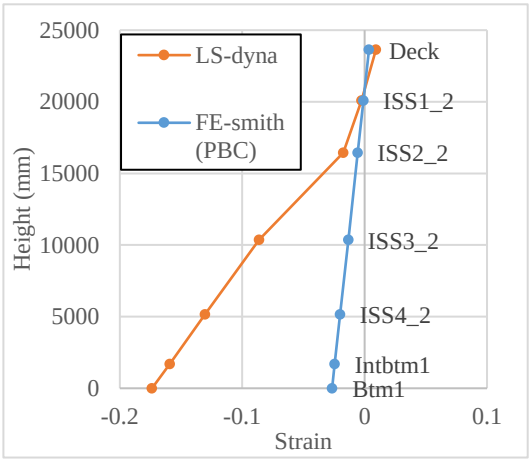

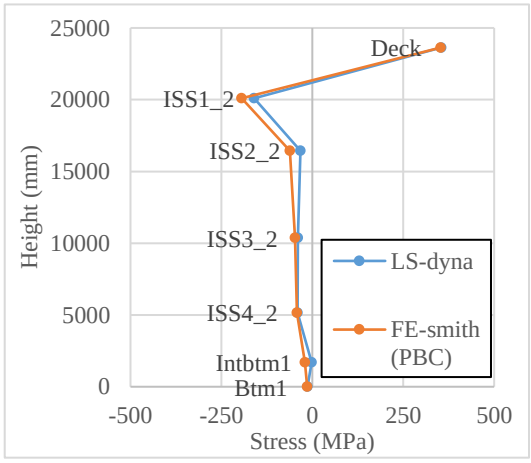

(b) Strain distribution and stress distribution at the end of loading

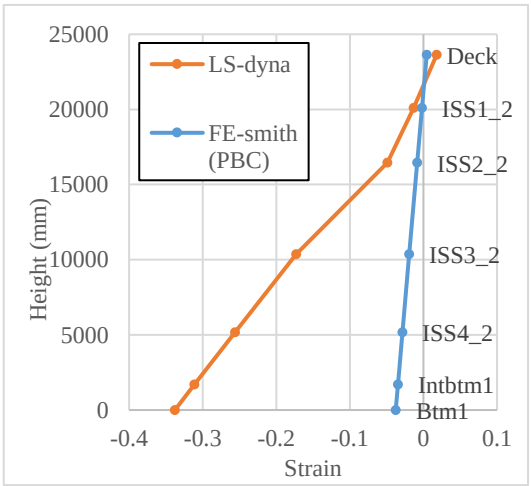

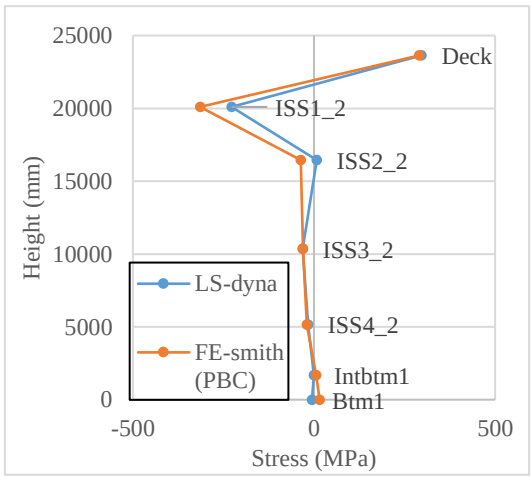

(c) Strain distribution and stress distribution at end of analysis

Fig 4. 31 Stress and strain distribution of cross-section (2.5sec load duration)

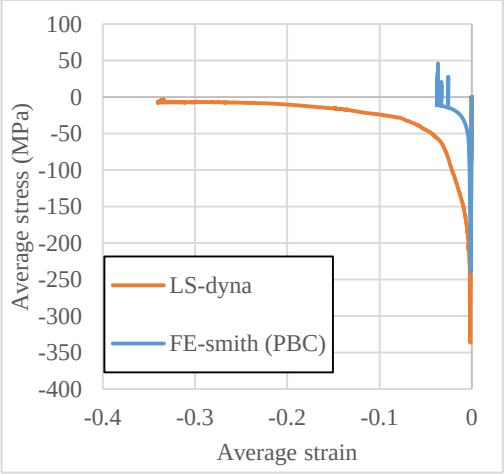

(a) Btm 1 element

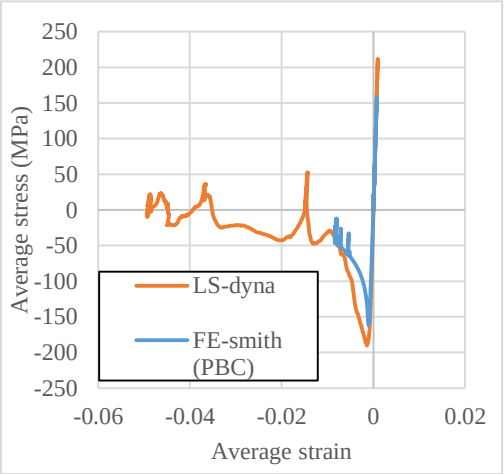

(d) ISS2_2 element

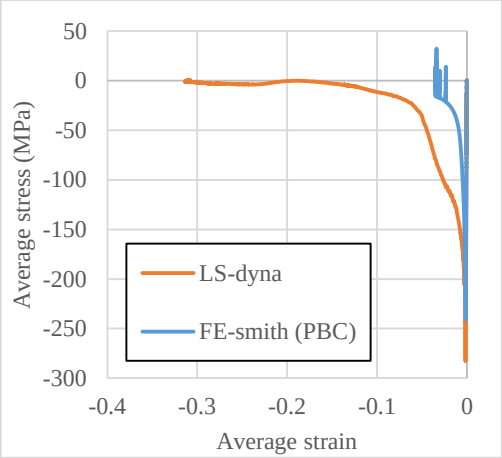

(b) Intbtm1 element

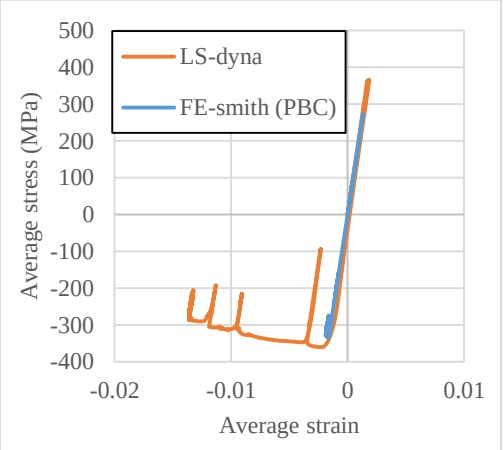

(e) ISS 1_2 element

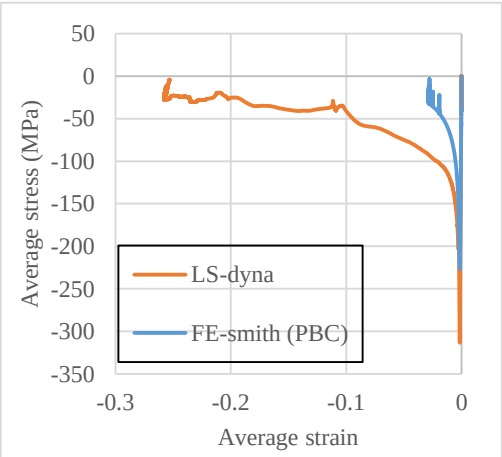

(c) ISS 4_2 element

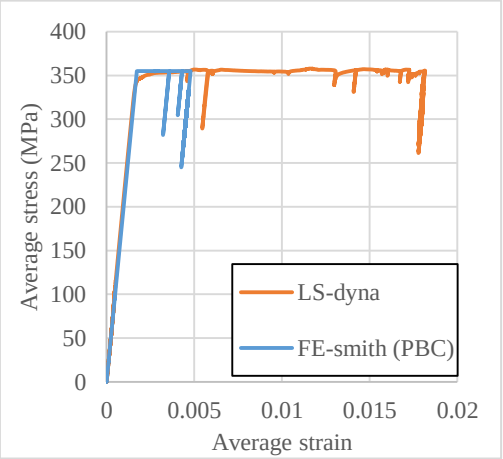

(f) Deck element

Fig 4. 32 Elements' average stress-strain during dynamic collapse (2.5sec load duration)

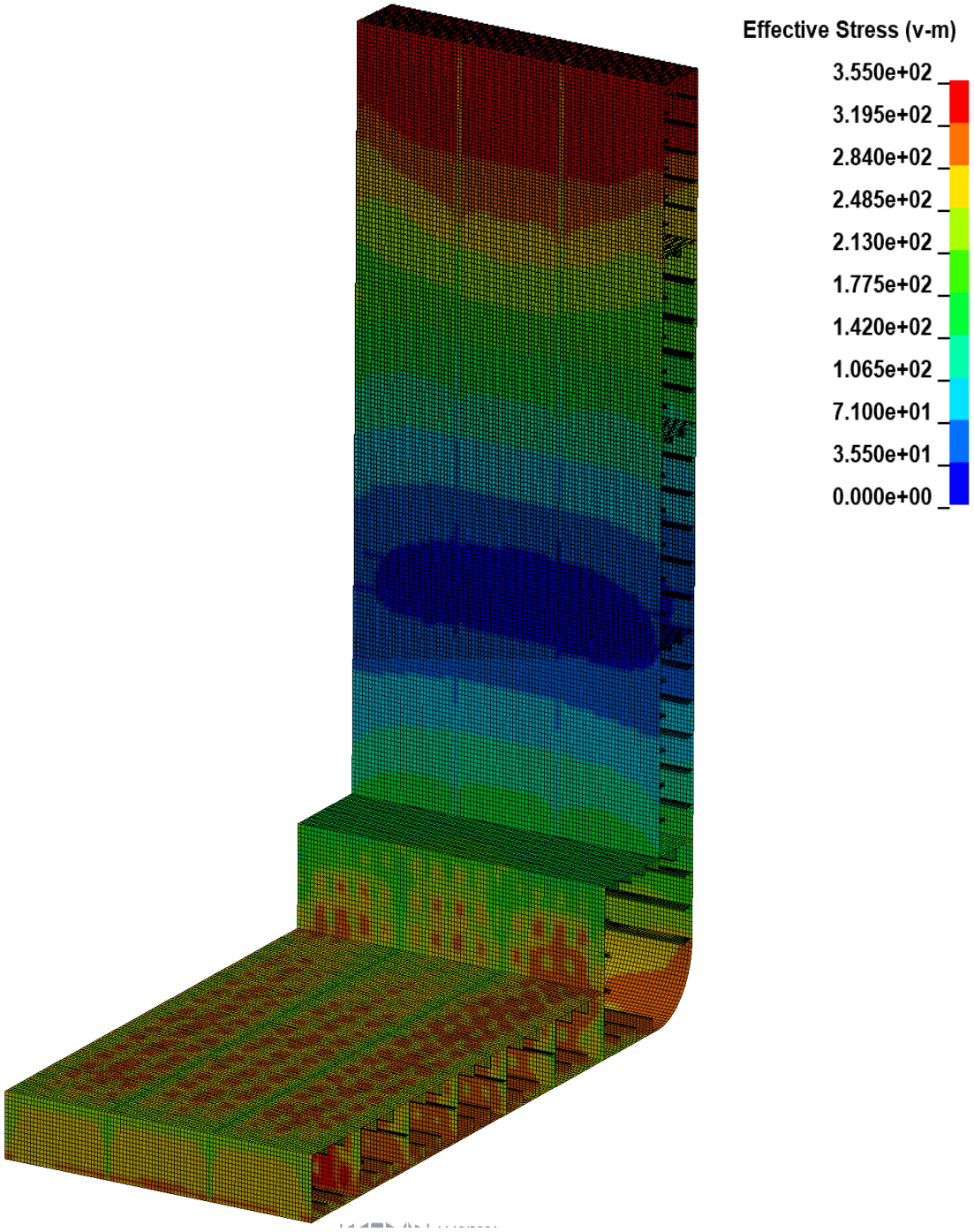

Fig 4. 33 Stress distribution of midship part at ultimate strength (2.5 sec load duration)

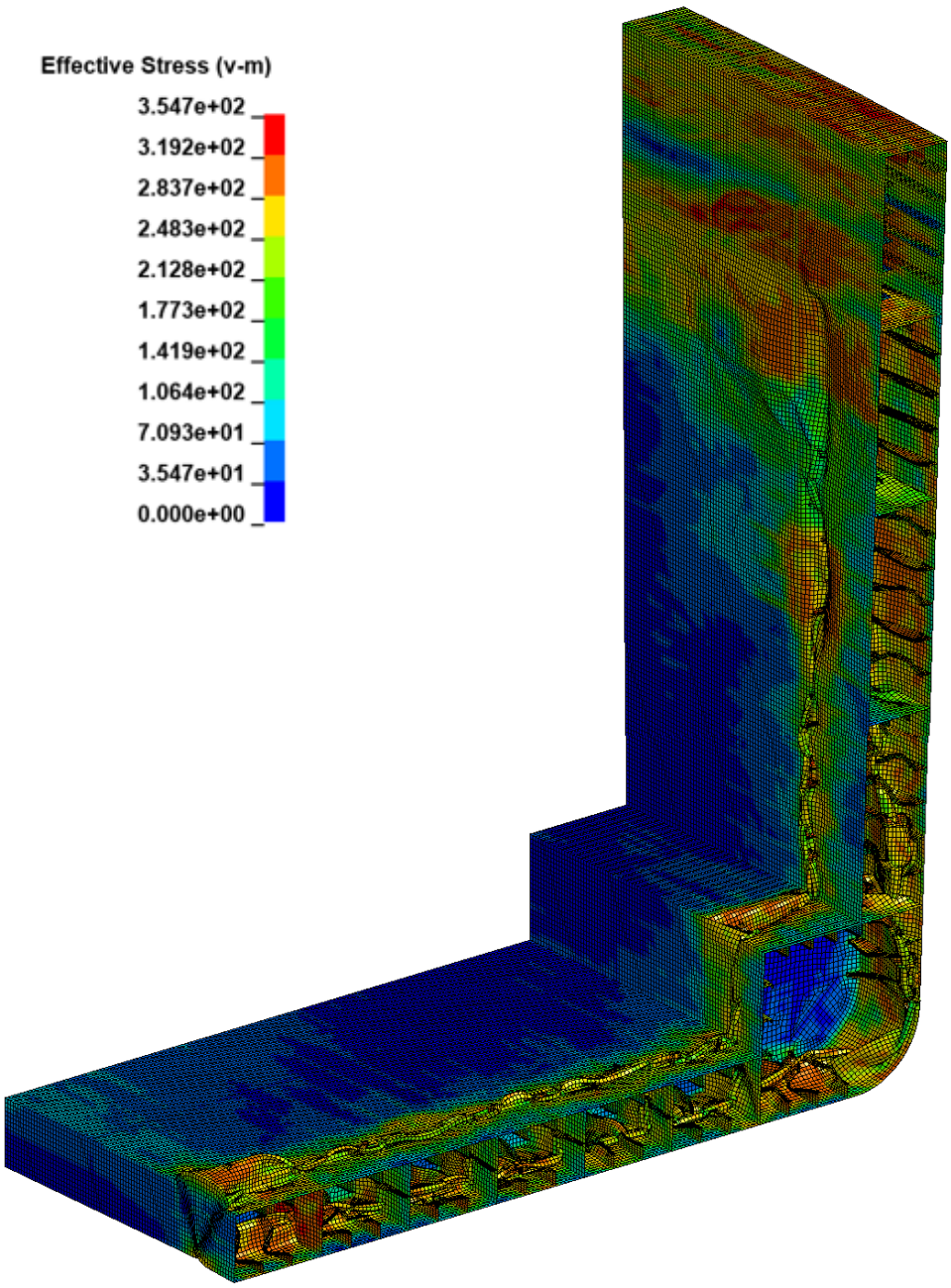

Fig 4. 34 Stress distribution of midship part at the end of anlaysis (2.5sec load duration)

In 3 sec load duration case, we can compare the FE-smith (CSR) result also since it also attained the ultimate strength. From Fig 4. 35, largest collapse extent can be found in LS-dyna, second largest in FE-smith (PBC) and third in FE-smith (CSR). Fig 4. 36,

Fig 4. 37 and Fig 4. 38 show stress-strain distribution of cross section, element stress-strain curves and time history of elements' strain during the dynamic collapse.

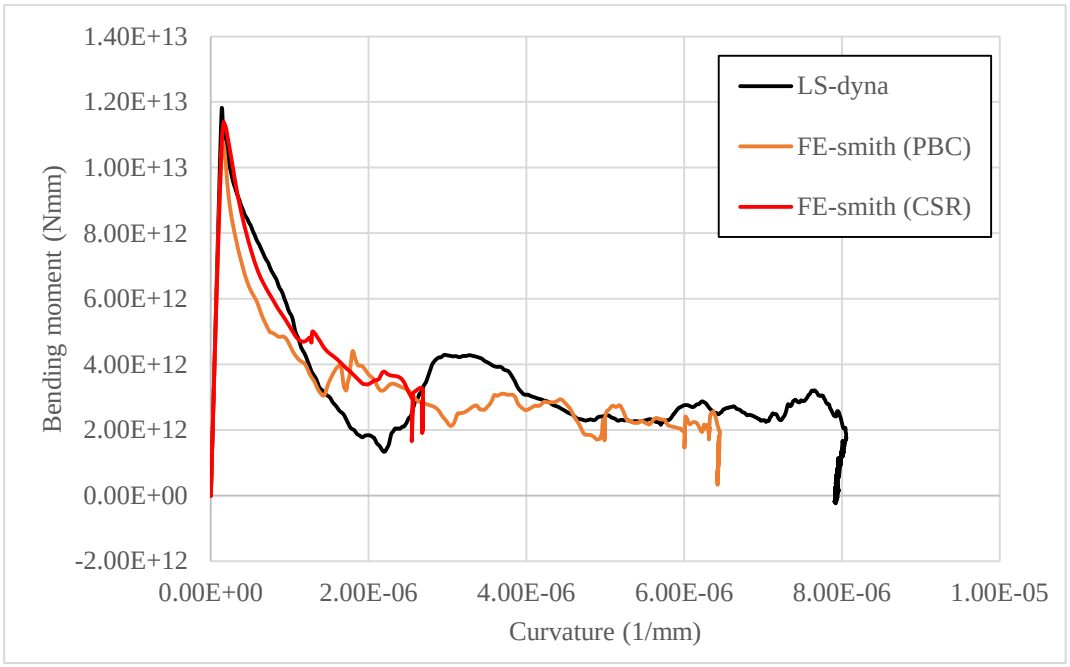

(a) Bending moment and curvature

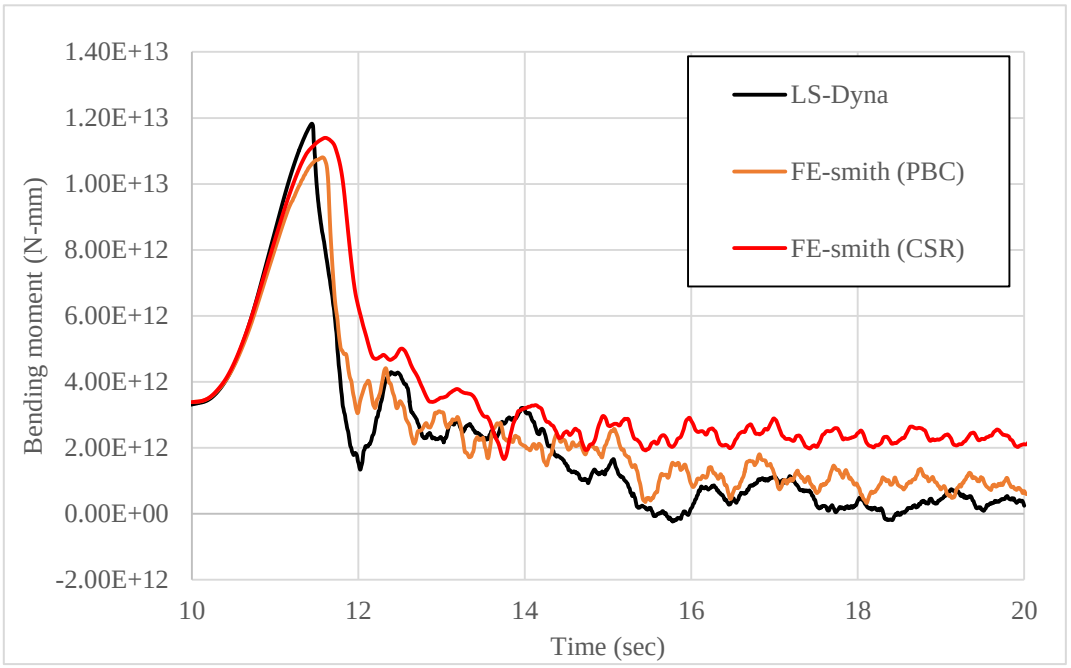

(b) Time history of moment

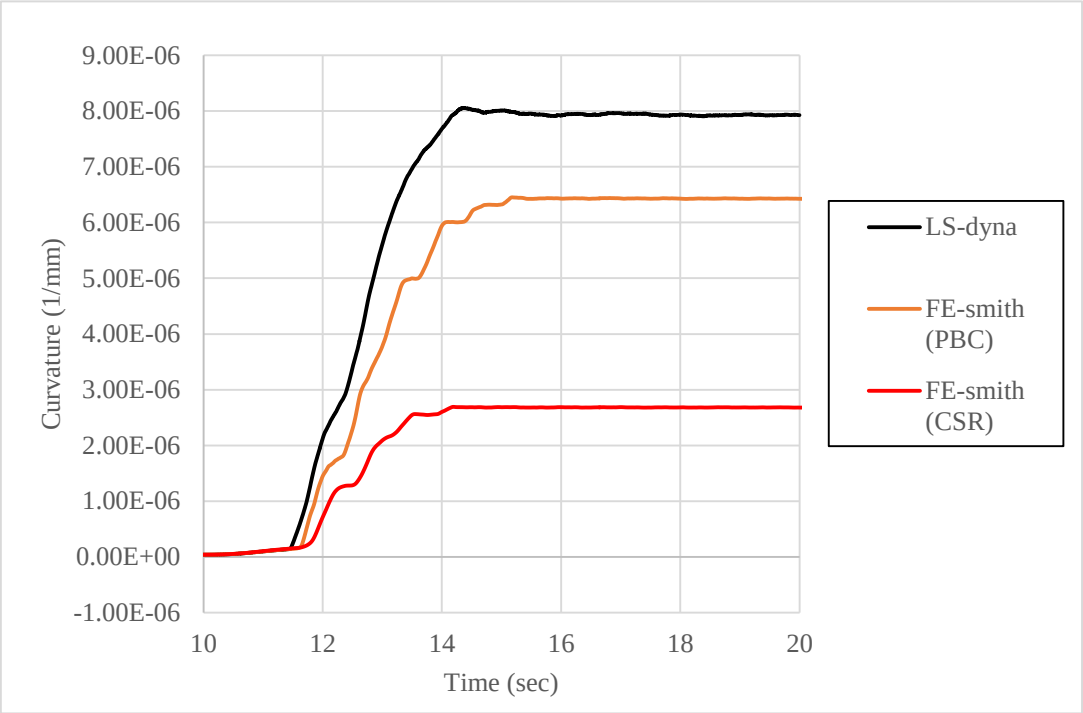

Fig 4. 35 Comparison between LS-dyna and FE-smith analyses

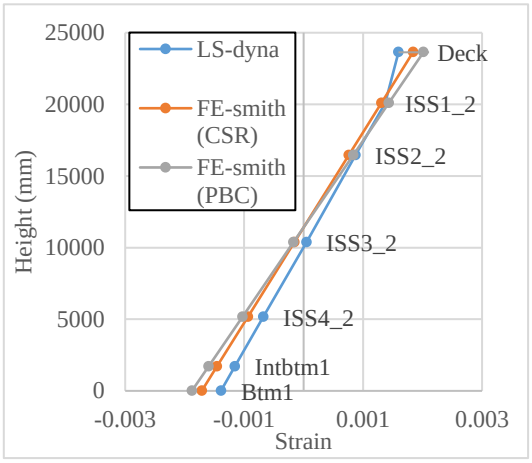

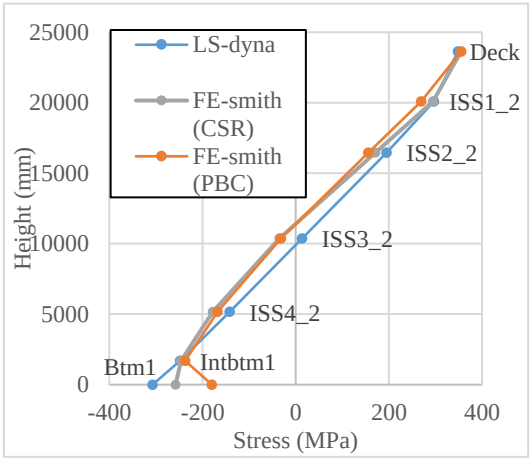

(a) Strain and stress distribution at ultimate strength

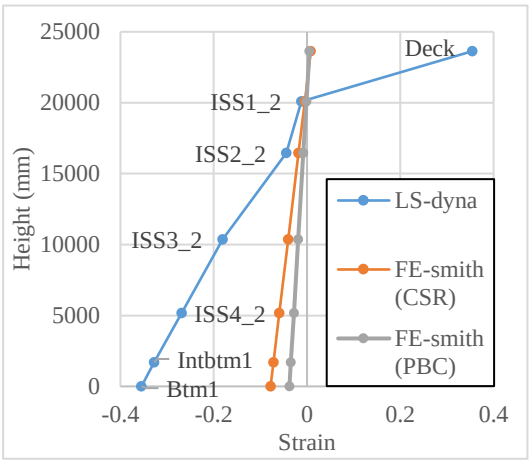

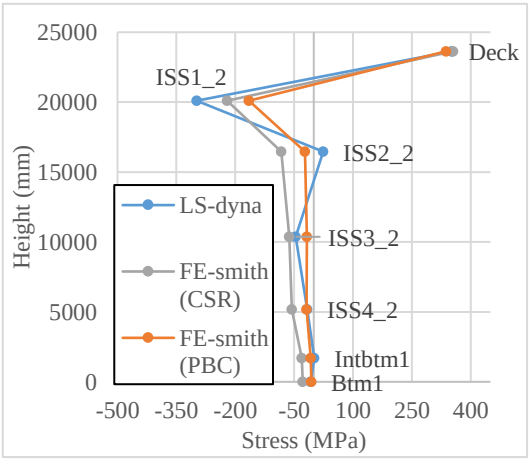

(b) Strain and stress distribution at the end of applied load

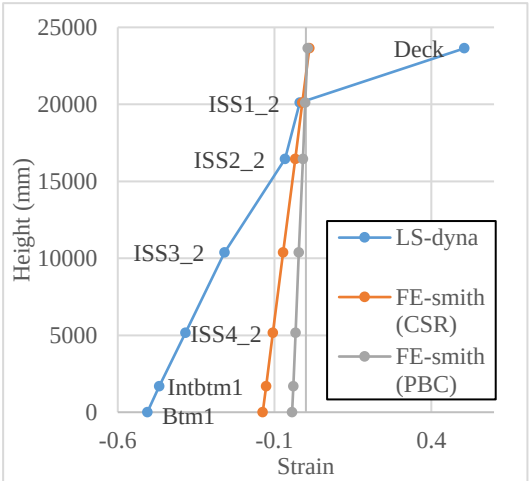

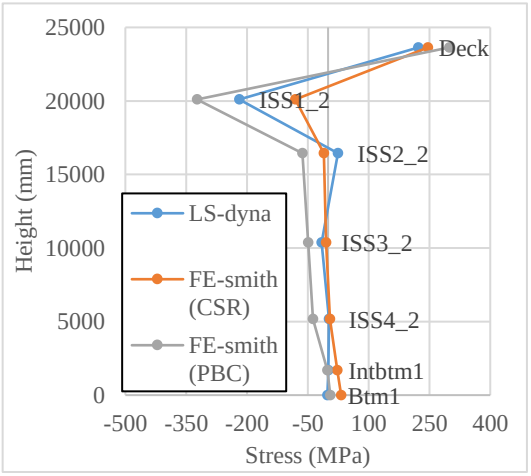

(c) Strain and stress distribution at the end of analysis

Fig 4. 36 Stress and strain contribution of cross section (3 sec load duration)

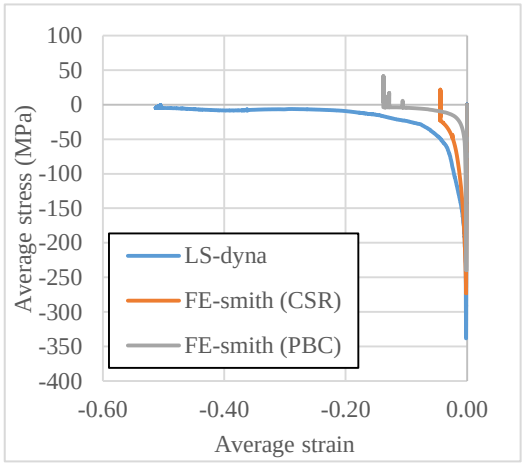

(a) Btm 1 element

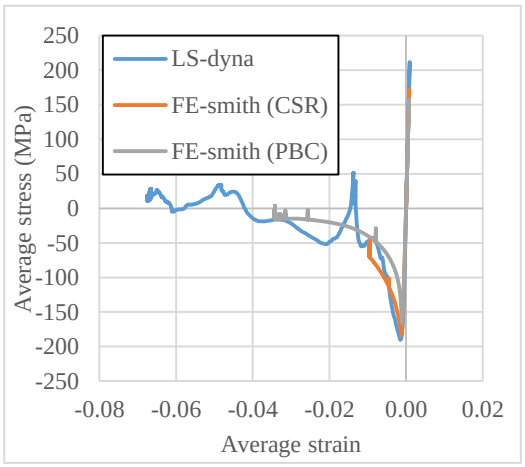

(d) ISS 3_2 element

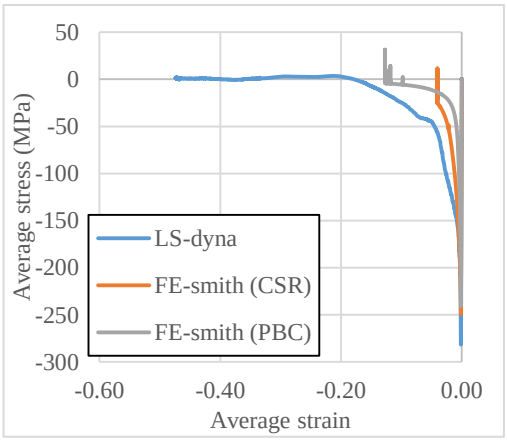

(b) Intbtm1 element

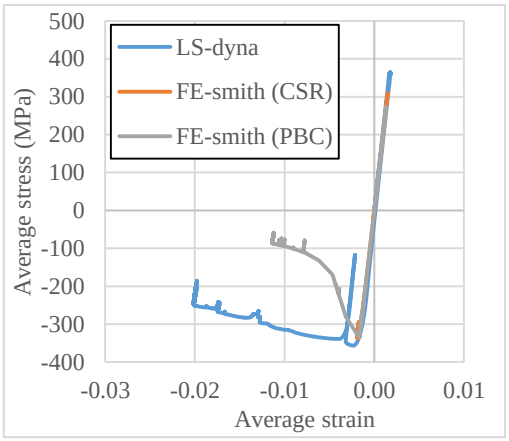

(e) ISS 2_2 element

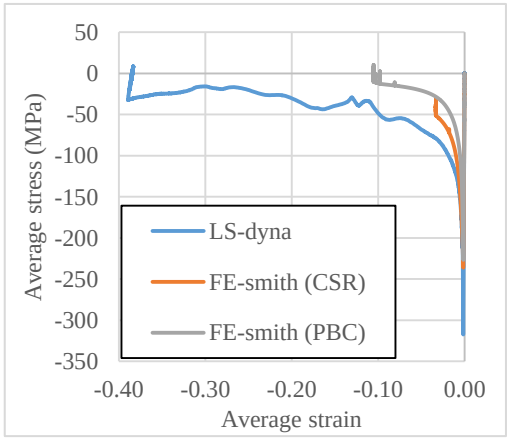

(c) ISS 4_2 element

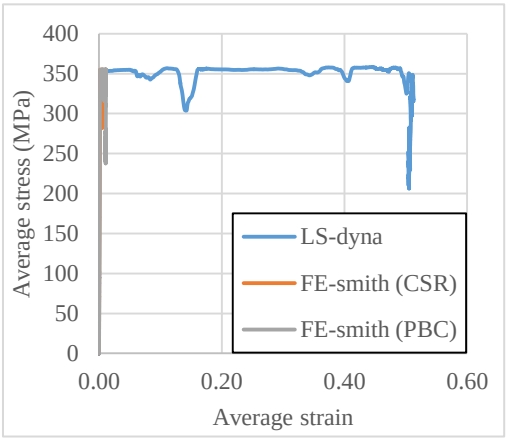

(f) Deck element

Fig 4. 37 Elements' average stress-strain during dynamic collapse (3sec load duration)

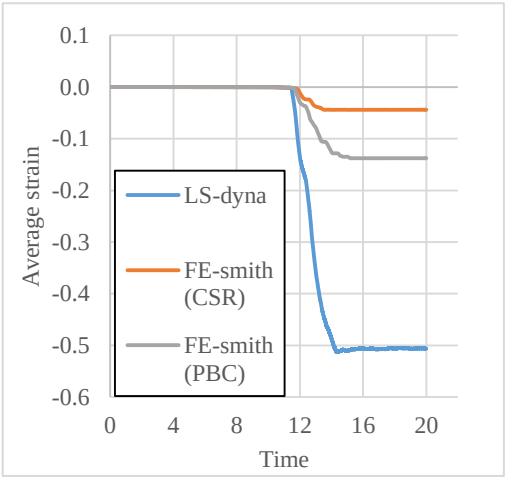

(a) Btm 1 element

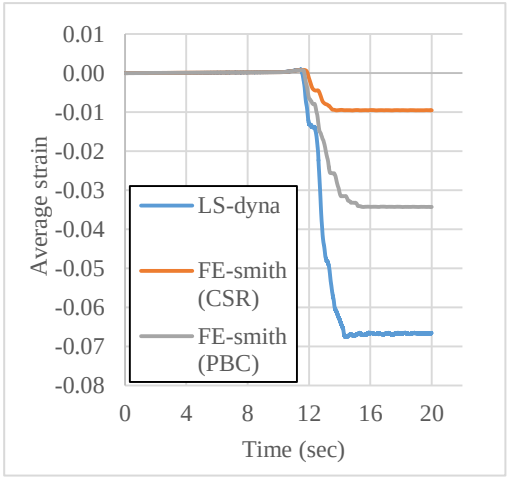

(d) ISS3_2 element

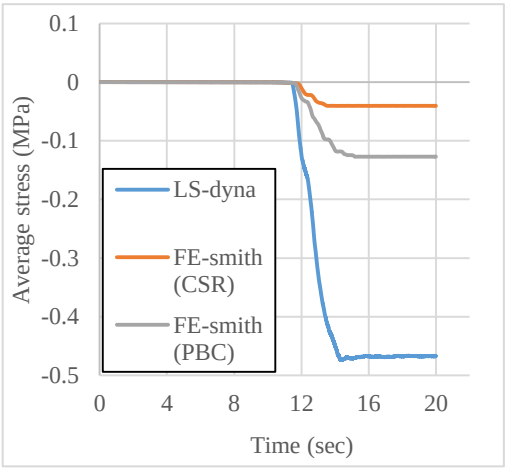

(b) Intbtm 1 element

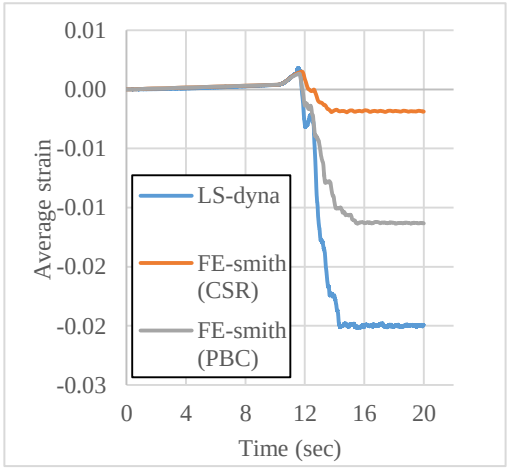

(e) ISS2_2 element

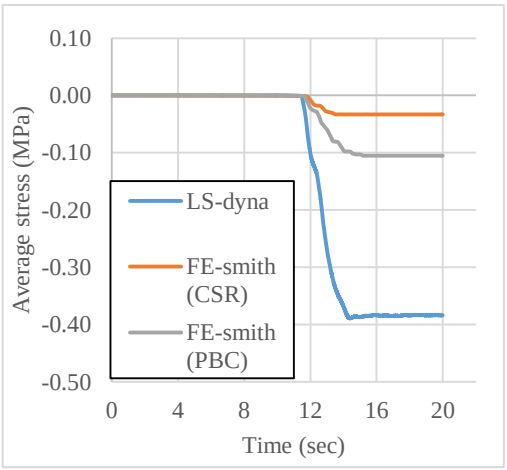

(c) ISS4_2 element

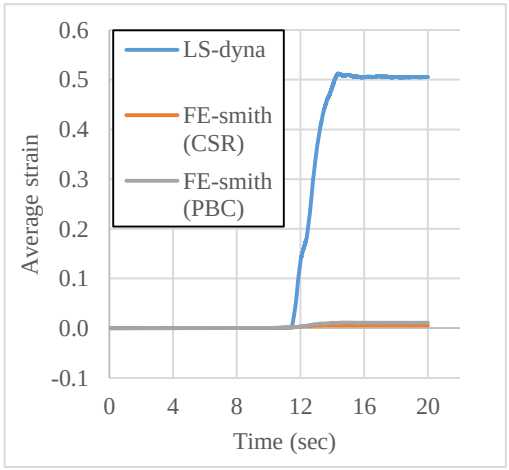

(f) Deck element

Fig 4. 38 Time history of element strain during dynamic collapse (3 sec load duration)

Fig 4. 39 shows the results of 3.5 sec load duration. For 3.5 sec case, LS-dyna analysis was terminated around 13 sec as the time step order becomes 10^{-11}. Results show the same behavior as previous cases.

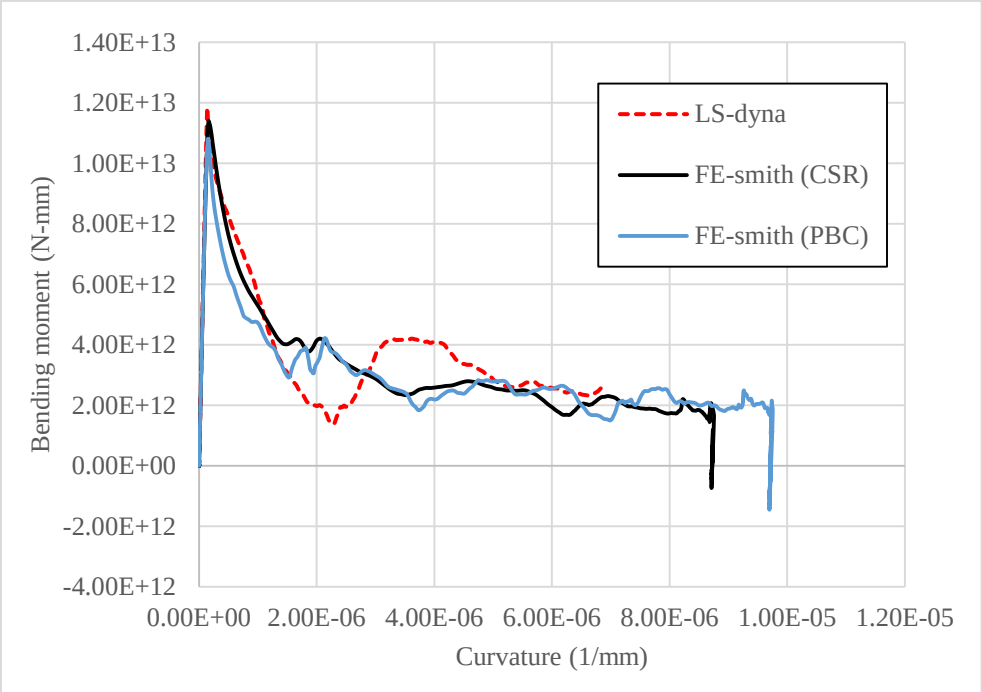

(a) Bending moment and curvature relationship

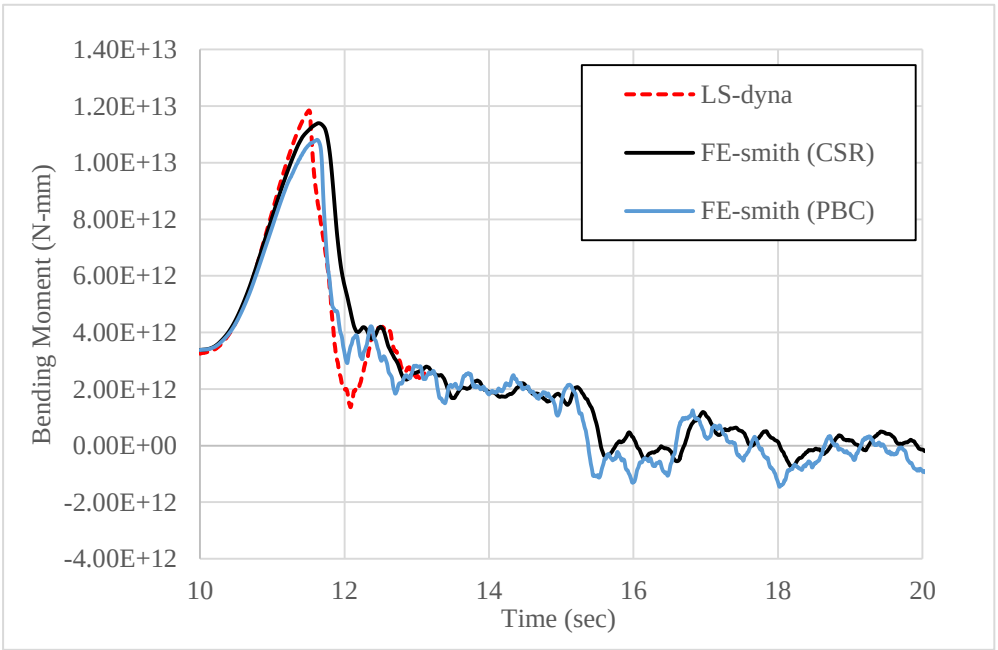

(b) Time history of bending moment

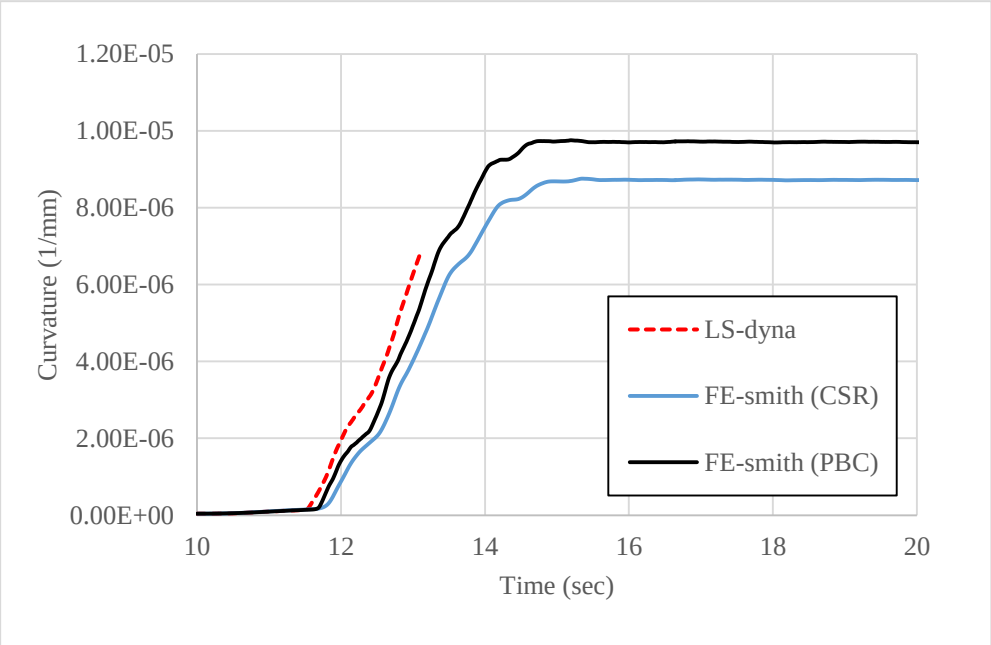

(c) Time history of curvature

Fig 4. 39 Comparison between LS-dyna and FE-smith analyses for 3.5 sec load duration

CPU time required for hull girder model by FE-smith and NFEA are summarized for different load duration cases in Table 4. 3. FE-smith is performed by i7-7600U CPU@2.80GHz and LS-dyna by i7-6700 CPU@3.4GHz.

Table 4. 3 Required CPU time

Load duration	Type	End time	FE-smith	LS-dyna
2.5 sec	Collapse analysis	20 sec	2.801 min	116.7 hours
3 sec	Collapse analysis	20 sec	3.365 min	120 hours
3.5 sec	Collapse analysis	13.1 sec	4.807 min	113 hours

4.6 Conclusions

Collapse analyses of uniform beam model and hull girder model are performed by using FE-smith NFEA and results are compared. Conclusions obtained from the results are

1. FE-smith can capture the dynamic collapse behavior of ship hull girder with reasonable accuracy in much shorter time compared to NFEA.
2. FE-smith (PBC) gives much closer result of collapse extent to NFEA than FE-smith (CSR). Discrepancy in collapse extent is due to the difference of adopted element stress-strain curves.
3. The assumption of plane cross section is one of the main source of the discrepancy between the results of FE-smith and NFEA.
4. Assumption of linear elastic unloading path leads to significant error in the post-unloaded or alternately loaded process. FE-Smith should be used up to the prediction of collapse extent due to first ultimate hull-girder failure. Further improvement is necessary concerning with the assumption of unloading stiffness.

Chapter 5

Parametric Dependency of Hull Girder Collapse Behavior

5.1 Introduction

Hull girder collapse is a complicated structural response influenced by dynamic factors such as added mass and damping as well as the structural strength. The degree of the dependency of collapse response on those factors will be different. Therefore, parametric dependency of hull girder collapse is investigated in this chapter using the hydro-elastoplastic beam model.

Xu et al. investigated the parametric studies on the collapse behavior of hull girder which is modelled as two rigid bodies connected with nonlinear rotational spring [32]. The effect of load duration, effect of amplitude of dynamic external moment, effect of added mass and effect of damping are investigated in their work.

There are common findings with regards to the effect on the collapse behavior and extent; i.e. the larger the applied load amplitude the larger the collapse extent; the larger the load duration the larger the collapse extent; the larger the damping the smaller the collapse extent. Xu et al. also showed that the added mass had the effect of reducing collapse extent. However, since the result was within the framework of a rigid body-spring model, the change of natural frequencies of hull girder vibration and the resulting effect on the bending moment time-history were not discussed. In this study, applying elastoplastic beam model, the added mass effects, which are more complex than the previous findings by Xu et al. has been discussed, together with interactive effects of different parameters.

5.2 Effect of load duration

Effect of load duration is as shown in Fig 5. 1, that is, the larger the load duration, the larger the collapse extent. This is because of the larger wave input energy for the larger load duration as was shown in Fig. 3.8. These input energy are mostly absorbed by the plastic deformation in the collapse process which leads to the larger collapse extent, i.e. residual deformation.

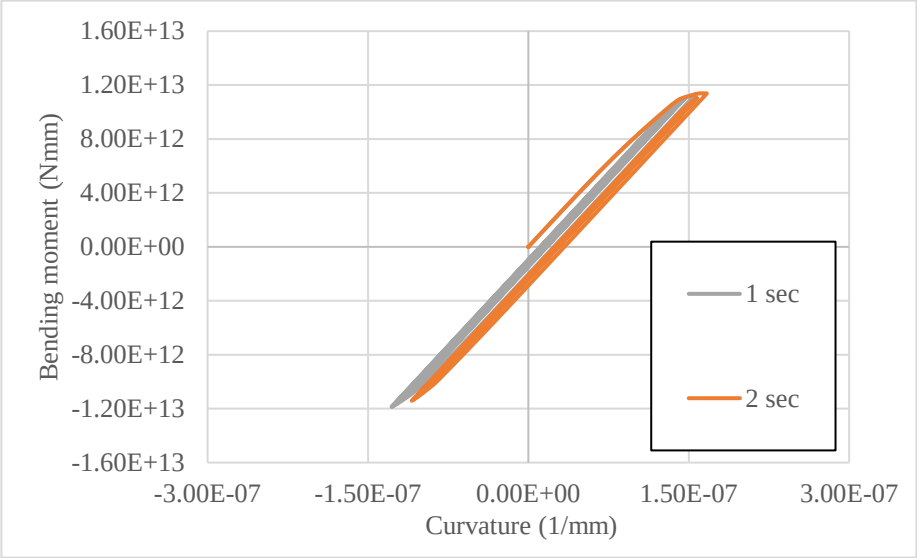

(a) Shorter load duration cases

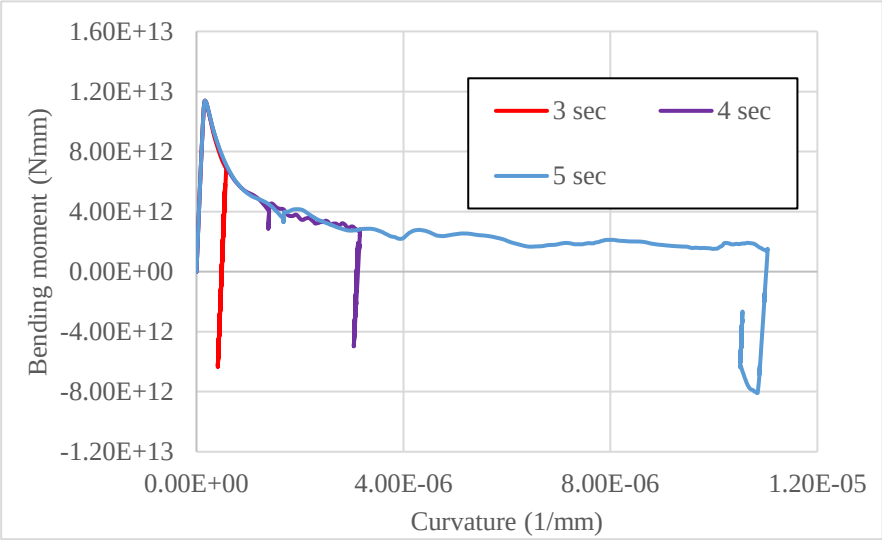

(b) Longer load duration cases

Fig 5. 1 Effect of load duration on hull girder collapse behavior

5.3 Effect of wave damping

Fig 5. 2 shows obtained elastic bending moment from the analyses of different wave damping value for different load duration cases. As described in section 3.4, added mass and damping coefficients are approximately calculated assuming a regular wave having a period of two times load duration. Those coefficients obtained for the target ship hull shape are here denoted by 100% and they are changed in the range of 20% to 100%. It is seen in Fig. 5.2 that the larger the damping coefficient, the smaller the elastic bending moment response. In the 1 sec load duration, only negligible effect is observed because hull girder deflection itself is small for smaller load duration case.

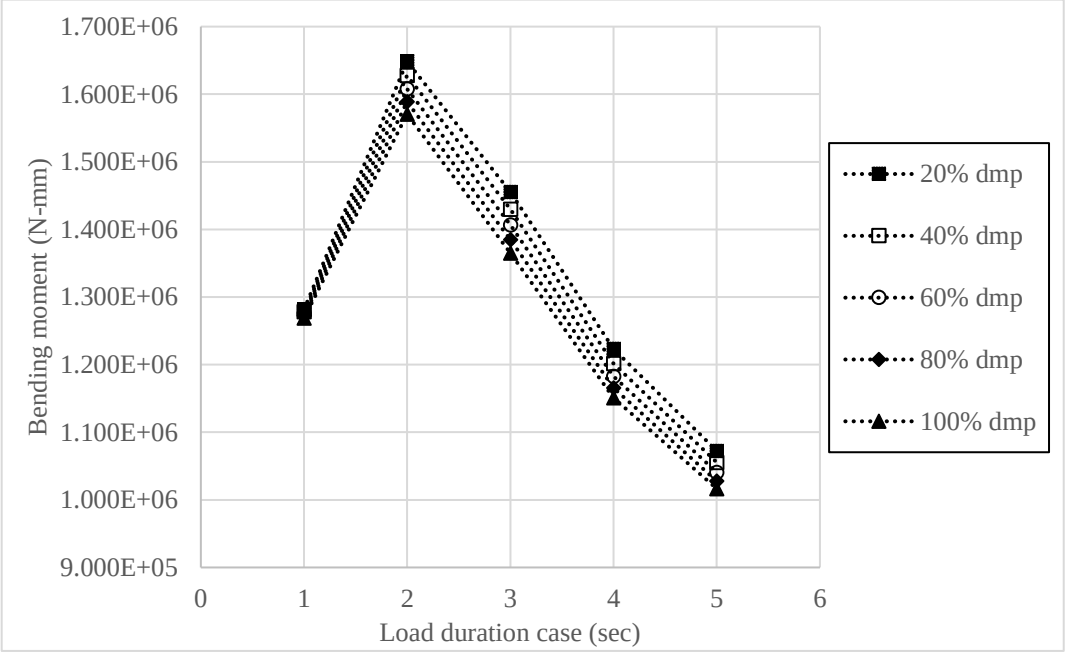

Fig 5. 2 Relationship between damping and elastic bending moment

Then the effect of wave damping on the collapse extent is investigated by two types of definition of applied impulsive load,

1. Case 1: Magnitude of the applied load is determined from the bending moment at collapsing section obtained by elastic analysis for 100% damping coefficient so that hull girder is subjected to 6% larger than its ultimate strength. Then the same magnitude of impulsive load is applied for collapse analysis of different wave damping coefficients.

2. Case 2: Magnitude of applied load is determined from the bending moment at collapsing section obtained by elastic analysis for different wave damping coefficient. The magnitude of load is determined so that hull girder is subjected to 6% larger than ultimate strength.

Fig 5. 3 shows the results of load duration of 2 sec, 3 sec and 5 sec under Case 1 condition. It can be concluded that the damping has significant influence on the collapse extent, namely the residual curvature, irrespective of the applied load duration, and the larger the damping coefficient, the smaller the collapse extent. This effect is particularly larger for shorter duration where the response velocities are relatively large. For the load duration of 2 sec, in Fig 5. 3(a), ultimate strength is not attained for the case of 100% damping whereas it is attained for other cases. These are essentially because larger amplitude of impulsive load relative to the ultimate strength is applied to smaller damping case for any duration time in Case 1. These results also show that the hull-girder collapse behavior must be basically treated as a dynamic response.

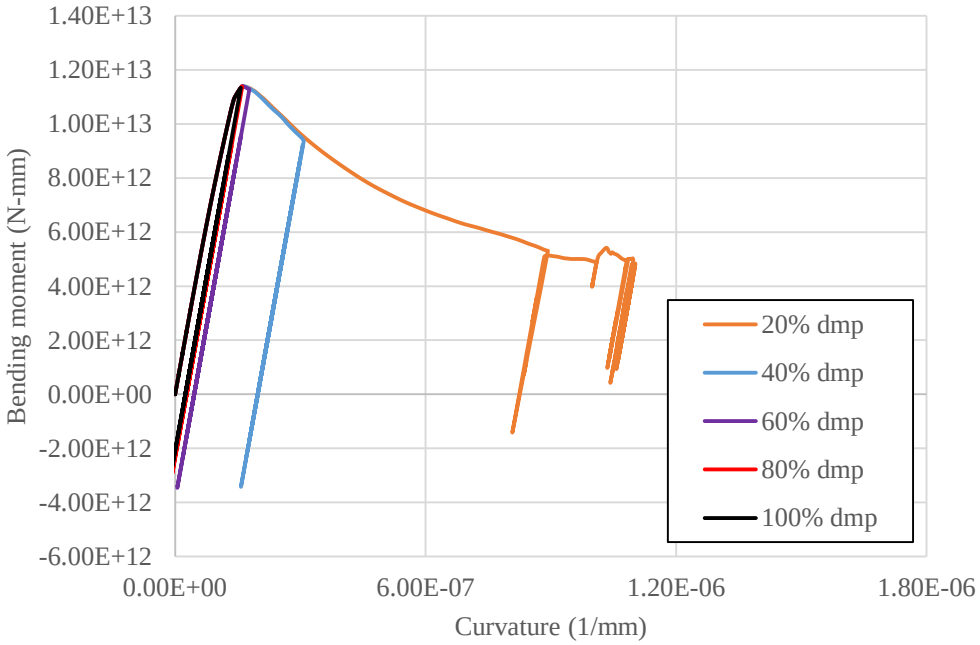

(a) 2 sec load duration

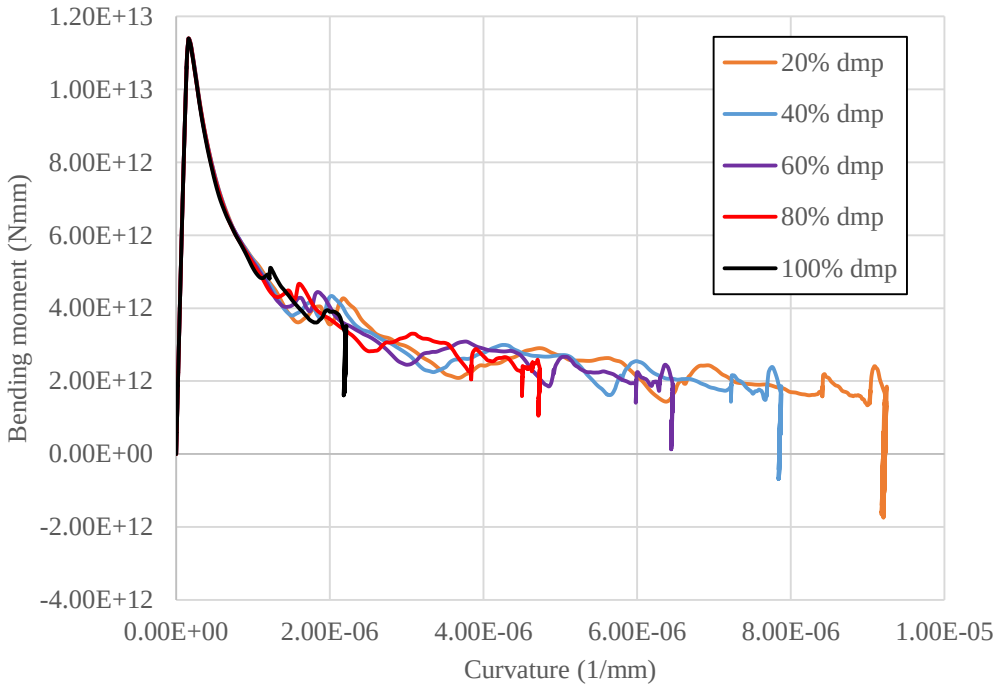

(b) 3 sec load duration

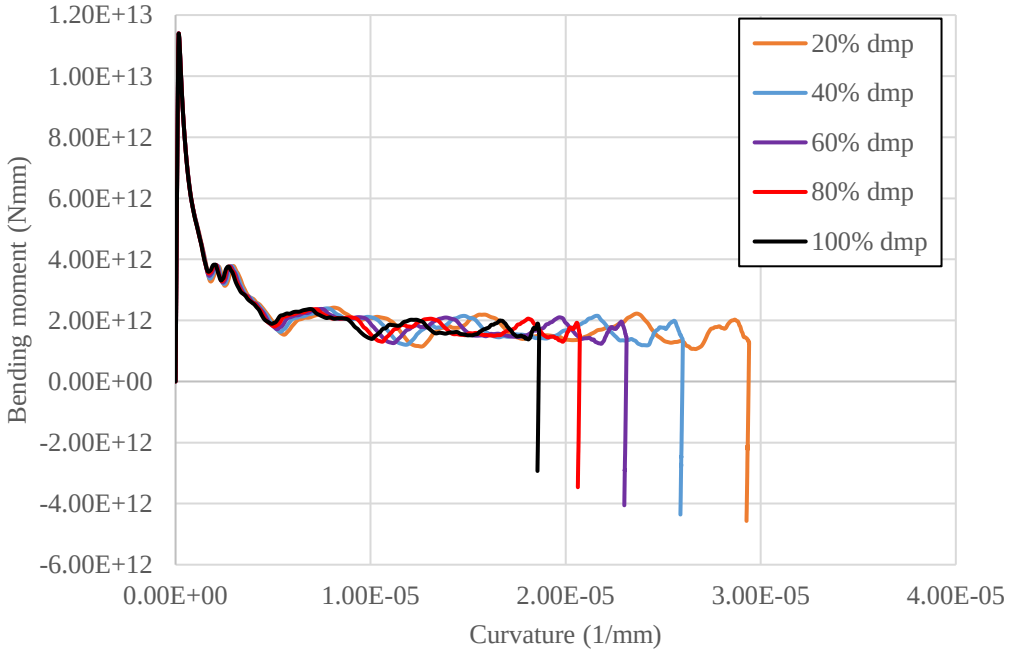

(c) 5 sec load duration

Fig 5. 3 Effect of wave damping on collapse extent (Case 1)

The results of Case 2 are given in Figs. 5. 4 to 5. 6. The results of small load duration cases are discussed firstly. Fig 5. 4 and Fig 5. 5 show the results of collapse analysis for 1 sec and 2 sec load duration cases. We can see that only small structural damage is observed for all cases and wave damping value does not have effect on the small plastic collapse. This is because wave damping value is small and effect of inertial force is much dominant in short load duration cases. The results of 5 sec load duration cases are drawn in Fig 5. 6. Although little damping effect is observed near the ultimate strength and some significant effect in the final collapse extent, because the plastic deformation more rapidly develops for smaller damping case.

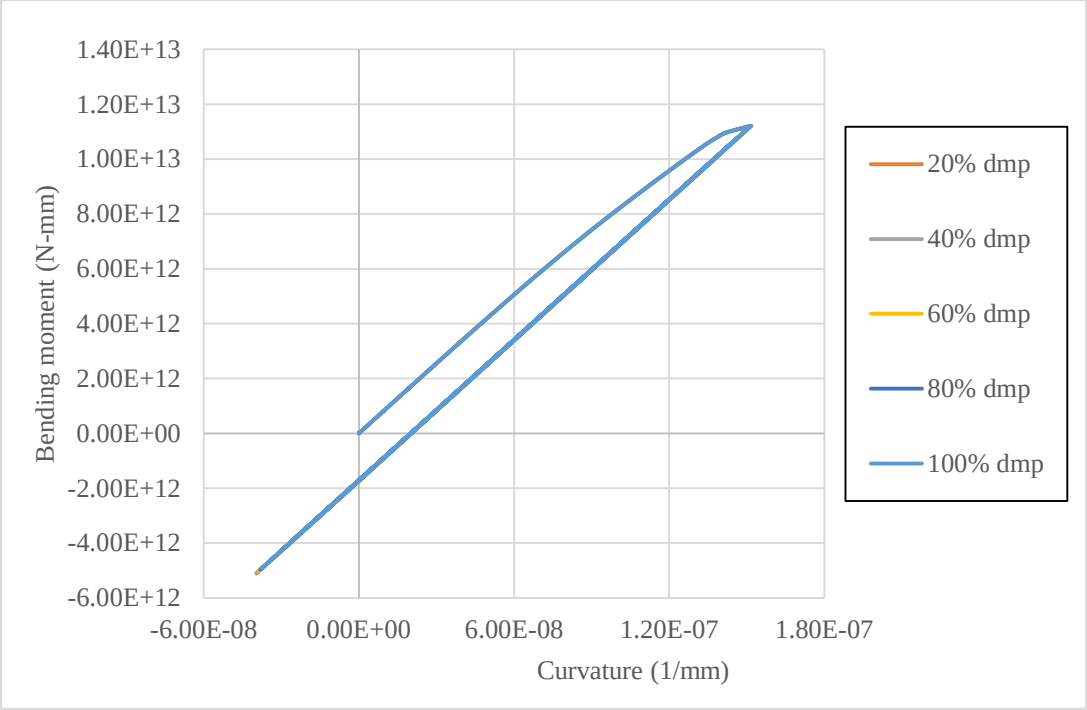

Fig 5. 4 Bending moment and curvature relationship of 1 sec load duration (Case 2)

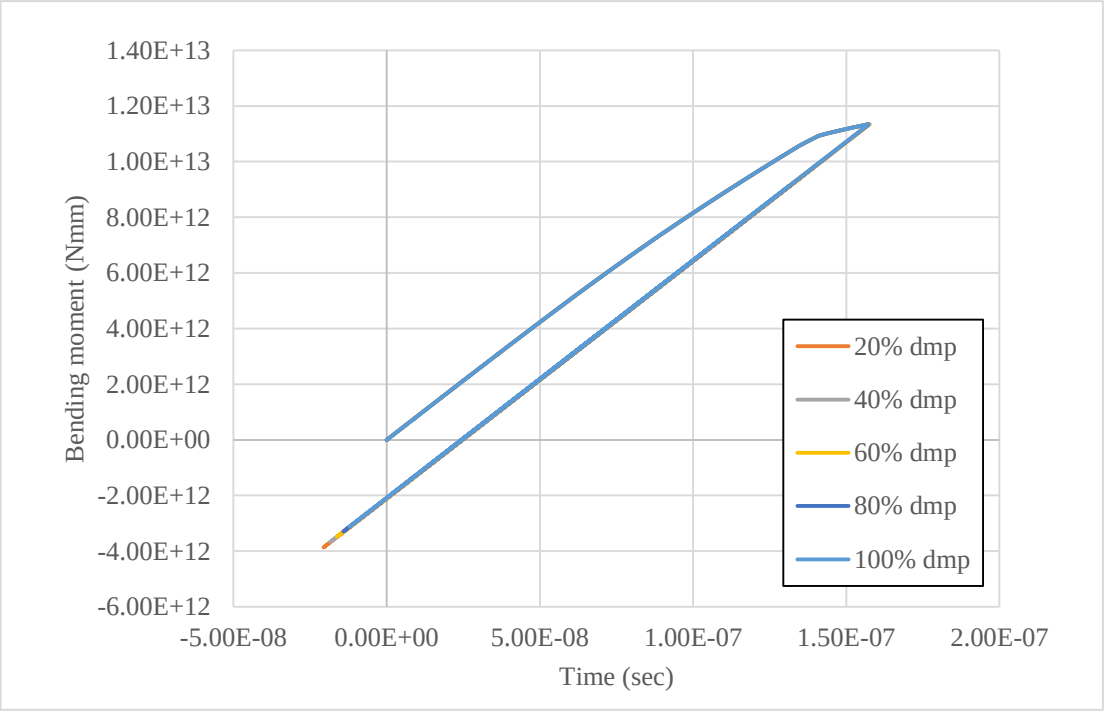

Fig 5. 5 Bending moment and curvature relationship of 2 sec load duration (Case 2)

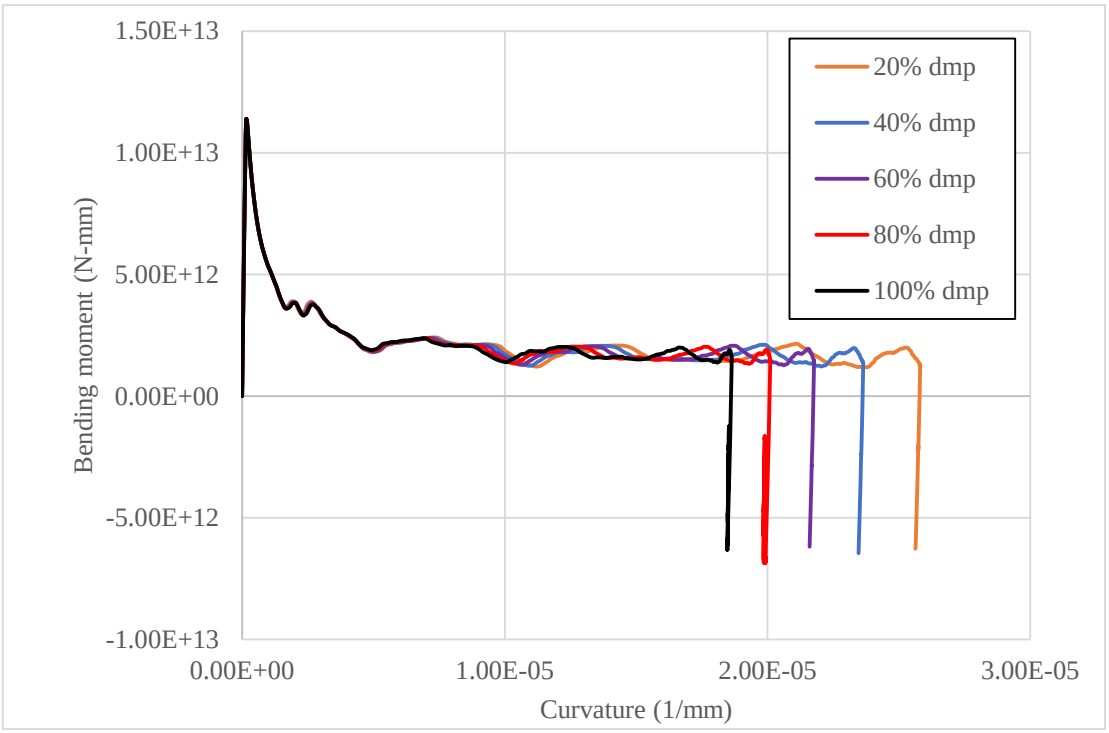

Fig 5. 6 Bending moment and curvature relationship of 5 sec load duration (Case 2)

5.4 Effect of added mass

According to the hydrodynamic theory, wave damping is decreased and becomes value of zero with increasing wave frequency. On the other hand, the added mass has different behavior. As the frequency is increased, added mass is increased and converged to a constant value. The added mass is related to the structural natural period. It is also highly related to the post-ultimate strength behavior, since the added mass generates the inertial force that is the main factor compensate the unbalance between external force and internal forces. Therefore, the effect of added mass is discussed in the following matters based on elastic analysis and collapse analysis.

(1) Natural period and load duration

(2) Correlation between wave damping with added mass

(3) Collapse extent

(1) and (2) are discussed from the elastic response analysis, and (3) from the collapse analysis.

5.3.1 Elastic analysis

(1) Natural period and load duration

Firstly, effect of added mass on elastic response is discussed. Analyses are performed by reducing the added mass by percentage. Natural period values of hull girder in waves with respect to the added mass percentage and load duration are shown in Fig 5. 7. It should be noted that in this study the added mass has been calculated from the linear harmonic heave motion of cross sections with period equal to the two times of applied load duration. The natural period therefore depends on the load duration.

As shown in Fig 5. 7, since the natural period is proportional to the square root of virtual mass, it increases with increase of the added mass value. It is seen that the natural period values are close to two times the load duration for the case of 1sec load duration but mostly smaller than two times the load duration for other cases. This means that dynamic effect is larger for short duration than the longer ones. Therefore, some different

duration times are selected to discuss. In addition, the analyses for selected load duration cases are carried out for four conditions as described in Table 5.1.

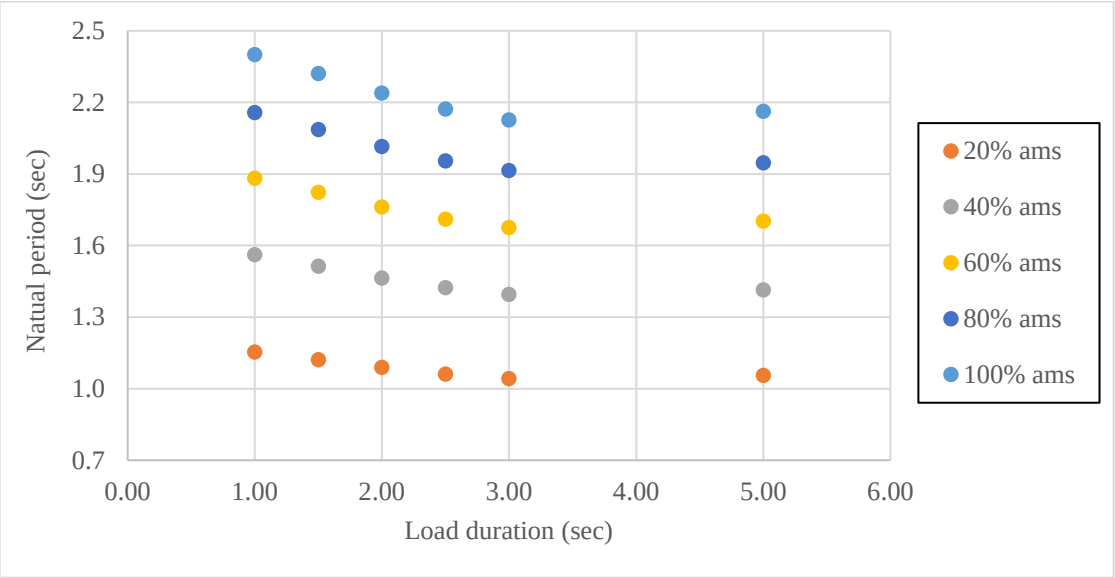

Fig 5. 7 Natural period of hull girder in relation with load duration and added mass

Table 5. 1 Conditions for analyses of parametric study of added mass

Analysis condition	Percentage of added mass	wave damping
A100_d0	100%	Not considered
A100_d1	100%	Considered
A20_d0	20%	Not considered
A20_d1	20%	Considered

(2) Correlation between wave damping with added mass

Firstly, only effect of added mass on elastic response is discussed. Fig 5. 8 shows the results of 5 sec load duration case. In the results obtained by A100_d0 and A20_d0, the vibration (bumps) in the bending moment response during load duration can be seen as the natural period is smaller than load duration in those cases. A20_d0 has more bumps because of its smaller natural period value compared to the load duration.

Then effect of wave damping in relation to added mass values is discussed. If we compare A100_d0 and A100_d1, wave damping just simply reduce the bending moment value. But in A20_d0 and A20_d1, added mass vibration during the load duration are all damped out due to the presence of wave damping. Therefore, elastic response and maximum bending moment occurrence time are different depending on the phase of velocity and acceleration.

Fig 5. 9 shows the results of 3 sec load duation. Same behavior as 5 sec load duration are observed except there is no phase difference after the load duration between A20-d1 and A20_d0. Fig 5. 10 shows the results of 2 sec load duration case. Here, phase lag after the load duration cannot be found in all conditions. Fig 5. 11 shows the results of 1 sec load duration case. In this case, added mass vibration is dominant and hull girder vibrates with natural period from the beginning. Also phase lag due to damping is not found after the load duration. This is because added mass effect is dominant compared to wave damping effect for smaller load duration case.

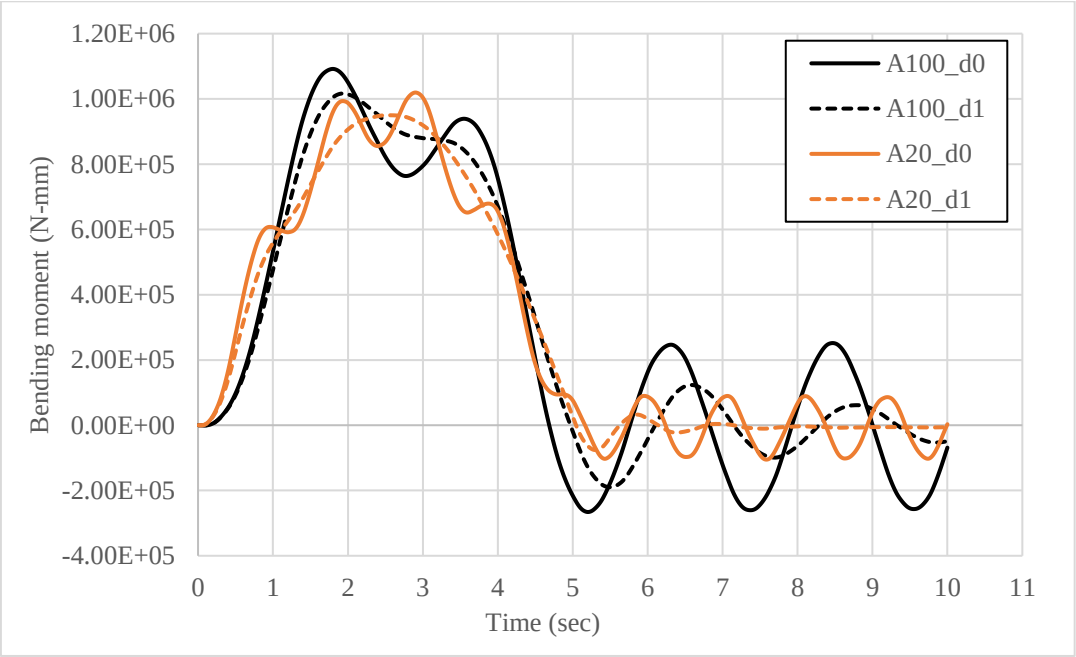

Fig 5. 8 Effect of added mass and damping on elastic response of 5 sec load duration

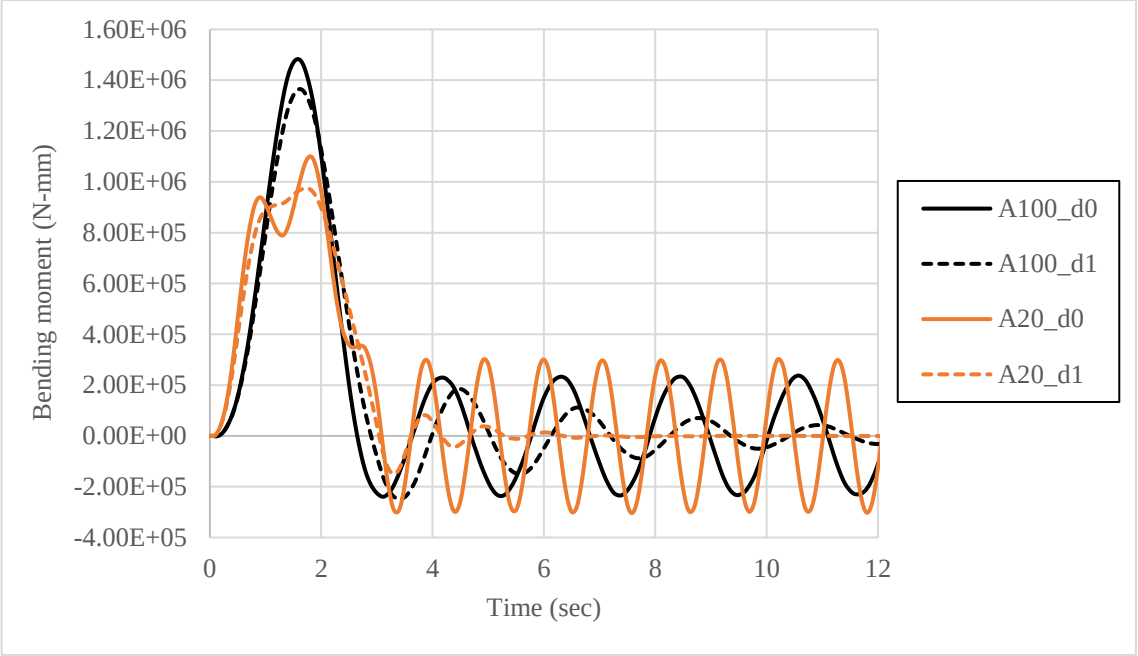

Fig 5. 9 Effect of added mass and damping on elastic response of 3 sec load duration

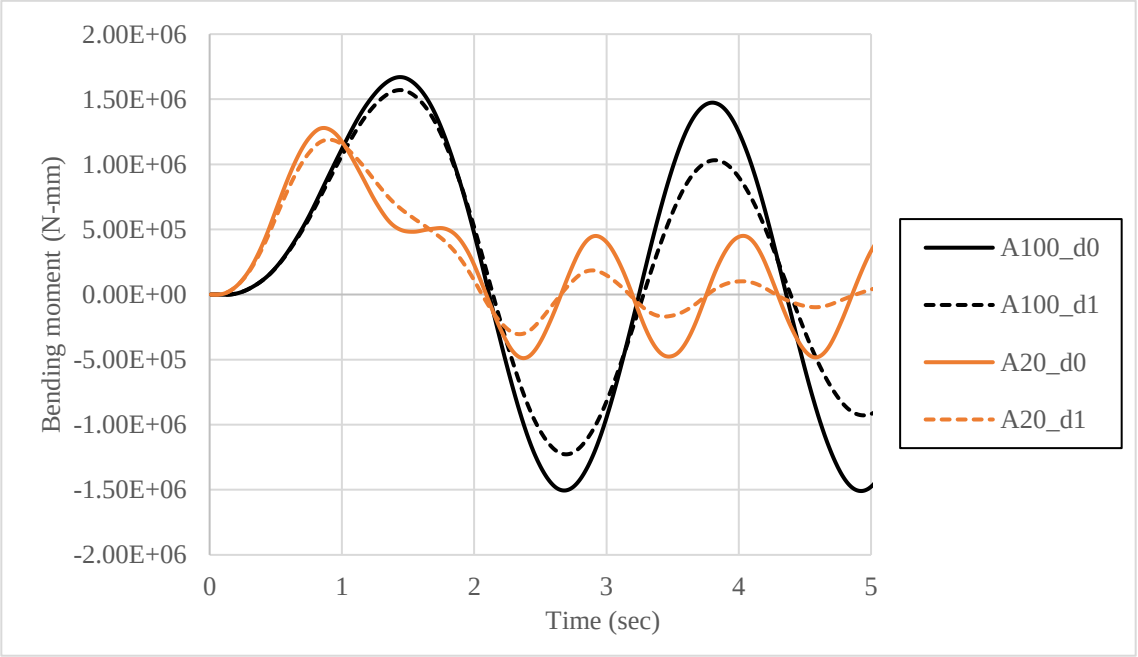

Fig 5. 10 Effect of added mass and damping on 2 sec load duration

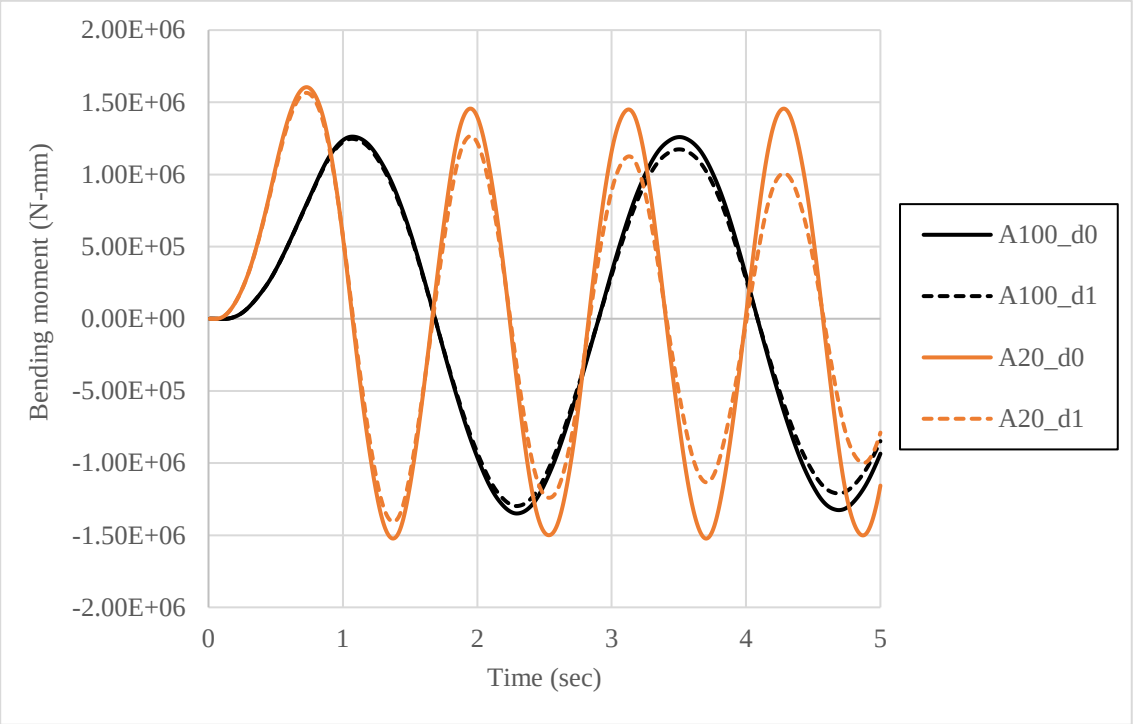

Fig 5. 11 Effect of added mass and damping on elastic response of 1 sec load duration

Regarding the maximum bending moment magnitude that directly affect the collapse behavior, it is noticed from Figs 5.9 to 5.11 that the maximum bending moment magnitude are different depending on the added mass and damping value. For 5 sec, 3 sec and 2 sec load durations, as shown in Fig 5. 8, 5.9 and 5.10, the maximum bending moment is larger when the added mass value is larger. For 1 sec load duration, bending moment is smaller when the added mass value is larger as shown in Fig 5. 11.

It is noted from the above results that compared to the effect of damping, the effect of added mass has larger influence on the response elastic bending moment. Bending moment magnitude and its occurrence time is directly related to relation between the natural period and load duration, and also phase of the velocity and accleration. The effect of added mass on collapse extent is discussed next.

5.3.2 Collapse analysis

Fig 5. 12 shows the relationship between bending moment and added mass obtained by elastic analysis without considering damping. For short duration of 1 sec, the bending moment is more dynamically exerted and the maximum value is smaller for larger added mass. For long duration, larger bending moment is exerted for larger added mass.

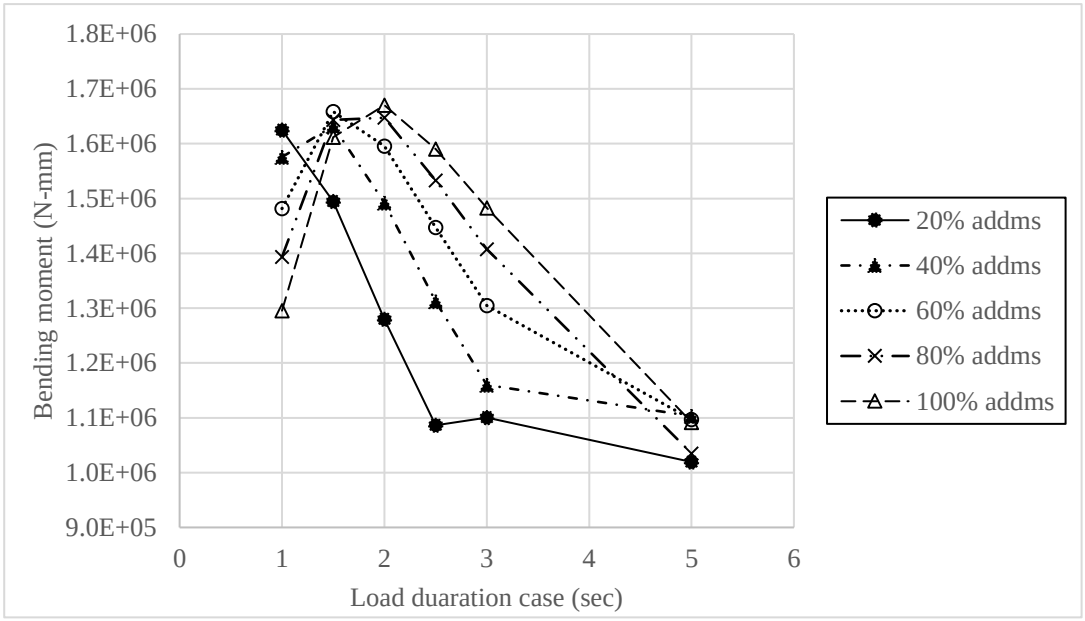

Fig 5. 12 Relationship between added mass and elastic bending moment

To discuss the effect of added mass on the collapse extent, two types of definition of applied impulsive load are considered in the same manner as parametric study on damping effects.

1. Case 1: Magnitude of the applied load is determined from the bending moment at collapsing section obtained by elastic analysis for 100% added mass so that hull girder is subjected to 6% larger than its ultimate strength. Then the same magnitude of impulsive load is applied for collapse analysis of different added mass.
2. Case 2: Magnitude of applied load is determined from the bending moment at collapsing section obtained by elastic analysis for different added mass. The

magnitude of load is determined so that hull girder is subjected to 6% larger than ultimate strength.

Results obtained by Case1 condition are discussed. Fig 5. 13 and Fig 5. 14 show the results of 2 sec and 3 sec load duration case. We can see that the collapse extent is smallest for 20% added mass case and it increases with the added mass. This is because the smaller bending moment is exerted for smaller added mass when the same magnitude of impulsive load is applied as shown in Fig 5. 12.

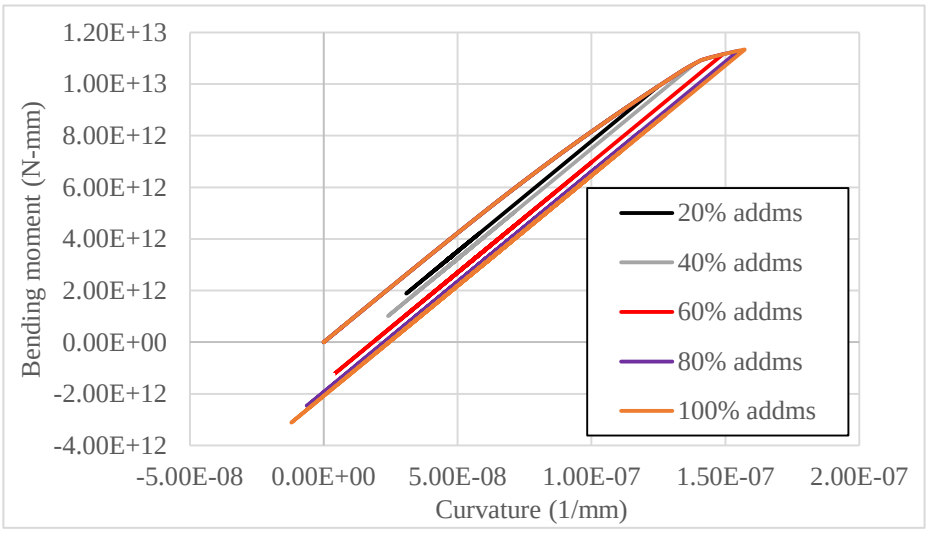

Fig 5. 13 Effect of added mass on collapse extent of 2 sec load duration (Case 1)

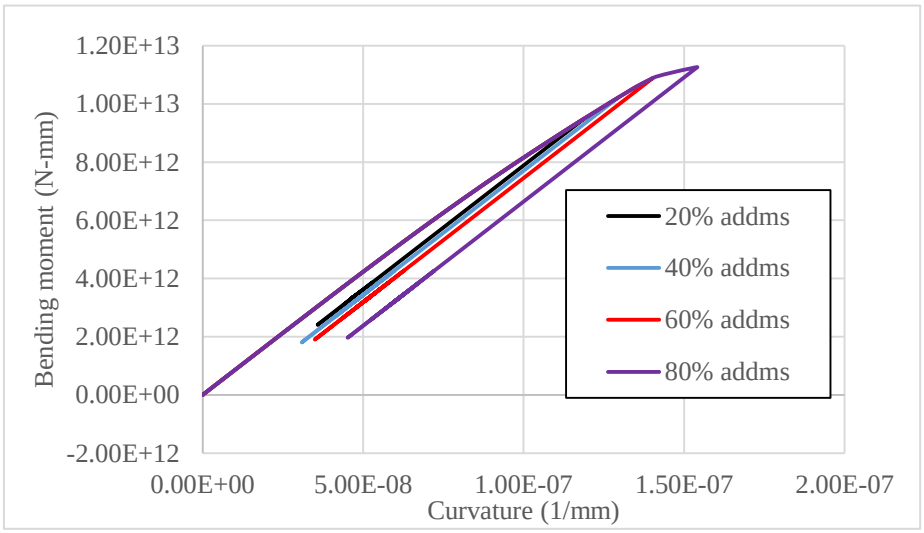

(a) 20% to 80% added mass

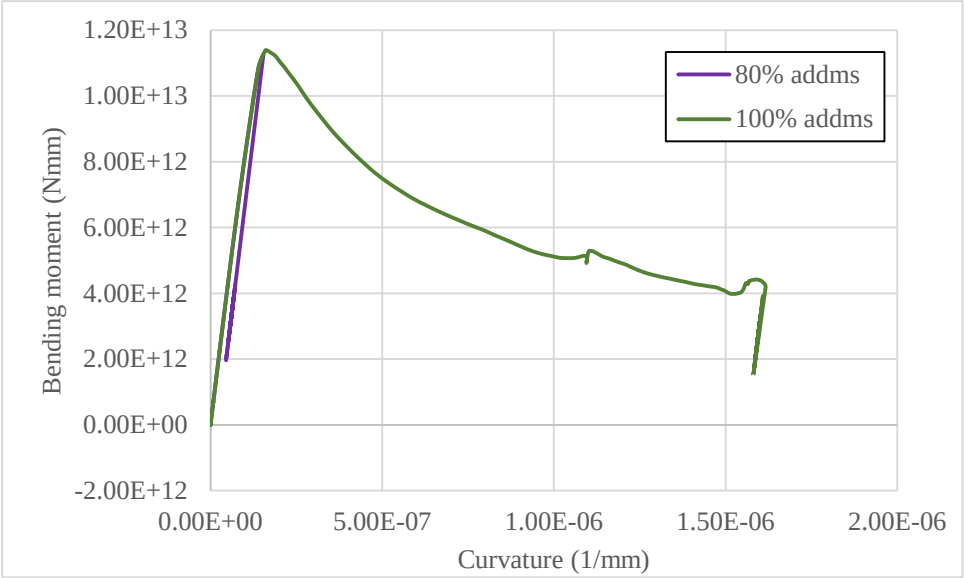

(b) 80% and 100% added mass

Fig 5. 14 Effect of added mass on collapse extent of 3 sec load duration (Case 1)

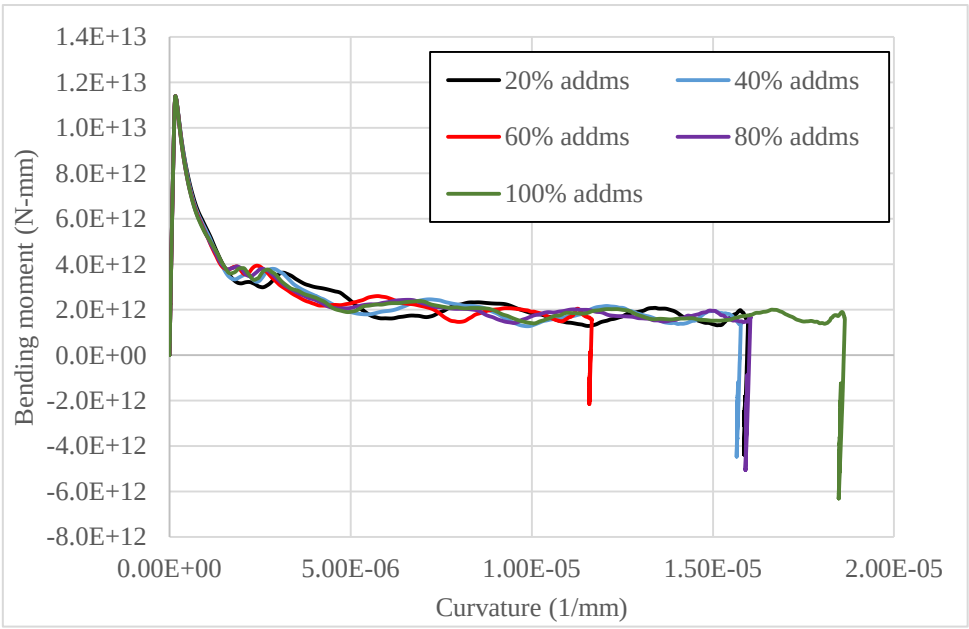

Fig 5. 15 Effect of added mass on collapse extent of 5 sec load duration (Case 1)

Fig 5. 15 shows the results of 5 sec load duration case. In 5 sec load duration case, we can see that elastic bending moment response is not changing proportionally to the value of added mass unlike other cases as can be seen in Fig 5. 12. This is because the natural period is much smaller than load duration compared to the other cases and the elastic bending moment response is highly affected by the change of added mass value and the resulting time history of vibration. This will be discussed later in Fig 5. 18 in more detail.

On the other hand, Fig 5. 16 shows the time history of curvature obtained for Case 2 of 2 sec duration time. The collapse extent is larger for smaller added mass. In Case 2, the same magnitude of maximum bending moment is exerted at the cross section. The difference in the collapse extent is therefore due to the difference of the inertia force that compensates the unbalanced force between the applied bending moment and the structural capacity. For larger added mass, the unbalance force can be compensated by smaller deformation and thus smaller associated acceleration. It can be concluded that the collapse extent is highly influenced by the added mass. It is therefore essential to consider the hydro-elastoplasticity to estimate the collapse extent after hull girder collapse.

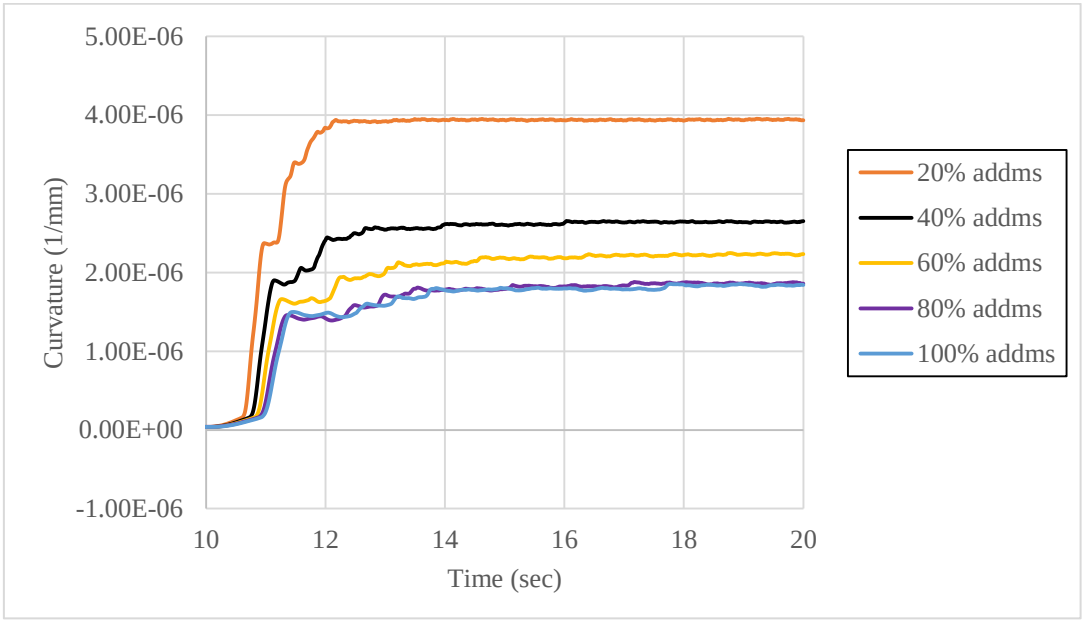

Fig 5. 16 Effect of added mass on collapse extent of 2 sec load duration (Case 2)

Similar behavior has been observed for shorter load duration mostly, but longer load duration shows different behavior. Fig 5. 17 show the time history of curvature obtained for Case 2 of 3 sec and 5 sec load duration time. In those cases, the dependency of the collapse extent on the added mass is not as simple as in Fig 5. 16.

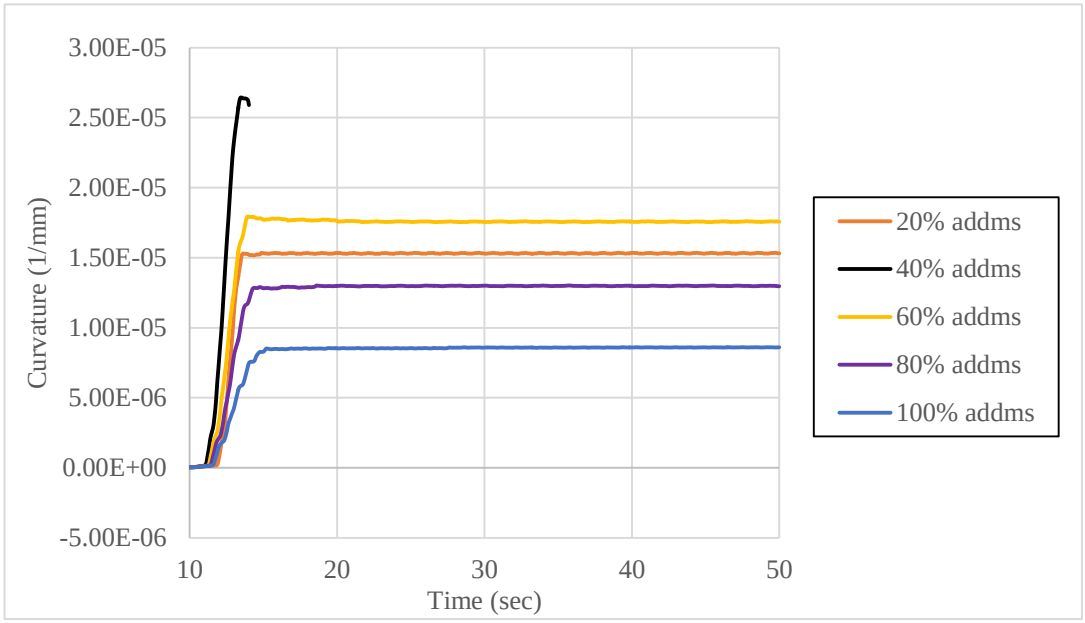

(a) 3sec load duration

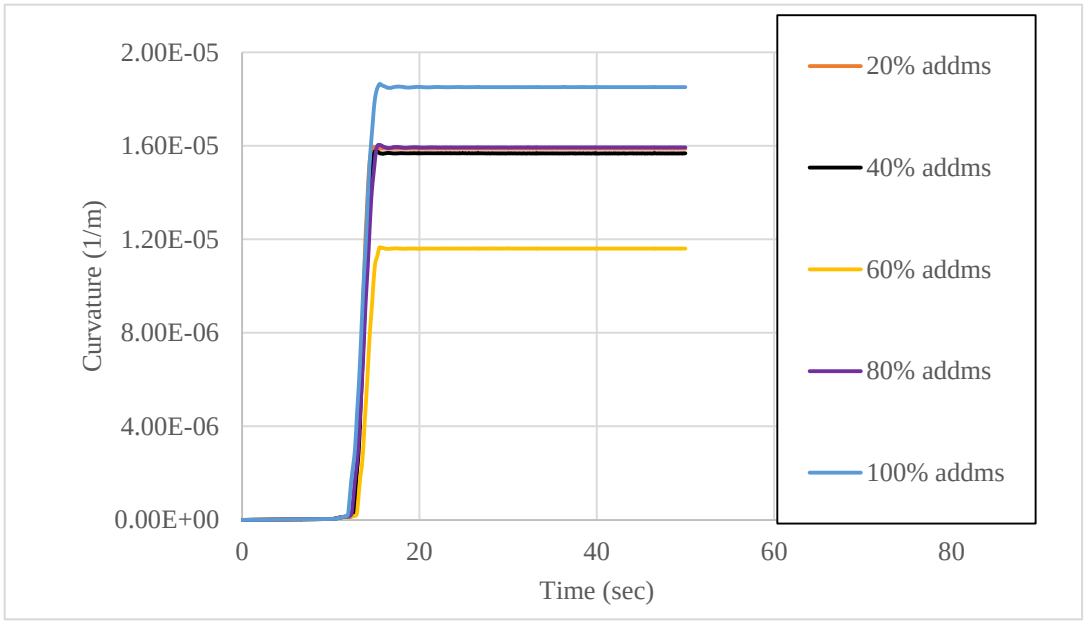

(b) 5 sec load duration

Fig 5. 17 Effect of added mass on collapse extent of longer load duration (Case 2)

To explore the possible reasons, the time histories of applied bending moment are compared as shown in Fig 5. 18. For the case of 2 sec load duration, Fig 5. 18(a), the bending moment due to vibration once increases and then decreases during an impulsive loading, while for 3 sec and 5 sec load duration, Fig 5. 18 (b) and Fig 5. 18 (c), some fluctuations of bending moment take place during an impulsive loading and this sometime enhance collapse extent and sometimes not. It is found that the collapse extent therefore depends not only the degree of inertia force generated by added mass but also on the relationship between the load duration and the natural period that also depends on added mass. Further study is needed to clarify the dependency of the collapse extend on the added mass.

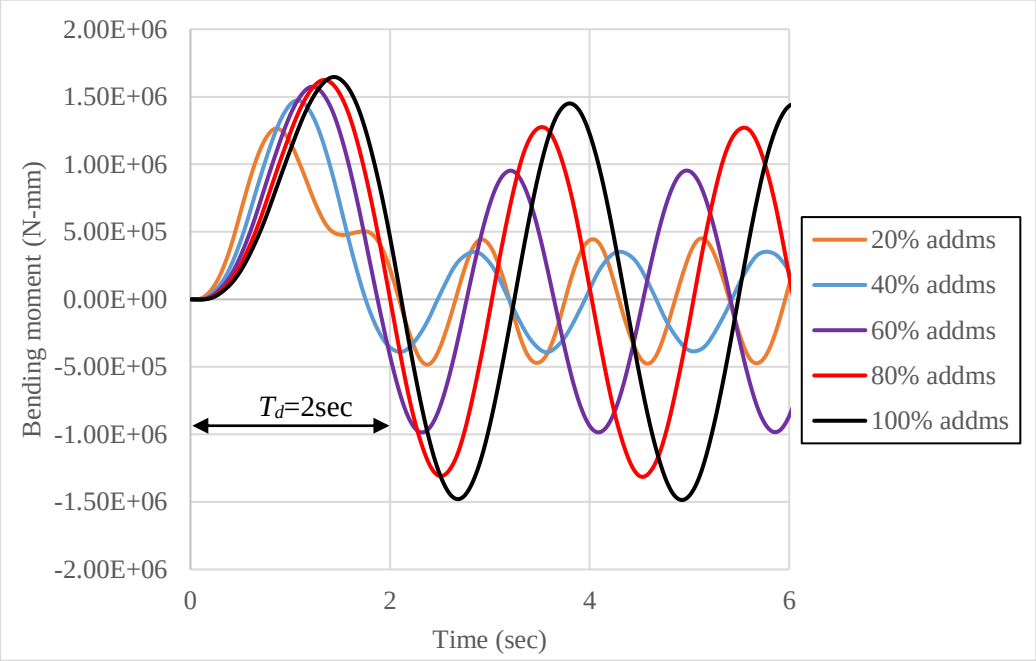

(a) Load duration of 2 sec

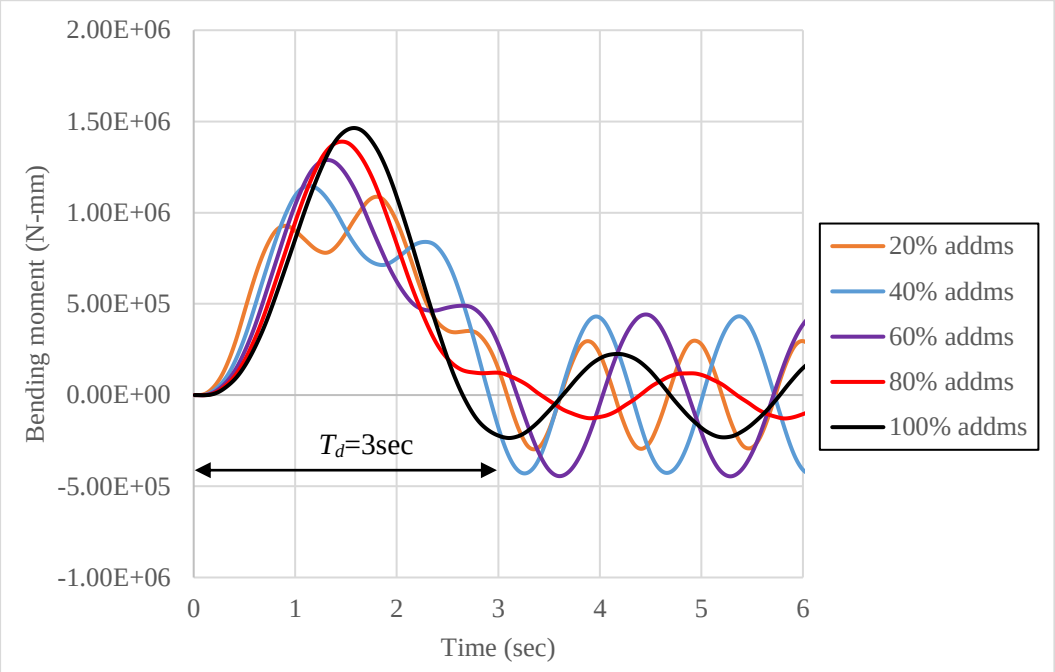

(b) Load duration of 3 sec

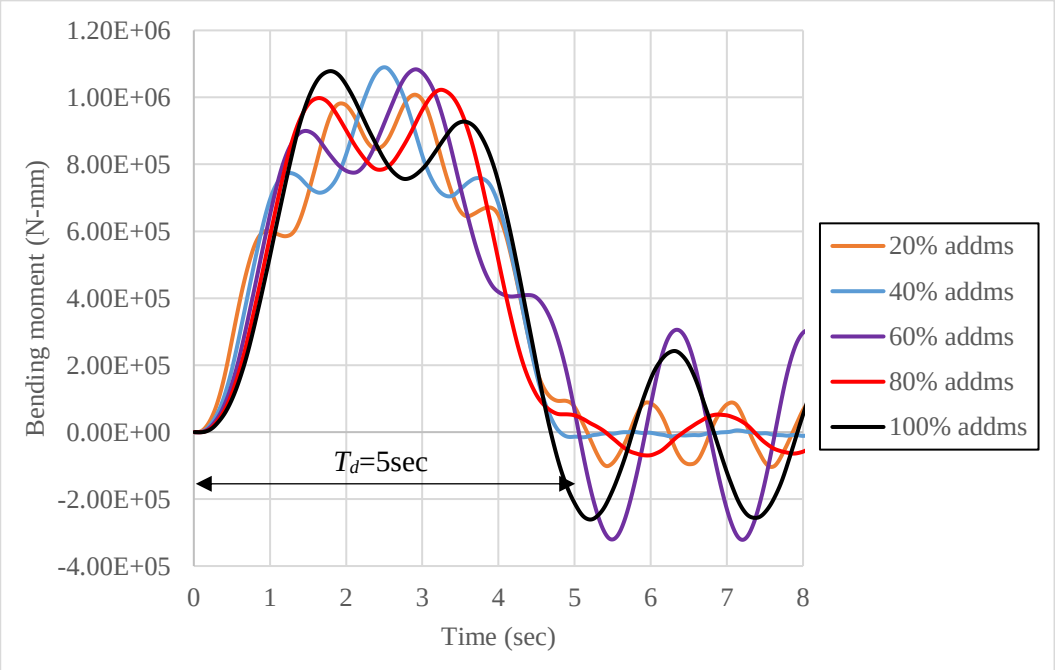

(c) Load duration of 5 sec

Fig 5. 18 Time history of bending moment at midship for different load duration

5.4 Conclusions

Effect of added mass and damping on the collapse extent of a hull girder under impulsive longitudinal bending moment are discussed taking the damping, added mass and load duration as parameters. Two cases of load conditions are considered; one considering the same magnitude of applied external load and the other considering the same magnitude of bending moment exerted at the collapsing cross section. The following conclusion can be drawn:

1. Damping has significant effect on the collapse extent, and the larger the damping coefficient, the smaller the collapse extent. This is the same conclusion as [32]. The effect is particularly large for shorter duration close to natural vibration period, where response velocities are relatively large.
2. Added mass has also significant and more complicated effect on the collapse extent. Collapse extent highly depends on the inertia force that compensates the unbalanced force between applied bending moment and post-ultimate structural capacity.
3. The collapse extent depends not only on the inertia force generated by the added mass but also on the relationship between the applied load duration and the natural period that also depends on the added mass. This point should be further addressed as a future work.

Chapter 6

Conclusions and suggestions for future work

6.1 Conclusions

A simplified method of the progressive collapse analysis of hull girder cross section has been proposed by incorporating the Smith method with the conventional beam finite element, namely FE-Smith method. Ultimate strength of ship hull girder cross section and post-ultimate strength behavior of ship hull girder is performed by using FE-smith method considering the fluid-structure interaction. Two types of average stress-average strain relationship are adopted in FE-smith method. One is obtained by CSR equation and the other by nonlinear FEM. Uniform beam model (box-shaped) and container ship hull model are used as target ships. Validation is done by performing the NFEA and accuracy is investigated. It can be concluded that

1. FE-smith method can give the reasonable collapse behavior in both static and dynamic analysis with much shorter computation time compared to NFEA.
2. It has been found that FE-smith method that employs the average stress-average strain curves obtained by nonlinear FEM can provide more reasonable prediction of the collapse behavior than those by CSR equation.
3. Limitation in the application of FE-smith method is mainly due to the assumption of a plane cross section for beam element and unloading stiffness assumption in average stress-average strain relationship of structural element.

Also parametric study is investigated for added mass, wave damping and load duration parameter. It can be concluded that

4. The longer the load duration, the larger the collapse extent. Short load duration like slamming load likely causes relatively small structural damage to the ship hull girder. It must be noted that repeating such small structural damage may lead to the dangerous condition for ship hull girder.

5. Wave damping simply resists the collapse extent. The larger the wave damping, the smaller the collapse extent.
6. The added mass has more complicated effects on the collapse extent, as it is related both to the reactions against accelerated hull girder deformation and to the natural vibrations that affects the bending moment history exerted at cross sections.
7. Correlation between the effect of wave damping and wave added is found in larger load duration. The time instance when maximum response bending moment occurs depends on the phase difference between velocity and acceleration. Phase lag of the vibration after the loading period also takes place due to the presence of wave damping.

6.2 Suggestions for future work

Although the assumptions of FE-smith's method limit the scope of its applicability, post-ultimate strength behavior can be captured with effective period of CPU time and quantitatively comparable with NLFEA. Since this is the fundamental study, further improvement is necessary concerning with the assumption to improve the accuracy. Suggestion for future works are

1. Unloading stiffness assumption should be improved considering the effect of residual deformation of structural elements on their elastic unloading behavior.
2. Model extent on NFEA and its effect on elastic hull girder stiffness should be investigated.
3. Transverse bending, shear and torsion effect should be taken into account for hull girder collapse behavior.
4. Average stress-average strain relationship of stiffened panel should be adopted from more reasonable approach having physically stiffer background than those obtained by CSR empirical equations. Analysis should be performed for stiffened panels under bi-axial, shear and torsion.
5. Assumed load distributions and histories have been applied to hull girder in this study. Collapse behavior of hull girder in waves must be enabled as a final goal of FE-Smith analysis.

Appendix A

Average stress-average strain curve

Two approaches used to calculate the average stress-average strain relationship in this study are

1. Gordo-Soares formulae (CSR equation)
2. Nonlinear Finite Element Analysis by Msc.Marc

CSR formulae for Smith method

Ship cross section is composed of 3 types of elements and elasto-plastic collapse behavior of all types of element under tension adopted the elastic-perfectly plastic property. Each element collapse behavior under compression are described below.

Hard corner element

Hard corner element does not have the hardening/softening behavior under compression loading. It means elastic-perfectly plastic stress-strain curve is adopted as shown in Fig A.1.

Plate element

Unlike hard corner element, buckling/yielding and softening behavior after the ultimate strength is considered in average stress-strain curve of plate element.

Stiffened panel element

For stiffened panel element, 3 types of failure modes are considered in CSR equation. They are

(1) beam column buckling

(2) torsional buckling and

(3) web local buckling.

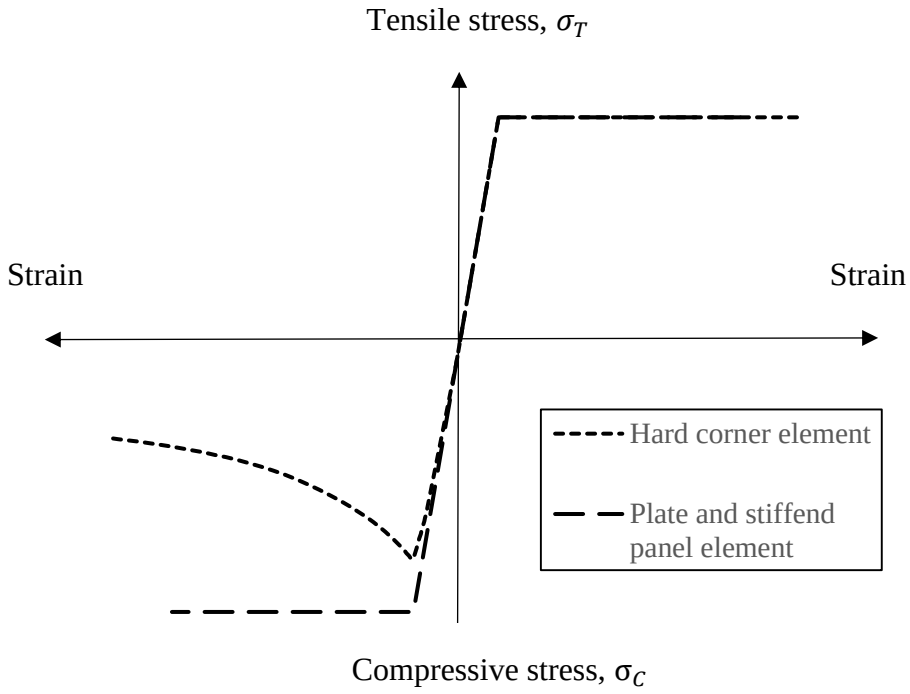

Fig A. 1 Average stress-average strain curve for elements in Smith method

Equations described for each element collapse mode are written in the [8]. In this study, plate elements are applied instead of hard corner elements according to Tatsumi et.al [33].

Nonlinear Finite Element Analysis by Msc.Marc

In case of NFEA by MSC.Marc, stiffened panel elements are analyzed under the uniaxial loading. In case of tension loading, elastic perfectly plastic material property is employed. For compression, arc-length method is used to obtain the softening behavior. Buckling half-wave is determined by the aspect ratio (*a/b*) of the stiffened panel. Length *a* means the panel length in longitudinal direction and *b* means panel breadth in transverse direction. Local initial deflection is considered by the following equations. α = 0.05 is used which is in between the slight and average condition.

$$w_{local} = B_0 \sin(\frac{m\pi x}{a}) \sin(\frac{n\pi y}{b}) \qquad \text{Eq (A.1)}$$

$$B_0 = \alpha\beta^2 t \qquad \text{Eq (A.2)}$$

$$\beta = \frac{b}{t}\sqrt{\frac{\sigma_Y}{E}} \qquad \text{Eq (A.3)}$$

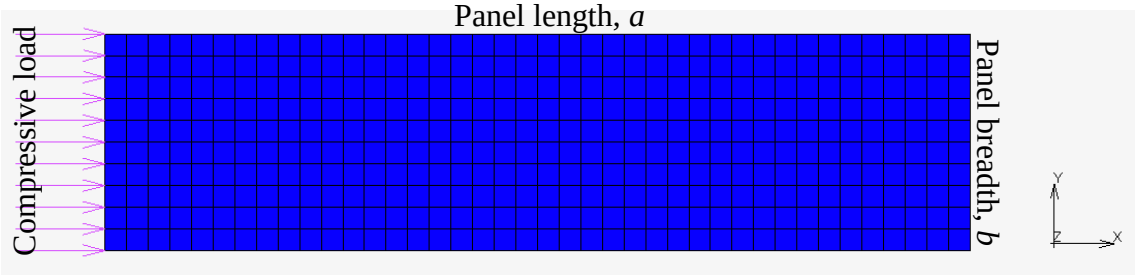

Fig A. 2 A stiffened panel

Global deflection is consider to be one half-wave (i.e. m=1 and n=1) for the region confined between the transverse frames and between the longitudinal girders.

$$w_{global} = A_0 \sin(\frac{\pi x}{a}) \sin(\frac{\pi y}{B}) \qquad \text{Eq (A.4)}$$

$$A_0 = 0.001 * a \qquad \text{Eq (A.5)}$$

Initial deflection of stiffener flanges is also having the same magnitude as the attached plate. Horizontal deflection of the stiffeners (stiffener tripping) are represented by

$$w_{global\_H} = A_0 \sin(\frac{\pi x}{a}) \frac{z}{h} \qquad \text{Eq (A.6)}$$

where h = height of stiffener

Elements of the ship cross section are called continuous stiffened panels as the longitudinal stiffeners of same size are usually attached to the plate in equal distance for corresponding region between the longitudinal girder. That means the deformation and structural configuration can be periodically repeated over the continuous stiffened panel. In that case, Periodic Boundary Condition (PBC) is used. Not necessarily taking the whole region, only a part stiffened panel of continuous panel can be taken and analyzed since the effect of continuity (symmetric condition) is defined by PBC.

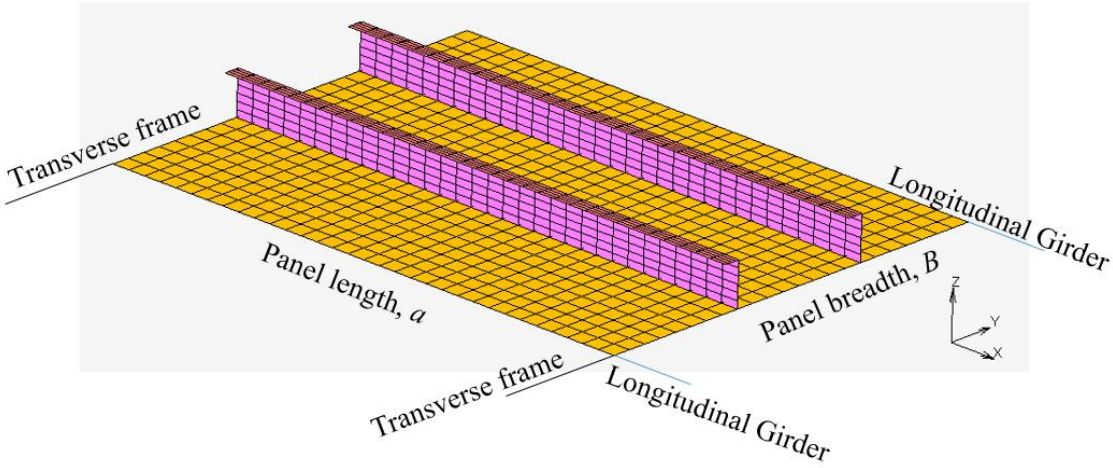

Fig A. 3 Global deflection applied region

In taking only a part of stiffened panel, the region (extent of model) to be considered is important. Model extend in longitudinal direction depends on the number of local half-buckling wave of longitudinal direction. Model extent in transverse direction depends not only on the loading condition but also on the types of stiffener, ie. flat bar , angle bar or t-bar. Longitudinal model extent region is shown in Fig A. 4 and periodic boundary condition imposed on CC and BB are

$$\text{u = uniform, } \theta_y = 0\,, \quad \theta_z = 0$$

and imposed on Fig 3.6(b) of AA and BB are

$$\text{u = uniform } y_{AA} = y_{BB}, z_{AA} = z_{BB}$$

$$\theta_{xAA} = \theta_{xBB}\,, \qquad \theta_{yAA} = \theta_{yBB}\,, \qquad \theta_{zAA} = \theta_{zBB}$$

Symmetry condition of transverse model extend is consider in the similar manner in which it depends on the rotation of the stiffeners. Detailed explanation can be found in [34].

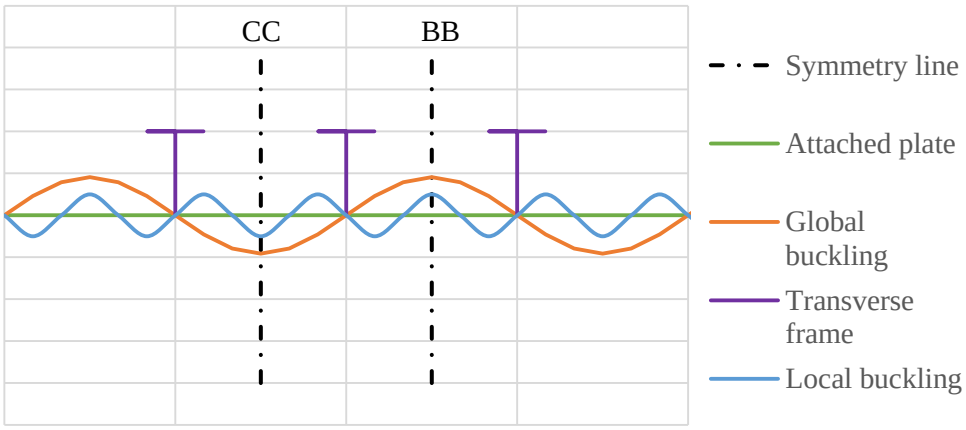

(a) PBC imposed region for odd number of local half buckling wave

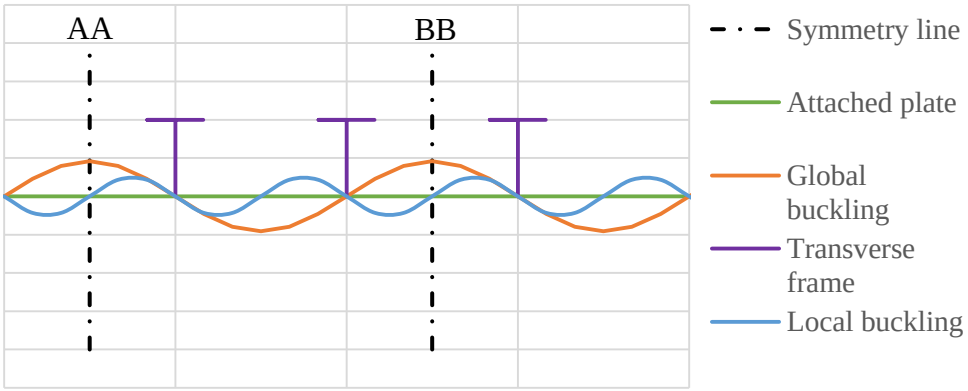

(b) PBC imposed region for even number of local half buckling wave

Fig A. 4 Model extend in longitudinal direction

Container midship cross section is composed of 315 elements. By taking out the same scantlings and same properties stiffened panel, 72 elements are required to analyze. Those 72 elements are named by Pbcid. Distance between transverse frame is 3200 mm and between longitudinal girder is 850 mm. Msc.Marc shell element type 75 is used for analysis. Number of integration point through the thickness is regarded as 5.

From the analyses, snap-back behavior are found in certain elements because of the capacity reduction and the associated localization of plastic deformation. The location of those elements and scantling are shown in Fig A.5. In reality, snap back behavior cannot be happened in hull girder cross section as adjacent elements support the collapse

element during unloading condition. Therefore, such post-buckling behavior is approximated by the straight line inclined around 10 degrees from vertical as shown in Fig A. 6.

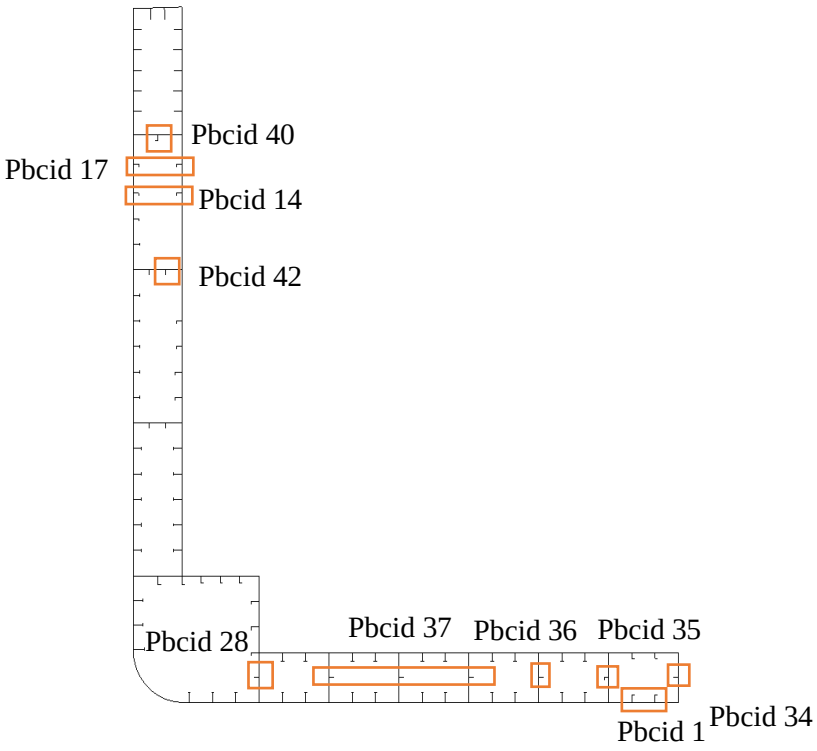

Fig A. 5 Elements having snap-back behavior

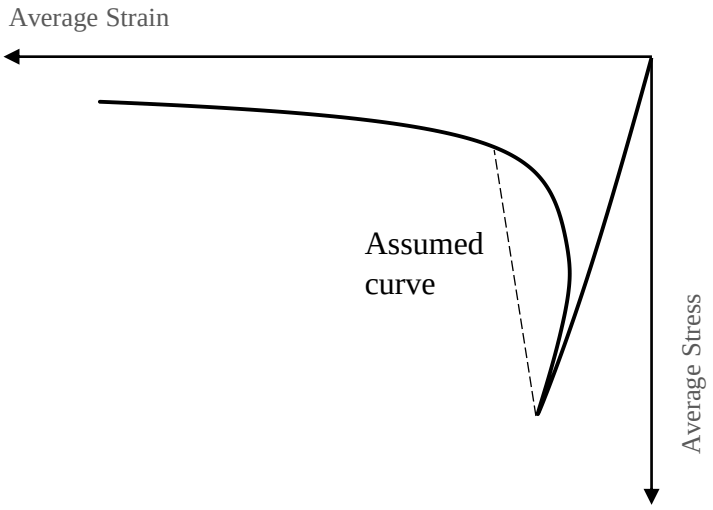

Fig A. 6 Snap-back behavior of Pbcid 34 and its treated curve

Table A. 1 Scantling of elements which have snap-back behavior

pbcid	Plate and Stiffener Scantling
1	850x12 --- L 200x9+90x15
14	930x32 --- L 200x9+90x14
15	990x32 --- L 200x9+90x14
23	930x32 --- L 200x9+90x14
24	990x32 --- L 200x9+90x14
28	845x13 --- I 180x9.5
34	845x14.5 --- I 180x9.6
35	845x13 --- L 150x9+90x15
36	845x19 --- I 180x9.5
37	845x13.5 --- I 180x9
40	890x20 --- L 200x9+90x14
42	474.67x11 --- I 180x9.5

Average stress-average strain curve obtained by Msc.Marc and Gordo-Soares formulae are described and compared in Appendix B. It can be seen that after the ultimate strength, Gordo-Soares formulae give the smooth unloading behavior compared to the NFEA. NFEA results shows the rapid load reduction rate in unloading region and also attain the smaller ultimate strength.

Although hull girder model have different cross-section, only midship section are considered for both approaches. Since the target collapse region is the midship section, the analysis is reasonable to perform under this condition.

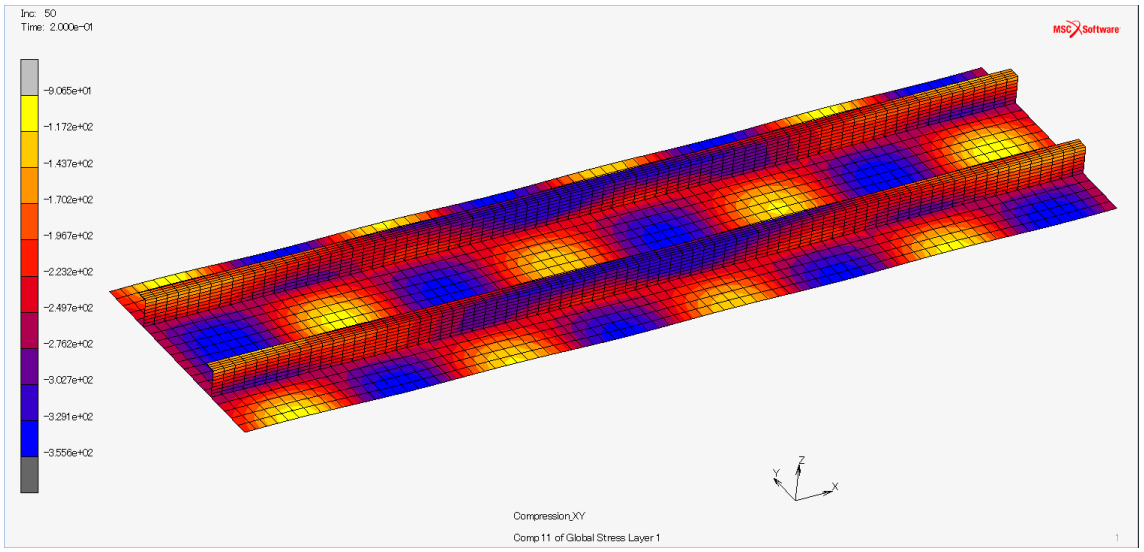

(a) Axial stress distribution at ultimate strength

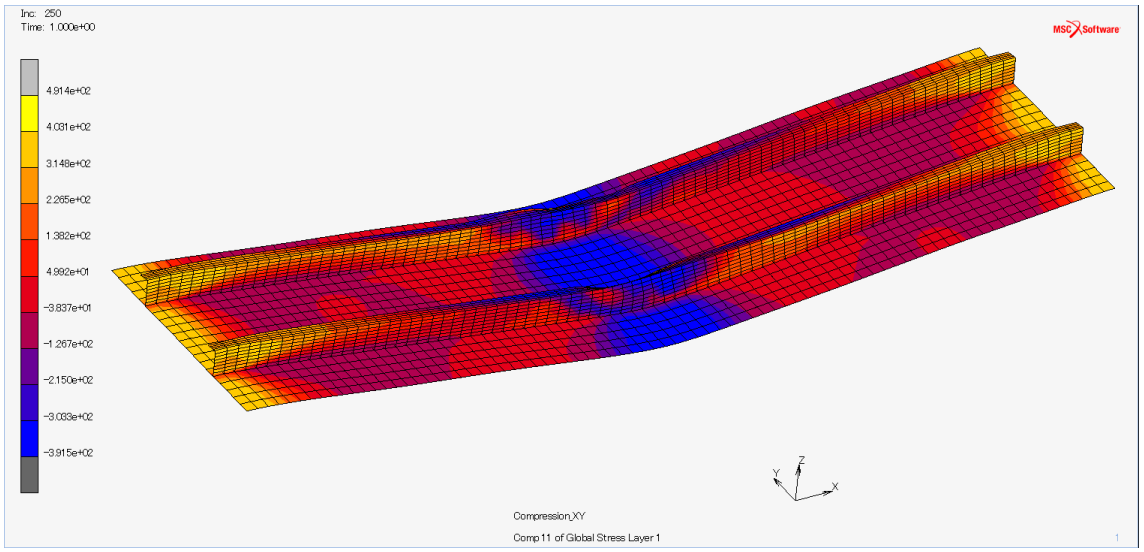

(b) Collapse mode at the end of analysis

Fig A. 7 Analysis of Pbcid34 panel

Appendix B

Comparison between CSR and PBC average stress- strain curves

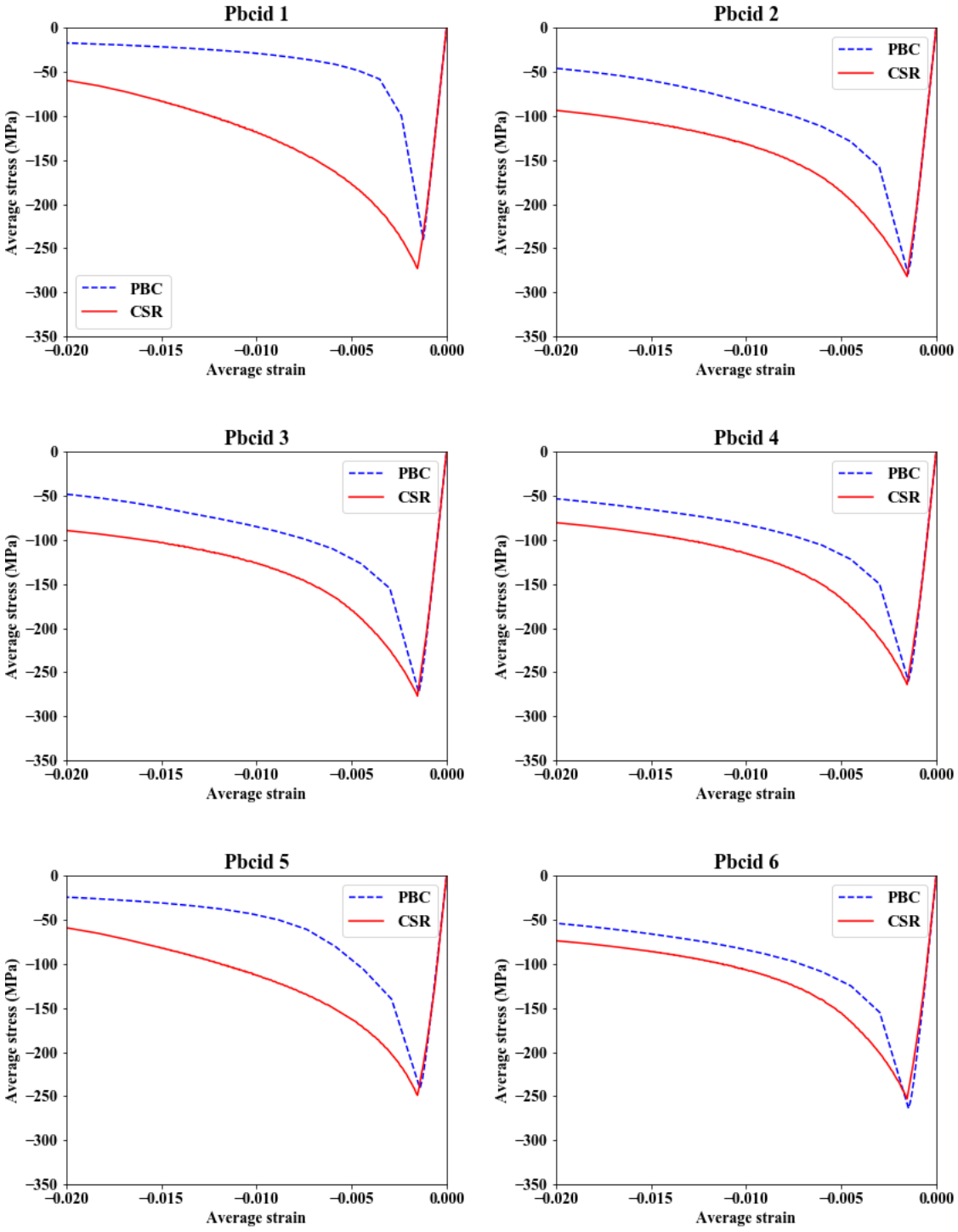

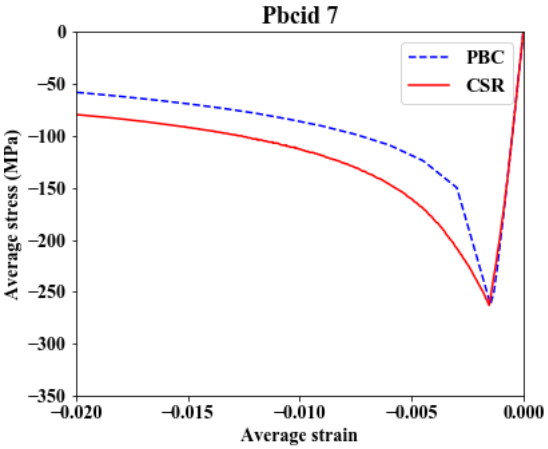
Pbcid 7
PBC
CSR
Average stress (MPa)
Average strain
0
−50
−100
−150
−200
−250
−300
−350
−0.020
−0.015
−0.010
−0.005
0.000

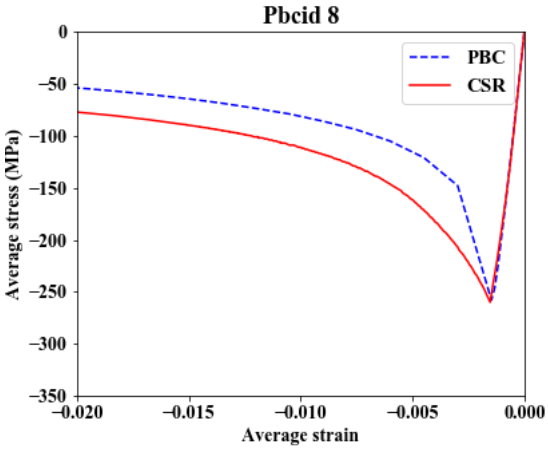
Pbcid 8
PBC
CSR
Average stress (MPa)
Average strain
0
−50
−100
−150
−200
−250
−300
−350
−0.020
−0.015
−0.010
−0.005
0.000

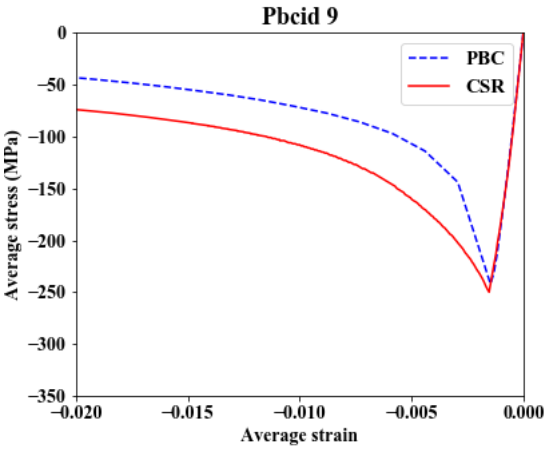
Pbcid 9
PBC
CSR
Average stress (MPa)
Average strain
0
−50
−100
−150
−200
−250
−300
−350
−0.020
−0.015
−0.010
−0.005
0.000

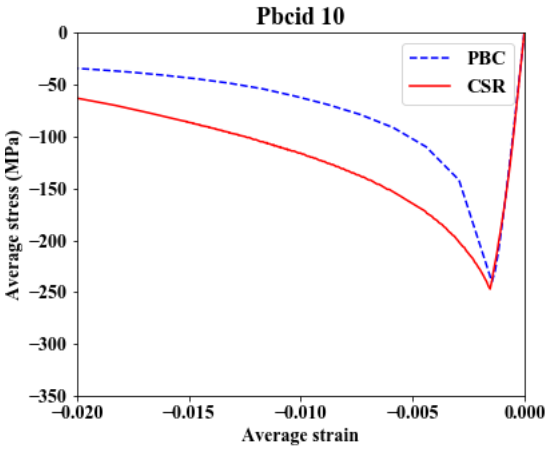
Pbcid 10
PBC
CSR
Average stress (MPa)
Average strain
0
−50
−100
−150
−200
−250
−300
−350
−0.020
−0.015
−0.010
−0.005
0.000

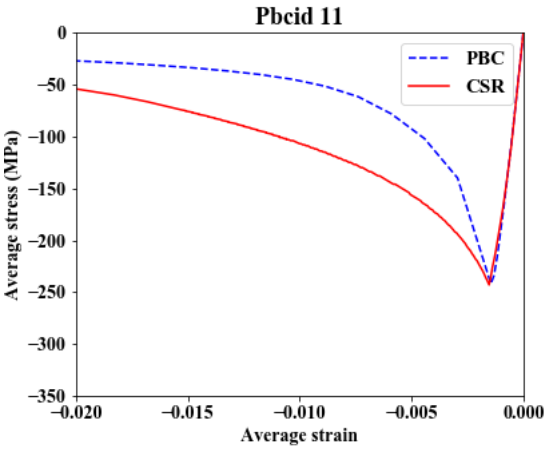
Pbcid 11
PBC
CSR
Average stress (MPa)
Average strain
0
−50
−100
−150
−200
−250
−300
−350
−0.020
−0.015
−0.010
−0.005
0.000

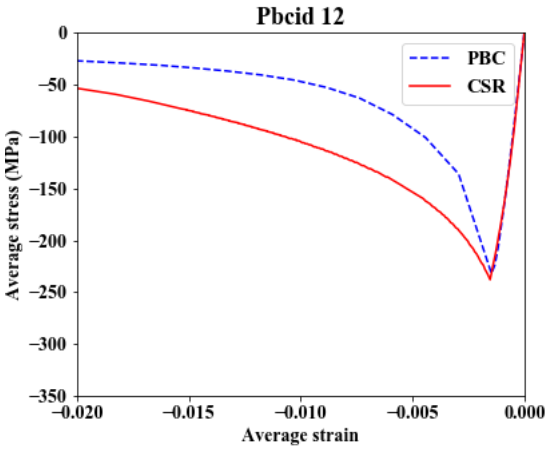
Pbcid 12
PBC
CSR
Average stress (MPa)
Average strain
0
−50
−100
−150
−200
−250
−300
−350
−0.020
−0.015
−0.010
−0.005
0.000

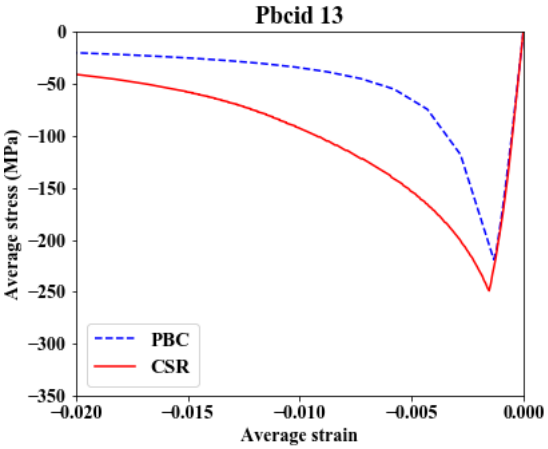
Pbcid 13
Average stress (MPa)
Average strain
PBC
CSR

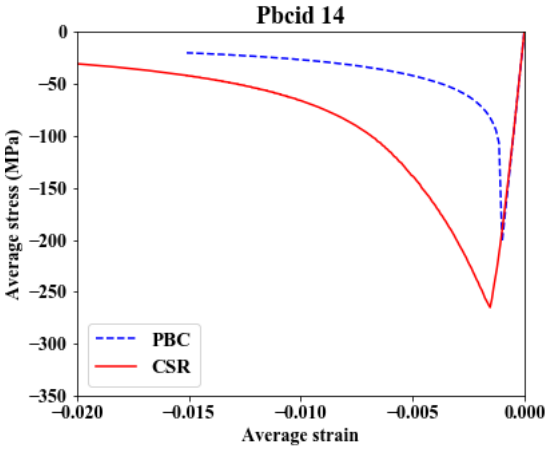
Pbcid 14
Average stress (MPa)
Average strain
PBC
CSR

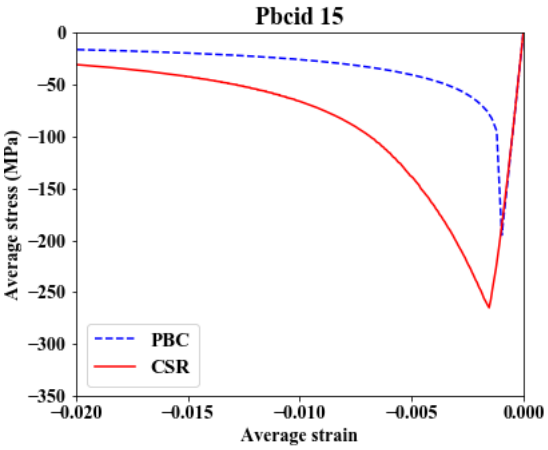
Pbcid 15
Average stress (MPa)
Average strain
PBC
CSR

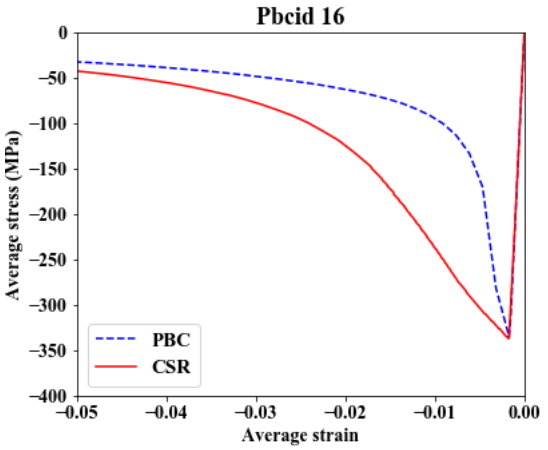
Pbcid 16
Average stress (MPa)
Average strain
PBC
CSR

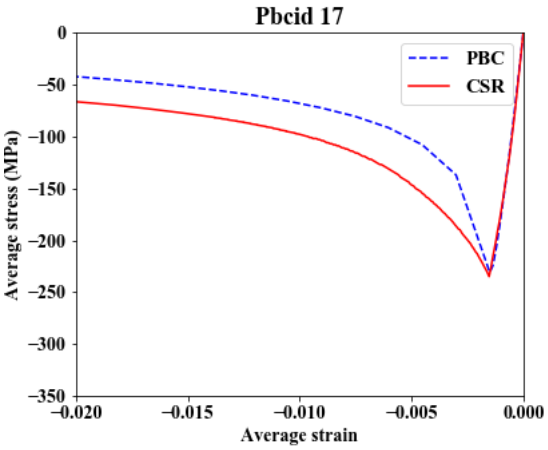
Pbcid 17
Average stress (MPa)
Average strain
PBC
CSR

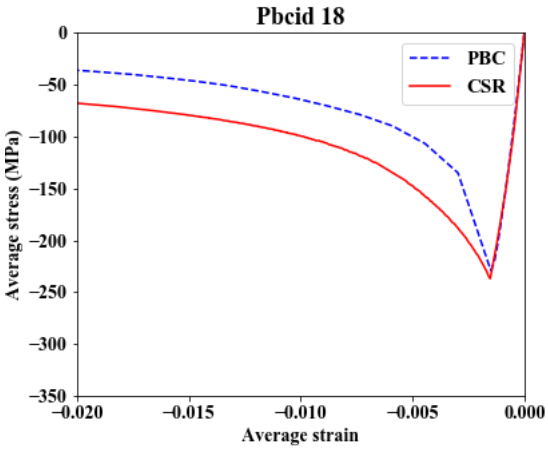
Pbcid 18
Average stress (MPa)
Average strain
PBC
CSR

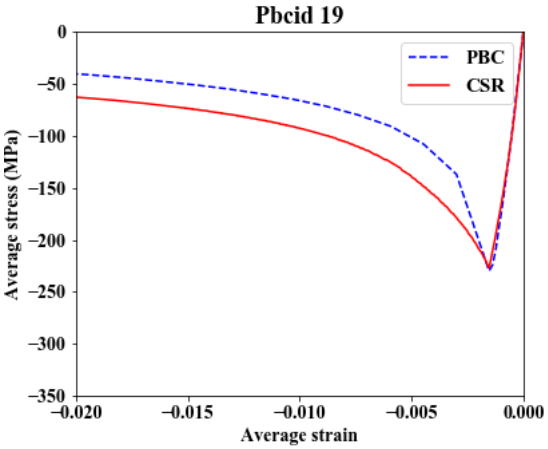
Pbcid 19
PBC
CSR
Average stress (MPa)
Average strain
0
−50
−100
−150
−200
−250
−300
−350
−0.020
−0.015
−0.010
−0.005
0.000

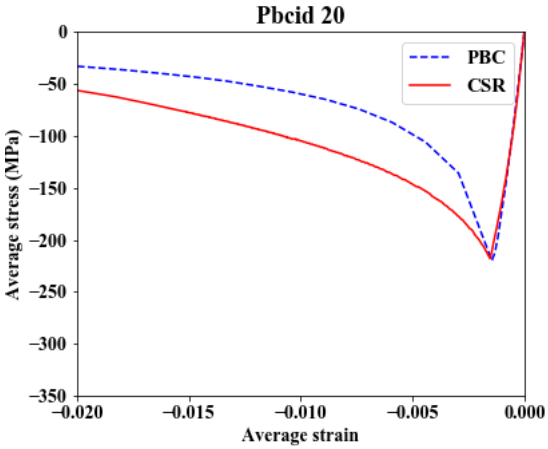
Pbcid 20
PBC
CSR
Average stress (MPa)
Average strain
0
−50
−100
−150
−200
−250
−300
−350
−0.020
−0.015
−0.010
−0.005
0.000

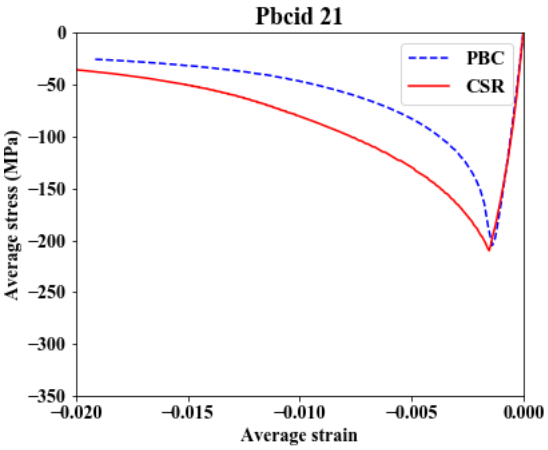
Pbcid 21
PBC
CSR
Average stress (MPa)
Average strain
0
−50
−100
−150
−200
−250
−300
−350
−0.020
−0.015
−0.010
−0.005
0.000

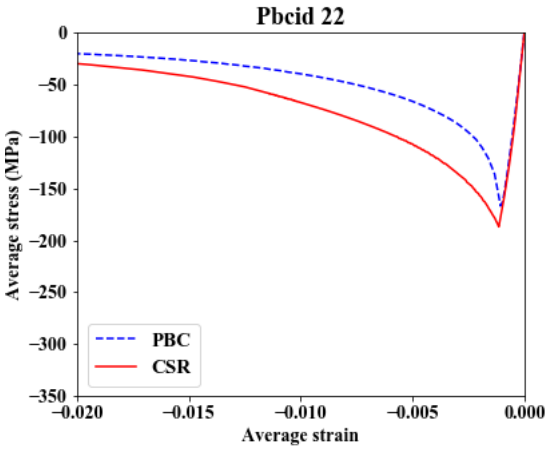
Pbcid 22
PBC
CSR
Average stress (MPa)
Average strain
0
−50
−100
−150
−200
−250
−300
−350
−0.020
−0.015
−0.010
−0.005
0.000

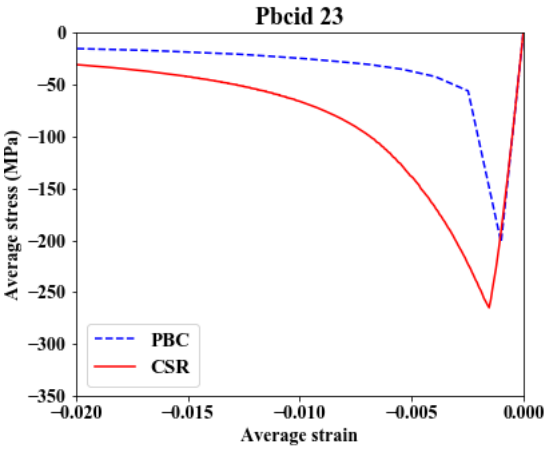
Pbcid 23
PBC
CSR
Average stress (MPa)
Average strain
0
−50
−100
−150
−200
−250
−300
−350
−0.020
−0.015
−0.010
−0.005
0.000

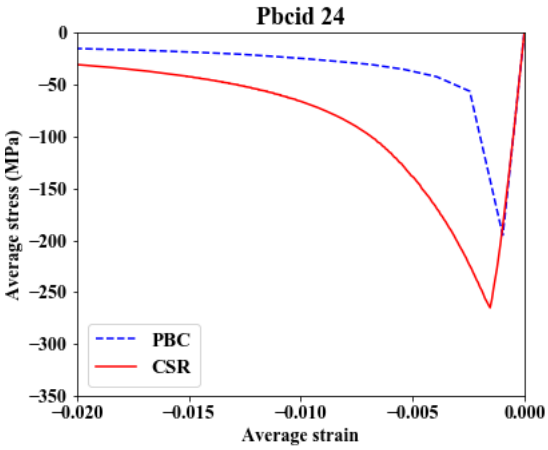
Pbcid 24
PBC
CSR
Average stress (MPa)
Average strain
0
−50
−100
−150
−200
−250
−300
−350
−0.020
−0.015
−0.010
−0.005
0.000

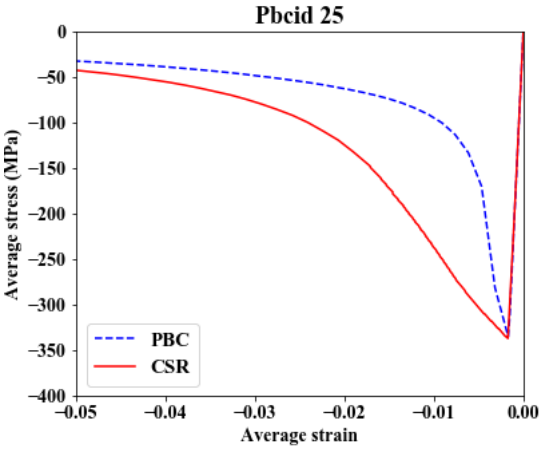
Pbcid 25
Average stress (MPa)
Average strain
PBC
CSR

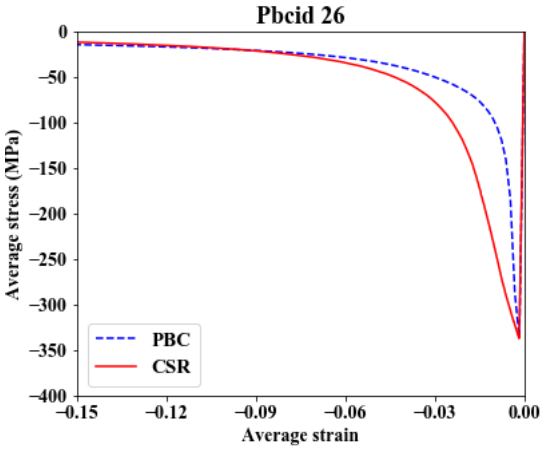
Pbcid 26
Average stress (MPa)
Average strain
PBC
CSR

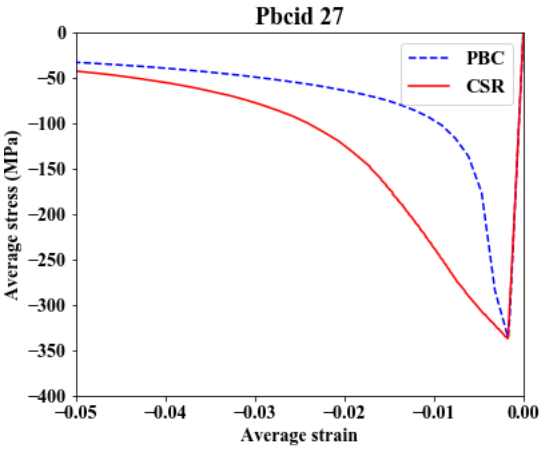
Pbcid 27
Average stress (MPa)
Average strain
PBC
CSR

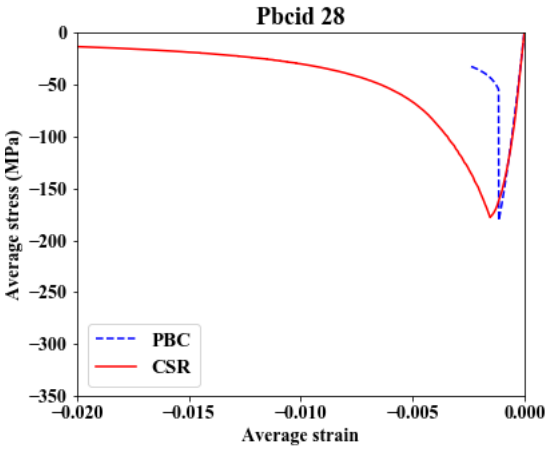
Pbcid 28
Average stress (MPa)
Average strain
PBC
CSR

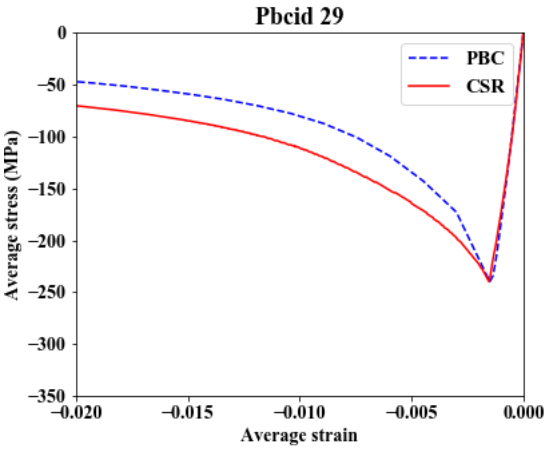
Pbcid 29
Average stress (MPa)
Average strain
PBC
CSR

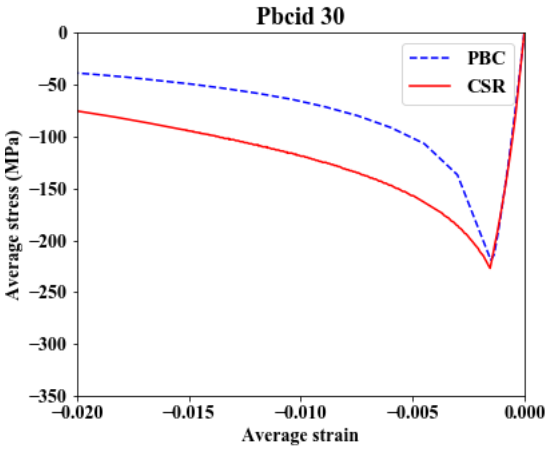
Pbcid 30
Average stress (MPa)
Average strain
PBC
CSR

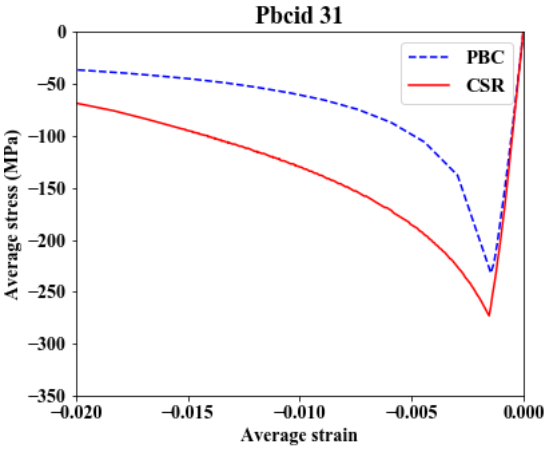
Pbcid 31
PBC
CSR
Average stress (MPa)
Average strain
0
−50
−100
−150
−200
−250
−300
−350
−0.020
−0.015
−0.010
−0.005
0.000

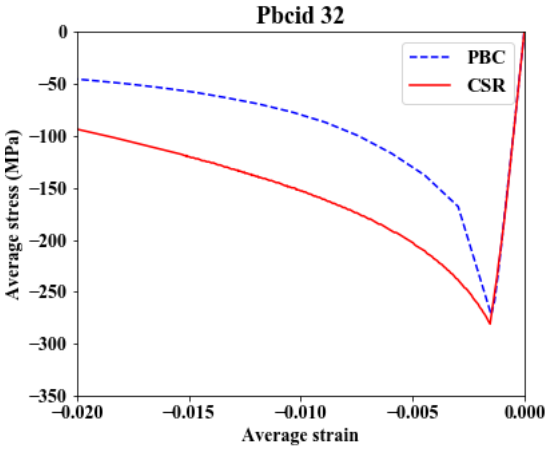
Pbcid 32
PBC
CSR
Average stress (MPa)
Average strain
0
−50
−100
−150
−200
−250
−300
−350
−0.020
−0.015
−0.010
−0.005
0.000

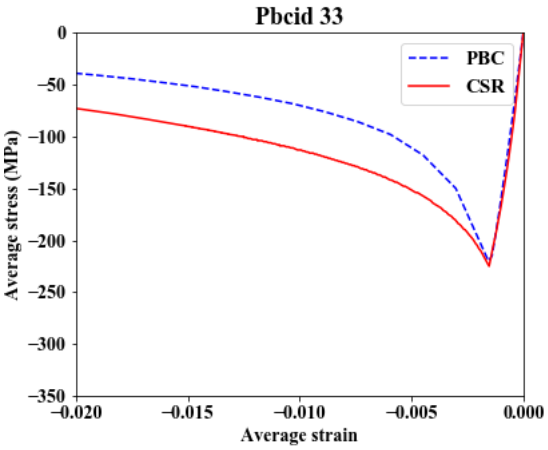
Pbcid 33
PBC
CSR
Average stress (MPa)
Average strain
0
−50
−100
−150
−200
−250
−300
−350
−0.020
−0.015
−0.010
−0.005
0.000

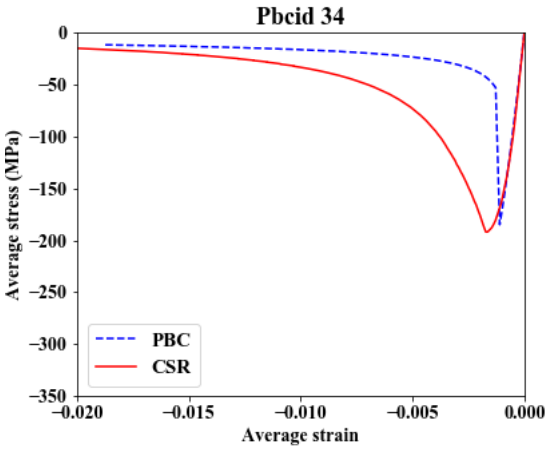
Pbcid 34
PBC
CSR
Average stress (MPa)
Average strain
0
−50
−100
−150
−200
−250
−300
−350
−0.020
−0.015
−0.010
−0.005
0.000

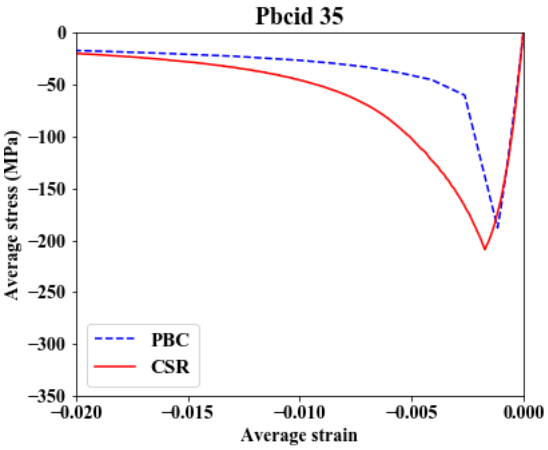
Pbcid 35
PBC
CSR
Average stress (MPa)
Average strain
0
−50
−100
−150
−200
−250
−300
−350
−0.020
−0.015
−0.010
−0.005
0.000

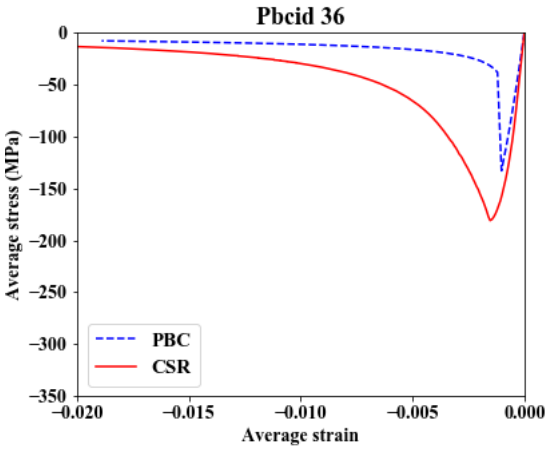
Pbcid 36
PBC
CSR
Average stress (MPa)
Average strain
0
−50
−100
−150
−200
−250
−300
−350
−0.020
−0.015
−0.010
−0.005
0.000

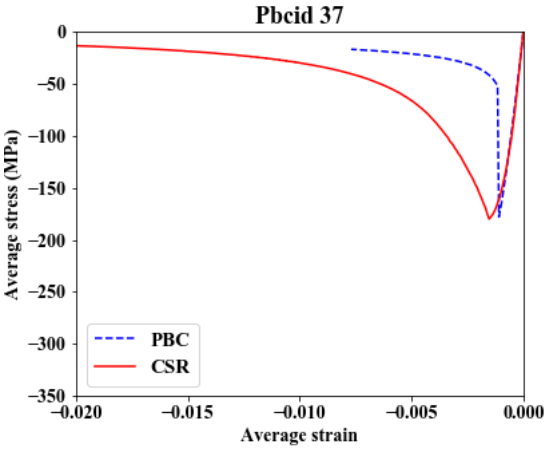
Pbcid 37
Average stress (MPa)
Average strain
PBC
CSR

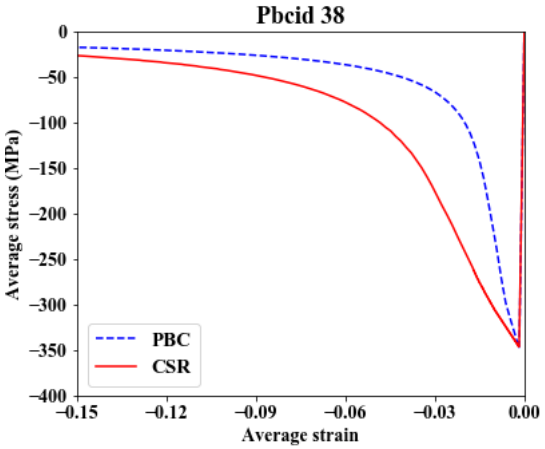
Pbcid 38
Average stress (MPa)
Average strain
PBC
CSR

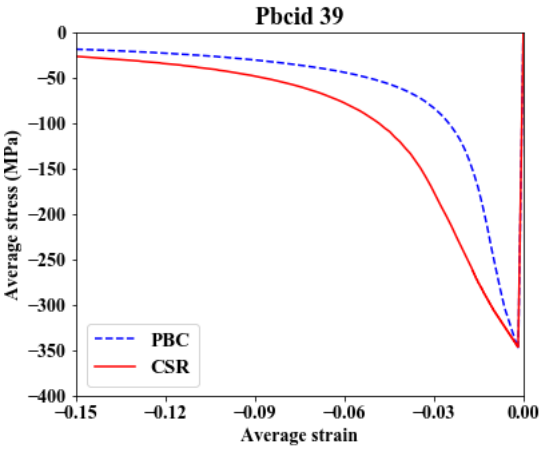
Pbcid 39
Average stress (MPa)
Average strain
PBC
CSR

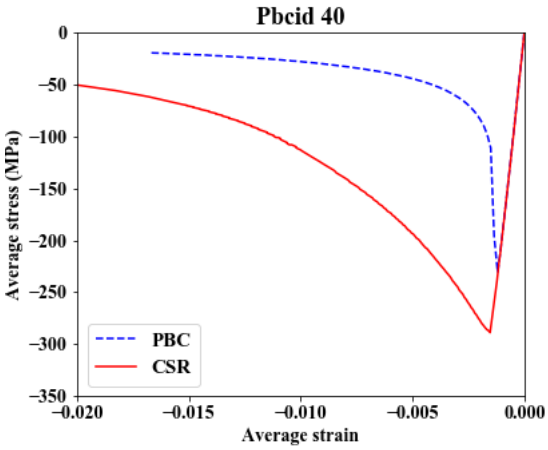
Pbcid 40
Average stress (MPa)
Average strain
PBC
CSR

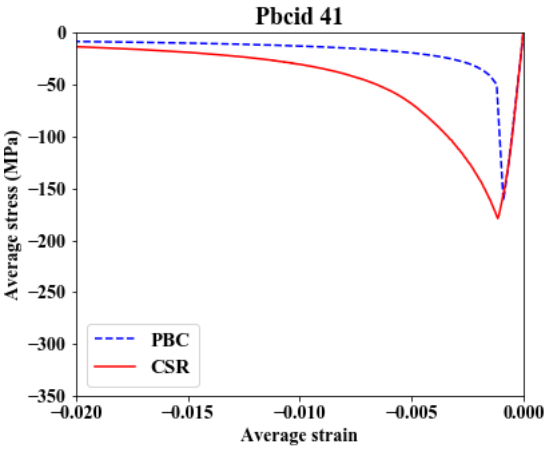
Pbcid 41
Average stress (MPa)
Average strain
PBC
CSR

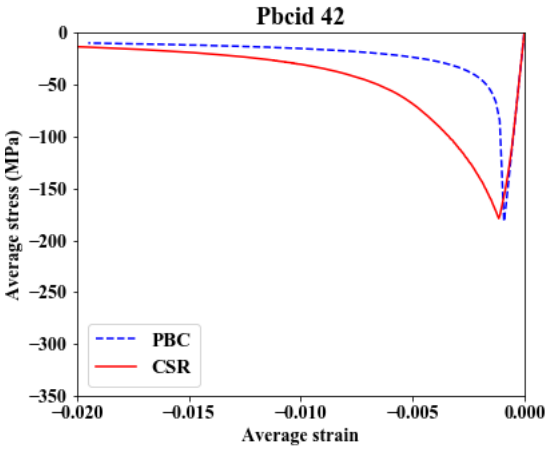
Pbcid 42
Average stress (MPa)
Average strain
PBC
CSR

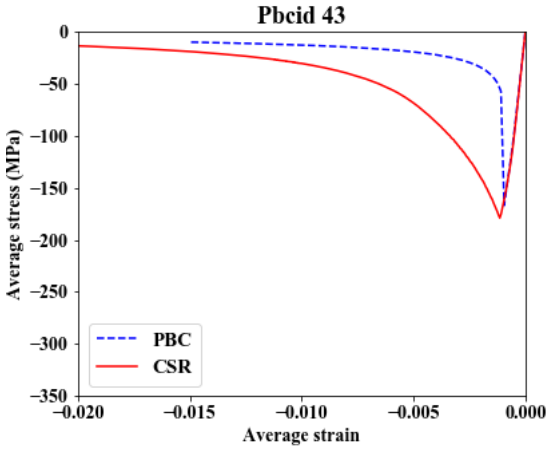
Pbcid 43
Average stress (MPa)
Average strain
PBC
CSR

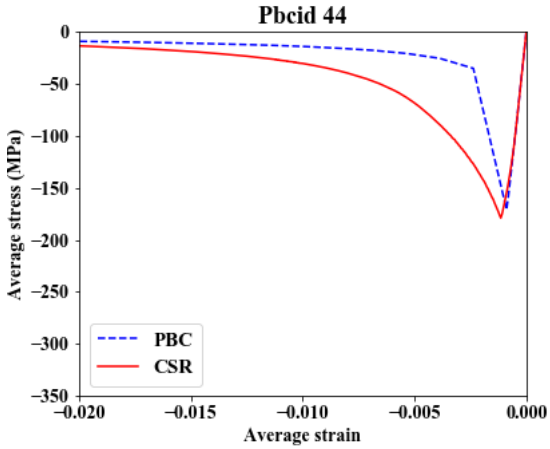
Pbcid 44
Average stress (MPa)
Average strain
PBC
CSR

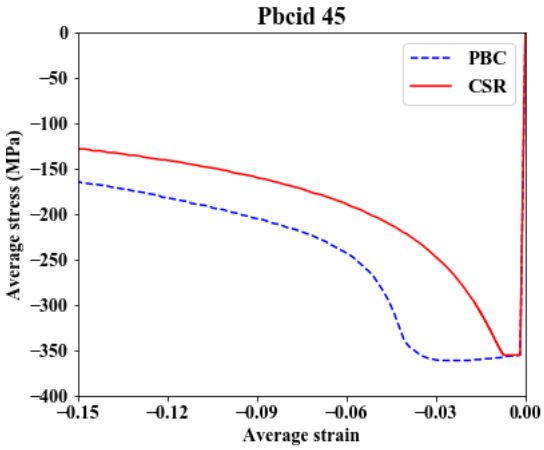
Pbcid 45
Average stress (MPa)
Average strain
PBC
CSR

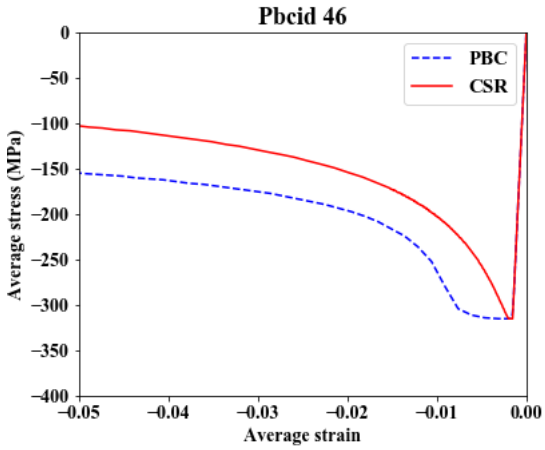
Pbcid 46
Average stress (MPa)
Average strain
PBC
CSR

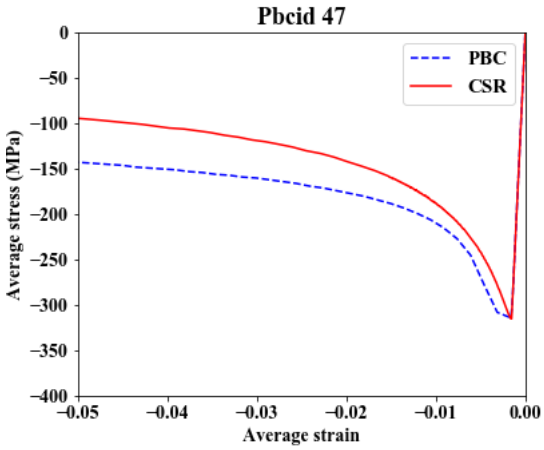
Pbcid 47
Average stress (MPa)
Average strain
PBC
CSR

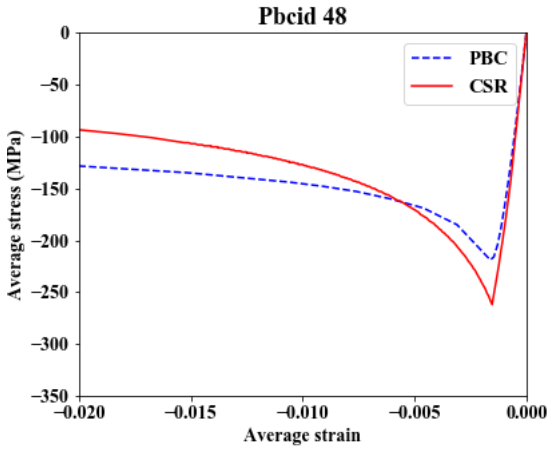
Pbcid 48
Average stress (MPa)
Average strain
PBC
CSR

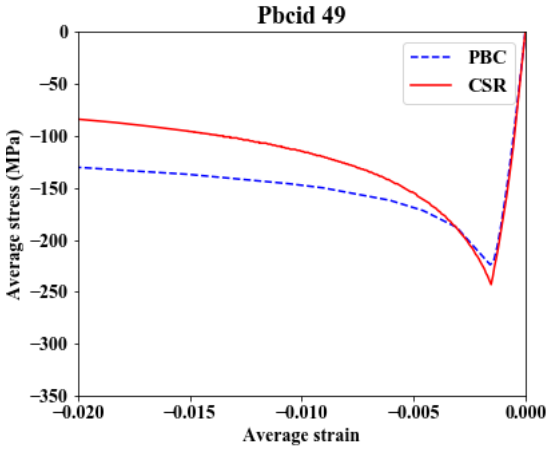
Pbcid 49
PBC
CSR
Average stress (MPa)
Average strain
0
−50
−100
−150
−200
−250
−300
−350
−0.020
−0.015
−0.010
−0.005
0.000

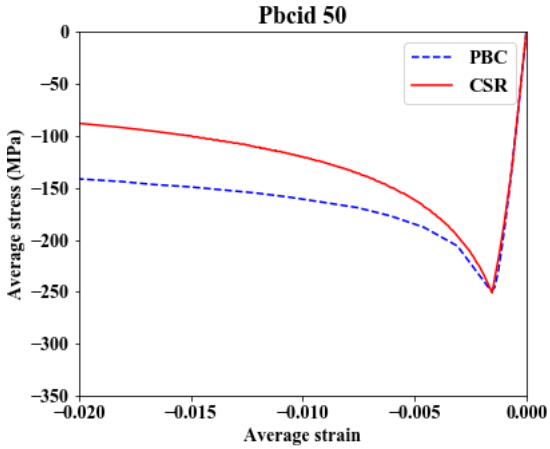
Pbcid 50
PBC
CSR
Average stress (MPa)
Average strain
0
−50
−100
−150
−200
−250
−300
−350
−0.020
−0.015
−0.010
−0.005
0.000

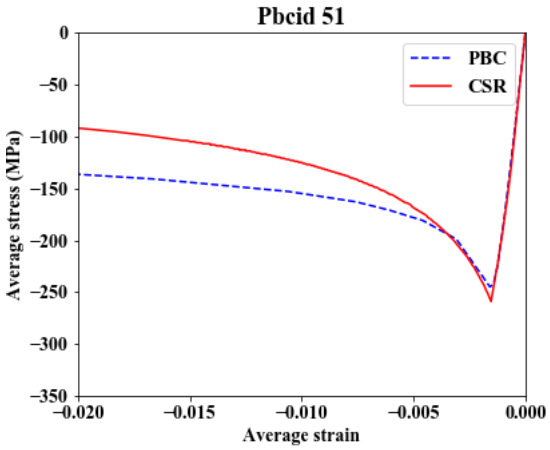
Pbcid 51
PBC
CSR
Average stress (MPa)
Average strain
0
−50
−100
−150
−200
−250
−300
−350
−0.020
−0.015
−0.010
−0.005
0.000

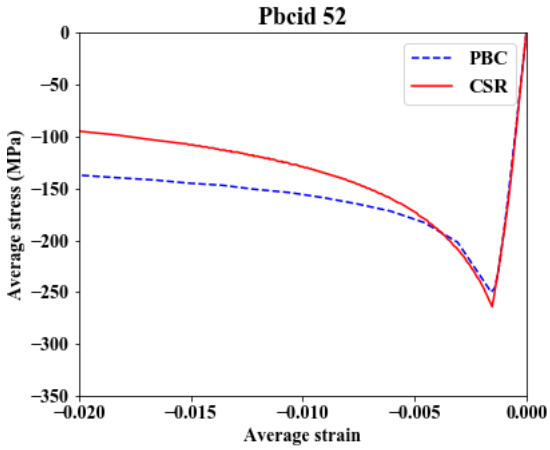
Pbcid 52
PBC
CSR
Average stress (MPa)
Average strain
0
−50
−100
−150
−200
−250
−300
−350
−0.020
−0.015
−0.010
−0.005
0.000

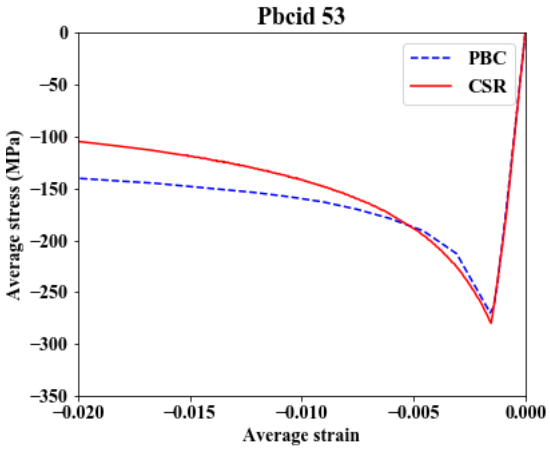
Pbcid 53
PBC
CSR
Average stress (MPa)
Average strain
0
−50
−100
−150
−200
−250
−300
−350
−0.020
−0.015
−0.010
−0.005
0.000

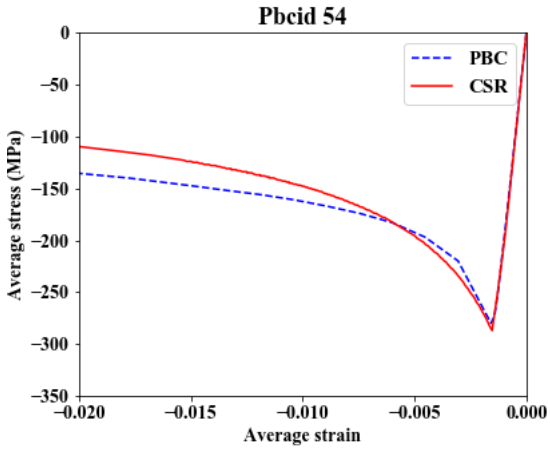
Pbcid 54
PBC
CSR
Average stress (MPa)
Average strain
0
−50
−100
−150
−200
−250
−300
−350
−0.020
−0.015
−0.010
−0.005
0.000

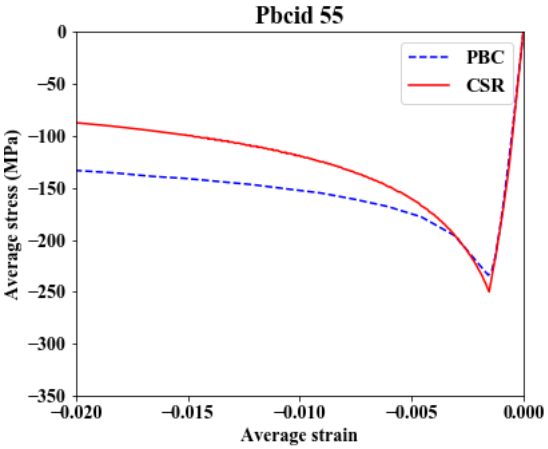
Pbcid 55
PBC
CSR
Average stress (MPa)
Average strain
0
−50
−100
−150
−200
−250
−300
−350
−0.020
−0.015
−0.010
−0.005
0.000

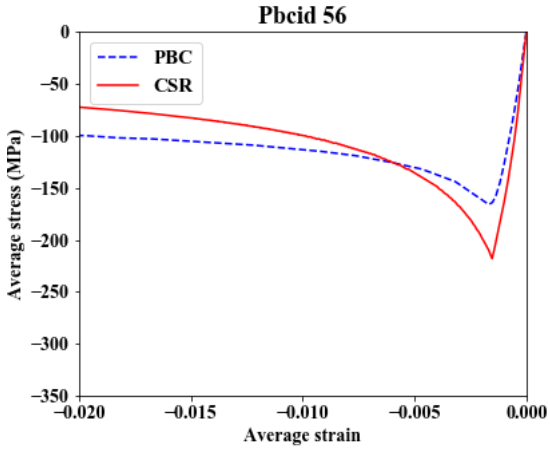
Pbcid 56
PBC
CSR
Average stress (MPa)
Average strain
0
−50
−100
−150
−200
−250
−300
−350
−0.020
−0.015
−0.010
−0.005
0.000

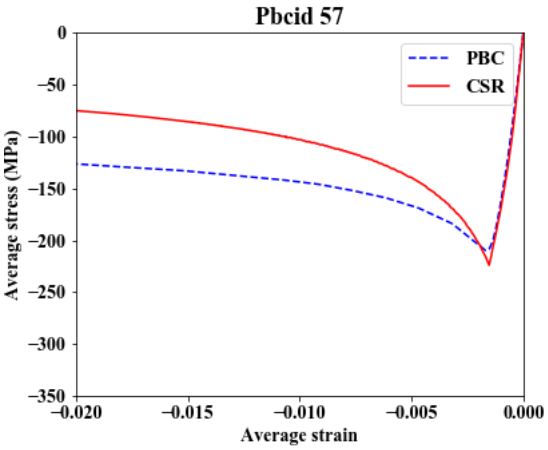
Pbcid 57
PBC
CSR
Average stress (MPa)
Average strain
0
−50
−100
−150
−200
−250
−300
−350
−0.020
−0.015
−0.010
−0.005
0.000

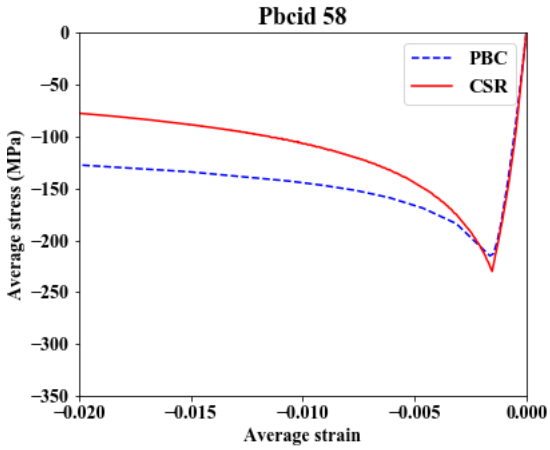
Pbcid 58
PBC
CSR
Average stress (MPa)
Average strain
0
−50
−100
−150
−200
−250
−300
−350
−0.020
−0.015
−0.010
−0.005
0.000

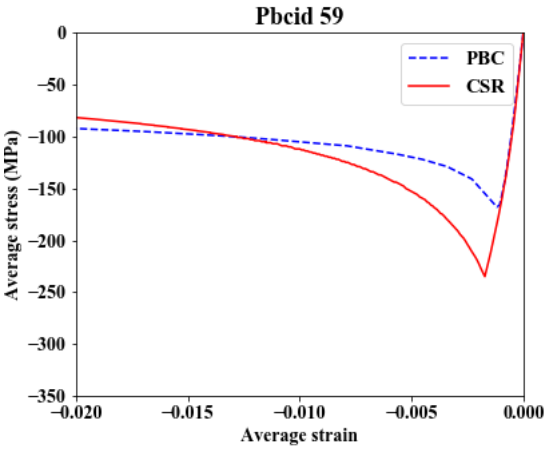
Pbcid 59
PBC
CSR
Average stress (MPa)
Average strain
0
−50
−100
−150
−200
−250
−300
−350
−0.020
−0.015
−0.010
−0.005
0.000

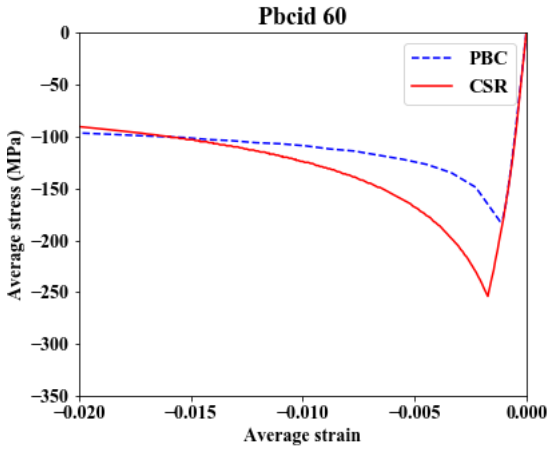
Pbcid 60
PBC
CSR
Average stress (MPa)
Average strain
0
−50
−100
−150
−200
−250
−300
−350
−0.020
−0.015
−0.010
−0.005
0.000

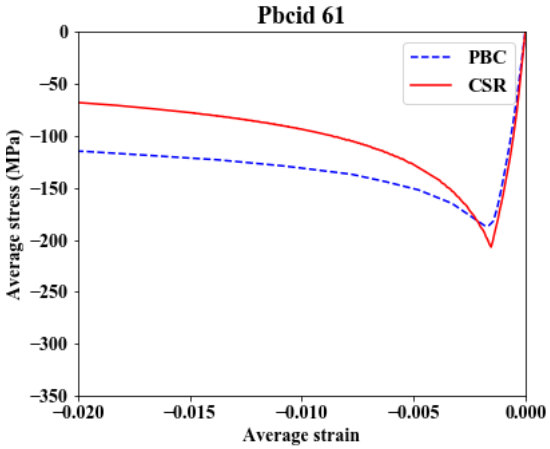
Pbcid 61
PBC
CSR
Average stress (MPa)
Average strain
0
−50
−100
−150
−200
−250
−300
−350
−0.020
−0.015
−0.010
−0.005
0.000

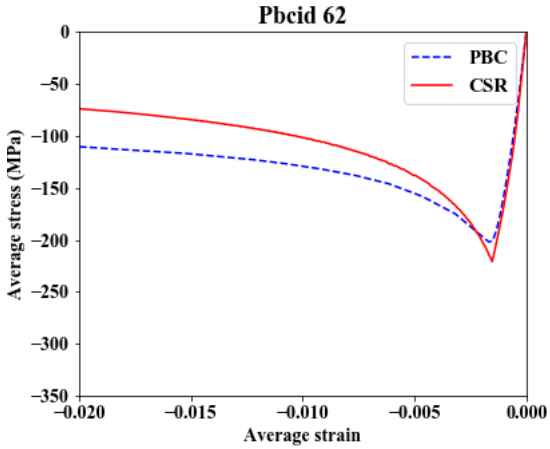
Pbcid 62
PBC
CSR
Average stress (MPa)
Average strain
0
−50
−100
−150
−200
−250
−300
−350
−0.020
−0.015
−0.010
−0.005
0.000

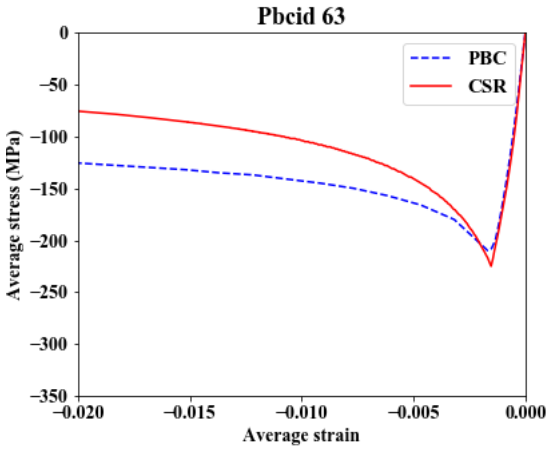
Pbcid 63
PBC
CSR
Average stress (MPa)
Average strain
0
−50
−100
−150
−200
−250
−300
−350
−0.020
−0.015
−0.010
−0.005
0.000

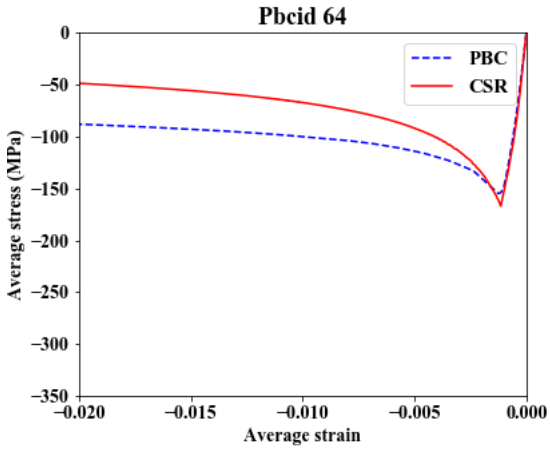
Pbcid 64
PBC
CSR
Average stress (MPa)
Average strain
0
−50
−100
−150
−200
−250
−300
−350
−0.020
−0.015
−0.010
−0.005
0.000

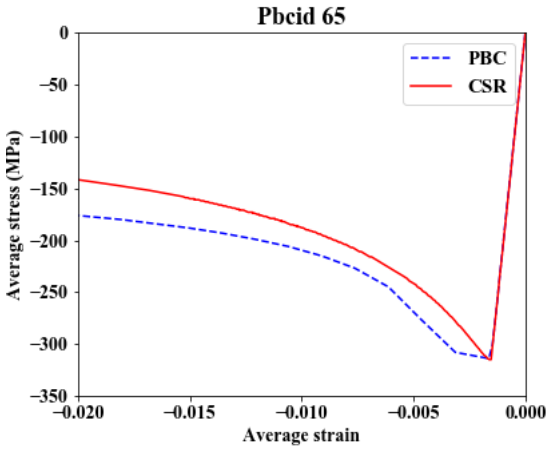
Pbcid 65
PBC
CSR
Average stress (MPa)
Average strain
0
−50
−100
−150
−200
−250
−300
−350
−0.020
−0.015
−0.010
−0.005
0.000

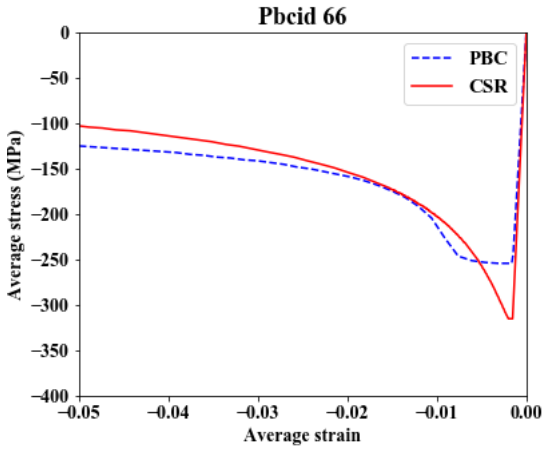
Pbcid 66
PBC
CSR
Average stress (MPa)
Average strain
0
−50
−100
−150
−200
−250
−300
−350
−400
−0.05
−0.04
−0.03
−0.02
−0.01
0.00

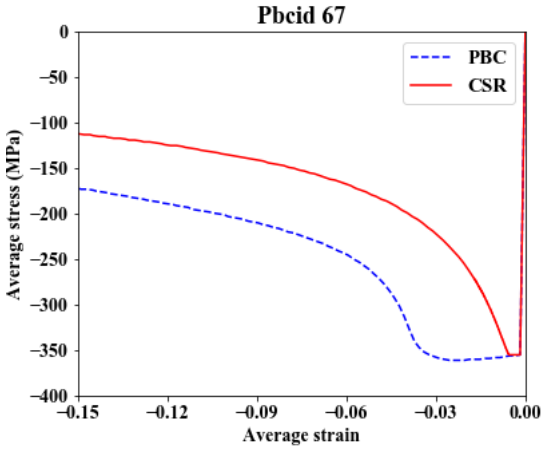
Pbcid 67
PBC
CSR
Average stress (MPa)
Average strain
0
−50
−100
−150
−200
−250
−300
−350
−400
−0.15
−0.12
−0.09
−0.06
−0.03
0.00

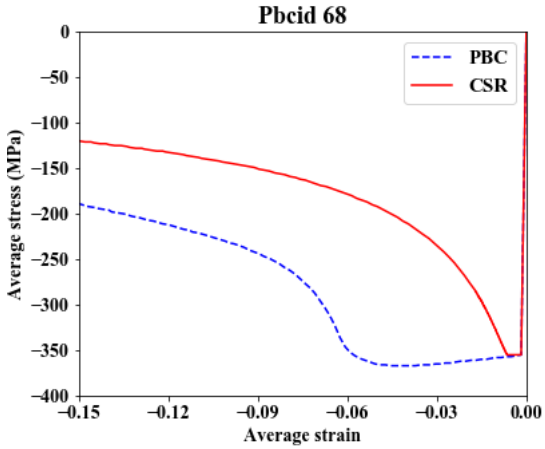
Pbcid 68
PBC
CSR
Average stress (MPa)
Average strain
0
−50
−100
−150
−200
−250
−300
−350
−400
−0.15
−0.12
−0.09
−0.06
−0.03
0.00

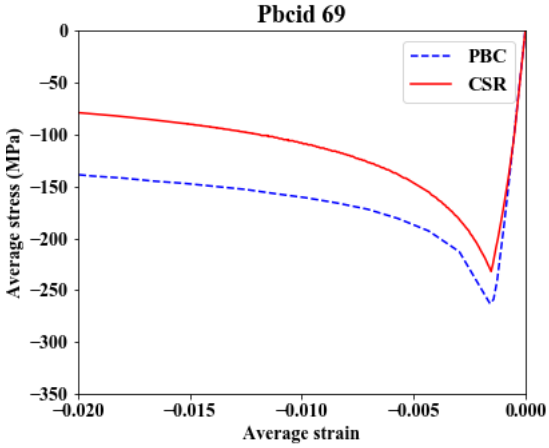
Pbcid 69
PBC
CSR
Average stress (MPa)
Average strain
0
−50
−100
−150
−200
−250
−300
−350
−0.020
−0.015
−0.010
−0.005
0.000

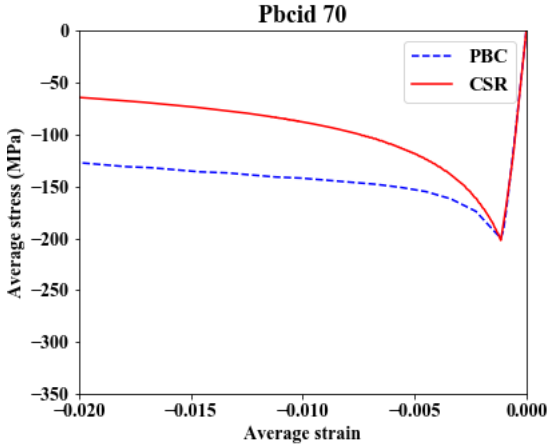
Pbcid 70
PBC
CSR
Average stress (MPa)
Average strain
0
−50
−100
−150
−200
−250
−300
−350
−0.020
−0.015
−0.010
−0.005
0.000

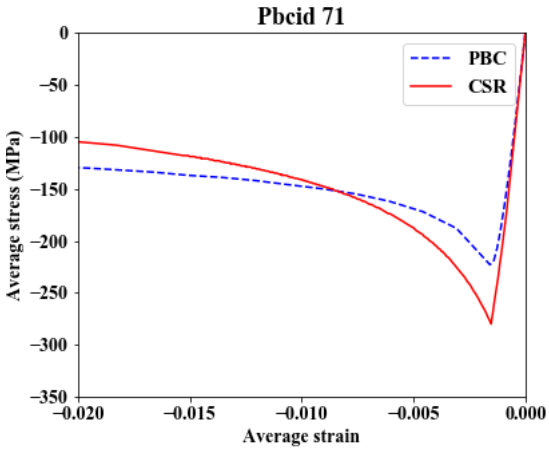
Pbcid 71
PBC
CSR
Average stress (MPa)
Average strain
0
−50
−100
−150
−200
−250
−300
−350
−0.020
−0.015
−0.010
−0.005
0.000

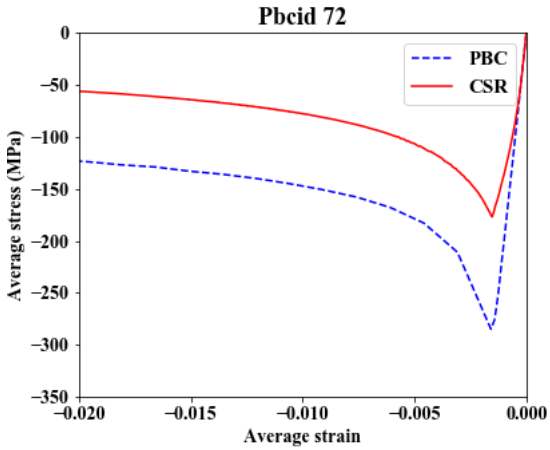
Pbcid 72
PBC
CSR
Average stress (MPa)
Average strain
0
−50
−100
−150
−200
−250
−300
−350
−0.020
−0.015
−0.010
−0.005
0.000

References

[1] Iijima, K., Kimura, K., Xu, W., and Fujikubo, M., 2011, "Hydroelasto-Plasticity Approach to Predicting the Post-Ultimate Strength Behavior of a Ship's Hull Girder in Waves," J. Mar. Sci. Technol.,16, pp- 379-389

[2] S.Timoshenko., 1983, History of Strength of Materials, pp- 434-449

[3] John, W.,1874, "On the Strength of Iron Ships," Trans R. Inst. Nav. Archit., 15, pp. 74-93

[4] Caldwell J.B., 1965, "Ultimate Longitudinal Strength," Trans R. Inst. Nav. Archit., **107**, pp. 411–430.

[5] Smith, C. S., 1977, "Influence of Local Compressive Failure on Ultimate Longitudinal Strength of a Ship's Hull," *Proceedings of the 1st International Symposium on Practical Design of Ships and Other Floating Structures*.

[6] Yao, T., and Nikolov, P. I., 1991, "Progressive Collapse Analysis of a Ship's Hull under Longitudinal Bending," J. Soc. Nav. Archit. Japan, **1991**(170), pp. 449–461.

[7] Yao, T., and Nikolov, P. I., 1992, "Progressive Collapse Analysis of a Ship's Hull under Longitudinal Bending (2nd Report)," J. Soc. Nav. Archit. Japan, **1992**(172), pp. 437–446.

[8] IACS, 2014, *Common Structural Rules for Bulk Carriers and Oil Tankers 1*.

[9] Gordo, J. M., and Guedes Soares, C., 1993, "Approximate Load Shortening Curves for Stiffened Plates Under Uniaxial Compression," Proc. Integr. Offshore Struct. - 5, (January), pp. 189–211.

[10] Hughes, T. J. R., and Liu, W. K., 1981, "Nonlinear Finite Element Analysis of Shells: Part I. Three-Dimensional Shells," Comput. Methods Appl. Mech. Eng., **26**(3), pp. 331–362.

[11] Hughes, T. J. R., and Liu, W. K., 1981, "Nonlinear Finite Element Analysis of Shells: Part II. Two-Dimensional Shells," Comput. Methods Appl. Mech. Eng. 10.1016/0045-7825(81)90148-1

[12] Belytschko, T., Tsay, C. S., and Liu, W. K., 1981, “A Stabilization Matrix for the Bilinear Mindlin Plate Element,” Comput. Methods Appl. Mech. Eng., **29**(3), pp. 313–327.

[13] Belytschko, T., Lin, J. I., and Chen-Shyh, T., 1984, “Explicit Algorithms for the Nonlinear Dynamics of Shells,” Comput. Methods Appl. Mech. Eng., **42**(2), pp. 225–251.

[14] Ted Belytschko, Bak Leong Wong, and Huai-Yang Chiang, 1992, “Advances in One-Point Quadrature Shell Elements,” Comput. Methods Appl. Mech. Eng., **96**(1), pp. 93–107.

[15] Chen K, Kutt L, Piaszczyk C, B. M., 1983, “Ultimate Strength of Ship Structures,” SNAME, pp. 149–168.

[16] Valsgaard, S., Jorgensen, L., Boe, A. A., and Thorkildsen, H., 1991, “Ultimate Hull Girder Strength Margins and Present Class Requirements,” pp. 1–19.

[17] IKEDA, A., Yao, T., Kitamura, O., Yamamoto, N., Yoneda, M., and Ohtsubo, H., 2001, “ASSESSMENT OF ULTIMATE LONGITUDINAL STRENGTH OF AGED TANKERS,” *Practical Design of Ships and Other Floating Structures. Proceedings of the Eighth International Symposium on Practical Design of Ships and Other Floating Structures*.

[18] Amlashi, H. K. K., and Moan, T., 2008, “Ultimate Strength Analysis of a Bulk Carrier Hull Girder under Alternate Hold Loading Condition - A Case Study. Part 1: Nonlinear Finite Element Modelling and Ultimate Hull Girder Capacity,” Mar. Struct.

[19] Amlashi, H. K. K., and Moan, T., 2009, “Ultimate Strength Analysis of a Bulk Carrier Hull Girder under Alternate Hold Loading Condition, Part 2: Stress Distribution in the Double Bottom and Simplified Approaches,” Mar. Struct.

[20] Tatsumi, A., and Fujikubo, M., 2020, “Ultimate Strength of Container Ships Subjected to Combined Hogging Moment and Bottom Local Loads Part 1: Nonlinear Finite Element Analysis,” Mar. Struct. 69, 108623

[21] Yukio, U., and Rashed, S. M. H., 1984, “The Idealized Structural Unit Method and

Its Application to Deep Girder Structures," Comput. Struct. 10.1016/0045-7949(84)90126-3

[22] Fujikubo, M., Kaeding, P., and Yao, T., 2000, "ISUM Rectangular Plate Element with New Lateral Shape Functions (1st Report)," J. Soc. Nav. Archit. Japan, **188**, pp. 209–219.

[23] Fujikubo, M., and Kaeding, P., 2000, "ISUM Rectangular Plate Element with New Lateral Shape Functions (2nd Report)," J. Soc. Nav. Archit. Japan, pp. 479–487.

[24] Paik, J. K., Thayamballi, A. K., Pedersen, P. T., and Park, Y. Il, 2001, "Ultimate Strength of Ship Hulls under Torsion," Ocean Eng.

[25] Pei, Z., Iijima, K., Fujikubo, M., Tanaka, Y., Tanaka, S., Okazawa, S., and Yao, T., 2013, "Collapse Behaviour of a Bulk Carrier under Alternate Heavy Loading Conditions," Int. J. Offshore Polar Eng., **23**(3), pp. 224–231.

[26] Cho, S., Czujko, J., and Estefen, S. F., 2006, "'Ultimate Strength (Committee III.1)'. 16th International Ship and Offshore Structures Congress," (August).

[27] Iijima, K., and Fujikubo, M., 2015, "Cumulative Collapse of a Ship Hull Girder under a Series of Extreme Wave Loads," J. Mar. Sci. Technol. 20, pp. 530–541

[28] Xu, W., Iijima, K., and Fujikubo, M., 2011, "Hydro-Elastoplasticity Approach to Ship's Hull Girder Collapse Behavior in Waves," *Advances in Marine Structures - Proceedings of the 3rd International Conference on Marine Structures, MARSTRUCT 2011*. 10.1201/b10771-28

[29] Tanaka, Y., Ogawa, H., Tatsumi, A., and Fujikubo, M., 2015, "Analysis Method of Ultimate Hull Girder Strength under Combined Loads," Ships Offshore Struct. Vol. 10, No. 5, 587–598

[30] Simo, J. C., and Hughes, T. J. R., 1998, *Computational Inelasticity*, Springer, New York, NY.

[31] de Souza Neto, E. A., Peri, D., and Owen, D. R. J., 2008, *Computational Methods for Plasticity*.

[32] Xu, W., Iijima, K., and Fujikubo, M., 2012, "Parametric Dependencies of the Post-

Ultimate Strength Behavior of a Ship's Hull Girder in Waves," J. Mar. Sci. Technol.17: pp.203-215

[33] Tatsumi, A., Ko, H. H. H., and Fujikubo, M., 2020, "Ultimate Strength of Container Ships Subjected to Combined Hogging Moment and Bottom Local Loads Part 2: An Extension of Smith's Method," Mar. Struct., **71**(May), p. 102738.

[34] Yao, T., and Fujikubo, M., 2016, *Buckling and Ultimate Strength of Ship and Ship-like Floating Structures*.